

ZEBRAFISH AS A MODEL TO STUDY MYELINATION DEFECTS IN CNS & PNS

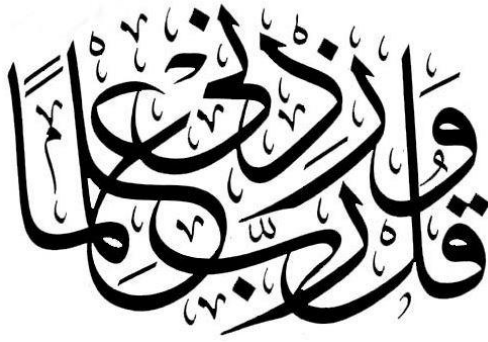
by

Nimah Alsomali



The
University
Of
Sheffield.

*Submitted for the degree of Doctor of Philosophy (PhD)
Sheffield Institute for Translational Neuroscience
University of Sheffield
October 2014*



“ My Lord! Increase me in knowledge.”
(Holy Quran, 20:114)

TABLE OF CONTENTS

LIST OF FIGURES	VIII
<i>CHAPTER I: INTRODUCTION</i>	1
1. MYELINATION	1
1.1 <i>CENTRAL NERVOUS SYSTEM MYELINATION</i>	3
1.1.1 Oligodendrocytes.....	3
1.1.2 Development of Oligodendrocytes.....	3
1.1.2.1 Oligodendrocyte Precursor Proliferation	4
1.1.2.2 Oligodendrocyte Precursor Migration	6
1.1.2.3 Oligodendrocyte Precursor Differentiation	8
1.1.2.4 Oligodendrocyte Myelination	11
1.2 <i>PERIPHERAL NERVOUS SYSTEM MYELINATION</i>	16
1.2.1 Schwann Cells (SCs).....	16
1.2.2 Schwann Cell Development.....	16
1.2.2.2 Schwann Cell Myelination	20
1.3 <i>MYELIN DISORDERS</i>	21
1.3.1 Multiple Sclerosis (MS)	22
1.4.2.1 MS Demyelination.....	23
1.4.2.2 MS Remyelination	24
1.3.2 Schizophrenia (SZ)	24
1.3.2.1 Myelin Associated Genes in SZ	26
1.3.2.2 Neuregulin 1.....	26
1.3.2.3 Disrupted-in-Schizophrenia 1 (DISC1).....	27
1.3.2.4 DISC1 Protein Interactions	28
1.3.2.4.1 Neuronal Migration.....	29
1.3.2.4.2 Neural Progenitor Proliferation	30
1.3.2.4.3 Neurosignaling.....	31
1.3.2.4.5 Synaptic Function	32
1.3.2.4.6 Other Protein Interactions.....	33
1.4 <i>ZEBRAFISH MODELS TO STUDY MYELINATION</i>	34
1.4.1 Development of Myelinating Cells in Zebrafish.....	35
1.5 <i>ZEBRAFISH GENETIC SCREENS</i>	36
1.5.1 Forward Genetic Screening.....	36

1.5.1.1 Chemical Mutagenesis.....	36
1.5.2 Reverse Genetic Screening	38
1.6 Hypothesis	41
1.7 Aims	41
CHAPTER II: MATERIALS AND METHODS	42
2.1 Materials	42
2.1.1 Zebrafish Maintenance	42
2.1.2 Solutions and Buffers	42
2.1.3 PCR primers used in this study.....	44
2.2 Methods	44
2.2.1 General Molecular Biology & Staining Methods.....	44
2.2.1.1 Bacterial Transformation	44
2.2.1.2 Bacterial Culture.....	45
2.2.1.3 Plasmid Purification.....	45
2.2.1.4 Digoxigenin (DIG)-Labelled Riboprobe Synthesis	46
2.2.1.5 Whole-Amount In situ Hybridization (WISH)	47
2.2.1.6 Cartilage Staining	49
2.2.1.7 Immunohistochemistry.....	49
2.2.1.8 Electron Microscopy	50
2.2.2 Genetic Methods.....	51
2.2.2.1 DNA Extraction.....	51
2.2.2.2 DNA purification.....	51
2.2.2.2.1 ExoSAP	51
2.2.2.2.2 Gel Extraction	52
2.2.2.2.3 Assay of DNA Concentration.....	53
2.2.2.3 Polymerase Chain Reaction (PCR).....	53
2.2.2.4 PCR Primer optimisation	54
2.2.2.5 Design Of PCR Primers.....	54
2.2.2.6 Agarose Gel Electrophoresis	54
2.2.3 Genetic Mapping Applications	54
2.2.3.1 Microsatellite (SSLP) Markers Scan	54
2.2.3.2 DNA Sequencing	55
2.2.3.4 BAC Rescue	55

2.2.3.4.1 BAC DNA Purification	55
2.2.3.4.2 Embryo microinjection.....	55
2.2.4 RNA-Based Methods.....	56
2.2.4.1 Total RNA Extraction From Zebrafish Embryos	56
2.2.4.2 cDNA Synthesis	56
2.2.4.3 Reverse Transcription RT-PCR.....	57
CHAPTER III: PHENOTYPIC CHARACTERSTION OF FB148.5	58
3 INTRODUCTION	58
3.1 FB148.5 Mutants Show Defects in Oligodendrocyte Specification in the Hindbrain.....	62
3.2 FB148.5 Zebrafish Show Abnormal Development of Lower Jaw Cartilages.....	65
3.3 FB148.5 Mutation May Impairs DISC1 Function.....	65
3.4 FB148.5 Mutants Show Neurogenesis Defects.....	68
3.5 FB148.5 Is Not Required For The Specification Of Serotonergic Neurons.....	71
3.6 FB148.5 Mutants Show Abnormal Axonal Development.....	71
3.7 FB148.5 May be Related To Sonic Hedgehog Signaling	74
3.8 FB148.5 Mutants Show Defects In Schwann Cell Development	76
3.9 DISCUSSION	78
CHAPTER IV: CHROMOSMAL MAPPING OF FB148.5 MUTANT ZEBRAFISH	82
4.1 INTRODUCTION	82
4.1.1 Intron-exon structure in zebrafish.....	82
4.1.2 Variant frequency in the zebrafish.....	83
4.2 Positional Cloning	84
4.2.1 FB148.5 Mapping Crosses.....	84
4.2.2 Linkage Analysis.....	85
4.2.3 The FB148.5 Mutation Maps To Linkage Group 8	89
4.2.4 Recombination Frequency Across LG8	94
4.2.5 Comparison Of Recombination Events In Individual Embryos	96
4.2.6 Sequencing of intronic regions	108
4.3 Candidate Genes	109

4.3.1 Genes Excluded By Genomic DNA Sequencing	109
4.3.2 Genes Excluded By cDNA Sequencing.....	112
4.3 Discussion.....	118
CHAPTER V: WHOLE GENOME SEQUENCING	122
5 INTRODUCTION.....	122
5.1 Whole Genome Sequencing.....	122
5.2 Mapping FB148.5 by Whole-Genome Sequencing.....	123
5.2.1. Whole-Genome Sequencing Failed to Identify The Causal Gene In FB148.5.....	125
5.2.2 Genes Excluded By WGS	129
5.2.3 GC Content	130
5.3 FB148.5 Rescue By BAC Clone Injection	137
5.3 Discussion.....	143
6. CHAPTER VI: GENERAL DISCUSSION.....	146
6.1 FUTURE WORK.....	153
Appendix.....	155
References	176

LIST OF TABLES

Table 2.1: List of buffers and reagents.....	44
Table 2.2 Probe synthesis reagents.....	47
Table 2.3 Proteinase K digestion stages and incubation time.....	49
Table 2.4 PCR programme for the DNA extraction	51
Table 2.5 ExoSAP Protocol	52
Table 2.6 PCR touchdown Programme	53
Table 4.1: list of SSLPs analysed from LG 8 with percentage recombination frequency observed.....	95
Table 4.2: Analysis of SSLPs linked with FB148.5 in individual embryos.	97
Table 4.3: List of genes that had intronic regions sequenced to identify novel SNPs linked with FB148.5.....	109
Table 4.4: Genes selected on the basis of known phenotypes.....	110
Table 5.1: Candidate LG8 genes identified by WGS and the polymorphism observed.	131
Table 5.2 List of BAC clones that were identified in the candidate interval with their size and genes encoded listed.....	139
Table 5.3: Quantification of attempted BAC rescue experiments.	142
Table 6.1 List of genes that were found to exhibit similar phenotypes to FB148.5 mutant zebrafish.....	150
Table .1: SSLP marker panel for initial mapping (genome scan).	155
Table 2 %G~C content in the genes in the LG8 candidate region	160

LIST OF FIGURES

Figure 1.1: Myelinating Cells in CNS and PNS Figure.	2
Figure 1.2: Progenitor domains in the spinal cord.	5
Figure 1.3: Oligodendrocyte developmental stages.	15
Figure 1.4: Stages of Schwann cell development.	17
Figure 3.1: Morphology of FB148.5 mutants.	59
Figure 3.2 Morphological and craniofacial defects induced by <i>disc1</i> knock-down	60
Figure 3.3 <i>disc1</i> is required for expansion of the populations of <i>olig2</i> and <i>sox10</i> -positive cells in the hindbrain.	61
Figure 3.4 <i>Olig2</i> and <i>sox10</i> expression in FB148.5 mutants and controls. ..	63
Figure 3.5 FB148.5 mutants show defects in oligodendrocyte development in the hindbrain.	64
Figure 3.6 Cartilage defects in FB148.5 mutants.	66
Figure 3.7 FB148.5 mutation affects <i>disc1</i> expression.	67
Figure 3.8 FB148.5 mutation affects <i>disc1</i> expression in hindbrain.	67
Figure 3.9 Neurogenesis defects in FB148.5 mutants shown by whole mount <i>in situ</i> hybridisation for <i>ash1b</i> expression.	69
Figure 3.10 Neurogenesis defects in FB148.5 mutants shown by whole mount <i>in situ</i> hybridisation for <i>ngn1</i> expression.	70
Figure 3.11: Normal production of neural stem cells in FB148.5 mutants shown by whole mount <i>in situ</i> hybridisation for <i>sox2</i> expression.	70
Figure 3.12: FB148.5 mutants showed relatively normal specification of serotonergic neurons.	72
Figure 3.13 FB148.5 mutants showed abnormal motor axon outgrowth by <i>znp-1</i> immunostaining.	73
Figure 3.14: Significant reduction in FB148.5 motor axon length.	73
Figure 3.15: FB148.5 mutants showed increased <i>ptc1</i> expression.	75
Figure 3.16: FB148.5 mutants show abnormal <i>gli1</i> expression by whole mount <i>in situ</i> hybridization.	75
Figure 3.17: FB148.5 is essential for Schwann cell development.	77
Figure 4.1 Mapping cross rationale.	84
Figure 4.2: Segregation of alleles in the mapping crosses.	86
Figure 4.3: Method for loading PCR products in agarose gels to enable direct comparison of alleles in mutant and sibling pools.	87
Figure 4.4: PCR products of 48 SSLPs markers used in initial mapping.	88
Figure 4.5: PCR products for the next 48 SSLPs.	90
Figure 4.6: PCR products for the next 48 SSLPs.	91
Figure 4.7: PCR products for the last 48 SSLPs.	92
Figure 4.8: PCR genotyping with SSLP z1068.	93
Figure 4.9: PCR genotyping with SSLP z15031.	93
Figure 4.10: Genotyping of mutant embryos with the SSLP marker z1068.	98

Figure 4.11: Genotyping of mutant embryos with the SSLP marker z7819, which is located at 30 cM.....	99
Figure 4.12: Genotyping of mutant embryos with the SSLP marker z15031, which is located at 28.2 cM.	100
Figure 4.13: Genotyping of mutant embryos with the SSLP marker z34962, which is located at 30 cM.....	101
Figure 4.14: Genotyping of single embryos with the SSLP marker z49543, which is located at 31 cM.....	102
Figure 4.15: Genotyping of single embryos with the SSLP marker z24511, which is located at 32 cM.....	103
Figure 4.16: Genotyping of single embryos with the SSLP marker z27391, which is located at 55.1 cM.	104
Figure 4.17: Map of SSLP markers between z1068 and z15031 on chromosome 8.	105
Figure 4.18 The genetic map of the candidate region between z1068 and z15031 contains around 50 genes	107
Figure 4.19: Sequence chromatograms for <i>Cldn5a</i>	111
Figure 4.20: Sequence chromatograms for <i>ufd11</i>	114
Figure 4.21: Sequence chromatograms for <i>lhx2b</i>	114
Figure 4.22: Direct sequencing of cDNA encoding <i>lhx2b</i> gene.	115
Figure 4.23: Direct sequencing of cDNA encoding <i>lhx2b</i> gene.	116
Figure 4.24 Candidate genes from the linkage interval.....	117
Figure 5.1: An example of high homozygosity score.	124
Figure 5.2: Plots showing homozygosity score levels in chr5, chr20 and chr23.....	126
Figure 5.3: Retesting of chromosomes 5, 20 and 23 for homozygosity with SSLP markers.	127
Figure 5.4: Homozygosity score level in chromosome 8.....	128
Figure 5.5: Sequencing of <i>dock5</i>	132
Figure 5.6: Sequencing of <i>fnbp11</i> SNP.....	133
Figure 5.7: Sequencing of <i>specc11a</i> SNP.	134
Figure 5.8: Sequencing of second <i>specc11a/b</i> SNP.....	135
Figure 5.9: Sequencing of <i>iqsec2</i> SNP.....	136
Figure 5.10: BAC clones locations in the linkage interval.....	139
Figure 5.11: BAC clones did not give mosaic rescue of oligodendrocyte defects in 5 d.p.f. FB148.5 larvae.	140
Figure 5.12: BAC clones did not give mosaic rescue of the oligodendrocyte defects in 5 d.p.f. FB148.5 larvae.	141
Figure 1: Intronic PCR primers used	161
Figure 2: Positions of primers used for sequencing <i>cldn5a</i>	171
Figure 3: Primers used for sequencing of <i>ccdc64</i>	172
Figure 4: Primers used for sequencing <i>rpl6</i>	173
Figure 5: Primers used for sequencing <i>ufd11</i>	174

Acknowledgement

PhD research is the result of four years of research work. However, it is impossible to complete the degree without the help and support of many people. It is pleasant that I finally have the opportunity to express my gratitude for all of them.

First and foremost, I would like to thank my first supervisor, Dr. Jon Wood, for his constant support in providing me opportunities to develop my scientific knowledge during these past four years. I appreciate all his contributions of ideas, time, patience and guidance to make my Ph.D. I will forever be grateful to him. Additionally, I have to thank my second supervisor Dr. Andy Grierson for his helpful suggestions and advice in general. I would like also to acknowledge Dr. Vincent Cunliffe and his lab members past and present; for their scientific advice and suggestions during our weekly lab meeting. I am also thankful to the Saudi Arabia's Ministry of Higher Education for funding me to complete this project.

My appreciation also goes to the wonderful staff and colleagues in the Sheffield Institute for Translational Neuroscience (SITraN) as well as in zebrafish facilities for always being so friendly and helpful.

I am also thankful for all my friends to look after me and the wonderful time we spent together all these years; these time would have been very hard without you. They were a great source of advice, support as well as friendships.

Lastly, I would like to express deepest love to my family for all their love and encouragement and without their care I would definitely have not been able to complete this thesis. Thank you!

ABSTRACT

Myelin is an electrical insulator sheath wrapped around axons. It is formed by myelinating oligodendrocyte cells in the CNS and by Schwann cells in the PNS. Myelin impairment has been linked with a number of neurological diseases such as multiple sclerosis (MS) and neuropsychiatric disorders such as schizophrenia.

Schizophrenia (SZ) is a severe mental disorder that affects approximately 0.5 to 1 % of the worldwide population. The causes of the illness are unclear but many studies have suggested the aetiology is a combination of genetic and environmental risk factors. Many genes implicated in SZ have important neurodevelopmental functions and Disrupted-in-schizophrenia 1 (DISC1) is one of the most widely studied SZ-susceptibility genes. Previous work has shown that knock down of *disc1* using morpholino antisense methods causes morphological abnormalities and inhibits the specification of *olig2*-positive oligodendrocyte precursors in the hindbrain. We identified an uncharacterized mutant (FB148.5) that showed very similar morphological defects to those seen in the *disc1* morpholino mutants (morphants).

Phenotypic characterisation of FB148.5 mutants revealed a number of neurological abnormalities similar to that found in *disc1* morphants including; specification of hindbrain oligodendrocytes, neurogenesis, Schwann cell development and motor axon outgrowth. Further mapping studies to identify the mutated gene in FB148.5 showed that the SSLP z1068 on linkage group 8 appears to be closely linked to the FB148.5 mutation. However, both the traditional mapping and high throughout strategies failed to find the mutated gene in this strain. Therefore, further work is needed to find the causative gene mutation.

CHAPTER I: INTRODUCTION

1. MYELINATION

The vertebrate nervous system is composed of the central nervous system (CNS) and the peripheral nervous system (PNS). The CNS consists of the brain and spinal cord and both contain grey matter and white matter. White matter contains glial cells and myelinated and non-myelinated axons, while grey matter primarily contains neurons and glia. The PNS consists of nerves that connect the central nervous system to the rest of the body. Myelin is an electrically insulating substance that is formed from multiple layers of myelin sheath which spread as compacted spirals to surround axons. Myelination in the (CNS) is performed by specialised glial cells, oligodendrocytes, whereas, in the (PNS) myelin is produced by Schwann cells (Geren and Schmitt 1954). In mammals, myelin sheaths cover large axons in both the central and peripheral nervous systems and axonal myelination is a unique feature of the vertebrate nervous system, whereas the invertebrate nervous system has ensheathing glia but no myelin is formed (Edenfeld, Volohonsky et al. 2006). Myelinated axons are segmented by unmyelinated gaps known as the nodes of Ranvier. The nodes are spread out at distances around 100 times the axonal diameter (Salzer 2003). These structures facilitate the rapid conduction of action potentials and conserve energy, which is essential for maintaining ion gradients (Siegel, Agranoff et al. 1999). Myelin is around 70% lipid and 30% protein and myelin sheath lipids consist mainly of un-esterified cholesterol. The ratio of cholesterol: phospholipids: glycolipids ranges from around 4:4:2 to 4:3:2 (Baumann and Pham-Dinh 2001). Myelinating cells can be detected using a number of myelin structural proteins as markers including, proteolipid protein (PLP), myelin basic

protein (MBP) and myelin associated glycoprotein (MAG) (Dubois-Dalcq, Behar et al. 1986) (Fig 1.1).

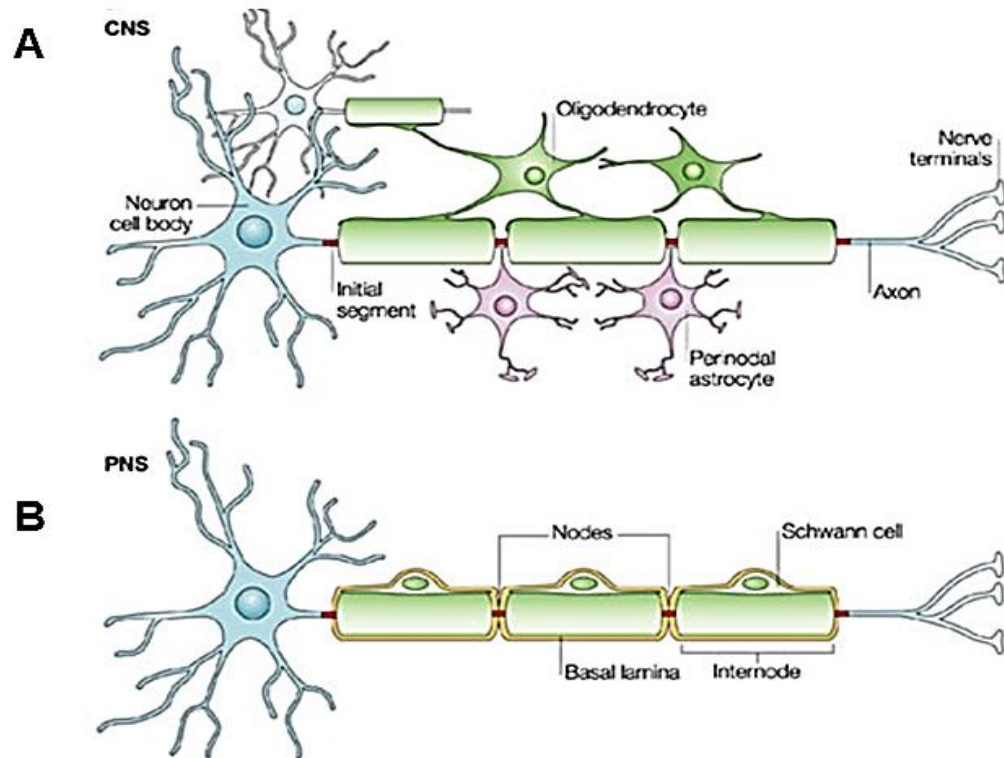


Figure 1.1: Myelinating Cells in CNS and PNS Figure.

(A) Oligodendrocytes in the CNS wrap multiple axons whereas (B) Schwann cells in the PNS wrap around a single axon. This figure is adapted from (Poliak and Peles 2003) with permission.

The importance of myelin in the normal functioning of the nervous system is emphasised by its roles in the aetiology of number of neurological diseases such as multiple sclerosis (MS) and neuropsychiatric disorders such as schizophrenia.

1.1 CENTRAL NERVOUS SYSTEM MYELINATION

1.1.1 OLIGODENDROCYTES

The term oligodendrocyte originates from Greek, meaning a cell with a few branches. Oligodendrocytes produce the myelin sheath that insulates CNS axons. A single oligodendrocyte can wrap up to 30-50 axons (Bunge 1968; Peters, Palay et al. 1991). Oligodendrocyte development occurs through number of differentiation steps from oligodendrocyte precursor cells (OPC) to mature myelinating cells which lead to dramatic alterations in the cell morphology, as well as expression of specific markers at different stages of development (Barateiro and Fernandes 2014).

1.1.2 DEVELOPMENT OF OLIGODENDROCYTES

Oligodendrocyte lineages develop in the mammalian brain and spinal cord through 4 main stages; oligodendrocyte precursor cells (OPC), pre-oligodendrocytes, immature oligodendrocytes and oligodendrocyte myelinating cells. In humans, OPCs start to proliferate at week 10 of gestation in the forebrain then reach their highest number at week 15 in the ventricular/sub-ventricular zone (Jakovcevski, Filipovic et al. 2009). In rodents, OPCs can be detected at E9.5 in the telencephalon (Timsit, Martinez et al. 1995). Between 18-28 weeks in humans and around postnatal day P2 in rodents, OPCs express specific markers such as OLIG2, A2B5 and SOX10 in order to differentiate to pre-oligodendrocytes. Then, between 28-40 weeks in humans, pre-oligodendrocytes give rise to immature oligodendrocytes from the pre-ventricular white matter and subsequently express a number of markers including MBP and MAG (Back, Luo et al.

2001; Craig, Ling Luo et al. 2003). At 36-40 weeks, myelin basic protein (MBP) expressing cells can be observed and the amount of myelinated white matter increases from 1-5% of total brain volume (Back, Luo et al. 2001). Similarly, in both mice and rats at around P7, MBP-expressing cells are observed and reach maximal numbers at around P14 (Hartman, Agrawal et al. 1979; Bjelke and Seiger 1989; Dean, Moravec et al. 2011; Barateiro and Fernandes 2014).

1.1.2.1 Oligodendrocyte Precursor Proliferation

OPCs are proliferating cells which originate from neuroepithelial progenitor cells in the ventral neural tube during development (Rowitch, 2004). During ventral spinal cord development, neuroepithelial cells are compartmentalised to generate the progenitor domains known as p3, p2, p1, pMN and p0 proceeding in a dorsal to ventral direction (Fig 1.2). Progenitor domains p0, p1 and p2 primarily give rise to interneurons and astrocytes, whereas motor neurons and OPCs originate mostly from the pMN domain (Vallstedt, Klos et al. 2005; Tripathi, Clarke et al. 2011). However, some OPCs arise in dorsal progenitor domains. OPCs are identified by expression of several genes such as the basic helix-loop-helix (bHLH) transcription factors OLIG1 and OLIG2, platelet derived growth factor receptor-alpha (PDGFR- α), SRY (sex determining region Y)-box 10 (SOX10) and chondroitin sulphate proteoglycan 4 (CSPG4) (also known as neuronal antigen 2 (NG2)). Neural progenitors in the pMN domain first give rise to motor neurons and later to OPCs (Poncet, Soula et al. 1996). Sonic hedgehog (Shh) signalling regulates this important switch (Park, Mehta et al. 2002). Shh is a secreted protein that is required for the specification of the progenitor domains as well as organizing the structure and function of the notochord and floor plate (Placzek 1995; Gritli-Linde, Lewis et al. 2001). Thus, the Shh signaling pathway is crucial for oligodendrocyte generation in both the spinal cord and forebrain (Orentas, Hayes et al. 1999; Nery,

Wichterle et al. 2001). During the specification of OPCs, these cells express *Olig1/2* which are essential for oligodendrocyte development in vertebrates. *Olig1/2* mutant zebrafish and mice demonstrate OPC specification defects in the spinal cord and brain (Lu, Sun et al. 2002; Park, Mehta et al. 2002; Zhou and Anderson 2002; Li, Lu et al. 2007). *Olig1* and *2* have different functions during OPC development, although they are similar in many ways (Rowitch, 2004).

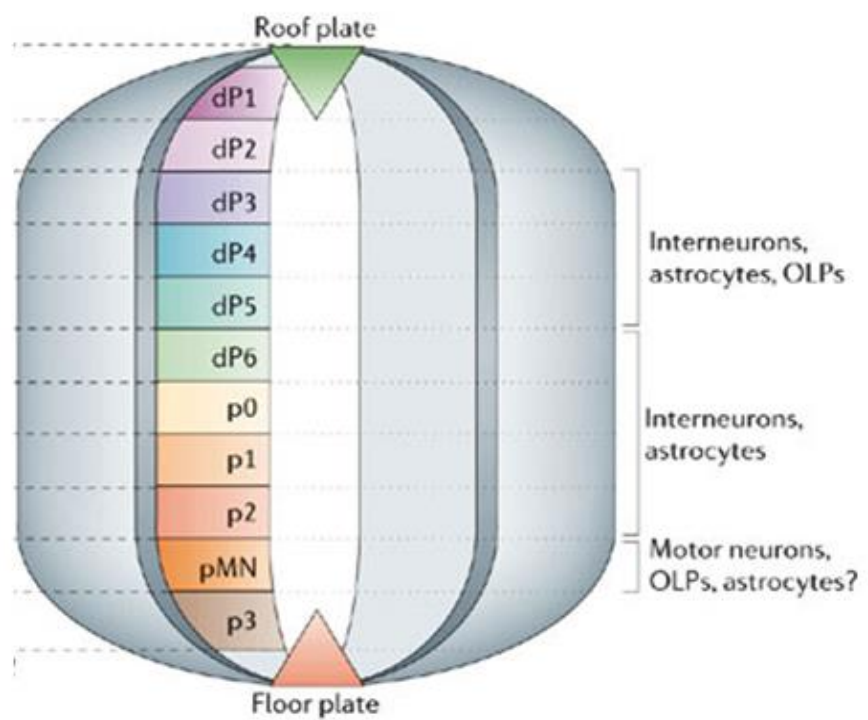


Figure 1.2: Progenitor domains in the spinal cord.

OPCs/OLPs are mainly generated from the pMN progenitor domain in the spinal cord. Image modified from (Richardson, Kessaris et al. 2006) with permission.

In the brain, OPCs are primarily generated in the ventral forebrain and then migrate dorsally to their final destinations in the cerebral cortex (Tekki-Kessaris, Woodruff et al. 2001 ;Rowitch, 2004; Kessaris, Pringle et al. 2008). As in the spinal cord, these OPCs express *Olig2* and *PDGFR- α* , and are generated under the control of Shh signalling (Tekki-Kessaris, Woodruff et al. 2001; Rowitch, 2004; Fuccillo, Rallu et al. 2004). It has been found that some subpopulations of OPCs are born independent of Shh signalling. Other studies have found that other signalling pathways in addition to Shh also regulate OPC production, and this includes fibroblast growth factor (FGF) signalling (Qian, Davis et al. 1997). FGFs are a family of signalling molecules that play multiple roles in controlling the development of the nervous system (Ford-Perriss, Abud et al. 2001; Hébert 2005; Aboitiz and Montiel 2007). It has been reported in zebrafish that FGF-receptor signalling regulates the production of OPCs by mediating the expression of *olig2* and *sox9* (Esain, Postlethwait et al. 2010). The SRY-box family transcription factors *Sox9* and *Sox10* have also been reported to have an important role in the development of OPCs by regulating *PDGFR- α* expression (Finzsch, Stolt et al. 2008). However, the molecular mechanisms underlying the production of OPCs under the control of FGF signalling in the forebrain are still unclear.

1.1.2.2 Oligodendrocyte Precursor Migration

There are different waves of OPC migration in the CNS and their final destination depends on the original site of specification. In the cerebellum the migration route of OPCs is not well studied unlike in the spinal cord where OPC migration has been studied in more detail. It has been reported that, in chick embryos, OPCs that originate from parabasal plate mesencephalon and diencephalon migrate to the cerebellar cortex (Mecklenburg, Garcia-López et al. 2011) or dorsal areas of the telencephalic and the diencephalon prosomeres (Garcia-Lopez and Martinez 2010). Additionally, OPCs

derived from the entopeduncular zone in the ventral forebrain, including the cerebral cortex, migrate through the entire telencephalon (Kessaris, Fogarty et al. 2005). Elsewhere, OPCs born in the rhombencephalon remain restricted to their original site in the rhombomeres (Olivier, Cobos et al. 2001). However, most OPCs derived from the ventricular zone of the spinal cord migrate along latero-ventral, ventral-dorsal and also rostro-caudal axes. Additionally, 20% of spinal cord OPCs originate from dorsal progenitor domains (Ono, Bansal et al. 1995). Other OPCs migrate through pre-formed axonal tracts such as from the pre-optic area along the optic nerve (Ono, Yasui et al. 1997; de Castro, Bribián et al. 2013). OPC migration involves interactions between OPC surface receptors and a number of environmental factors including chemokines, adhesion molecules, neurotransmitters and secreted growth factors (de Castro, Bribián et al. 2013).

Chemokines are proteins characterised by their small size and the presence of four cysteine residues in conserved locations that are essential to the formation of their 3-dimensional structure. The C-X-C chemokine receptor type 4 (CXCR4) has been shown to play a central role in OPC migration in response to the chemokine CXCL12 also known as stromal cell-derived factor-1 (SDF-1) (Banisadr, Frederick et al. 2011). The CXCL1 chemokine receptor (CXCR2) also facilitates the development of oligodendrocytes in the spinal cord (Tran and Miller 2003). CXCR2 is expressed mainly in spinal cord OPCs but it is also found in the cerebral cortex. CXCR2 appears to act as a stop signal for OPC migration in the spinal cord (Tsai, Frost et al. 2002).

During OPC migration, numerous adhesion contact-mediated molecules have been reported to be supporters of OPC migration via cell-cell interactions and subsequently regulate the speed of OPC motility. These molecules include extracellular matrix

proteins such as fibronectin, merosin, PSA-NCAM, anosmin-1 and tenascin-C (de Castro, Bribián et al. 2013).

In addition, a number of chemoattractant molecules which are known to assist cell movements, have been linked to OPC migration. FGF2, PDGF-AA and VEGF-A are important growth factors but have also been shown to act as chemoattractant molecules that affect OPC migration (Zhang, Vutskits et al. 2003; Zhang, Vutskits et al. 2004). Vascular endothelial growth factor (VEGF)-A, plays a central role in angiogenesis, and also mediates OPC migration independent of the presence of FGF2 (Zhang, Vutskits et al. 2003). It has been shown that the activation of PDGF receptors via the PDGF-AA growth factor increases OPC migration (Fruttiger, Karlsson et al. 1999). Shh also acts as a chemoattractant through the canonical Shh receptor, patched-1 (Ptc1) in optic nerve OPCs (Merchán, Bribián et al. 2007). Other chemoattractant molecules including netrin-1, semaphorin 3A and neuregulin-1 have significant functions in OPC migration (de Castro, Bribián et al. 2013). At the end of the migration process, various studies have reported multiple factors that act as stop signals to arrest OPC migration, and these include anosmin-1, endothelin-1, CXCL1 and FGF2 (de Castro, Bribián et al. 2013).

When OPCs have migrated to their final destination, most of them differentiate in to myelinating oligodendrocytes. However, some OPCs remain undifferentiated and may subsequently contribute to adult myelination, and these are thought to number 5-8% of total glial cells (Jones, Jolson et al. 2003).

1.1.2.3 Oligodendrocyte Precursor Differentiation

As OPCs differentiate to mature oligodendrocytes, their morphology becomes more complex and they extend multipolar short processes. A number of intrinsic and extrinsic factors have been reported to be involved in the OPC differentiation process. The

intrinsic factors include neural transcription factors and epigenetic mechanisms, while, the extrinsic factors include extracellular ligands and secreted molecules (Emery 2010).

There are numerous transcription factors that act as negative differentiation regulators in OPCs in order for the differentiation process to initiate. These transcription factors include Id2, Id4 and Hes5, which when they are active block the expression of myelin genes and keep OPCs undifferentiated. However, stimulation of extracellular signals leads to the down-regulation of these negative factors by affecting their cellular localization, causing pro-differentiation factors to express myelin genes and start differentiation (Kondo and Raff 2000; Wang, Sdrulla et al. 2001; Liu, Li et al. 2006). Consequently, a number of transcription factors work as positive regulators in the differentiation phase, most notably Olig1, Mash-1, Nkx2.2, Sox10, and YY1 (Wegner 2008). Additionally, Zinc-finger protein 191 (Zfp191) is a transcription factor that has been found to control late stages of oligodendrocyte differentiation. It has been found that Zfp191 mutant mice lose the ability to start myelin sheath formation (Howng, Avila et al. 2010).

MicroRNAs (miRNAs) are small, noncoding RNA molecules that are expressed by eukaryotic organisms. MicroRNAs function in the control of gene expression by targeting specific mRNAs and activating RNA degradation or inhibiting translation processes (Iorio, Ferracin et al. 2005). Interestingly, miRNAs have been shown to regulate CNS myelination through two miRNAs that have crucial roles in oligodendrocyte differentiation. These microRNAs are miR-338 miR-219, and they influence genes that usually act to keep OPCs in the undifferentiated condition, for instance Hes5, Sox6 and PDGFR α (Dugas, Cuellar et al. 2010; Zhao, He et al. 2010). This suggests a relationship between changes in gene expression and the signalling molecules which regulate OPC development during the differentiation process.

During differentiation OPCs express sulfatides recognised by the O4-antibody to develop to pre-oligodendrocytes (Bansal, Stefansson et al. 1992). In contrast, expression of PDGFR- α , A2B5 and NG2 are down-regulated in the pre- oligodendrocytes. Subsequently, these cells express galactocerebroside (GalC) along with O4 antigen and then pre-OPCs develop into pre-myelinating cells and start to express myelin related proteins (Barateiro and Fernandes 2014).

In addition, ligands for several receptors have been reported to control oligodendrocyte differentiation/myelination, such as Jagged, which signals via Notch in OPCs, as well as PSA-NCAM and Leucine-rich repeat and immunoglobulin domain-containing protein 1 (LINGO-1). Additionally, the Wnt/ β -catenin pathway appears to be a key factor in the initiation of terminal differentiation (Emery 2010). This pathway was suggested to act through Tcf4/Tcf7l2, a transcription factor that mediates the transcriptional effects of Wnt signaling. Furthermore, it has been reported that Tcf4 was found to be down-regulated in mature oligodendrocytes and play a role in re-myelination (Fancy, Baranzini et al. 2009). Therefore, this suggested that Wnt signaling may regulate complex pathways in oligodendrocyte differentiation and myelination via connecting with Tcf4 to regulate oligodendrocyte differentiation (Ye, Chen et al. 2009).

Pervious evidence showed that the ErbB2 receptor tyrosine kinase has a significant role in oligodendrocyte differentiation (Park, Mehta et al. 2002; Kim, Sun et al. 2003). A recent study demonstrated that LINGO-1 affects ErbB2 signalling to regulate oligodendrocyte differentiation via decreasing ErbB2 phosphorylation. LINGO-1 is known as a negative regulator of oligodendrocyte differentiation (Mi, Miller et al. 2005; Lee, Shao et al. 2014). Additionally, several studies found that hepatocyte growth factor (HGF)–cMet signalling mediates OPC differentiation and proliferation (Ohya, Funakoshi et al. 2007). HGF is affected by CD82 activity which inhibits HGF/cMet

during oligodendrocyte development. Therefore, HGF acts as an inhibitory regulator of OPC differentiation with CD82 alleviating this block (Mela and Goldman 2013). In addition to the previously discussed factors, G protein–coupled receptor (GPCR) Gpr17 is known to be expressed during oligodendrocyte differentiation and overexpression of this protein was reported in both *in vivo* and *in vitro* systems to inhibit oligodendrocyte differentiation. Thus, it might play a role in regulating the differentiation process (Chen, Wu et al. 2009). Rab family proteins are a group of small GTPases that are involved in vesicular trafficking with more than 60 Rab proteins having been identified in mammals and several of these proteins are linked to oligodendrocytes development. Rab35 has been described as a unique Rab protein that acts as a negative regulator for OPC differentiation through ACAP2 by inhibiting Arf6 (Miyamoto, Yamamori et al. 2014).

1.1.2.4 Oligodendrocyte Myelination

In the final phase of oligodendrocyte development, mature oligodendrocytes spread their membrane to form compact myelin sheaths around axons. This process is controlled by the axonal contact surface, axon thickness and electrical activity. Mature oligodendrocytes start to express a number of myelin- related proteins including myelin basic protein (MBP) and proteolipid protein (PLP) (Verity and Campagnoni 1988), 2',3'-cyclic nucleotide 3'-phosphodiesterase (CNPase), myelin-associated glycoprotein (MAG) myelin oligodendrocyte glycoprotein (MOG) and oligodendrocyte–myelin glycoprotein (OMgp) (Miron, Kuhlmann et al. 2011).

Several signals that originate from the axonal membrane have been reported to regulate the oligodendrocyte myelination process. Studies have reported that PSA-NCAM is expressed constantly during the early stages of oligodendrocyte development. Then, before starting the myelination process, PSA-NCAM expression is down-regulated. This suggested that expression of PSA-NCAM acts as a negative regulatory signal for

oligodendrocyte myelination (Jakovcevski, Mo et al. 2007). Previous studies found that axonal electrical activity plays a central role during myelination. For example, tetrodotoxin (TTX), which blocks voltage-gated sodium channels, was found to inhibit myelination (Charles, Hernandez et al. 2000). However, losing PSA-NCAM has no effect on the ability of TTX to inhibit myelin formation. Thus, myelination required positive axonal signals such as TTX-sensitive electrical activity and negative signals such as down-regulation of PSA-NCAM (Charles, Hernandez et al. 2000). There are other factors from the axonal membrane that are involved in the myelination process, for example L1, a cell-adhesion molecule and one of the immunoglobulin superfamily, which is known to be an inhibitory regulator of myelination during early contact between the oligodendrocyte and axons (Barbin, Aigrot et al. 2004).

In the CNS, a master molecular regulator that guides the myelination process by oligodendrocytes has not been reported yet. However, in the PNS Neuregulin-1 (NRG1) has been described as the major regulator on the axonal membrane that leads to myelination by Schwann cells (Taveggia, Zanazzi et al. 2005). The role of NRG1 signalling in CNS myelination is controversial. Early evidence suggested that NRG1 is a key factor in spinal cord oligodendrocyte development (Vartanian, Fischbach et al. 1999). On the other hand, it has been reported that CNS myelination may proceed independently of NRG1 signalling; therefore, it is most likely that in the CNS there are other signalling pathways that play a similar role to that of NRG1-ErbB signalling in PNS myelination (Brinkmann, Agarwal et al. 2008).

The Akt-1 signalling pathway has also been shown to play a role in CNS myelination. A number of growth factors including NRG1 type III, insulin growth factor (IGF-1) and steroids, which activate the myelination process in the CNS, cause phosphorylation of Akt-1 by phosphatidylinositol 3-kinase (PI3K). PI3K-Akt-1 signalling increases

myelination by activating mTOR, the mammalian target of rapamycin (Taveggia, Feltri et al. 2010).

FGF receptors 1 and 2 are expressed in mature oligodendrocytes and it has been found through studies in animal models that contain mutations in these genes, that they are not required for normal OPC differentiation and axonal ensheathment. In contrast, the overall CNS myelin thickness was affected, suggesting that FGF signalling regulates CNS myelin thickness in some way (Furusho, Dupree et al. 2012).

Recently, it has been reported that CNS myelin thickness is also regulated by calcium/calmodulin-dependent kinase type II β (CaMKII β), which is a serine/threonine kinase that primarily works through actin cytoskeleton pathways (Waggener, Dupree et al. 2013). Additionally, it has been found that Laminin receptors in the CNS activate oligodendrocyte differentiation and survival during myelin wrapping (Colognato, French-Constant et al. 2005). Also, β 1 integrin-deficient mice showed decreased myelin sheath thickness and dysmyelinated axons. This study suggested that β 1 integrins aid oligodendrocyte myelin formation through activating AKT (Barros, Nguyen et al. 2009).

Finally, oligodendrocytes wrap axons according to their diameter; mainly myelinating axons that have diameter greater than 0.2 μ m (Waxman and Bennett 1972). The myelin sheath wraps multiple times around an axon and the number of myelin wraps is proportional to the axon's diameter (Voyvodic 1989). Moreover, each oligodendrocyte is able to myelinate up to 60 axons (Remahl and Hildebrand 1990). It has been recently reported in zebrafish that oligodendrocytes have a short time window for formation of the myelin sheath (Czopka, French-Constant et al. 2013). Myelin thickness is measured by calculating the g-ratio which is the ratio of the axonal diameter divided by the diameter of the myelin sheath. It has been reported that the g-ratio for any given animal is the same, around 0.6 to 0.7. Therefore, axons that have large diameters are

ensheathed by thick myelin (Sherman and Brophy 2005). Finally, non-myelinating oligodendrocytes have been reported to undergo apoptosis (Barres and Raff 1999).

In summary, the development of myelinating oligodendrocytes is mediated by multiple cellular signalling pathways as well as transcription factors. However, it is still not fully understood how these pathways guide myelin formation at all developmental stages.

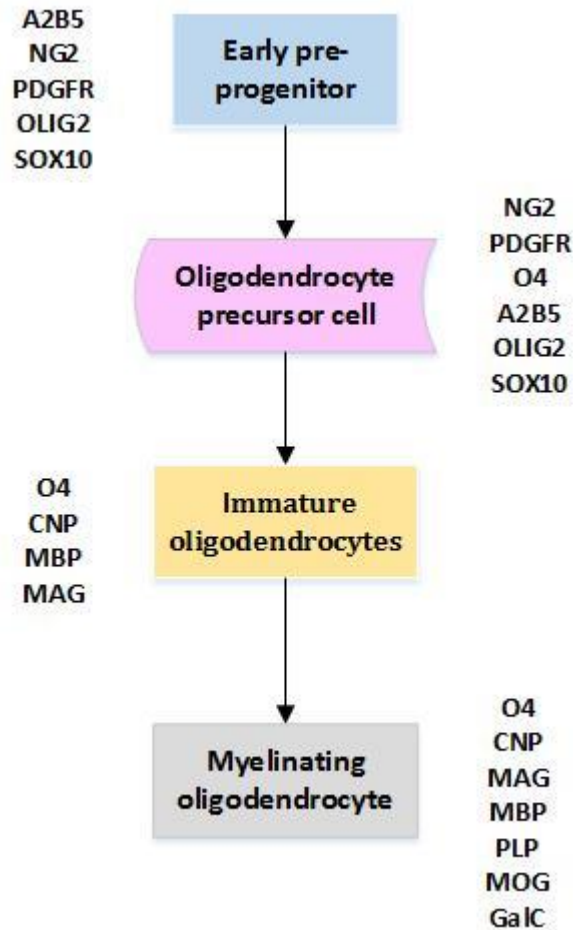


Figure 1.3: Oligodendrocyte developmental stages.

Oligodendrocytes are derived from early pre-progenitors which then develop into late progenitors, which then become oligodendrocyte precursors (OPCs) which can be identified on the basis of specific markers. OPCs then develop into immature oligodendrocytes which later become mature oligodendrocytes. Mature oligodendrocytes create the specific elements of myelin and become mature myelinating oligodendrocytes.

1.2 PERIPHERAL NERVOUS SYSTEM MYELINATION

1.2.1 SCHWANN CELLS (SCS)

The main role of Schwann cells is to myelinate the axons of the peripheral nervous system (PNS). Schwann cells are the glial cells of the PNS and they are derived from neural crest cells which migrate throughout the PNS where they differentiate into Schwann cell precursors (Jessen, Brennan et al. 1994). After migration is complete, Schwann cell precursors become immature Schwann cells, and finally differentiate into mature Schwann cells which can either form a sheath around a single large diameter axon or wrap several thin diameter axons. Schwann cell development has been shown to be regulated by many transcription factors and pathways which tightly regulate this process (Jessen and Mirsky 2005).

1.2.2 SCHWANN CELL DEVELOPMENT

Neural crest cells are derived from the dorsal part of the neural tube and migrate along different pathways that determine the lineage development of various cell types. These include neural cells of the autonomic sensory nervous system plus several non-neural cell types such as cardiac smooth muscle, melanocytes in the skin, cartilage, craniofacial bones and connective tissue. Cells that migrate laterally mainly give rise to non-neural cells (Woodhoo and Sommer 2008), while cells that migrate ventrally become neural cells or give rise to Schwann cell precursors (SCPs). This process takes place around E12- 13 in mice and E14/15 in rats, and then SCPs differentiate into immature Schwann cells. In rodents, myelinating SC formation proceeds around E15 to E17 in rats and E15 in mice. Lastly, immature Schwann cells give rise to myelinating and non-myelinating SC. Schwann cell ensheathement of axons in nerves was reported

around E17-18 in rats and E15-16 in mice (Mirsky, Jessen et al. 2002; Jessen and Mirsky 2005).

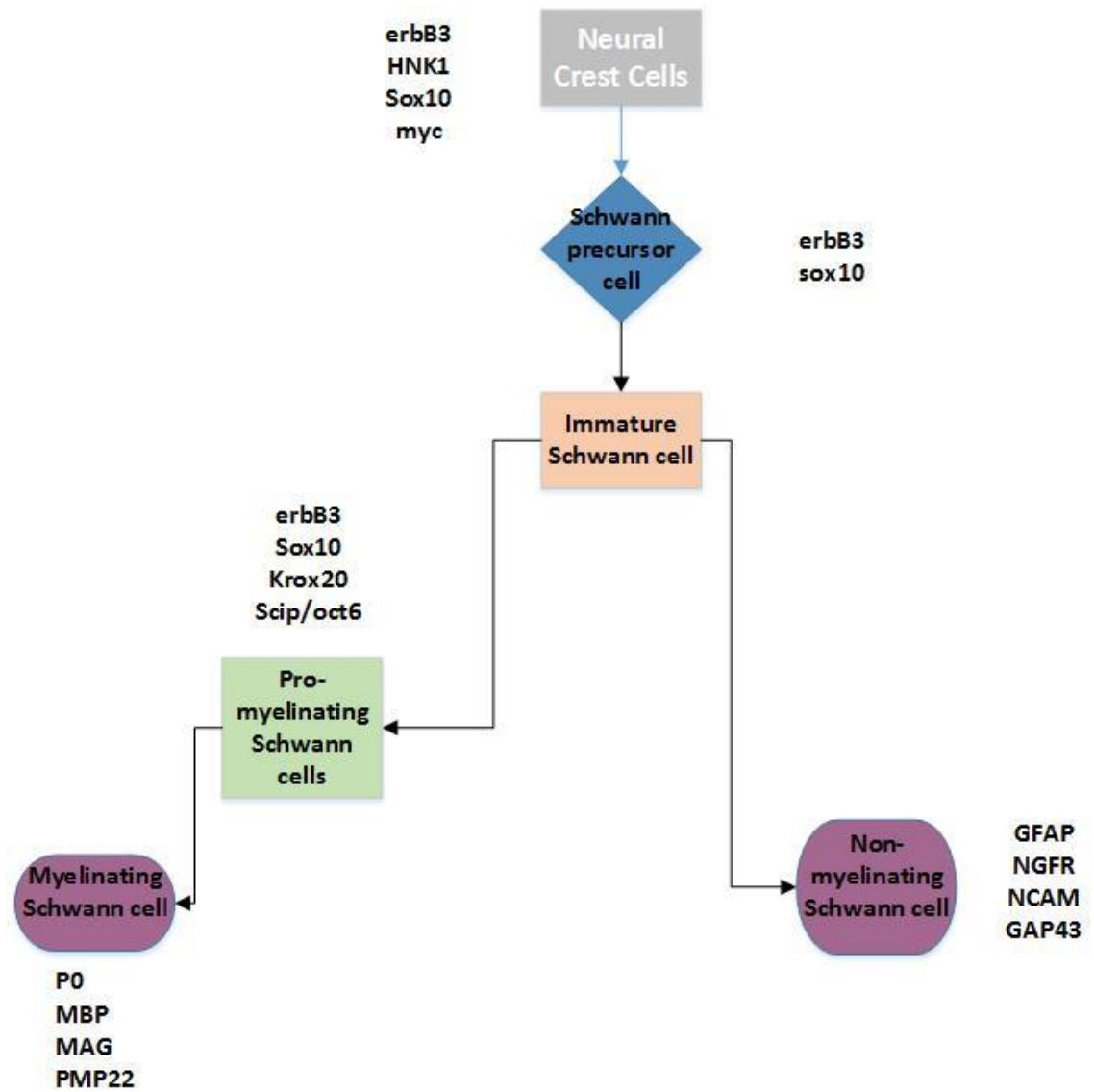


Figure 1.4: Stages of Schwann cell development.

Schwann cells start to differentiate from neural crest cells into Schwann precursor cells, and then they develop into immature Schwann cells. Immature Schwann cells can become non-myelinating or myelinating Schwann cells.

1.2.2.1 Schwann Cell Proliferation and Migration

In order to proliferate and differentiate from SCP to immature SC these cells respond to several signals and express specific transcription factors. The transcription factor Sox10 is expressed by neural crest cells as well as SCPs and is required for the transition from the neural crest to immature SC, however; in immature SCs Sox10 expression is reduced (Britsch, Goerich et al. 2001). The neuregulin (NRG) protein family and ErbB receptor tyrosine kinases, which are NRG-receptors, are known to be key regulators in numerous SC developmental stages (Brinkmann, Agarwal et al. 2008). Several studies have reported that NRG1 is required for the migration and proliferation of SCPs. NRG1 type III isoform mutation in mice leads to a dramatic decrease in SCPs number at E14 in the spinal cord (Taveggia, Zanazzi et al. 2005). Additionally, both in mice and zebrafish, ErbB receptors 2 and 3 have been reported to regulate both proliferation and migration of Schwann cells (Riethmacher, Sonnenberg-Riethmacher et al. 1997; Lyons, Pogoda et al. 2005). Taken together, these studies suggest that NRG1-ErbB signalling plays significant roles in SC development. Other factors have been shown to regulate SC proliferation as well as process extension and stabilization including Cdc42 and Rac1 during radial sorting. Cdc42 was found to be activated by neuregulin-1 (NRG1), while Rac1 has been linked to β 1-integrin signaling to promote SC process extension and stabilization (Benninger, Thurnherr et al. 2007). This suggested that NRG1 signalling may also play indirect roles in regulating SC development. In addition to NRG1, another mitogen that affects SC proliferation and migration is transforming growth factor (TGF-beta). Studies *in vivo* as well as *in vitro* showed that TGF-beta may play a key role in SC proliferation (Atanasoski, Notterpek et al. 2004).

Laminin, which is one of the extracellular matrix molecules that forms the basal lamina around non-myelinating SCs, has also been reported to regulate SC proliferation

because animals that lack laminin $\gamma 1$ displayed a reduction in SC proliferation in pre-myelinating stages (Yu, Feltri et al. 2005).

In addition, endothelin and its receptor are expressed in embryonic nerves, and its expression has been shown to impair SCP maturation in rats. This suggested that endothelin is a negative regulator of Schwann cell maturation (Brennan, Dean et al. 2000). Another factor that acts to negatively control Schwann cell maturation is the transcription factor AP-2, specifically AP2 α , because it was found to be down-regulated *in vivo* as Schwann cell precursors are generated (Stewart, Brennan et al. 2001). Also, *in vitro* overexpression of AP2 α leads to delayed SCP generation. These findings suggest that AP2 α may act as an inhibitory factor during SCs maturation (Stewart, Brennan et al. 2001). It has been reported that there are several stop or death signals that contribute to regulating SC apoptosis. These signals include nerve growth factor (NGF), which acts via its receptor p75 in immature SCs and has also been shown to be important in SC death after injury (Syroid, Maycox et al. 2000) and TGF- β 2 receptors (D'Antonio, Droggiti et al. 2006). Another negative signal which is involved in SCP differentiation, is the c-Jun-amino (N)-terminal kinase (JNK) pathway which is inhibited at the beginning of myelination by Krox-20 signalling, whereas it is activated by TGF β and NRG-1 in immature Schwann cells (Parkinson, Bhaskaran et al. 2004).

Notch 1 is expressed by neural crest cells and it has been shown that Notch signals activate immature SC proliferation both *in vivo* and *in vitro*. However, it is down regulated when mature SCs start myelination which suggests that Notch acts as an inhibitory signal during myelination (Woodhoo, Alonso et al. 2009).

Finally, immature Schwann cells express multiple transcription factors that act as positive regulators for SC development and induce the expression of myelin specific proteins to promote the development of immature SCs to myelinating SCs. These

factors include Krox20, which is also known as early growth response protein 2 (EGR2), Oct6, also known as POU domain class 3 transcription factor 1 (POU3F1) and Brn2 (Ghislain and Charnay 2006). Besides the above factors, the TGF- β inhibitor Ski is another protein that has been found to be an essential factor in the signalling pathways that control SC myelination. Ski is mainly expressed *in vivo* by myelinating SCs and promotes the expression of myelin-related genes. Lack of this factor caused failure in SC myelination in an appropriate culture system (Atanasoski, Notterpek et al. 2004). The transcription factor NF-kappa B is another factor that plays a central role in pre-myelinating SC formation. NF- κ B is expressed in SCs and preventing its expression results in impairment of myelination (Nickols, Valentine et al. 2003). It is unclear how these different transcription factors are interconnected and relate with other components and molecules to regulate SC myelination.

In addition, cAMP signalling has been found to control SCP proliferation and differentiation during development via activating Krox20 and upregulating P₀ and MAG expression in cultures studies (Monuki, Weinmaster et al. 1989; Ogata, Yamamoto et al. 2006). Also, Gpr126 is a G protein coupled receptor which has been reported to promote SC development in zebrafish at the pro-myelinating stage through activating adenylate cyclase (Monk, Naylor et al. 2009).

1.2.2.2 Schwann Cell Myelination

Prior to myelination, pro-myelinating SCs form bundles around axons radially and separate them into smaller bundles at a 1:1 ratio with each axon to wrap them. This phenomenon is defined as radial sorting (Webster, Martin et al. 1973). Similarly, non-myelinated SCs are generated around sensory axons which have diameter less than ~1 μ m to form Remak bundles (Sherman and Brophy 2005). Although is not fully understood yet how SCs interact with axons to be myelinated, multiple factors are

known to be involved such as cell adhesion molecules such as PSA- NCAM and L1 which are thought to be expressed by non-myelinated axons and then repressed during axonal myelination (Sherman and Brophy 2005).

It is well known that signals from axons are critical in the development of the Schwann cell lineage. NRG1 type III has been reported to be the main signal that controls myelin thickness around myelinated axons (Taveggia, Zanazzi et al. 2005). In addition, NRG1 type III has a key function in Remak bundle generation in non-myelinating SCs (Taveggia, Zanazzi et al. 2005).

Prior to maturation, Schwann cells begin to control their survival through producing a number of survival factors that block apoptosis by participating in an autocrine circuit. These factors include neurotrophin 3 (NT3), insulin-like growth factor 2 (IGF2), leukaemia inhibitory factor (LIF), lysophosphatidic acid (LPA), and platelet-derived growth factor- β (PDGFB) (Jessen and Mirsky 2005). In addition, several studies showed that Laminin/ β 1 integrin is essential for radial axonal sorting. β 1 integrin has been shown to mediate the activation of Rac1 which subsequently promotes SC myelination and axonal wrapping (Nodari, Zambroni et al. 2007). Another molecule that has key functions during the late stage of myelination is Neurofascin-186 (NF186), an immunoglobulin cell adhesion molecule, which has been shown to be responsible for the clustering of sodium channels at the nodes of Ranvier (Lyons and Talbot 2012).

1.3 MYELIN DISORDERS

Myelin abnormalities and oligodendrocyte deficiency has been linked to several psychiatric disorders including autism, schizophrenia and depression (Edgar and Sibille 2012). Additionally, similar abnormalities have also been reported in a number of neurodegenerative diseases such as multiple sclerosis, Alzheimer's disease and

amyotrophic lateral sclerosis (ALS). Postmortem brain tissue from Alzheimer's disease patients revealed a reduction in the expression of myelin related proteins such as CNPase, MBP and PLP (Vlkolinský, Cairns et al. 2001). Moreover, white matter defects have been shown by neuroimaging studies in Alzheimer patients, suggesting that these abnormalities might be related to the myelin damage that has been detected in postmortem brain tissue from patients (El Waly, Macchi et al. 2014). In addition, a recent study revealed that oligodendrocytes fail to perform normal myelination as well as providing inadequate trophic support to neurones in mutant superoxide dismutase 1 (*SOD1*) transgenic mice, a commonly used mouse model of ALS (Philips, Bento-Abreu et al. 2013).

1.3.1 MULTIPLE SCLEROSIS (MS)

Multiple sclerosis (MS) is a recurrent autoimmune disease of myelin in the CNS. A high prevalence of the disease occurs in young adults between 20-40 making MS the most common neurological disorder in young adults. It affects around 2.5 million people worldwide (Milo and Kahana 2010), with a higher incidence in females than males (Taylor, Devon et al. 2003). The disease etiology is not fully understood, but it is assumed that MS results from a combination of genetic susceptibility and environmental factors that lead to immune attack of myelin sheaths throughout the CNS (Milo and Kahana 2010).

MS is thought to be partly a genetic disease due to linkage and genome wide association studies which have identified a number of genetic loci, although twin studies have shown a modest rate of coincidence (around 30%) in identical twins. In contrast, non-identical twins have shown 3-5% higher risk in MS (Sadovnick, Armstrong et al. 1993). The human leukocyte antigen (HLA) system, which is located on chromosome 6, consists of many genes that are involved in the major histocompatibility complex

(MHC), and contains the most susceptibility genes for MS (Baranzini 2011). Additionally, GWAS have discovered a number of genes outside the HLA region that slightly effect MS incidence. Infectious agents have been identified as an environmental factor for MS (Kakalacheva and Lünemann 2011). Vitamin D deficiency, influenza A virus, Epstein-Barr virus (EBV) and smoking have also been associated with MS (Milo and Kahana 2010).

MS is a complex disease that clinically has different forms. The first form of MS disease is characterised by neurological defects such as numbness, weakness, incoordination and double or loss of vision in one eye. These symptoms can be rescued completely or moderately after a few days, and this pattern is known as the relapsing-remitting subtype of MS (RRMS). In some cases MS can lead to disability without any relapses and remissions, which is the secondary progressive subtype of MS (SPMS). Small numbers of MS patients are diagnosed with the primary progressive form (PPMS) which is characterised by a constant progression from onset. Many cases undergo complete disability due to the disease pattern or from immunosuppressive drug complications (Fleming 2013).

1.4.2.1 MS Demyelination

MS lesions in the CNS are caused by autoimmune inflammatory reactions that are mediated by T cell and B cells against myelin sheath and oligodendrocyte proteins which leads to white matter damage (Fingerprinting 2007). Demyelinated lesions in MS are created from activation of CD4+ T cells which leads to secretion of pro-inflammatory cytokines. These cytokines then stimulate microglia and astrocytes as well as other immune cells. It has been reported that immune cells secrete self-antibodies that might target the myelin sheath and oligodendrocytes (Gandhi, Laroni et al. 2010).

1.4.2.2 MS Remyelination

Remyelination or the myelin regenerative process is very similar to myelination during development and the only difference between them is that during development, myelination occurs in a healthy environment, while in MS, remyelination occurs in an abnormal environment (Buckley, Goldsmith et al. 2008). In MS, remyelinating lesions are observed by immunohistochemistry using antibodies against myelin related proteins including MBP, CNPase and PLP. This type of lesion has thinner myelin sheaths and fewer axons and therefore shows a weak staining of myelin proteins termed a “shadow plaque”. However, remyelination does not occur in some MS patients and large numbers of their lesions display no remyelination (Hanafy and Sloane 2011).

1.3.2 SCHIZOPHRENIA (SZ)

Schizophrenia (SZ) is a severe mental disorder that affects approximately 0.5 to 1 % of the worldwide population. It is characterized by a combination of symptoms such as delusions, hallucinations, disorganized thoughts and cognitive defects. SZ appears in late adolescence or early adulthood (Ross, Margolis et al. 2006). The causes of the illness are unclear but several studies have suggested the etiology as a combination of genetic risk factors, which includes a number of genes, such as *Neuregulin 1*, *DISC1* and *Dysbindin*, as well as environmental factors (Chubb, Bradshaw et al. 2007). A recent GWAS found 108 loci with most of them being expressed in brain and including several genes that are linked with glutamatergic neurotransmission, neurodevelopment and the immune system. This study therefore identified new insights in SZ etiology (Consortium 2014).

The existing treatment for SZ is considered only sedative and due to the poor knowledge of the disorder’s etiology and pathogenic mechanisms, therapeutic

development is extremely limited. The incidence of SZ is 1.4 times higher in men than women (Aleman, Kahn et al. 2003). The clinical symptoms of SZ vary but the most common symptoms are positive symptoms such as delusions and hallucinations, whereas negative symptoms are symptoms that are recognized by the absence of normal behaviors, including social withdrawal and abnormal emotional responses. So far there is no specific laboratory test to diagnose SZ and cases are diagnosed on the basis of symptoms after excluding other psychotic disorders such as delirium. However, it has been discovered that many of the clinical symptoms of SZ overlap with bipolar disorder symptoms (Ross, Margolis et al. 2006). Endophenotypes is a term that was used firstly by Gottesman in 1973, and is defined as clinical features which are heritable phenotypes that present at higher rates in the non-affected family members than in the general population. These phenotypes should co-segregate within families with psychiatric illness (Gottesman and Gould 2003). In SZ cases, endophenotypes have been applied to help describe neural abnormalities under genetic control. Thus, SZ has been associated with eye movement disorders (Ettinger, Picchioni et al. 2006), while the P300 wave, which tests cortical activity, has been used to identify deficits in memory function and attention in SZ patients and is also used as an endophenotype in SZ (Bramon, Dempster et al. 2006). Cognitive impairments, for example, learning difficulties, abnormal attention and poor memory performance, have been shown to be significantly altered in SZ. Additionally, there is some evidence of abnormalities in neurodevelopment in SZ, which has led to the neurodevelopmental hypothesis of SZ. For instance, abnormalities in neuronal positioning (Akbarian, Bunney et al. 1993) have been reported as well as decreases in the cortical neuropil volume (Selemon and Goldman-Rakic 2001).

1.3.2.1 Myelin Associated Genes in SZ

During normal development of brain, the myelination process leads to increased white matter volume. This process appears post-natally and normally continues into middle age. It has been found that increased white matter volume is linked with normal development of cognitive skills (Paus 2010). Since, SZ has its peak incidence during early adulthood, several studies have suggested myelin dysfunction in SZ as a causal factor in disease pathology. Abnormalities in brain white matter areas including the anterior commissure, fornix and corpus callosum have reported in SZ patients. Additionally, myelin dysfunction and reduction in oligodendrocyte numbers have been shown in SZ cases (Fields 2008; Jaaro-Peled, Hayashi-Takagi et al. 2009). In addition, numerous genetic studies have provided evidence of abnormal expression of oligodendrocyte and myelin related genes in SZ. These genes include *CNP*, *MAL*, *HRBB3*, *MAG*, *TF* and *GSN* (Hakak, Walker et al. 2001). Additionally, myelin related genes such as *MBP*, *MOP*, *MP2*, *PMP22* and *MAG* have also been reported to show decreased expression in SZ (Aston, Jiang et al. 2004; Prabakaran, Swatton et al. 2004). In spite of this, there are several reports that showed negative results, for instance; *MAG*, *CNP* and *OLIG2* with SZ (Mitkus, Hyde et al. 2008; Maycox, Kelly et al. 2009).

1.3.2.2 Neuregulin 1

NRG1 is one of four neuregulin related proteins. The *NRG1* gene was first linked to SZ when an association study in the Icelandic population pinpointed *NRG1* in a candidate region that had already been linked to SZ (Stefansson, Petursson et al. 2002). These findings were confirmed by other association studies in Caucasian and Asian populations (Li, Collier et al. 2006). *NRG1* has therefore been considered a pivotal candidate gene for SZ, although it has not been implicated by recent GWAS findings. The gene is found on chromosome 8p12.21 and encodes a signalling protein that

interacts with receptor tyrosine kinases of the ErbB family. The *NRG1* gene is expressed in most brain areas that have been correlated with SZ (Law, Shannon Weickert et al. 2004).

There are many studies that have investigated the possible role of *NRG1* in SZ. For example, Li et al (2005) provided evidence that *NRG1* is required for neural progenitor proliferation, suggesting that defects in this gene's activity might lead to abnormal brain development. Also, NRG1-ErbB4 signalling has a role in controlling axon guidance as well as neural migration (Rio, Rieff et al. 1997; López-Bendito, Cautinat et al. 2006). Furthermore, it has been shown that *NRG1* is required for axon myelination and oligodendrocyte differentiation, which has been observed in a zebrafish model as well as in cell and mouse studies (Corfas, Velardez et al. 2004; Wood, Bonath et al. 2009).

1.3.2.3 Disrupted-in-Schizophrenia 1 (DISC1)

Disrupted-in-Schizophrenia 1 (DISC1) is found on chromosome 1 and contains 13 exons, which generate four alternative splice forms. The *DISC1* gene was initially identified when a large Scottish family study found that the *DISC1* locus was disrupted by a balanced t (1; 11), (q42.1; q14.3) chromosomal translocation associated with psychiatric disorders (Millar, Wilson-Annan et al. 2000). Subsequently, *DISC1* has been associated with SZ in a number of different populations, for example Finnish, African American, central European, Chinese and Caucasian populations (Hennah, Varilo et al. 2003; Qu, Tang et al. 2007; Hodgkinson, Yuan et al. 2008; Schumacher, Laje et al. 2009). Additionally, a strong association was found with schizoaffective disorder close to the *DISC1* locus at 1q42 (Hamshere, Bennett et al. 2005). Therefore, interest in *DISC1* has increased as a potential candidate gene in SZ as well as in other mental disorders. Genetic analysis of *DISC1* has detected several SNPs and haplotypes of *DISC1* that are related to brain functions and structural abnormalities such as abnormal

cognitive function, decreased grey matter and hippocampal volume (Cannon, Hennah et al. 2005; Hennah, Tuulio-Henriksson et al. 2005; Thomson, Harris et al. 2005). Therefore, *DISC1* has been considered one of the most promising candidate genes for SZ. However, there are several GWAS studies that showed negative or no significant results for *DISC1* (Sullivan, Lin et al. 2008; O'Donovan, Craddock et al. 2009; Crowley, Hilliard et al. 2013). In addition, there are a number of association studies that failed to find linkage between *DISC1* and SZ in some populations, for instance Japanese and Korean populations (Devon, Anderson et al. 2001; Kim, Park et al. 2008).

It was first shown that *DISC1* might have a significant role in oligodendrocyte differentiation during neurodevelopment in the zebrafish (Wood et al, 2009). Subsequently, it was shown in a mouse model that *Disc1* mutants showed impairment of oligodendrocyte differentiation (Katsel, Tan et al. 2011). In addition, *DISC1* mutation has linked to agenesis of the corpus callosum (AgCC) pathology in humans, and abnormal development of the cerebral hemispheres in mice (Clapcote and Roder 2006). Abnormal callosal function has also been linked to schizophrenia (Innocenti, Ansermet et al. 2003). This indicates that aberrant *DISC1* function may underlie the mechanisms of agenesis of the corpus callosum (Osun, Li et al. 2011). Human brain imaging in the context of *DISC1* polymorphisms in SZ cases have reported large clusters of reduced grey matter (Duff, Macritchie et al. 2013).

1.3.2.4 *DISC1* Protein Interactions

DISC1 is recognised as a multifunctional scaffold protein that interacts with several proteins which are necessary for cAMP signalling, neuronal migration, neural progenitor proliferation, cytoskeletal modulation and synaptic function (Chubb, Bradshaw et al. 2007). The mechanisms and pathways suggested to involve *DISC1* protein function are many.

1.3.2.4.1 Neuronal Migration

Amyloid precursor protein (APP) is a transmembrane glycoprotein which plays a key role in Alzheimer's disease. Previously, it has been reported that APP knockdown using siRNA in the cortex leads to abnormal neuronal migration (Young-Pearse, Suth et al. 2010). A recent study suggested that the N-terminal domain of DISC1 interacts with the intracellular domain of APP which then promotes DISC1 protein distribution to the centrosome. Consequently, these results suggest that DISC1 controls neuronal migration in the cortex (Young-Pearse, Suth et al. 2010).

DIX domain containing 1 (DIXDC1) is the mammalian homologue of zebrafish Ccd1 that contains a Dishevelled-Axin (DIX) domain and controls Wnt/ β -catenin activity (Shiomi, Uchida et al. 2003). It has been reported that suppression of *Disc1* or knockdown of *Dixdc1* leads to defects in neural migration. Interestingly, the over-expression of degradation-resistant β -catenin or over-expression of both genes (*Disc1* & *Dixdc1*) did not reverse the neuronal migration abnormalities. Thus, neuronal migration is regulated by *Disc1* and *Dixdc1* genes independent of Wnt/ β -catenin signaling (Singh, Ge et al. 2010). Furthermore, it has been found that *Dixdc1* interacts with Ndel1 through phosphorylation of *Dixdc1* by Cyclin-dependent kinase 5 (Cdk5) on serine 250. *Dixdc1* also has a pivotal role in neuronal progenitor cell proliferation by interacting with DISC1 via Wnt-GSK3 β / β -catenin signaling (Singh, Ge et al. 2010). Thus, Cdk5 is required to switch the DISC1 protein function from neuronal progenitor cell proliferation to post-mitotic neuronal migration (Singh, Ge et al. 2010).

LIS1, also known as *PAFAH1B1*, encodes the lissencephaly 1 protein. *LIS1* gene mutation causes a severe neurodevelopmental disease called lissencephaly. This disease is recognized by serious brain malformation caused by defective neuronal migration (Lo Nigro, Chong et al. 1997). It has been found that LIS1 protein plays a vital role in

neuronal migration and neuroblast proliferation, and *Lis1* mutations lead to abnormal neurogenesis in the hippocampus in mice (Baraban 2007). Furthermore, it has been found that LIS1 is involved in the conserved nuclear transport pathway. The nuclear distribution (*nud*) mutants were discovered in *Aspergillus nidulans*. LIS1 is the mammalian orthologue of *nudf*, while NDE1 and NDEL1 are orthologues of *nude*. Subsequently, LIS1 was shown to form a complex with NDE1 and NDEL1 proteins. NDE1 and NDEL1 also have a central role in neuronal migration and LIS1 interacts with DISC1 through the NDEL1-LIS1 complex (Chubb, Bradshaw et al. 2007).

NDE-Like 1 (NDEL1) and Nuclear Distribution Factor E Homolog 1 (NDE1) share 60% identity and 80% similarity at the amino acid level. DISC1 was found to bind to NDEL1 protein in a number of yeast two-hybrid studies (Morris, Kandpal et al. 2003; Ozeki, Tomoda et al. 2003; Brandon, Handford et al. 2004). It has been found that NDEL1 is important for the connection between the centrosome and nucleus during neuronal migration. This neuronal migration system involves dynein, microtubules and the LIS1-NDEL1 protein complex. Impairment of the LIS1-NDEL1 complex leads to inhibition of neuronal migration by preventing the centrosome from integrating with the nucleus. Additionally, NDEL1 has been shown to act as an endo-oligopeptidase that cleaves neuropeptides. Interestingly, NDEL1-DISC1 interaction prevents this activity which is important in neurite outgrowth (Hayashi, Guerreiro et al. 2010).

1.3.2.4.2 Neural Progenitor Proliferation

DISC1 plays a critical role in neurogenesis and the proliferation of neural progenitor cells during mouse brain development (Mao, Ge et al. 2009). These results were seen in cultured brain slices, where use of short hairpin RNA (shRNA) against *Disc1* lead to decreased differentiation of progenitor cells. In contrast, DISC1 over-expression lead to increased production of neural progenitor cells (Mao, Ge et al. 2009). It has long been

known that wnt/ β -catenin signaling controls neural progenitor proliferation (Chenn and Walsh 2002). Recent research in 2009 by Mao et al found that DISC1 controls β -catenin activity. Additionally, the over-expression of degradation resistant β -catenin was shown to rescue the effect of *Disc1* loss (Mao, Ge et al. 2009).

Interestingly, Mao et al reported that glycogen synthase kinase-3 β protein (GSK3 β) interacts with DISC1 and is inhibited by DISC1. The mechanism that was suggested to explain this process is that the N-terminal domain of DISC1 interacts directly with GSK3 β and leads to inhibition of GSK3 β activity. For this reason β -catenin is stabilized, which then supports the proliferation of neural progenitor cells (Ming and Song 2009). Importantly, antipsychotic treatment (lithium) was also found to inhibit GSK3 β activity (Mao, Ge et al. 2009). GSK3 β is regulated by different factors such as Ser 9 phosphorylation via the AKT pathway (Mao, Ge et al. 2009) and recently it has been found that APP also regulates GSK3 β activity (Hernández, Gómez de Barreda et al. 2010).

1.3.2.4.3 Neurosignaling

The phosphodiesterase 4 (PDE4) family consists of four genes PDE4A-D that encode at least twenty different protein isoforms. PDE4s are enzymes consisting of two upstream conserved regions (UCR1, UCR2) and a catalytic N-terminal domain. DISC1 interacts with the UCR2 domain in PDE4. PDE4s play a critical role in the regulation of cyclic adenosine monophosphate (cAMP) signaling in the CNS. It has been reported that mutation in the DISC1-PDE4 binding site in mice leads to decreased PDE4 activity (Clapcote, Lipina et al. 2007). PKA (protein kinase A) phosphorylates the UCR1 domain in PDE4 leading to activation of PDE4 isoforms. When the cAMP concentration rises, this leads to dissociation of PDE4 and DISC1 and also increases PKA phosphorylation and activation of PDE4. Therefore, DISC1 plays a regulatory role

in PDE4 function. Additionally, decreasing DISC1 expression in cultured rat cells using RNAi, causes a decline in the extracellular signal- related kinase (ERK) level. ERK is considered as a key regulator of PDE4s catalytic activity. Therefore, DISC1 has a crucial role in controlling PDE4 activity (Chubb, Bradshaw et al. 2007).

Girdin protein, also known as KIAA1212, is expressed in cells of the dentate gyrus of the hippocampus and regulates the serine /threonine kinase AKT through direct binding with AKT (Enomoto, Asai et al. 2009). Girdin protein was found to interact with DISC1 in 2007 using a yeast two-hybrid screen (Camargo, Collura et al. 2006). Further studies have found that the DISC1- Girdin interaction leads to inhibition of AKT signaling (Zheng, Wang et al. 2012).

In summary, DISC1 is a key regulator of some of the most important signaling pathways in neurodevelopmental disorders. DISC1 controls Wnt/ β - catenin signaling by inhibiting GSK3 β activity, cAMP signaling by interacting with PDE4 and inhibiting AKT/mTOR signaling by binding with Girdin. Altogether, DISC1 plays a central role in neurosignaling and understanding these pathways may offer new approaches to neuropsychiatric treatment.

1.3.2.4.5 Synaptic Function

Kalirin7 is a GDP/GTP exchange factor for Rac1 of the Rho protein family. Kal-7 has a critical function in regulating dendritic spine formation and was linked with DISC1 by a yeast two-hybrid screen (Hayashi, Guerreiro et al. 2010). Traf2 and Nck-interacting Kinase (TNIK) is a serine/threonine kinase is another DISC1 protein partner. TNIK – DISC1 protein interaction was demonstrated in a yeast two hybrid screen (Camargo, Collura et al. 2006). TNIK is expressed in neurons that are enriched in PSD proteins and TNIK activity is inhibited by DISC1 protein. Reducing TNIK activity affects the stability of post synaptic proteins and neuronal activity (Wang, Charych et al. 2010).

1.3.2.4.6 Other Protein Interactions

Several studies have found other proteins that interact with DISC1 and have a role in brain structure and function, for example, 14-3-3 epsilon and Kinesin-1. 14-3-3ε protein is vital for brain function and has been linked with various neurological disorders. Loss of 14-3-3ε was shown in Miller-Diker syndrome as a consequence of disarrangement of the NDEL1 and LIS1 complex and subsequently leads to migration defects (Chubb, Bradshaw et al. 2007).

Function of 14-3-3ε protein has been linked with DISC1 in rat PC12 cells. The NDEL1-LIS1-14-3-3ε complex is regulated by DISC1 and Kinesin-1, another DISC1 binding protein. Additionally, it has been found that the Kinesin-1 interaction with DISC1 is important for axonal growth and microtubule organization (Taya, Shinoda et al. 2007). Together, these results suggest that DISC1 plays a role as a cargo receptor for transport of NDEL1, LIS1, 14-3-3ε complexes by Kinesin-1 (Chubb, Bradshaw et al. 2007).

Fasciculation and Elongation Factor Zeta1 (FEZ1) is another DISC1 protein partner that is implicated in the regulation of neuronal outgrowth. It has been reported that FEZ1-DISC1 interaction affects neural differentiation in PC12 cells (Miyoshi, Honda et al. 2003). This finding suggested that the DISC1-FEZ1 interaction has a role in brain function (Chubb, Bradshaw et al. 2007).

DISC1 was also found to bind to the centrosome via Pericentrin, which is also called Kendrin, and acts as a regulator for Pericentriolar material 1 (PCM1) function in microtubule organization. Importantly, PCM1 also interacts with DISC1 at the centrosome and it is critical for the production of newborn neurones (Ge, Frank et al. 2010). It has been found that Ser704Cys and Leu607Phe, which are amino acid variants of DISC1, lead to abnormal positioning of PCM1 at the centrosome. This suggests that DISC1 alleles might affect PCM1 localization (Eastwood, Walker et al. 2010).

In summary, the DISC1 protein is a scaffold protein with multiple isoforms and functions. These cause complex DISC1 interactions with several proteins which already have central roles in brain development and function. DISC1 may regulate these proteins at distinct times and different location in brain. Understanding these functions will lead to better understanding of the SZ etiology and pathology (Bradshaw and Porteous 2011).

1.4 ZEBRAFISH MODELS TO STUDY MYELINATION

Zebrafish (*Danio rerio*) were initially used by George Streisinger for scientific research in 1981 (Streisinger, Walker et al. 1981). Since then, zebrafish have been utilised as a high-throughput *in vivo* model which has become widely used in the last decade for therapeutic drug screens and to understand the mechanisms underlying a range of human diseases. Zebrafish have a number of advantages that make this model particularly suitable for the analysis of early development. The most important advantage is that zebrafish show rapid development of most organs, for example; the heart develops within two days post-fertilization (d.p.f) (Kimmel, Ballard et al. 1995).

Additionally, the developmental stages of the embryos can be easily observed due to external fertilization, which allows *in vivo* studies of cell structure and function. Moreover, zebrafish are relatively cheap to maintain. The ability to lay large numbers of embryos (around 100 to 300 embryos weekly per female) is another advantage of zebrafish as a model system (Buckley, Goldsmith et al. 2008).

Several techniques are available for both forward and reverse genetic studies to manipulate gene function. For example; gene knock down can be achieved using morpholino antisense oligonucleotides to inhibit splicing or translation of mRNA encoding a gene of interest (Skromne and Prince 2008). In addition, to generate gene

mutations in zebrafish, the chemical mutagen N-ethyl-N-nitrosurea (ENU) has been widely used. This method generates random mutations throughout the genome and can be used to isolate mutants by phenotype (Wienholds, Schulte-Merker et al. 2002). ENU-mutagenesis based screening is then followed by positional cloning techniques to identify the mutant gene (Talbot and Schier 1998).

In addition, the zebrafish has gained favour as a model organism for myelination research through the use of *in vivo* imaging techniques to visualize neural cell behavior and the relationships between neurons and glia during myelination.

1.4.1 DEVELOPMENT OF MYELINATING CELLS IN ZEBRAFISH

Zebrafish oligodendrocytes possess the same morphological structures of the myelin sheath as other vertebrates and express similar myelin-specific proteins throughout the development of myelinating cells, including *sox10*, *krox20*, *oct6* and *mbp* (Jeserich and Waehneltdt 1986; Sivron, Cohen et al. 1990; Jeserich and Stratmann 1992; Brösamle and Halpern 2002; Jeserich, Klempahn et al. 2008)

However, the main difference between zebrafish and mammals in myelin protein expression is that in the CNS, zebrafish express myelin protein zero (MPZ), which is only present in the PNS in mammals (Brösamle and Halpern 2002; Waehneltdt, Matthieu et al. 1986; Avila, Tevlin et al. 2007; Jeserich, Klempahn et al. 2008). Moreover, zebrafish often express a pair of orthologous genes for each vertebrate gene, as is the case for PLP/DM20 (Schweitzer, Becker et al. 2006; Brösamle and Halpern 2002). For this reason, some myelin-specific proteins are considerably less conserved in zebrafish compared to mammals. In zebrafish, oligodendrocytes in both the spinal cord and hindbrain arise from multipotent *olig2*-positive precursor cells of the motor neuron precursor (pMN) domain (Richardson, Smith et al. 2000; Rowitch 2004). Previously, it

has been reported that OPCs can be detected in the zebrafish by 2 days post fertilization (d.p.f.) in the hindbrain and that OPC differentiation occurs around 3 d.p.f. (Park et al., 2002). Additionally, *mpb*-expressing cells can be observed at 4 d.p.f. in the ventral hindbrain while compact myelin was reported around 7 d.p.f. (Brösamle and Halpern 2002). In contrast, another study reported that myelinated tracts can be observed as early as 54 h.p.f. in the zebrafish spinal cord using a *plp*:EGFP transgenic line (Yoshida and Macklin 2005). More recently, it was reported that myelination might start in zebrafish spinal cord at 3 d.p.f. (Buckley, Marguerie et al. 2010). Taken together, these findings demonstrate that zebrafish can be used as a model system to study and understand the complex mechanisms of myelination and model diseases of myelin.

Similar to mammals, mutant *erbb2* and *erbb3* zebrafish show impairments in SC proliferation and survival (Lyons, Pogoda et al. 2005). In addition, ErbB signalling was found to be required for radial sorting as well as directed migration of SC along their axons (Gilmour, Maischein et al. 2002; Raphael, Lyons et al. 2011). In addition, *gpr126*, a member of the adhesion family of G proteins, has been studied in zebrafish and it was found that *gpr126* mutants lack SC myelination. Further research found that *gpr126* up-regulates *krox20* and *oct6* functions in SC development (Monk, Naylor et al. 2009).

1.5 ZEBRAFISH GENETIC SCREENS

1.5.1 FORWARD GENETIC SCREENING

1.5.1.1 CHEMICAL MUTAGENESIS

Forward genetic screens aim to identify mutations that yield specific classes of phenotype. N-ethyl-N-nitrosourea (ENU) is a chemical mutagen that has been widely

used in large scale zebrafish forward genetic screens to produce point mutations (Grunwald and Streisinger 1992).

Point mutations are generated throughout the entire genome in pre-meiotic germ cells where ethyl group transfer to individual bases of the DNA causes base substitutions in the subsequent DNA replication (Pastink, Vreeken et al. 1989). ENU mainly induces recessive mutations, so in order to purify mutants to homozygosity, multi-generation backcrosses are utilised. Mutagenized adult male zebrafish are crossed with wild-type females in what is known as the parental generation (P) to create the F1 generation. The first generation (F1) offspring are heterozygous for individual mutations which are crossed for a second time with wild-type females, to generate the second generation (F2), which are then randomly inter-crossed to create the third generation (F3) families in which homozygous mutations appear. Ultimately, the F3 embryos are selected based on morphological criteria using microscopy between 1-5 dpf. Subsequently, positional cloning is used to link a particular gene to a point mutation (Solnica-Krezel, Schier et al. 1994; Lawson and Wolfe 2011). It is worth noting that zebrafish genomes are highly polymorphic between strains and obtaining a homozygous line requires multiple background out-crosses. The high level of polymorphic variability allowed scientists to use SNP mapping which is a relatively rapid and inexpensive tool to resolve the genetic linkage between phenotype and genotype in zebrafish strains.

Such screens have been performed to identify myelination mutants. Myelination defects can be observed as a secondary effect of some early developmental mutations, thus *mpb* expression in otherwise normal appearing embryos has been used to screen for mutations that cause specific myelination abnormalities (Czopka and Lyons 2011). One screen identified four mutants that were associated with Schwann cell and oligodendrocyte development and differentiation defects (Kazakova, Li et al. 2006).

Additionally, another large scale screen was performed in zebrafish which identified 10 different genes carrying 13 mutations that carried myelination defects (Pogoda, Sternheim et al. 2006). It was from this screen that *erbb3* and *erbb2* mutant lines were identified through disruption of *mbp* expression along PNS axons (Lyons, Pogoda et al. 2005).

In this study, a large-scale zebrafish mutagenesis phenotypic screen was previously performed using ENU by the Ingham laboratory in the Centre for Developmental and Biomedical Genetics at Sheffield University. This screen identified a small number of zebrafish lines that showed myelination defect phenotypes (A.J Grierson unpublished), for which further genetic mapping is required to determine the causal genes. Through this screen the FB148.5 mutation zebrafish strain was identified which is the main subject of this project.

1.5.2 REVERSE GENETIC SCREENING

Reverse genetic methods have been used in myelination research to study specific myelin-related gene functions by analysing the phenotypes caused by loss of gene function. A number of reverse genetic approaches have been used to study myelination in zebrafish including morpholino antisense oligonucleotides (MOs), Zinc finger nuclease (ZFN) technology, Targeted Induced Local Lesions in Genomes (TILLING), Transcription activator-like effector (TALE) nucleases (TALENs) and Clustered regulatory interspaced short palindromic (CRISPR) (Heasman 2002, Moens, Donn et al. 2008; Hwang, Fu et al. 2013).

The MO approach is utilized to analyse gene function through either blocking mRNA translation initiation or preventing the normal splicing of pre-mRNA (Nasevicius and Ekker 2000; Eisen and Smith 2008). However, this technique has disadvantages in that

it can give profound off target effects and is only suitable for early developmental stages since the effects of MOs are transient. The abnormal side effects include increased cell death, neural degradation (Heasman 2002) and p53 activation (Robu, Larson et al. 2007). As myelination is known to initiate at 3-4 days in zebrafish when the effect of MOs microinjected at the 1-cell stage will be wearing off, other techniques such as focal electroporation have been used (Concha, Russell et al. 2003; Czopka and Lyons 2011).

Another reverse genetic screening method is Targeted Induced Local Lesions in Genomes (TILLING) and it has been performed in several species including plants, mice and zebrafish (Wienholds, van Eeden et al. 2003). This approach again uses ENU to perform random mutagenesis to generate a library of mutation carrying fish and then sequencing of genomic DNA or use of other methods to identify mutants in a specific gene of interest (Moens, Donn et al. 2008). This approach could also aid myelination research by isolating specific mutant alleles in genes that are involved in myelination.

Zinc finger nucleases (ZFN) are one of the more recent reverse genetic approaches that has been used in zebrafish. ZFNs are artificial restriction enzymes that generate double-stranded DNA breaks by cleaving specific sequences. In respect to myelination, these powerful genome-editing methods can be used to provide new insight into understanding myelin formation and maintenance because they allow targeting and modification of specific alleles that cause human myelination disorders in zebrafish (Czopka and Lyons 2011).

In addition, Transcription activator-like effector (TALE) nucleases (TALENs) have recently appeared as an alternative genome engineering tool in many different organisms including mouse, rat, yeast, frog and zebrafish (Sun and Zhao 2013). TALENs are fusions of the FokI cleavage domain and DNA-binding domains derived from TALE proteins. This tool introduces site specific chromosomal double-strand

breaks, which is similar to the ZFN technique, and can be used for gene disruption, insertion, deletion or replacement. This approach can be applied to create targeted mutation in zebrafish which could help in myelination research (Sander, Cade et al. 2011).

Clustered regulatory interspaced short palindromic repeats have emerged recently as a powerful genetic editing technology. In zebrafish, the CRISPR-Cas9 has been applied with bacterial type II CRISPR systems to serve as RNA-guides that direct DNA cleavage by the Cas9 endonuclease in zebrafish embryos to induce targeted mutations similar to those obtained by ZFN and TALEN methods (Gaj, Gersbach et al. 2013; Hwang, Fu et al. 2013).

1.6 HYPOTHESIS

Previous unpublished research in Sheffield identified an uncharacterized mutant (FB148.5) that showed very similar morphological defects to those seen in the *disc1* morpholino mutants (morphants). Therefore, we hypothesized that the gene mutated in FB148.5 is functionally related to *disc1* and may be of relevance to psychiatric disease.

1.7 AIMS

There were two main aims at the outset of this project:

- To perform a detailed phenotypic characterisation of CNS development in FB148.5 mutants using whole mount *in situ* hybridization (WISH) and antibody staining against a panel of oligodendroglial and neuronal markers.
- To map the FB148.5 mutation by out-crossing FB148.5 onto the polymorphic wild-type WIK strain for two generations, and then use a panel of microsatellite markers to identify the linkage group harbouring the mutated gene as part of a positional cloning strategy. Further mapping and sequencing studies would then be undertaken to identify the FB148.5 mutation.

CHAPTER II: MATERIALS AND METHODS

2.1 MATERIALS

2.1.1 ZEBRAFISH MAINTENANCE

Wild-type zebrafish (AB and TL strains) were obtained by natural mating and maintained at 28.5°C in E3 medium. FB148.5 mutant zebrafish were induced by N-ethyl-N-nitrosourea (ENU) mutagenesis and isolated in an F3 lethal screen in the laboratory of Professor Philip Ingham at the Centre for Developmental Genetics at the University of Sheffield. The mutation is inherited in a recessive Mendelian mode and reveals abnormal morphological phenotypes, including small eyes, curved body axis and misshapen head. In addition, mutant embryos were distinguished by myelination defects through *mbp* and *olig2* expression patterns in the hindbrain using *ISH* at 48 hpf (Wolff, Roy et al. 2004). The heterozygous FB148.5 strain carrying the ENU induced mutation was originally generated in the AB strain background but was crossed several times to the London Wild Type (LWT) strain while maintaining the line, and later were out-crossed to the WIK strain to perform positional cloning. These multiple grandparental crosses exhibit different sets of SNPs which may interfere with mapping resolution and consequently yield false positive results.

Procedures in this study were performed according to local animal welfare regulations.

2.1.2 SOLUTIONS AND BUFFERS

Buffers	Recipes
Phosphate buffered saline (PBS)	Provided as tablets from Sigma,

	each tablet was dissolved in 200ml of H ₂ O
1X E3 medium	5 mM NaCl, 0.17 mM KCl, 0.33 mM CaCl ₂ , 0.33 mM MgSO ₄ , 20 µl of 0.03 M Methylene Blue per 1L was added to prevent fungal growth
PBT	2% (v/v) sheep serum, 0.2% (w/v) bovine serum albumin (BSA) , 0.1% (w/v) Tween 20 in PBS
20x SSC	300 mM Sodium citrate, 3 M NaCl
PTW	0.1 % (w/v) Tween 20 in PBS
Fish fix	0.1 M phosphate buffer pH 7.4, 4% (w/v) paraformaldehyde, 4% (w/v) sucrose, 0.12 mM CaCl ₂
Hybridization solution	5×SSC, 0.1% Tween 20, 500 µg/ml RNase free tRNA, 50 µg/ml Heparin, 50% Formamide, 9.2 mM citric acid.
Staining buffer	100 mM Tris-HCl pH9.5, 100

	mM NaCl, 50 mM MgCl ₂ , 0.1% (w/v) Tween20
PBDT	1% (v/v) DMSO, 1% (w/v) BSA & 0.5% (w/v) Triton X-100 in PBS.
5×TBE buffer	450 mM Tris, 450 mM Boric acid, 10 mM EDTA pH 8.3 – 8.7
DEPC-H ₂ O	0.1% (v/v) DEPC in dH ₂ O, autoclaved
50X TAE buffer	2 M Tris base, 1 M Glacial acetic acid, 50 mM EDTA pH 8.4

Table 2.1: List of buffers and reagents

2.1.3 PCR PRIMERS USED IN THIS STUDY

All primers that were used in this project were ordered from Sigma (Poole, UK).

2.2 METHODS

2.2.1 GENERAL MOLECULAR BIOLOGY & STAINING METHODS

2.2.1.1 BACTERIAL TRANSFORMATION

To perform bacterial transformations, DH5 α competent cells (Life Technologies, Paisley, UK) were thawed on ice and then 50 μ l of cells was transferred to a 1.5 ml micro-centrifuge tube that had been chilled on wet ice. Then, 1 μ l of DNA solution was added to the cells and mixed gently. After that, the tube was incubated on ice for 30 min, and then a heat shock was done to the cells for 20 s in a 37°C water bath. The tube was subsequently placed on ice for 2 min then 950 μ l of pre-warmed LB medium was added. After that, the tube was incubated at 37°C for 30 min at 225rpm. Finally, 0.5 ml from the transformation was spread on an LB-agar plate containing 50 μ g/ml of carbenicillin (Sigma), and then the plate was incubated overnight at 37°C.

2.2.1.2 BACTERIAL CULTURE

Using a sterile loop, a single colony was selected and used to inoculate 2 ml of LB medium (Fisher Bioreagents) containing 50 μ g/ml of carbenicillin. After that, the tube was placed on a shaking incubator at 37°C and 250rpm for 8 hr. Next, 100 μ l of the starter culture were transferred to 100ml of fresh growth medium in a 500ml flask which then was incubated overnight on the shaking incubator at 37°C.

2.2.1.3 PLASMID PURIFICATION

To purify DNA from bacteria, a Plasmid Midiprep Kit (QIAGEN GmbH) was used according to the manufacturer's instructions. Briefly, the bacterial cells were harvested by centrifugation at 600 x g for 15 min at 4 C. Then, cells were re-suspended in 4 ml of Buffer P1 and transferred to a 50 ml tube. After that, 4 ml of Buffer P2 was added to the tube and the contents were mixed thoroughly by inverting the sealed tube 4-6 times, and then incubated at room temperature for 5 min. Next, 4 ml of chilled Buffer P3 was added and the tube was thoroughly mixed and incubated on ice for 15 min. Following this, the tube was centrifuged at 20,000g for 30 minutes. The supernatant from this centrifugation contained the plasmid DNA which was removed carefully to a fresh tube.

The tube was centrifuged once more for 15 min at 20,000g and the supernatant was removed carefully. After that, the supernatant was applied to a column and it was allowed to enter the resin by gravity flow. Next, the QIAprep column was washed twice by adding 10 ml of Buffer QC. The column was placed in a clean labelled 15 ml tube and the plasmid DNA was eluted by the addition of 5 ml of elution buffer QF. Then, the tube was incubated at room temperature for 10 minute and then centrifuged for 30 minutes and the DNA was collected. The DNA was resuspended in 10 mM Tris buffer and stored in the freezer at -20°C until further use.

2.2.1.4 DIGOXIGENIN (DIG)-LABELLED RIBOPROBE SYNTHESIS

To prepare DIG-labeled riboprobes, plasmid templates were first linearised with appropriate restriction endonucleases. Linearised templates were purified using phenol: chloroform extraction and ethanol precipitation following standard protocols. Probe synthesis reactions contained the following:

Reagent	Amount
DNA	1 µg
10× transcription buffer (Roche)	2 µl
10× DIG labelling mix (Roche)	2 µl
RNA polymerase (T7,T3,SP6, all from Roche)	2 µl
RNase inhibitor (New England BioLabs)	1 µl
DEPC-treated water	To a final volume of 20 µl

Table 2.2 Probe synthesis reagents

The probe synthesis mixture was mixed gently and centrifuged briefly, then incubated for 2 h at 37°C. After this incubation 0.5 µl was removed for agarose gel electrophoresis. Subsequently, to purify the probe 2.5 µl of 10× DNase buffer and 2.5 µl (5U) of RNase-free DNase was added to the reaction which was then incubated for a further 15 min at 37°C. The probe was then precipitated with 2.5 µl 4M LiCl and 75 µl ethanol at -80°C overnight. The next day, the precipitated probe was collected by centrifugation at 13,000 rpm for 20 min at 4°C. The pellet was washed with 100 ml 70% ethanol then re-centrifuged for 15 min at 4°C. The pellet was air-dried for 5 min at RT and then re-suspended in 50 µl of DEPC-treated water. Recovery of the probe was checked by agarose gel electrophoresis. Finally, 50 µl of formamide (Sigma) was added to the probe which was then stored at -20°C.

2.2.1.5 WHOLE-AMOUNT *IN SITU* HYBRIDIZATION (WISH)

Whole-mount *in situ* hybridization (WISH) was applied to study spatial and temporal gene expression. Embryos were collected at 24, 31, 52 and 72 hours post fertilization (h.p.f.) in this study and were manually dechorionated using fine forceps. To prevent embryo pigmentation, 0.2 mM 1-phenyl-2-thiourea (PTU) (Sigma) was added at 8 h.p.f. Before fixation, embryos were washed with PBS then fixed with fish fix at 4°C overnight.

The next day embryos were rinsed with PBS, then washed with 50:50 PBS: methanol (MeOH) and stored at -20°C in 100% MeOH. The hybridization protocol started by washing the embryos in 50:50 PBS: MeOH then was followed with four washes with PBS + 0.1% Tween 20 (PTW) (5 min per wash). Proteinase K (Sigma) was applied to embryos at 10 µg/ml in PTW for appropriate time according to (table 2.3). After that, embryos were re-fixed in fish fix for 20 min, then washed four times with PTW and pre-

hybridized with fresh hybridization solution (200-300 μ l) at 65-70 $^{\circ}$ C for 3 hours. Embryos were then hybridized overnight with a 1:200 dilution of DIG-labelled antisense probe in hybridization solution at 65-70 $^{\circ}$ C.

On day 2, washing steps were performed. This started with a 20 min wash in a 1:1 mix of hybridization solution and 2 \times SSC. After that, the solution was replaced with 2 \times SSC for 20 min, then the embryos were washed with 0.2 \times SSC twice for 60 min each wash. Next, the embryos were blocked for 3 hours in PBT solution at room temperature then incubated overnight with an alkaline phosphatase-conjugated anti-DIG-antibody (Roche) at 4 $^{\circ}$ C.

On day 3, the embryos were washed 6 times with PBT for 20 minutes each wash then rinsed with staining buffer. Afterwards, NBT/BCIP (Roche) staining solution was applied to the embryos for colour development until the staining was optimal as judged by light microscopy. Embryos were then re-fixed at 4 $^{\circ}$ C in fish fix. The next day, embryos were washed with PTW then cleared with sequential washes in 10, 20, 40, 60 and 80% glycerol/PBS. After the last wash, the embryos were stored at 4 $^{\circ}$ C. Finally, images were obtained using differential interference contrast (DIC) light microscopy with a Leica microscope (LEICA DFC420C) and images were captured by LASAF software (Leica).

Embryos age	Incubation time in Proteinase K digestion
24 (h.p.f.)	10 min
2 (d.p.f.)	25 min
3 (d.p.f.)	25 min

4 (d.p.f.)	30 min
------------	--------

Table 2.3 Proteinase K digestion stages and incubation time

2.2.1.6 CARTILAGE STAINING

To observe embryonic jaw cartilage development in FB148.5 embryos at 5 d.p.f., alcian blue staining was performed. After fixation, embryos were rinsed with 0.1% Tween 20 (Sigma) in H₂O. After that alcian blue stain (Sigma) (0.05% Alcian blue, 5% acetic acid) was added then the embryos were stored at room temperature overnight. The next day, embryos were washed with 0.1% Tween 20 then in 30% (saturated) sodium borate solution. Afterwards, embryos were incubated with 100 µg/ml trypsin (Sigma) in 30% sodium borate solution for 3-4 hours to digest the tissue around the cartilages. Then, the embryos were cleared using 25% followed by 50% glycerol and stored at 4°C until images were taken by DIC microscopy.

2.2.1.7 IMMUNOHISTOCHEMISTRY

In this study we used anti-acetylated tubulin (AAT) (Sigma) and znp-1 (Developmental Studies Hybridoma Bank) mouse monoclonal antibodies to observe axonal development in mutant and sibling embryos. The procedure was done as follows: Fixed embryos in 100% MeOH were washed gradually in 75%, 50% and 25% MeOH/H₂O (5 min each). Embryos were then rinsed with 0.1% Triton X-100/H₂O. Embryos older than 2 days were treated with trypsin solution (0.25% trypsin in PBT) on ice, while embryos younger than 2 days were treated with acetone at -20°C for 7-10 min. After that, 0.1% TX-100/H₂O was again added to wash the embryos 3 times, and then block solution (PBDT + 5% normal serum) was applied to the embryos for 2 h using a shaking platform at room temperature. Next, the blocking solution was replaced with PBDT + 5% normal serum containing the primary antibody (AAT at 1/2000 or znp-1 at 1/500) then the embryos were incubated overnight at 4°C.

The next day, embryos were washed 4 times with PBDT + 5% normal serum, and then incubated overnight at 4°C in the Vectastain biotinylated secondary antibody at 1/400 (Vector Laboratories). Day 3 started with washing the embryos 4 times in PBDT + 5% normal serum over a 2 h period. Avidin-biotin complex (ABC) was prepared during the last wash and left on the bench for 30 min before use. Afterwards, the AB complex was added and the embryos were incubated at room temperature for 90 min on a shaking platform. Then, PBDT + 5% normal serum washes were performed 4 times (30 min each) followed by 3 washes with PBS + 0.5% TX-100 over a 1 h period.

After that, 3,3'-Diaminobenzidine (DAB) staining was performed with a DAB Peroxidase Substrate Kit according to the manufacturer's protocol (Vector Laboratories). After the DAB staining solution was added to the embryos they were incubated at room temperature with continuous monitoring until colour development was optimal. Finally, the embryos were washed with PBS 3 times and then fixed with fish fix overnight at 4°C. The next day, the embryos were passed through a glycerol series (10%, 20%, 40%, 60%, and 80%) to clear them prior to mounting.

2.2.1.8 ELECTRON MICROSCOPY

Fish at 5 dpf were prepared for transmission electron microscopy (TEM) as described elsewhere (Czopka and Lyons 2011). They underwent primary fixation in 2% glutaraldehyde, 4% formaldehyde, 0.1 M sodium cacodylate using microwave stimulation, followed by 2 h at room temperature. The biophysical basis of microwave-stimulated processing is not understood; full experimental details are provided in Czopka and Lyons 2011. Specimens were decapitated prior to secondary fixation with 2% osmium tetroxide, 0.1 M sodium cacodylate, 0.1 M imidazole, pH 7.5. Secondary fixation was also microwave assisted then continued overnight. Specimens were thoroughly rinsed in deionised water then stained with saturated uranyl acetate with

microwave stimulation. After that, specimens were dehydrated by passing through an ethanol series (50%, 70%, 95% and 100%), followed by 3 x 10 min acetone washes. Dehydration steps were also microwave assisted. Specimens were infiltrated with 1:1 EMBED:acetone at room temperature overnight, then embedded in 100% EMBED in wells of embedding molds. Specimens were allowed to cure for 72 h at 65°C. Sectioning, staining and transmission electron microscopy was performed by Chris Hill in the Electron Microscopy Unit, Department of Biomedical Science, University of Sheffield. G-ratios (myelin thickness) and axon diameters were measured using imageJ and GraphPad Prism6 with 2-tailed tests. Statistical significance was set at $P < 0.05$.

2.2.2 GENETIC METHODS

2.2.2.1 DNA Extraction

DNA was extracted using QuickExtract solution; each embryo was transferred to a 0.2ml microcentrifuge tube with 30 μ l of QuickExtract solution then processed using a G storm PCR machine with the following DNA extraction protocol.

Temperature	Time
65°C	120 min
98°C	2 min
4°C	hold

Table 2.4 PCR programme for the DNA extraction

Next, the extracted embryos were vortexed for 15 s, centrifuged for 1 min at 1700 r.p.m. then stored at -20°C.

2.2.2.2 DNA purification

2.2.2.2.1 *ExoSAP*

To remove excess dNTPs and primers from PCR products prior to sequencing, two enzymes, shrimp alkaline phosphatase (SAP; United States Biochemical) and Exonuclease 1(New England BioLabs) were used. 0.5 U of SAP and 1 U of Exonuclease I was added to 4 µl of H₂O and 5 µl of PCR product. The following PCR programme was used:

Temperature	Time
Starting temperature	37°C to 45 minutes
Denature	80°C to 15 minutes
Storing temperature	12°C for ever

Table 2.5 ExoSAP Protocol

2.2.2.2.2 Gel Extraction

To extract DNA from agarose gel slices, gel extraction was performed using the QIAEX II kit (Qiagen) according to the manufacturer's instructions. DNA bands were excised from the agarose gel using a clean sharp scalpel. They were transferred to 1.5ml micro-centrifuge tubes and weighed. Next, 3 volumes of Buffer QX1 were added to each volume of DNA fragments. Then, Qiaex II (10 µl) was added to tubes and they were incubated at 50°C for 15 minutes during which the tubes were mixed by vortexing for every 2 minutes. After that, tubes were then centrifuged at 13,000g for 30 seconds and the supernatant was removed. Then, the pellet was washed with 500µl of Buffer QX1 and then was re-suspended by vortexing and centrifuged for 30 seconds at 13000 g. All traces of supernatant were removed with a pipette. Subsequently, pellets were washed twice with 500µl of buffer PE. In each wash, the pellets were re-suspended in the buffer

by vortexing and then centrifuged for 30 seconds then the supernatant was removed. Afterwards, the pellets were air dried for 10 to 15 minutes and then the DNA was eluted by adding 20µl of 10mM Tris-Cl, pH8.5 or sterile water. The beads were then incubated for 5 minutes at room temperature, followed by a 30-second centrifugation. Supernatant containing the eluted DNA was placed in a fresh micro-centrifuge tube. DNA was quantified using a Nanodrop spectrophotometer and were stored at -20°C.

2.2.2.2.3 Assay of DNA Concentration

The concentration of DNA solutions was measured by spectrophotometry using a Nanodrop ND-1000 spectrophotometer. DNA concentration was determined by measuring the absorbance at 260 nm and the extinction coefficient used was an absorbance of 1 for 50µg/ml double stranded DNA.

2.2.2.3 Polymerase Chain Reaction (PCR)

PCR was used to amplify the DNA samples using a touchdown programme according to table of conditions below;

Temperature	Period
Starting (Temp) 94°C	5 min
Touchdown temp 65-50°C	Cycles 35
Denature (Temp) 94°C	30 sec
Annealing (Temp) 58°C	45 sec
Elongation (Temp) 72°C	1.30 min
Storing (Temp) 72°C	10 min

Table 2.6 PCR touchdown Programme

A PCR master mix was prepared by adding 0.5 µM primers (Sigma) and sterile deionised water to 5x FirePol PCR mix (Solis Biodyne). After mixing, 9 µl of the

master mix was transferred to PCR tubes then 1 μ l of each DNA sample was added. Samples were amplified using a G-Storm GS2 thermal cycler. To check the PCR reaction's quality, both positive (previously validated template) and negative (no template) controls were used.

2.2.2.4 PCR PRIMER OPTIMISATION

To optimise primers, PCR reactions were performed with different concentration of forward and reverse primers (0.1 μ M and 0.2 μ M). Additionally, PCR reactions were done with different annealing temperatures (58°C-68 °C). Several DNA concentrations were also used (0.04- 0.2 ng/ μ l).

2.2.2.5 DESIGN OF PCR PRIMERS

PCR primers were designed using the publicly available Primer design tools web page at NCBI (<http://www.ncbi.nlm.nih.gov/tools/primer-blast/>). All primers that were used in this study were ordered from Sigma (Poole, UK).

2.2.2.6 AGAROSE GEL ELECTROPHORESIS

Amplified DNA products were visualized using agarose gel electrophoresis. To analyse SSLPs, MetaPhor® Agarose (Lonza), which is a high resolution grade agarose, was used with 0.5X TBE buffer. Ethidium bromide was added to gels to enable visualisation of DNA by UV transillumination. 5 μ l of each PCR product or 7 μ l of DNA ladder (Hyperladder V, Bionline) was loaded in each well of the gel. Gels were electrophoresed at 200 Volts for 2 hours then the DNA bands visualised using a Geni gel documentation system (Syngene, UK).

2.2.3 GENETIC MAPPING APPLICATIONS

2.2.3.1 MICROSATELLITE (SSLP) MARKERS SCAN

DNA from 25 mutant embryos and 25 wild-type embryos were pooled separately. Mutant pool DNA was placed into the odd-numbered columns of a 96-well plate whereas, even-numbered columns contained wild-type DNA. PCR was performed to genotype 192 microsatellite markers (SSLP) which cover all of the 25 zebrafish linkage groups. PCR products were analysed using a 3.5% agarose gel and samples were loaded using a multichannel pipette.

2.2.3.2 DNA SEQUENCING

The Core Sequencing Facility at the University of Sheffield performed the sequencing procedure, using the Big Dye Terminator v3.1 Cycle Sequencing Kit (Applied Biosciences) following the manufacturer's instructions. Sequence data was analysed and manually modified using Finch TV and Sequencher 5.1 programmes.

2.2.3.4 BAC RESCUE

2.2.3.4.1 BAC DNA Purification

The CHORI-211 BAC library was searched in the candidate interval using ZFIN (<http://zfin.org/>). BACs in the candidate region were obtained from Dr Sarah Baxendale. LB cultures were inoculated and grown in 12% Chloramphenicol (Sigma) LB plates (12 mg/ml). BACs were isolated from cultures using the Qiagen large construct kit as described by the manufacturer.

2.2.3.4.2 Embryo microinjection

BAC DNA (50ng/μl) was mixed with 0.5% phenol red to give a final concentration of 0.05% to enable the sample to be viewed through the injection process. A 1% agarose mold was made in a 10 cm petri dish with grooves to hold the embryos in place during injection. Fine microinjection needles were pulled from glass capillaries using a micropipette puller (Sutter Instrument Co., USA) and the volume of injected liquid calibrated by measuring the droplet size in Halocarbon Oil Series 27 (Sigma) in a small

petri dish over a graticule. Embryos were aligned in rows in the agarose dish using fine forceps and injected at the 1 to 2 cells stage directly into the fertilised cell. Embryos were then placed in E3 medium and incubated at 28°C. Un-injected embryos were kept as controls. Embryos were checked every day for survival rate. Subsequently, embryos were fixed at 4 d.p.f. and analysed for *mbp* expression using *in situ* hybridization.

2.2.4 RNA-BASED METHODS

2.2.4.1 TOTAL RNA EXTRACTION FROM ZEBRAFISH EMBRYOS

Pools of 20 mutant embryos and 20 siblings were collected and washed several times with DEPC/H₂O to remove residual medium and egg debris. Then, 250 µl of Trizol (Invitrogen) was added and the samples homogenized by passing through a syringe needle 2 to 3 times. After that, samples were incubated at RT for 5 min for cell lysis. Chloroform (50 µl) was added to each tube and shaken vigorously for 15 s then incubated for 3 min at RT. Tubes were centrifuged for 15 min at 4°C at 13000g then the aqueous, upper phase was transferred to a fresh tube with a filter tip. 83 µl of isopropanol was added to the supernatant, mixed gently by pipetting up and down then incubated for 10 min at RT before being centrifuged at 13000g for 15 min at 4°C. Then, the supernatant was carefully removed and the pellet washed with 250 µl of 75% ethanol (in DEPC/H₂O). This was followed by centrifugation for 5 min at 4°C at 13000g. After that, the ethanol was removed then the pellet was air-dried at RT for 10 min. Finally, the RNA was resuspended in 50-100 µl DEPC/H₂O, and then total RNA was stored at -80°C.

2.2.4.2 cDNA SYNTHESIS

To synthesise cDNA the SuperScript® III First-Strand Synthesis System (Invitrogen) was used. Total RNA was converted to cDNA by mixing 2 µg of total RNA, 1 µl of 50 mM oligo(dT)₂₀ primer, 1 µl of 10 mM dNTPs and DEPC/H₂O to a final volume of 14

μ l. This was incubated for 5 min at 65C and next placed on ice for 1 min. The following components were then added together: 2 μ l of 10X RT buffer, 4 μ l of 25 mM MgCl₂, 2 μ l of 0.1 M DTT, 1 μ l of RNaseOUT™ (40 U/ μ l) and 1 μ l of SuperScript® III RT (200 U/ μ l). This mixture was then added to the cDNA synthesis tube and mixed gently. Next, the reaction was incubated for 50 min at 50C then the reaction was terminated at 85C for 5 min followed by chilling on ice. Tubes were then centrifuged and 1 μ l of RNase H was added and incubated for a further 20 min at 37C. Finally, the cDNA was stored at -20C.

2.2.4.3 REVERSE TRANSCRIPTION RT-PCR

To amplify products from cDNA, RT- PCR was carried out using the same reaction and program described in section 2.2.2.3. Instead of adding 1 μ l of genomic DNA, 1 μ l of cDNA was added to the mixture.

CHAPTER III: PHENOTYPIC CHARACTERSTION OF FB148.5

3 INTRODUCTION

The Ingham laboratory in the Centre for Developmental and Biomedical Genetics at Sheffield University performed a large-scale zebrafish mutagenesis phenotypic screen using the chemical mutagen N-ethyl-N-nitrosourea (ENU) (Wolff, Roy et al. 2004). From this screen, the FB 148.5 mutant was isolated and previous work by the Grierson laboratory in SITraN has identified axonal and myelination defects in the CNS and PNS of FB148.5 mutants. FB148.5 mutant embryos show a morphological phenotype from around 48 h.p.f. At 2 d.p.f., mutants can be clearly distinguished from their wild type siblings, as mutants display a number of morphological abnormalities including small eyes, cardiac oedema and a mis-shapen head, as well as later phenotypes such as a curved body axis and abnormal swim bladder. The severity of the phenotype increases from 2-5 d.p.f. leading to embryonic lethality of FB148.5 mutants at around 5-7 d.p.f.. Interestingly, these phenotypes are very similar to those described in *disc1* morpholino mutants (Figs. 3.1 and 3.2). Preliminary characterization of FB148.5 mutants showed very similar oligodendrocyte specification defects to those in *disc1* morphants (Wood, Bonath et al. 2009). Therefore, we hypothesized that the gene mutated in FB148.5 may be functionally related to *disc1* and therefore be of relevance to psychiatric disease mechanisms.

As mentioned previously, the preliminary phenotypic characterisation that has been performed on FB148.5 identified a number of neurological defects. However, further detailed studies are needed to characterise the CNS phenotypes more fully. Therefore, in this chapter, further phenotypic studies have been done and these revealed that the

FB148.5 gene is essential for different stages of nervous system development, including specification of hindbrain oligodendrocytes, Schwann cell development, neurogenesis, and motor axon outgrowth,.



Figure 3.1: Morphology of FB148.5 mutants.

Lateral view of live FB148.5 mutant embryo at 5 dpf. The FB148.5 phenotype is characterized by a curved body axis, small eyes, cardiac oedema (**black arrowhead**), mis-shaped head, abnormal swim bladder and abnormal lower jaw (**red arrow**). (n= 45, technical repeat x3).

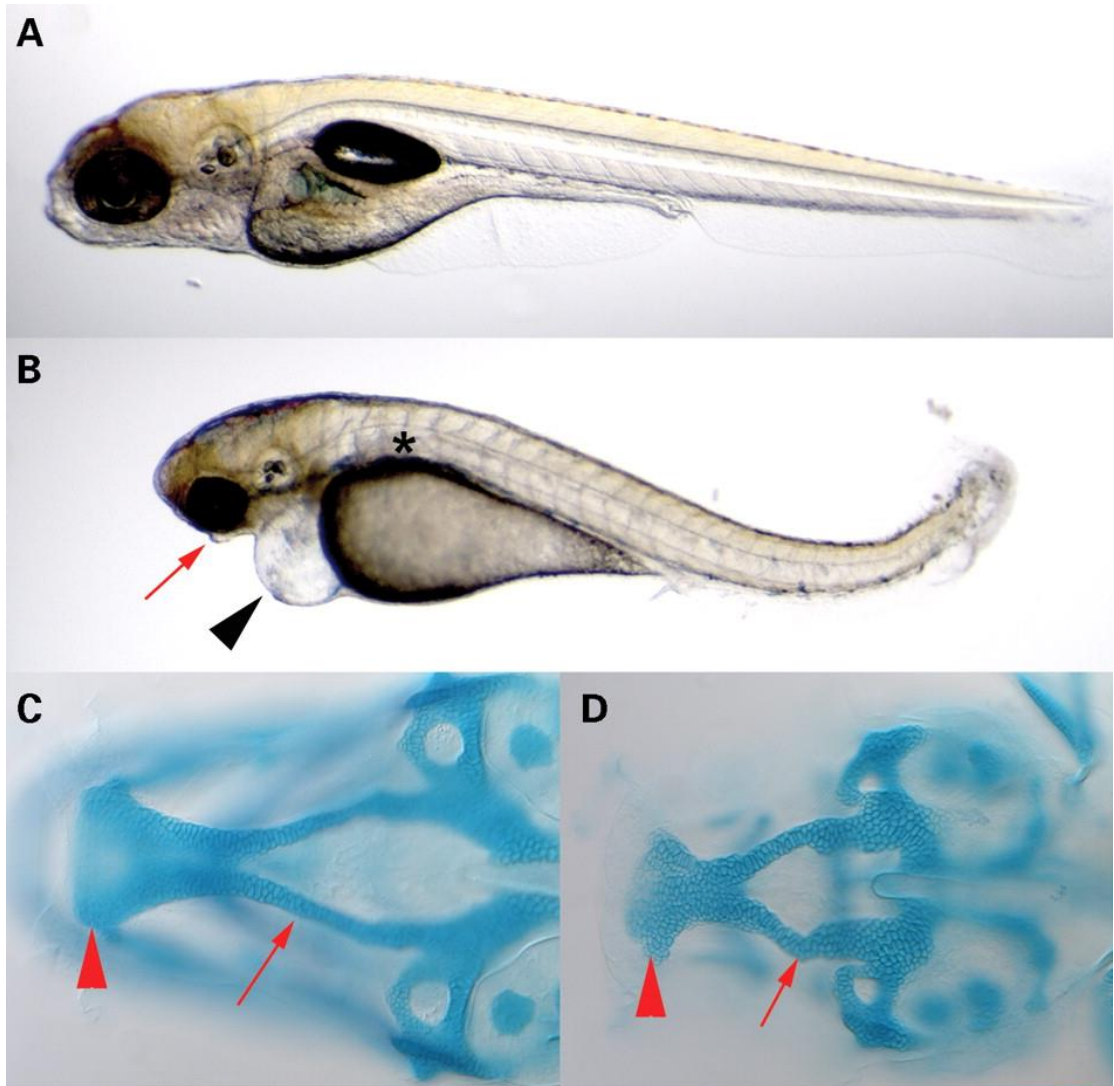


Figure 3.2 Morphological and craniofacial defects induced by *disc1* knock-down
(A) Lateral image of live 5 d.p.f. wild type embryo control. **(B)** Live 5 d.p.f. *disc1* morphant shows mis-shapen eyes, mis-shapen head, pericardial oedema, (**black arrowhead**), abnormal lower jaw (**red arrow**), upward curving trunk and tail, and failure of swim bladder to inflate (**asterisk**). Ventral views of 5 d.p.f. control embryo **(C)** which has normal cartilage elements and *disc1* morphant **(D)** showing that the trabeculae (**red arrow**) and ethmoid plate (**red arrowhead**) are smaller but appropriately shaped. **Images were obtained from Jonathan D. Wood et al. Hum. Mol. Genet. 2009;18:391-404.**

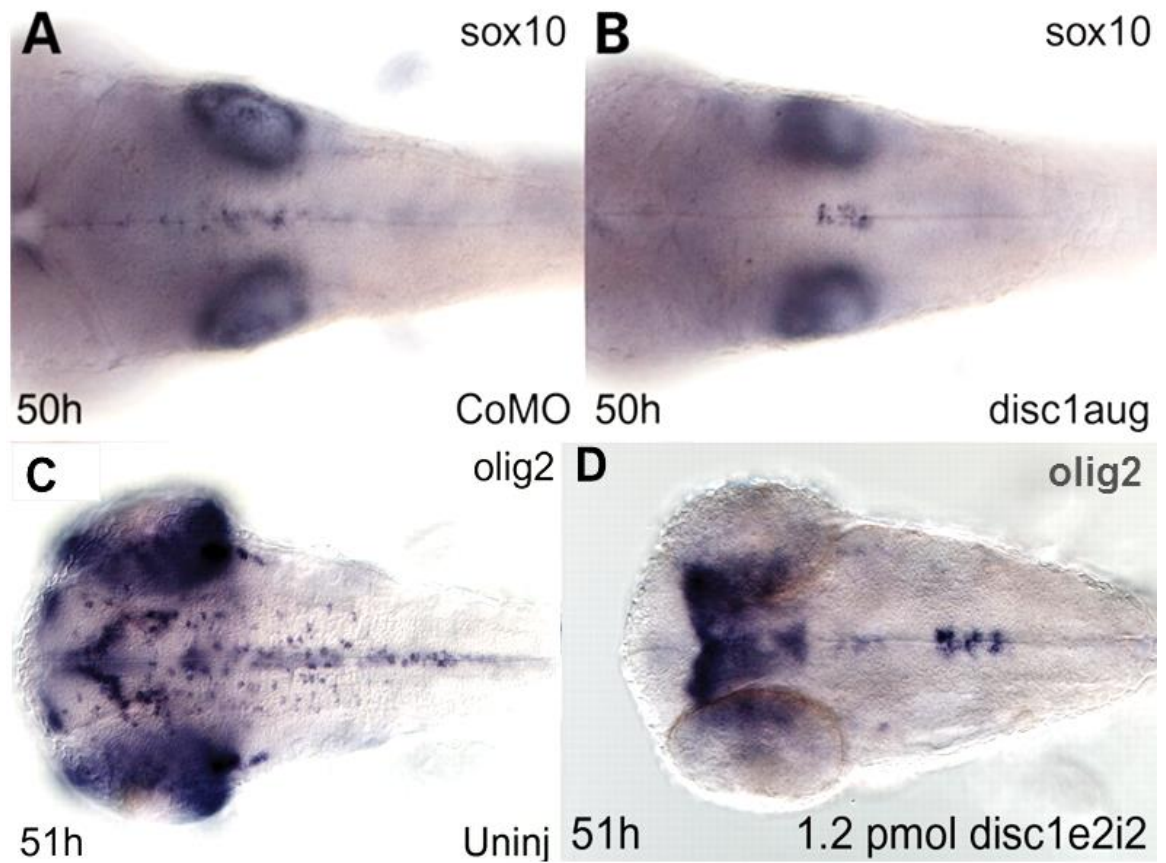


Figure 3.3 *disc1* is required for expansion of the populations of *olig2* and *sox10*-positive cells in the hindbrain.

(A) Normal *sox10* expression in the hindbrain midline in control embryos. (B) *disc1aug* morpholino embryos at 50 h.p.f. show reduced *sox10* expression in the hindbrain. (C) Image of 51 h.p.f. un-injected embryo showing that the expression of *olig2* is detected along the entire length of the hindbrain midline of un-injected embryos. (D) Expression of *olig2* remained restricted to the midline of rhombomeres 5 and 6 in embryos injected with a *disc1* splice site morpholino. Images were obtained from Jonathan D. Wood et al. *Hum. Mol. Genet.* 2009;18:391-404.

3.1 FB148.5 MUTANTS SHOW DEFECTS IN OLIGODENDROCYTE SPECIFICATION IN THE HINDBRAIN

Previous work on *disc1* morphant zebrafish found that *disc1* is required for oligodendrocyte production and development through regulating the specification of *olig2*-expressing precursor cells in the hindbrain (Fig 3.3 C and D) (Wood, Bonath et al. 2009). Since the neurological and morphological abnormalities that are seen in FB148.5 mutants are very similar to those found in *disc1* morphants (Fig 3.2 & 3.3), we hypothesized that these two genes may act together in common developmental pathways.

Specifically, it was found that *disc1* is expressed in a region that also expresses *olig2* in the hindbrain in a region that is populated with midline ventricular zone progenitors (Wood, Bonath et al. 2009). Oligodendrocytes arise from *olig2*-expressing OPCs and expression of *Sox10* regulates the differentiation of OPCs in mice (Stolt, Rehberg et al. 2002). To determine whether FB148.5 is necessary for the production and specification of oligodendrocytes, the expression of the OPC markers *olig2* and *sox10*, as well as the expression of markers for terminally differentiated oligodendrocytes, *plp1b* and *mbp*, was analysed in FB148.5 mutants and sibling embryos.

We found that expression of *sox10* and *olig2*, markers for the early production of OPCs, was absent or greatly reduced and restricted to hindbrain rhombomeres 5 and 6 in mutant embryos (Fig 3.4 B and D), compared with the normal expression pattern in sibling embryos (Fig. 3.4 A and C). At 5 d.p.f., expression of myelin basic protein (*mbp*) and proteolipid protein 1b (*plp1b*), markers for oligodendrocyte differentiation, was distributed throughout the hindbrain in wide-type siblings (Fig.3.5 A and C), while the expression of these markers in mutants was almost completely eliminated (Fig.3.5 B

and D). These results demonstrate that FB148.5 mutants show severe defects in oligodendrocyte lineage development in the zebrafish hindbrain caused by defects in the specification of oligodendrocyte progenitors.

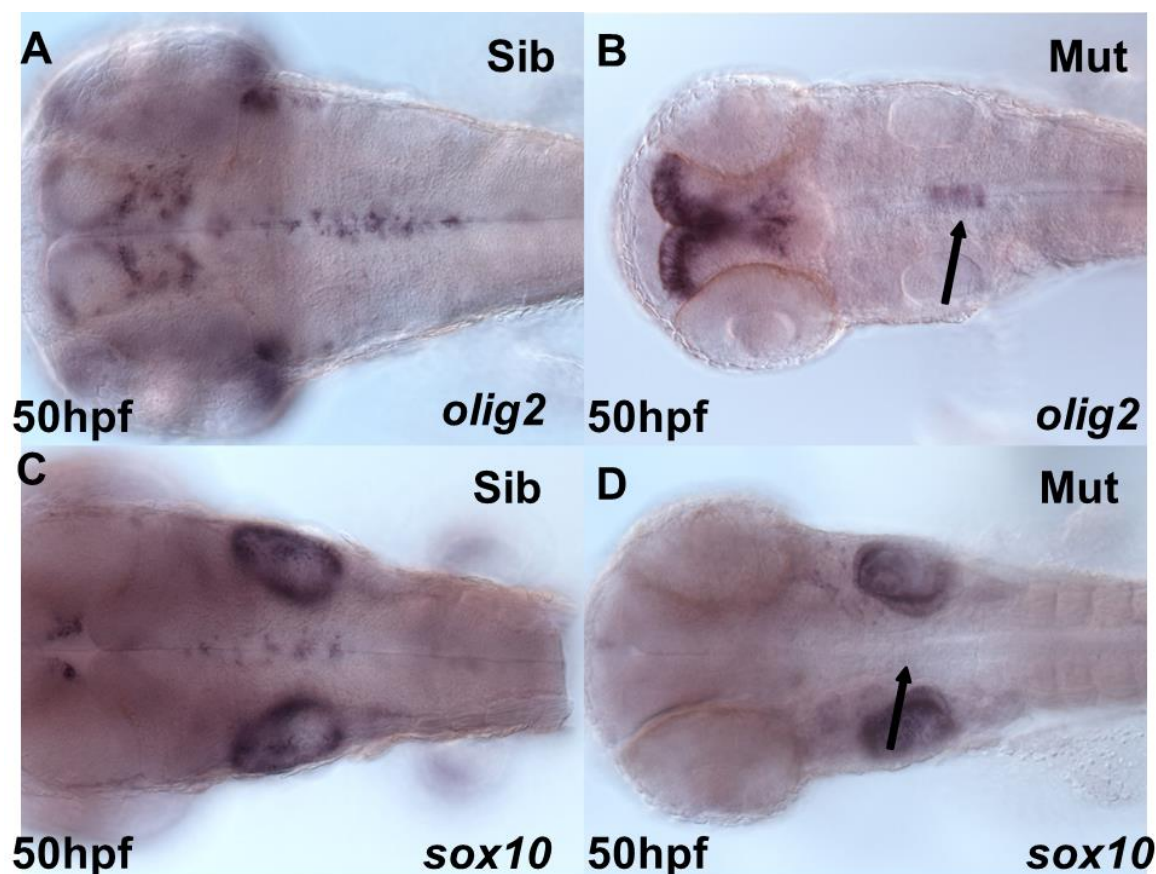


Figure 3.4 *Olig2* and *sox10* expression in FB148.5 mutants and controls.

(A) Whole mount *in situ* hybridisation for *olig2* expression at 50 h.p.f. in control embryos shows strong expression throughout the midline of the hindbrain. (n=60, t =2, b =3). (B) The expression of *olig2* in FB148.5 mutants is significantly reduced in the midline of the hindbrain (n=13, t =2, b =3). (C) Intense *sox10* expression in the hindbrain midline in control embryos (n=55, t =2, b =3). (D) Mutant embryos at 50 h.p.f. show a complete loss of *sox10* expression in the hindbrain (n=11, t=2, b=3). The black arrows indicate the hindbrain rhombomeres 5 and 6 (B, D). Magnification x20 (all panels). Note; no negative sense control probe has been used. This data was interpreted according to the known expression patterns of *olig2* and *sox10* obtained from ZFIN.

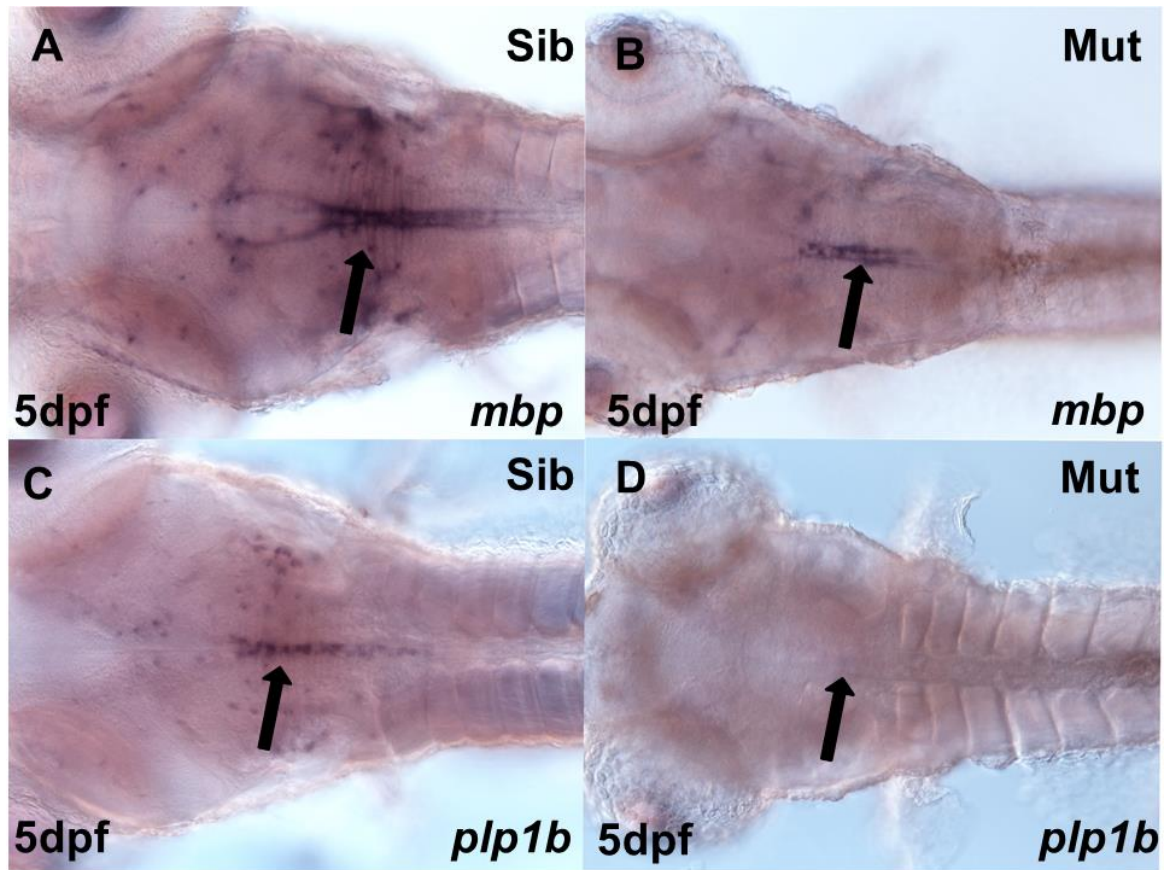


Figure 3.5 FB148.5 mutants show defects in oligodendrocyte development in the hindbrain.

(A) Whole mount *in situ* hybridisation for *mbp* expression at 5 dpf in control embryos shows strong expression throughout the hindbrain (n=71, t=3, b=3). (B) The expression of *mbp* in FB148.5 mutants is restricted to the hindbrain midline (n=19, t=3, b=3). (C) Robust *plp1b* expression in the hindbrain in control embryos (n=111, t=3, b=3). (D) Mutant embryos at 5 dpf show a total absence of *plp1b* expression in the hindbrain (n=25, t=3, b=3). The black arrows indicate the hindbrain midline area. Magnification x20 (all panels). Note; no sense probe negative control has been used. This data was interpreted according to the known expression patterns obtained from ZFIN.

3.2 FB148.5 ZEBRAFISH SHOW ABNORMAL DEVELOPMENT OF LOWER JAW CARTILAGES

Alcian blue staining demonstrated that most of the lower jaw cartilage elements in FB148.5 embryos were missing. The Meckel's and ceratohyal cartilages were completely absent in the mutants compared to siblings (Fig. 3.6 C and D). In addition, the basihyal, ceratobranchial and basibranchial cartilages were also lacking in FB148.5 mutants. FB148.5 mutants show shorter trabeculae and a small ethmoid plate with relatively normal shape (Fig. 3.6 A and B). We conclude that the correct development of many cartilage elements requires FB148.5 function. These defects are also very similar to those reported to be caused by *disc1* knock-down (Fig 3.2 C and D), (Drerup, Wiora et al. 2009; Wood, Bonath et al. 2009).

3.3 FB148.5 MUTATION MAY IMPAIRS DISC1 FUNCTION

In order to test, whether the FB148.5 mutation may affect *disc1* function, we analyzed *disc1* expression in FB148.5 embryos. We found that *disc1* was strongly expressed in the cranial neural crest-derived cartilages of the lower jaw in sibling embryos at 2 d.p.f. (Fig. 3.7 A), while in mutant embryos the expression was present but clearly decreased in intensity (Fig. 3.7 B). Additionally, expression of *disc1* in control embryos was prominent in the hindbrain, while the expression in this area was reduced in mutant embryos (Fig. 3.8 A and B). These findings suggested that the mutated gene in FB148.5 is required for *disc1* function or that *disc1* functions in cell types regulated by FB148.5 and subsequently they might act in the same or similar pathways regulating development.

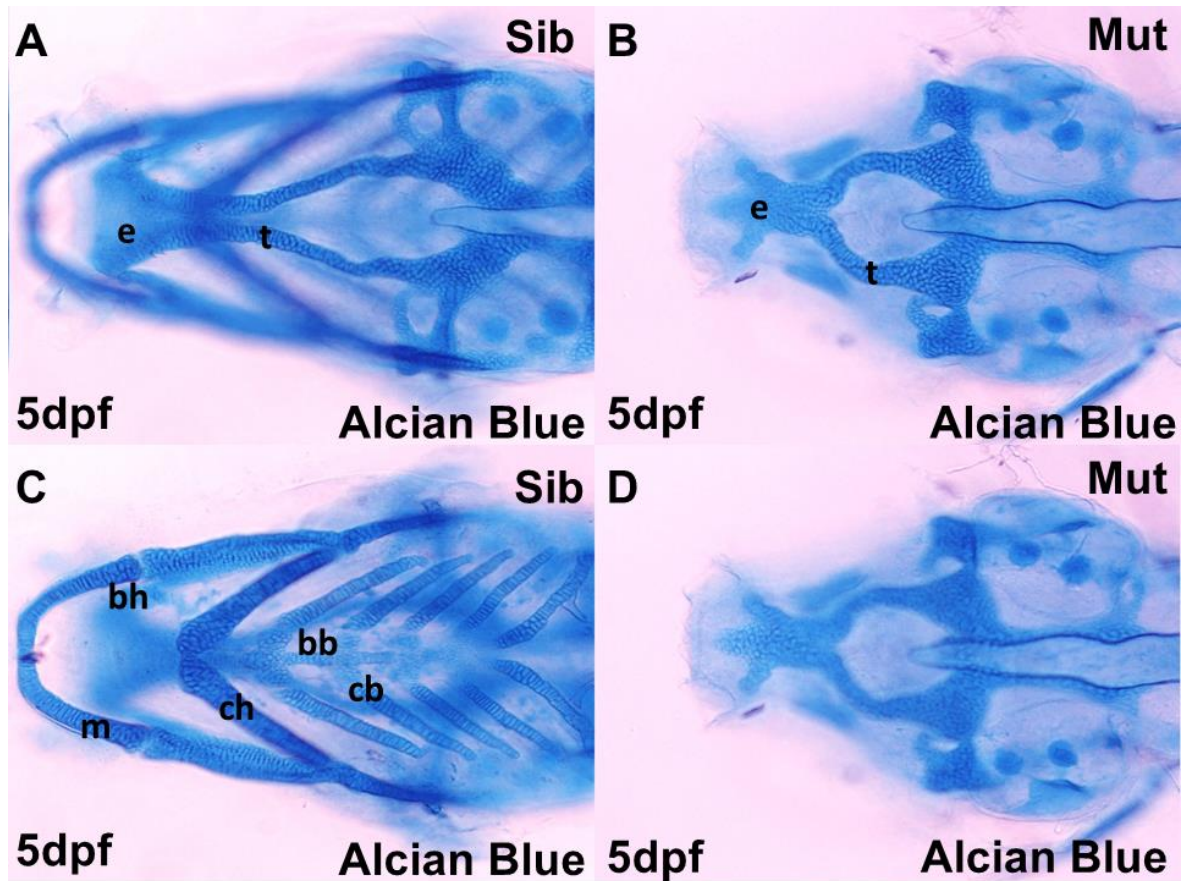


Figure 3.6 Cartilage defects in FB148.5 mutants.

Ventral views of Alcian blue stained embryos at 5 dpf. **(A)** FB148.5 sibling shows the ethmoid plate (e) and trabeculae (t) (n=35, t=1, b=3). **(B)** FB148.5 mutants failed to form the proper structure of the ethmoid plate (e) and trabeculae (t) (n=6, t=1, b=3). **(C)** FB148.5 sibling showing Meckel's cartilage (m), basihyal (bh), ceratohyal (ch), basibranchials (bb), and ceratobranchials (cb). **(D)** FB148.5 mutants lack all these structures. Magnification x20 all panels.

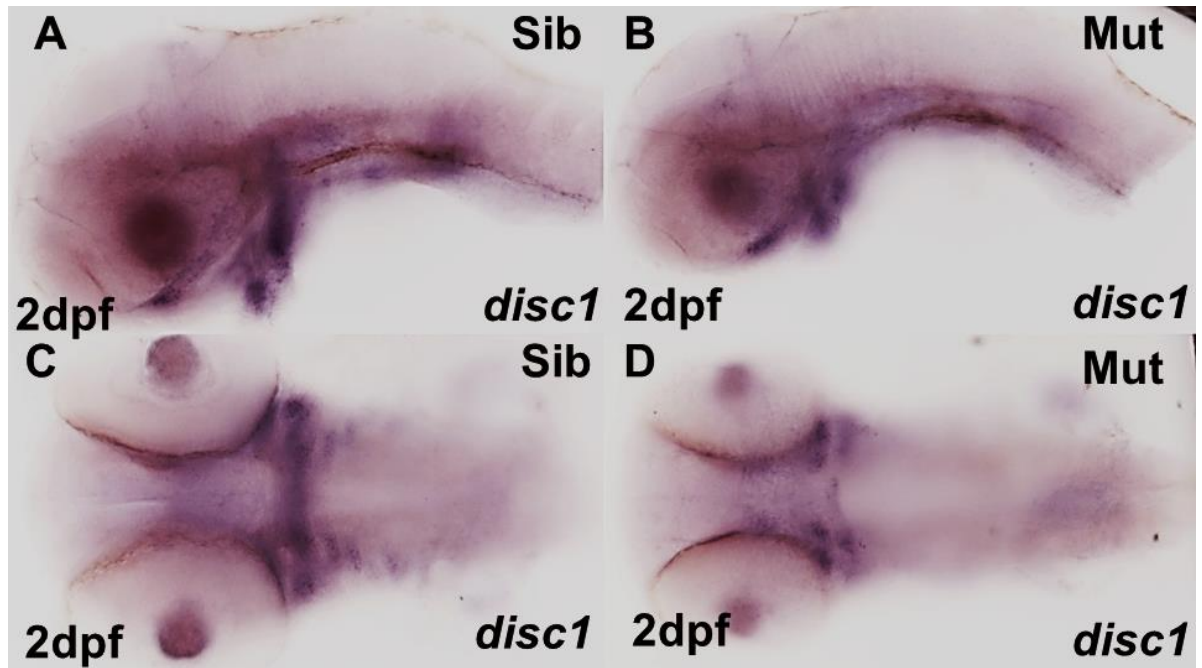


Figure 3.7 FB148.5 mutation affects *disc1* expression.

Images show whole mount *in situ* hybridisation for *disc1* expression in FB148.5 (B, D) and sibling (A, C) embryos at 2 d.p.f. (A,B) Lateral views of the head showing strong *disc1* expression in lower jaw cartilages in Sibling embryo (A) (n=27, t=1, b=3). compared to mutant embryo (B) (n=5, t=1, b=3). (C, D) Ventral view showing strong *disc1* expression in lower jaw cartilages in control embryo (C) compared to FB148.5 embryo (D). Magnification x10 all panels Note; no sense probe negative control has been used, however this data was interpreted according to the known expression pattern obtained from ZFIN.

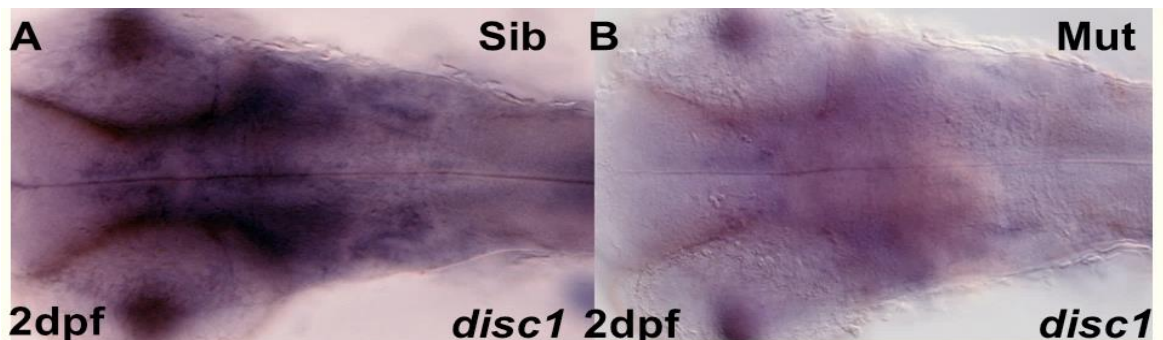


Figure 3.8 FB148.5 mutation affects *disc1* expression in hindbrain.

(A) Dorsal view of 2 d.p.f. embryo (n=27, t=1, b=3) showing *disc1* expression in the hindbrain compared to mutant (B) embryo (n=5, t=1, b=3). Magnification x10 all panels Note; no negative control has been used, however this data was interpreted according to the known expression pattern obtained from ZFIN.

3.4 *FB148.5* MUTANTS SHOW NEUROGENESIS DEFECTS

Neurogenesis is defined as the process through which undifferentiated neural progenitors become mature functional neurones. This process consists of the induction of neural progenitor cells and then their proliferation and asymmetric division to form committed precursors. Subsequently, they differentiate into mature neurones and each of these steps is regulated in a spatially and temporally controlled way (Schmidt, Strähle et al. 2013).

FB148.5 mutants have a small brain so in order to investigate whether the mutated gene in *FB148.5* affects neurogenesis, the expression patterns of the pro-neural genes *ash1b* (Allende and Weinberg 1994) and *ngn1* (Blader, Fischer et al. 1997) were analyzed. At 26 h.p.f. it was not possible to discern mutant and sibling embryos on the basis of the expression of these genes. However, *FB148.5* mutant embryos show a significant reduction in both *ash1b* and *ngn1* expression at 31 h.p.f. compared to their siblings (Fig. 3.9B and D, 3.10B). Both *ash1b* and *ngn1* transcripts are seen in clusters of cells either side of the midline in each of the rhombomeres in siblings at 31 h.p.f. (Fig. 3.9A and 3.10A). These findings indicate that the *FB148.5* gene product is necessary for neurogenesis in the zebrafish brain which may support the observed brain malformation phenotype. Expression of *sox2*, a marker of neural stem cells, was found to be only slightly reduced in mutants compared to siblings. This suggests that the *FB148.5* mutation does not dramatically affect the production of neural stem cells (Fig. 3.11A and B), but affects later stages of neurogenesis instead.

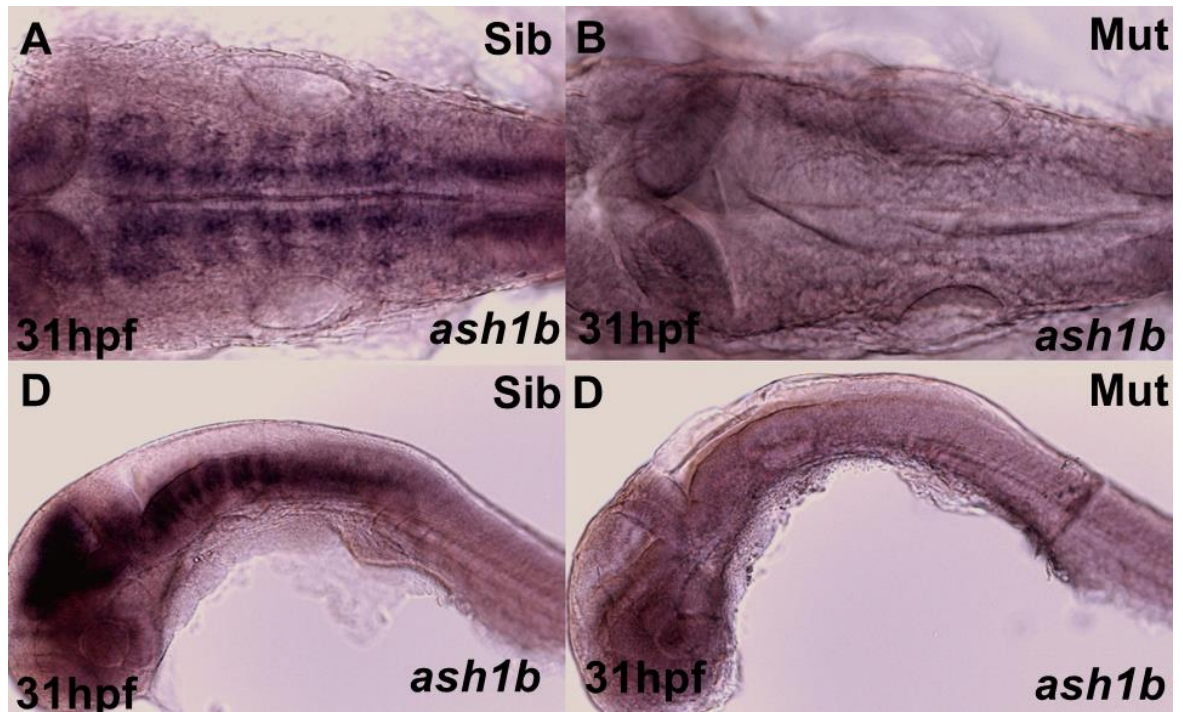


Figure 3.9 Neurogenesis defects in FB148.5 mutants shown by whole mount in situ hybridisation for *ash1b* expression.

(A) Dorsal view of *ash1b* expression at 31 h.p.f. in a sibling embryo which shows strong expression in the hindbrain (n=127, t=4, b=3). (B) Mutant FB148.5 embryo showing dramatic loss of *ash1b* expression in the hindbrain (n=29, t=4, b=3). (C) Lateral view of control embryo showing robust *ash1b* expression in the hindbrain. (D) Expression of *ash1b* in mutant FB148.5 showing complete loss of expression throughout the midbrain and hindbrain. Magnification x20 in (A and B) and x10 in (C and D). Note; no negative sense probe control has been used, however this data was interpreted according to the known expression pattern obtained from ZFIN.

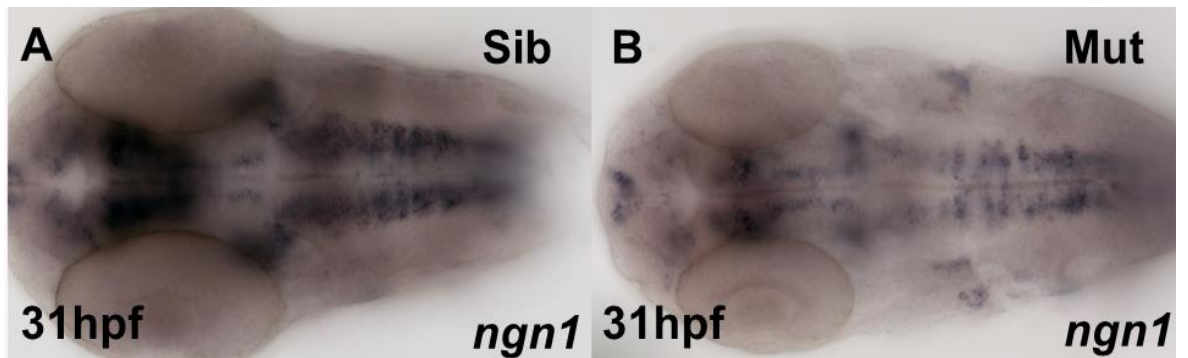


Figure 3.10 Neurogenesis defects in FB148.5 mutants shown by whole mount *in situ* hybridisation for *ngn1* expression.

(A) Dorsal view of *ngn1* expression at 31 h.p.f. in sibling embryo which shows intense staining for *ngn1* expression in the hindbrain (n=43, t=2, b=3). (B) Mutant FB148.5 embryo shows a diminished expression of *ngn1* in the hindbrain (n=9, t=2, b=3). Magnification x20 in (A and B) Note; no negative sense probe control has been used, however this data was interpreted according to the known expression pattern obtained from ZFIN.

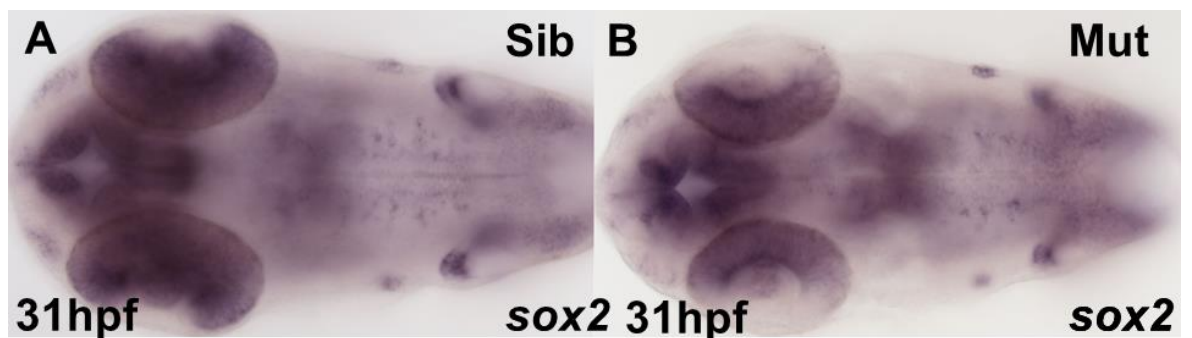


Figure 3.11: Normal production of neural stem cells in FB148.5 mutants shown by whole mount *in situ* hybridisation for *sox2* expression.

(A) Dorsal view of *sox2* expression at 31 h.p.f. in sibling embryo which shows normal pattern of expression in the hindbrain (n=95, t=3, b=3). (B) Mutant FB148.5 embryo showing a very similar pattern of *sox2* expression in the hindbrain (n=21, t=3, b=3). Magnification x20 in (A and B). Note; no negative sense control probe has been used; however this data was interpreted according to the known expression pattern obtained from ZFIN.

3.5 FB148.5 IS NOT REQUIRED FOR THE SPECIFICATION OF SEROTONERGIC NEURONS

It has been reported that *monorail/Foxa2*, which encodes a winged-helix transcription factor, affects specification of both hindbrain OPCs and Raphe neurons. Moreover, *monorail/Foxa2* function has been related to sonic hedgehog (Shh) signalling and causes increased expression of Hh related genes such as *tiggywinkle hedgehog (twhh)* and *sonic hedgehog (shh)* (Norton, Mangoli et al. 2005). Thus, defects in OPC specification may also be associated with Raphe neuron abnormalities. To investigate the specification of serotonergic Raphe nuclei in FB148.5 mutant embryos, expression of tryptophan hydroxylase 2 (*tph2*), which is an enzyme involved in the biosynthesis of serotonin, was examined. However, no apparent difference in the number or location of serotonergic cells in FB148.5 mutants was observed (Fig. 3.12). This result suggests that the FB148.5 mutation has little effect on serotonergic neuron specification. Also, this suggests that the Raphe neurones are not derived from *olig2*-positive precursors since we have found significant loss of *olig2*-positive neuroepithelial precursors and OPCs, but no obvious loss of Raphe neurones, in FB148.5 mutants.

3.6 FB148.5 MUTANTS SHOW ABNORMAL AXONAL DEVELOPMENT

Previous work on FB148.5 embryos has reported abnormal axonal development in the brain using anti-acetylated tubulin staining at 52 h.p.f. (Fan Yang & Andy Grierson, unpublished). In order to further characterise axonal defects in FB148.5 mutants,

embryos were analysed by immunostaining with monoclonal antibody znp-1. Then, quantitative measurements of spinal motor axon length were performed to determine the mean motor axon lengths in FB148.5 mutant and sibling embryos. FB148.5 mutants showed abnormal axons which are shorter and more branched compared to axons in siblings (Fig 3.13). The quantitative analysis found a significant reduction in FB148.5 axon length (mean 75 μ m and SD 3.2) compared to siblings (mean 96 μ m and SD 5.5) (Fig. 3.14). These results suggest that the gene mutated in FB148.5 is essential for normal motor axon development and outgrowth.

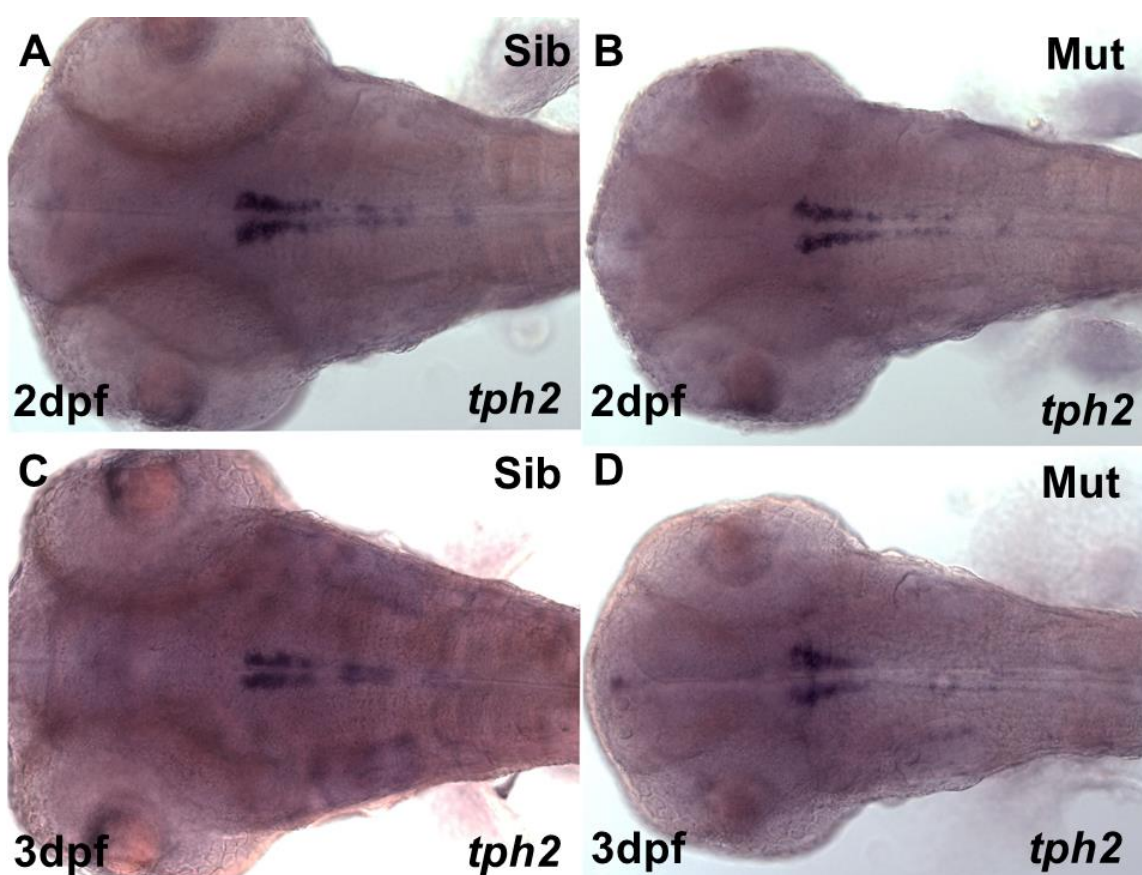


Figure 3.12: FB148.5 mutants showed relatively normal specification of serotonergic neurons.

Whole mount *in situ* hybridisation for *tph2* was performed. (A) Dorsal views of *tph2* expression at 2 d.p.f. in control embryos shows strong expression in the hindbrain (n=88, t=3, b=3). (B) The expression of *tph2* in FB148.5 mutants displayed no obvious change in the hindbrain (n=19, t=3, b=3). (C) At 3 (d.p.f.), strong *tph2* expression in the hindbrain in control embryos (n=106, t=3, b=3). (D) Mutant embryos at 3 (d.p.f.) may show a slight loss of *tph2* expression in the posterior part of the hindbrain (n=24, t=3, b=3). Magnification x20 (all panels). Note; no negative sense control probe has been

used, however this data was interpreted according to the known expression pattern obtained from ZFIN.

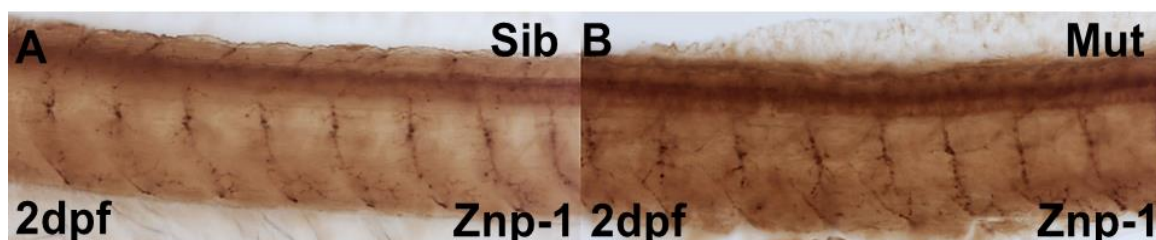


Figure 3.13 FB148.5 mutants showed abnormal motor axon outgrowth by *znp-1* immunostaining.

(A) At 52 h.p.f. sibling embryo shows normal motor axon outgrowth (n=74, t=3, b=3). (B) Mutant FB148.5 embryo stained with *znp-1* demonstrates shorter and prematurely branched motor axons (n=18, t=3, b=3). Magnification x10 in (A and B).



Figure 3.14: Significant reduction in FB148.5 motor axon length.

FB148.5 mutants showed a significant reduction in motor axon length from 96 to 75 µm. Statistical significance was determined using an un-paired t-test, ****P<0.0001. (n=18 WT and 18 mutant, axons, n=144 t=3, b=3). 97.94 ± 1.200 , n=18, 74.50 ± 0.7421 , n=18.

3.7 *FB148.5* MAY BE RELATED TO SONIC HEDGEHOG

SIGNALING

Previously, it has been reported that sonic hedgehog (shh) is essential for control of *olig2* expression and specification of motor neurons and oligodendrocyte progenitors in the zebrafish hindbrain (Esain et al, Development 2010). To determine whether shh signaling is affected in *FB148.5*, we analysed the expression of shh regulated genes in *FB148.5* mutant and sibling embryos. We focused on Patched1 (*ptc1*) and GLI family zinc-finger transcription factor 1 (*gli1*), which are regulators of shh signalling and are well-characterised transcriptional targets of the shh pathway (Wolff, Roy et al. 2004; Koudijs, den Broeder et al. 2008). We found that at 52 h.p.f., *ptc1* expression in mutant embryos was significantly increased in the forebrain, midline of the hindbrain, mid-diencephalon boundary, midbrain-hindbrain boundary and in the pharyngeal endoderm (Fig. 3.15B). Similarly, *gli1* expression was prominently increased in the regions showing mis-expression of *ptc1* in *FB148.5* mutants (Fig.3.16B). Taking these results together, we conclude that the *FB148.5* mutation leads to aberrant activation of the shh signaling pathway in several regions, especially in the CNS.

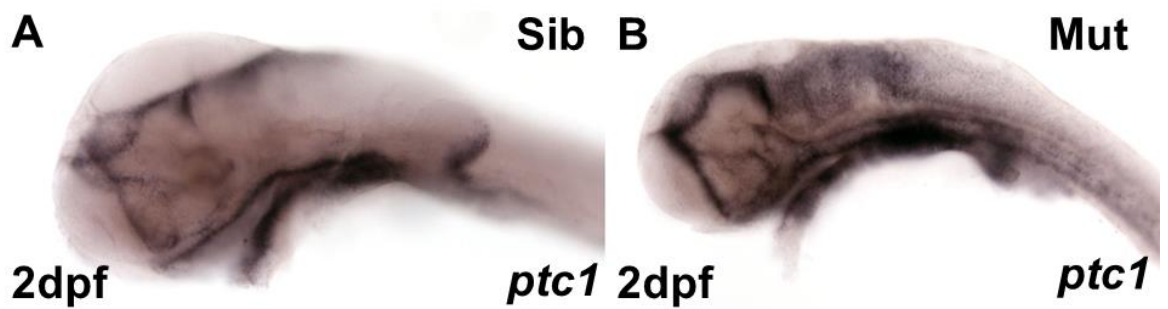


Figure 3.15: FB148.5 mutants showed increased *ptc1* expression.

(A) Wild-type embryo showing normal expression of *ptc1* by whole mount *in situ* hybridisation (n=84, t=1, b=3). (B) *ptc1* expression is regionally increased in FB148.5 mutant embryos (n=21, t=1, b=3). Magnification x10 in (A and B). Note; no negative sense control probe has been used, however this data was interpreted according to the known expression pattern obtained from ZFIN.

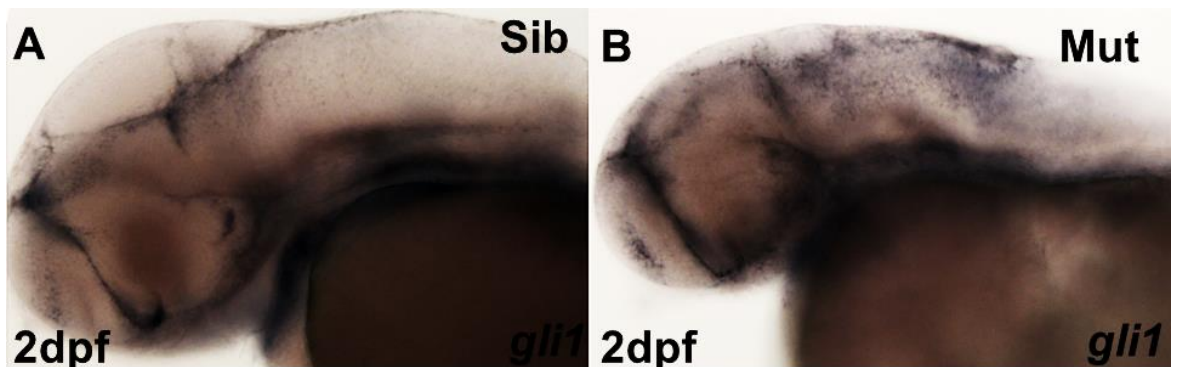


Figure 3.16: FB148.5 mutants show abnormal *gli1* expression by whole mount *in situ* hybridization.

mRNA ISH for *gli1* at 2 d.p.f. showing prominent expression in the brain, demonstrates that *gli1* expression is increased in mutants (B) (n=32, t=1, b=3) compared to sibling embryos (A) (n=62, t=1, b=3). Magnification x10 in (A and B). Note; no negative sense control probe has been used, however this data was interpreted according to the known expression pattern obtained from ZFIN.

3.8 FB148.5 MUTANTS SHOW DEFECTS IN SCHWANN CELL DEVELOPMENT

Given that FB148.5 mutants display CNS myelination defects, we assessed whether PNS myelination was also affected in these mutants. We found that the expression of *mbp* at 4 d.p.f. in FB148.5 mutants was decreased, with gaps in the staining of the posterior lateral line nerve (PLLn) apparent (Fig. 3.17B), compared with *mbp* expression in wild-type siblings, where it was expressed strongly along the full length of the PLLn (Fig. 3.17A). In order to determine whether the *mbp* expression defects that were identified were due to SC development defects or secondary to axonal outgrowth defects, the lateral line nerve was analysed by anti-acetylated tubulin antibody staining (data not shown). It was found that in both the FB148.5 mutant and sibling embryos the PLLn axons extended the full length of the trunk, suggesting that these defects are as a result of defects in Schwann cell development. Moreover, to verify this finding, we analysed *sox10* expression at 3 d.p.f., which marks neural crest derived cells, including Schwann cell precursors along the PLLn. We found that *sox10* expression along the PLLn was also disrupted in FB148.5 mutants compared with siblings at 3 d.p.f. (Figure 3.17C, D). This result suggests that the mutated gene in FB148.5 has functions that are essential for development of Schwann cells in the peripheral nervous system and that the loss of peripheral *mbp* expression is likely due to defects in the development of Schwann cells.

To further confirm the effect of the FB148.5 mutation on PNS myelination, expression of *krox20*, which is expressed in Schwann cells committed to myelination (Topilko, Schneider-Maunoury et al. 1994) was also examined. Analysis of *krox20* expression also showed a reduction in staining along the PLLn in FB148.5 mutants (Fig. 3.17F) compared with sibling controls (Fig. 3.17E). This result is consistent with the findings

of the loss of *mbp* and *sox10* expression which suggests that FB148.5 function is necessary for the normal development of SCs.

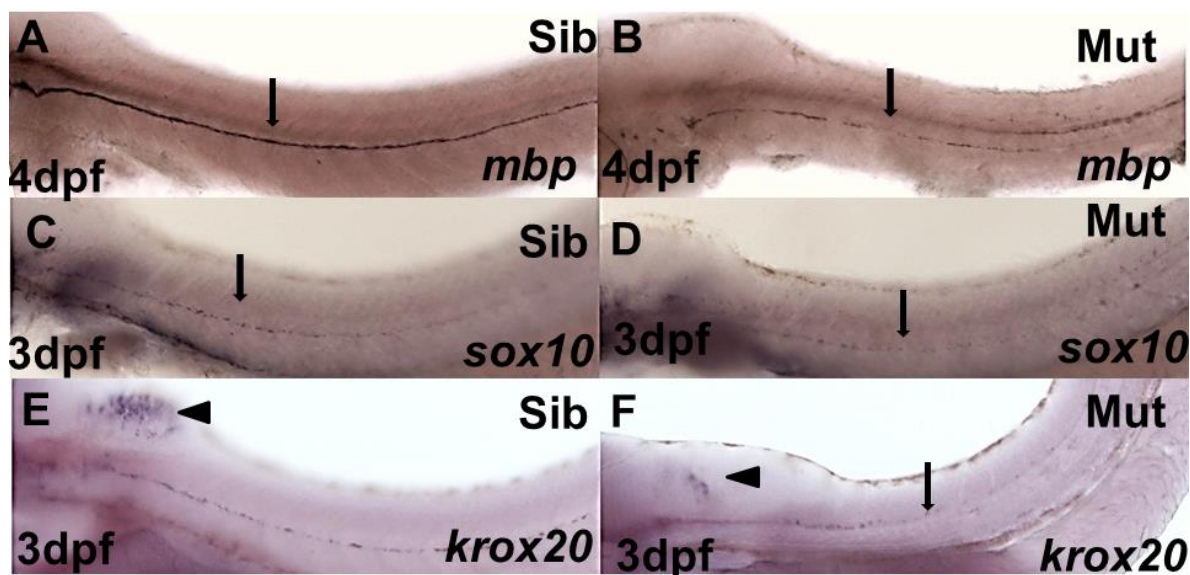


Figure 3.17: FB148.5 is essential for Schwann cell development.

ISH of (A) Sibling (n=54, t=2, b=3) and (B) FB148.5 mutant (n=11, t=1, b=3) zebrafish larvae at 4 d.p.f., showing *mbp* mRNA expression in PLLn Schwann cells (arrows). (C) WT zebrafish embryo at 3 d.p.f., showing *sox10* expression in PLLn; Schwann cell precursors indicated (arrow) (n=68, t=2, b=3). (D) FB14.5 mutant larva at 3 d.p.f. showing weak *sox10* expression in PLLn Schwann cell precursors (arrow) (n=15, t=2, b=3). (E) Sibling larvae at 3 d.p.f., show normal *krox20* mRNA expression in PLLn Schwann cell precursors (arrow) and in the brain (arrowhead) (n=79, t=2, b=3). (F) *krox20* expression along the PLLn in FB148.5 mutant larvae is diminished (arrow), with a loss of expression also seen in the brain (arrowhead) (n=18, t=2, b=3). Magnification x10 in all panels. Note; no negative control sense probes were used, however this data was interpreted according to the known expression patterns obtained from ZFIN.

3.9 DISCUSSION

The *DISC1* gene has been considered one of the most important candidate genes for SZ since it was shown to be disrupted by a balanced t (1; 11), (q42.1; q14.3) chromosomal translocation associated with psychiatric disorders in a large Scottish family (Millar, Wilson-Annan et al. 2000). More recently, *DISC1* mutation has been linked with agenesis of the corpus callosum (AgCC), suggesting that *DISC1* is essential for development of the corpus callosum (Osburn, Li et al. 2011). Oligodendrocytes are the brain cells responsible for myelin sheath formation in the central nervous system (CNS) and they are derived during development from oligodendrocyte precursor cells. A number of studies have suggested that DISC1 has important functions in oligodendrocytes. Analysis of zebrafish *disc1* morphants found that *disc1* is crucial for oligodendrocyte production and development through controlling the production of *olig2*-expressing precursor cells in the zebrafish hindbrain (Fig 3.3) (Wood, Bonath et al. 2009). DISC1 protein expression has been reported in oligodendrocytes in tissue sections as well as *in vitro* cultures which supports a possible role of DISC1 in oligodendrocytes (Seshadri, Kamiya et al. 2010; Katsel, Tan et al. 2011). In addition, a recent study has found that DISC1 is expressed in mouse corpus callosum oligodendrocytes and the authors suggested that DISC1 functions to negatively regulate oligodendrocyte differentiation through down-regulating the expression of *Sox10* and/or *Nkx2.2* (Hattori, Shimizu et al. 2014). Together, these studies support a role for DISC1 in oligodendrocyte development. A number of abnormal morphological phenotypes were reported in zebrafish *disc1* morphants (Drerup, Wiora et al. 2009; Wood, Bonath et al. 2009). Interestingly, very similar phenotypes to those found in *disc1* morphants were shown in FB148.5 mutant zebrafish (Figs. 3.1 and 2), so we hypothesized that these two genes may act together in a common developmental pathway.

In order to investigate the role of the gene mutated in FB148.5 in oligodendrocyte development, the expression of oligodendrocyte lineage markers was analysed, including *olig2*, *sox10*, *mbp* and *plp1b*. Both *sox10* and *olig2*, which are expressed by oligodendrocyte precursor cells (Park, Mehta et al. 2002) were found to be restricted to rhombomeres 5 and 6 in the hindbrain (Fig. 3.4). Furthermore, expression of *mbp* and *plp1b*, which encode myelin structural proteins and are expressed in mature myelinating oligodendrocytes (Carson, Worboys et al. 1997), was decreased dramatically in the hindbrain (Fig. 3.5). These findings suggested that like *disc1*, the gene mutated in FB148.5 is critical for oligodendrocyte development. This supports the idea that *disc1* and the gene mutated in FB148.5 might overlap in their function to control oligodendrocyte specification and development. It is of note that several previous studies have documented myelin and oligodendrocyte deficits in SZ (Uranova, Orlovskaya et al. 2001; Katsel, Davis et al. 2005; Kerns, Vong et al. 2010). *OLIG2* has been reported as a candidate gene in SZ, potentially interacting with other genes that have been linked with oligodendrocyte development such as *ERBB4* and *CNP* (Georgieva, Moskvina et al. 2006). Therefore by characterizing FB148.5 we hoped to shed new light on pathways that *disc1* functions in with potential relevance to schizophrenia.

Several lines of evidence demonstrate that *Disc1* is necessary for neurogenesis during early brain development (Austin, Ky et al. 2004; Schurov, Handford et al. 2004; Mao, Ge et al. 2009). It has also been reported that reducing *Disc1* expression using RNAi leads to abnormal neuronal migration in mice (Kamiya, Kubo et al. 2005; Mao, Ge et al. 2009; Singh, Ge et al. 2010; Lee, Fadel et al. 2011). Zebrafish *disc1* morpholino mutants probed for expression of the neurogenesis marker *ash1b* showed slightly decreased expression in the mutant hindbrain, suggesting that *disc1* also contributes to neurogenesis during zebrafish brain development (Wood, Bonath et al. 2009). However,

FB148.5 mutant embryos showed a dramatic loss of the pro-neural transcription factors *ash1b* and *ngn1* in the hindbrain at 31h.p.f. (Fig 3.9 and 3.10), suggesting that the FB148.5 gene and *disc1* may have different functional roles in neurogenesis. In contrast, the neural stem cell marker *sox2* showed only a minor reduction of expression in the hindbrain of FB148.5 mutant embryos at the same stage (Fig 3.11). It is possible that the reduction in pro-neural gene expression within the FB148.5 mutant hindbrain reflects a block in pro-neural gene expression or premature differentiation of neuroblasts into neurons. Immunostaining for HuC, a marker for post-mitotic neurons, might indicate whether there was premature differentiation of neuroblasts.

To determine whether FB148.5 might regulate *disc1* expression, we analysed *disc1* expression in FB148.5 mutants and observed decreased expression in the cranial neural crest-derived cartilages of the lower jaw (Fig. 3.7 and 3.8). It has been reported that *disc1* negatively regulates *sox10* expression, a neural crest marker, (Drerup, Wiora et al. 2009). Therefore, this may suggest that the FB148.5 mutation affects NC development through influencing *disc1* expression directly or indirectly. However it may simply reflect a defect in NC development so it would be important to test other NC markers such as *sox9* and *snailb* to confirm the NC defect in FB148.5 (Cheung and Briscoe 2003). Neural crest defects have been suggested in Schizophrenia since many patients exhibit mild craniofacial abnormalities (Sivkov and Akabaliev 2003), although this has not been reported in the Scottish DISC1 family (Blackwood, Fordyce et al. 2001). Expression of *disc1* in mutant embryos was also reduced in the pectoral fin buds and sensory patches of the inner ear.

Both *disc1* morphants and FB148.5 mutants have a curved body axis, although the direction of curvature is different between them. A downward curved body axis is seen in many cilia mutants, which can have secondary effects on Sonic hedgehog (Shh)

signaling. Therefore, we investigated hedgehog signaling in FB148.5 mutant zebrafish. Shh is one of a small family of proteins that regulates the development of many tissues during vertebrate embryogenesis. Shh binds to Patched which in the absence of Shh inhibits the function of the membrane protein Smoothed (smo). The Shh-Patched complex releases smoothed from inhibition which then activates a signaling cascade ending with the activation of Gli transcription factors (Pan, Bai et al. 2006). Patched is therefore a negative regulator of the Shh pathway and is itself induced by Shh signaling as part of a negative feedback loop. We examined Shh signaling in FB148.5 mutant embryos by analyzing the expression of the Shh target genes *gli1* and *ptch2*. A significant increase in expression of both *gli1* and *ptch2* was shown in FB148.5 mutants (Fig.3.15 and 16) suggesting that Shh signalling is altered in FB148.5 mutants. This result could indicate also that the FB148.5 gene affects the formation of primary cilia since the link between the primary cilium and Shh signaling is well established (Huangfu, Liu et al. 2003; Park, Haigo et al. 2006; Vierkotten, Dildrop et al. 2007). Further experiments to investigate whether FB148.5 has a role in cilia formation were not undertaken, but this finding suggested that cilia-related genes might be good candidates in the FB148.5 locus.

To conclude, the phenotypic characterization of FB148.5 clearly illustrated that the mutated gene has multiple roles in nervous system development and is required for oligodendrocyte precursor specification, neurogenesis, motor axon outgrowth and Schwann cell development. It was hoped that this information would be informative for prioritizing candidate genes for sequencing in the FB148.5 locus.

CHAPTER IV: CHROMOSMAL MAPPING OF FB148.5 MUTANT ZEBRAFISH

4.1 INTRODUCTION

Positional cloning allows the identification of a mutated gene based on its chromosomal map position using the principle of genetic linkage. Genetic linkage is defined as the tendency of genes that are close together on the same chromosome to be inherited together during meiosis. Forward genetic screens in zebrafish have been widely used to identify the genes mutated in numerous mutants that are involved in a variety of biological processes. Typically, the first stage for identifying the mutation causing a mutant phenotype is to perform bulked segregant analysis (BSA) through scanning the polymorphic zebrafish genome with genetic markers called simple sequence length polymorphisms (SSLPs) to analyse the genetic linkage between the mutant phenotype and these SSLPs (Geisler, Rauch et al. 2007). Next, individual mutant fish are screened to calculate the recombination or cross-over frequency. This works on the principle that the closer two genes or markers are to each other on a chromosome, the less likely it is that a crossover will occur between them. Thus, the percentage of recombination frequency between two genes is a measure of how close those two genes are which allows us to refine the candidate area in which a particular mutation lies. Finally, candidate genes within promising region are screened for deleterious mutations by sequencing genomic DNA or cDNA.

4.1.1 INTRON-EXON STRUCTURE IN ZEBRAFISH

Introns are a major non-coding component of genomes. They can contain gene regulatory elements (Majewski and Ott 2002) which have essential effects on transcription and alternative splicing (Mironov, Fickett et al. 1999). Intron size and

frequency diverge significantly across species (Long and Deutsch 1999; Lynch and Conery 2003). In the zebrafish, has been reported that it has an atypical distribution of intron sizes, with a greater number of larger introns in general and a notable peak in the frequency of introns of approximately 500 to 2,000 bp compared with other fish. This report also concluded that 47% of zebrafish introns are composed of repetitive sequences (Gelfman, Burstein et al. 2012). In addition, analyses of vertebrate exons showed similar distributions of exon numbers in human, mice, and zebrafish. A study of exon number in all protein-coding genes in several species, including human, mouse and zebrafish, showed that vertebrate genes consist of more exons on average than invertebrate genes (Gelfman, Burstein et al. 2012).

4.1.2 VARIANT FREQUENCY IN THE ZEBRAFISH

Zebrafish have a high degree of variation between strains and a lower level of variation within each zebrafish strain (Bradley, Elmore et al. 2007; Coe, Hamilton et al. 2009). It has predicted that approximately more than 50,000 high-quality SNPs cover the zebrafish genome with average resolution of 41 kbp (Guryev, Koudijs et al. 2006). Even with the low number of embryos that were genotyped, it possibly provides one informative SNP every 500 nucleotides. For example, on linkage group 14, the average frequency of candidate SNP is 1 per 41 kbp, and the largest gap between two nearby variants is 2 Mb (Guryev, Koudijs et al. 2006). Moreover, in the zebrafish genome, the majority of the candidate zebrafish SNPs are C to T, or G to A transitions similar to human and mice genome. Though, in zebrafish the ratio of these SNPs is remarkably less than in human (Coe, Hamilton et al. 2009).

4.2 POSITIONAL CLONING

4.2.1 FB148.5 MAPPING CROSSES

In order to perform positional cloning, polymorphic FB148.5 mutation carriers were generated by out-crossing homozygous WIK/WIK wild type fish with heterozygous FB148.5/LWT fish. The resulting fish were considered as the F1 generation, and half of them would be predicted to be heterozygous carriers. The F2 mapping generation was then created by inter-crosses between pairs from the F1 generation and mapping pairs identified on the basis of approximately 25% of embryos showing the mutant phenotype (Fig. 4.1). 8 pairs of FB148.5/WIK were identified and then around 150 homozygous FB148.5 mutant embryos were collected from these pairs of parents for genetic linkage analysis.

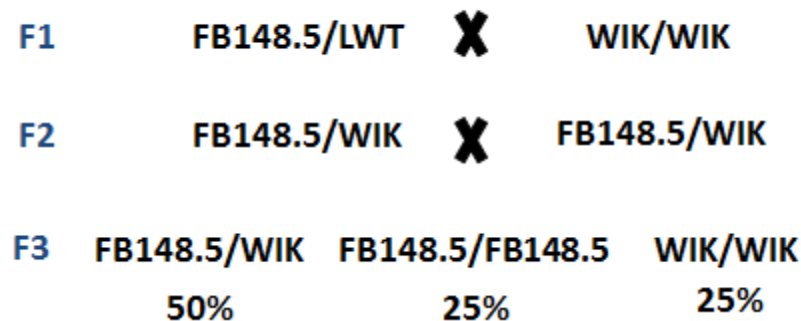


Figure 4.1 Mapping cross rationale.

A polymorphic hybrid strain was generated by out-crossing homozygous WIK/WIK wild type fish with heterozygous FB148.5/LWT carriers. This yielded the F1 family, with half of them expected to be heterozygotes. F2 fish were then created by inter-crossing heterozygous pairs from the F1 generation, so that approximately 25% of embryos should show the mutant phenotype (n of $M=186=25\%$, Sibling= 590, $t=5$, $b=8$).

4.2.2 LINKAGE ANALYSIS

Linkage analysis was used to define the chromosomal region in which the phenotype causing gene is located using a panel of SSLP markers. The genetic map is measured in centimorgans (cM), 1 cM corresponding to 1% recombination frequency. However, in the physical map, 1 cM typically corresponds approximately to 1 million DNA base pairs (1 megabase, 1 Mbp), but this is variable. To genetically link FB148.5 to a specific chromosome, pools were made by mixing equal amounts of DNA from 25 homozygous mutant and 25 wild-type embryos (a mixture of homozygous WT and heterozygous embryos) and then genotyped with 192 SSLP markers (see appendix 1 list of SSLPs), which were spaced roughly equally across all 25 zebrafish linkage groups (LG) (Fig 4.4). A linkage group is defined as a set of genes that are inherited together in a cross and each LG represents a single chromosome (Kelly, Chu et al. 2000). The SSLP markers are microsatellites which normally consist of TA, CA or GT dinucleotide repeats. The lengths of these repeats differ between many of the zebrafish strains that are commonly used, enabling them to be used as polymorphic genetic markers (Rauch, Granato et al. 1997) (Fig.4.2). SSLP markers were amplified by PCR according to section 2.2.2.3, then the PCR products electrophoresed in 3.5% agarose gels loaded with a multichannel pipette (Figure 4.3) for at least 2 h at 200 V to separate different alleles (see 2.2.2.5). Genetic linkage should be apparent when the WIK allele is absent in the mutant pool and present in the sibling pool (Figure 4.2), i.e. homozygosity for a polymorphic marker should be apparent in the mutant pool. This suggests that the two alleles (SSLP and mutated gene) are very close to each other, thus they will inherit together. However, if there is a large distance between SSLP and mutation loci, this will allow recombination to occur between them. On the initial genome scan performed, one of the linkage group 8 (LG8) markers (z1068) showed apparent increased homozygosity

in the mutant pool compared with the sibling pool (red arrow in Fig.4.4A). This marker was re-tested on DNA pools from the progeny of three separate mapping pairs to confirm the potential linkage of the FB148.5 mutation with this marker on LG8 (see section 4.2.3 below).

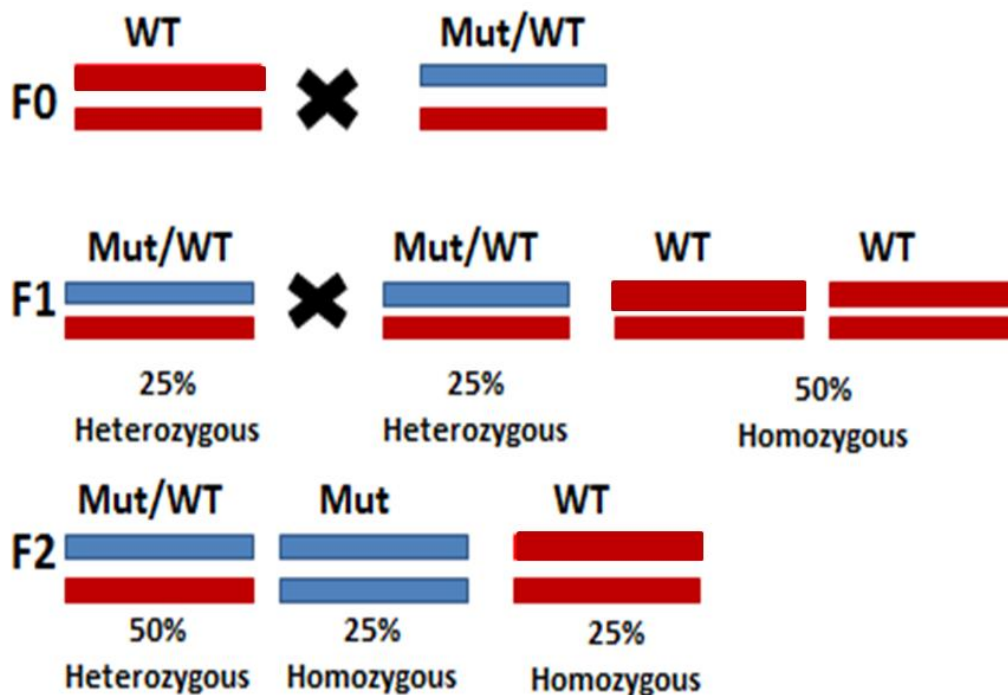


Figure 4.2: Segregation of alleles in the mapping crosses.

Red represents the WT allele and blue represents the mutant allele. The F1 heterozygous carriers are crossed to each other to generate the F2 generation for genetic mapping. One quarter of the normal F2 progeny are homozygous for the WT allele while two quarters of them are heterozygotes. All F2 mutants will be homozygous for the mutated allele.

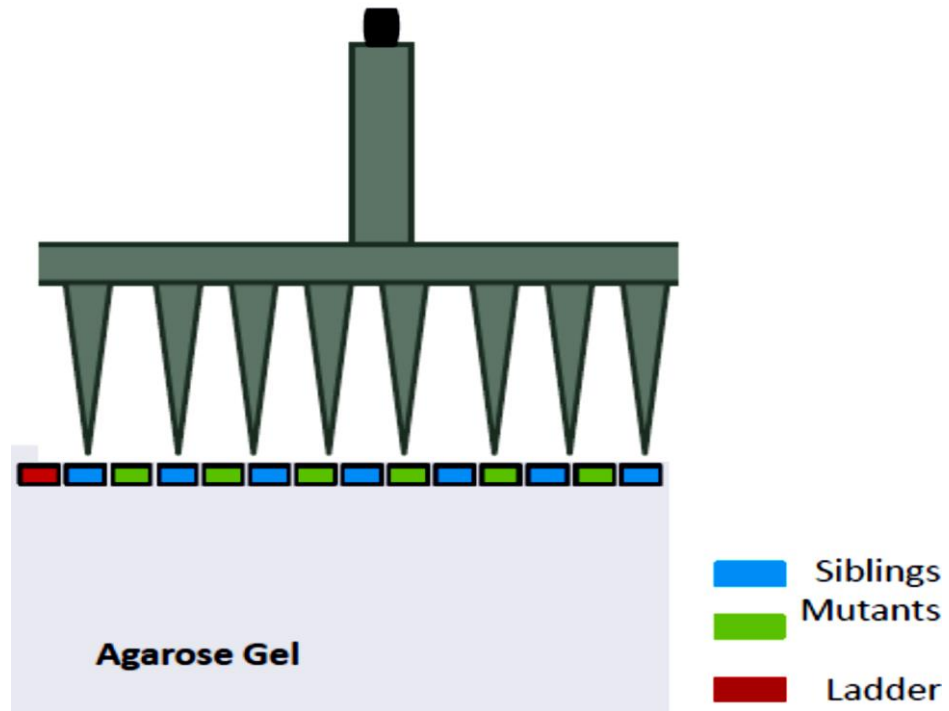


Figure 4.3: Method for loading PCR products in agarose gels to enable direct comparison of alleles in mutant and sibling pools.

A large electrophoresis tank was used that enabled simultaneous analysis of 200 PCR reactions by agarose gel electrophoresis. Mutant and sibling PCR reactions were performed in separate 96 well plates, then using a multi-channel pipette, PCR products from siblings were loaded in alternating wells with the mutant samples loaded in the intervening wells, thus, mutant and sibling samples for each marker were loaded next to each other.

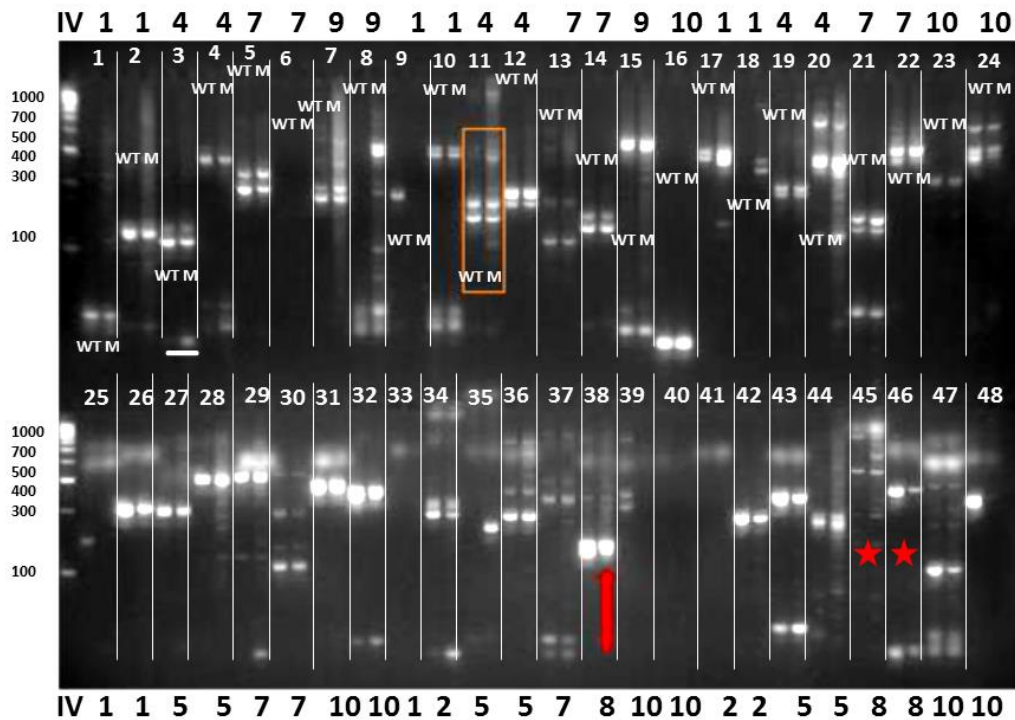


Figure 4.4: PCR products of 48 SSLPs markers used in initial mapping.

A total genome scan was performed with 192 SSLP markers spaced evenly across the 25 zebrafish linkage groups (see Table 1 Appendix). The figure shows PCR products for 48 SSLPs; each marker was tested on mutant (M) and wild-type (WT) DNA pools. The red box shows an unlinked marker because the mutant DNA pool and sibling DNA pool both show equal intensity for the two polymorphic allele products. The red arrow indicates polymorphic allele products where the upper band appears to be enriched in the mutant pool indicating that this SSLP (z1068 on linkage group 8) may be linked to the FB148.5 mutation (see Figure 4.5 which confirmed the genetic linkage). Z4324 and z13412 SSLP are also located in LG 8 and are labelled with red stars, but neither allele amplified well in both pools. (Hyperladder IV was loaded on all gels and the LG for each marker is indicated in black above or below the gel).

4.2.3 THE FB148.5 MUTATION MAPS TO LINKAGE GROUP 8

The BSA analysis shown in the previous section suggested that the FB148.5 mutation may locate to chromosome 8 (Fig. 4.4). SSLP z1068 showed a very broad product band in the sibling DNA pool, while the homozygous FB148.5 mutant DNA pool gave a narrower product band, indicating homozygosity for a polymorphic allele. This suggested that FB148.5 was linked with this marker which is found on LG 8 (Fig. 4.4). In order to validate that the candidate marker z1068 at 13 cM was genetically linked with the mutation, it was analysed in three separate mutant and sibling DNA pools which contained 25 embryos for each that were derived from three different mapping pairs. Genetic linkage was suggested in all 3 pools with the mutants showing homozygosity for the middle allele of three alleles detected in the siblings (Figure 4.8). Three alleles were amplified by PCR due to FB148.5 having been maintained on different genetic backgrounds since it was first identified in an ENU mutagenesis screen over 10 years ago. Similarly, z15031 at 28.2cM was showed strong genetic linkage with mutation. Genotyping of z15031 SSLP was tested with the three DNA pools which showed homozygosity for the upper allele confirming that the FB148.5 mutation is likely to be located on LG 8 (Figure 4.9).

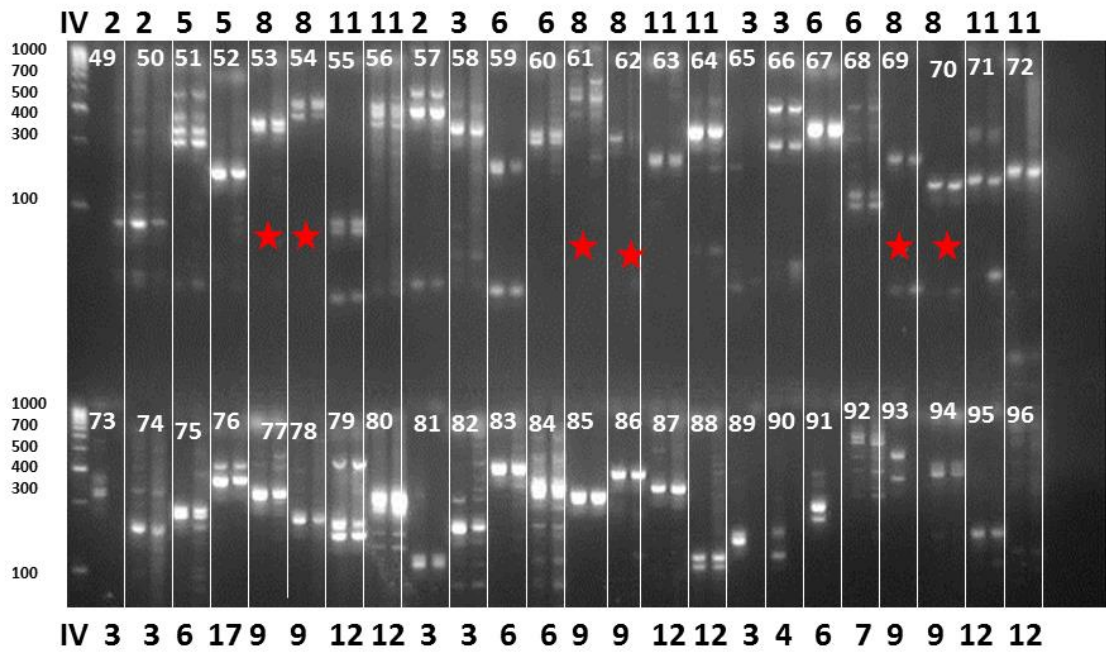


Figure 4.5: PCR products for the next 48 SSLPs.

The figure shows PCR products for 48 SSLP markers; each marker was tested on mutant (M) and (WT) wild-type DNA pools. A total genome scan was performed with 48 SSLP markers (see Appendix Table 1). Markers which are labelled with stars are z27391, z21115, z7130, z14670, z9279 and z10929 respectively, all of which are located in LG 8 (see Table 4.1). (Hyperladder IV was loaded on all gels and the LG for each marker is shown in black above or below the gel).

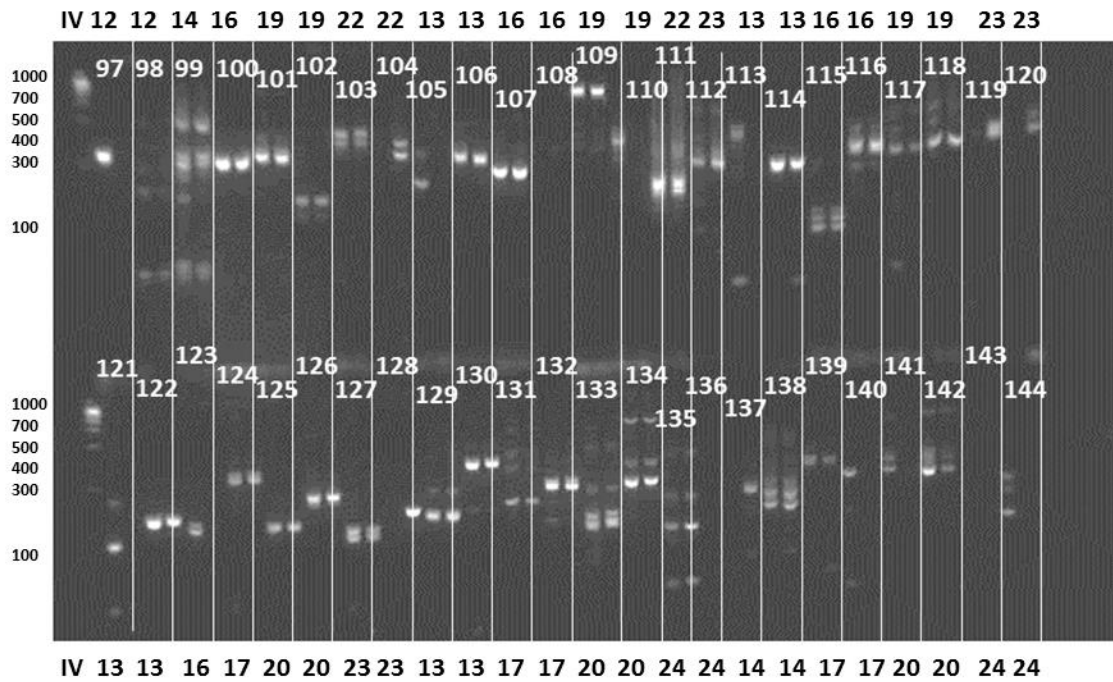


Figure 4.6: PCR products for the next 48 SSLPs.

The figure shows PCR products for 48 SSLP markers; each marker was tested on mutant DNA (M) and (WT) wild-type DNA pools (see Appendix table 1). (Hyperladder IV was used on all gels and the LG for each marker is indicated in black above and below the gel).

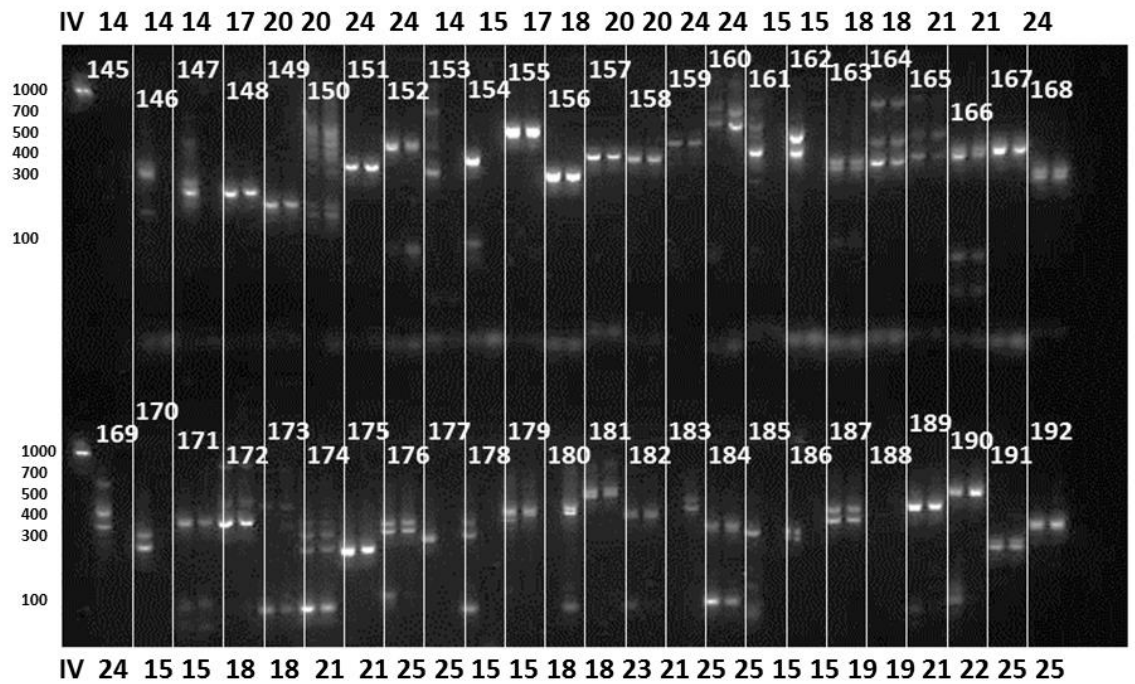
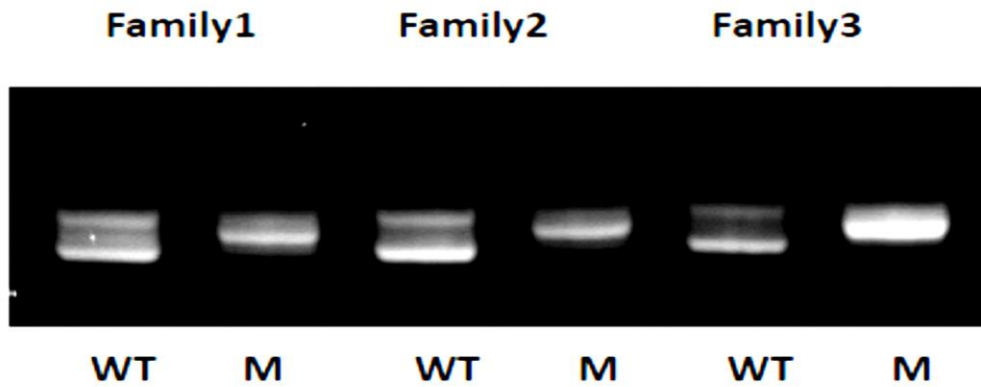


Figure 4.7: PCR products for the last 48 SSLPs.

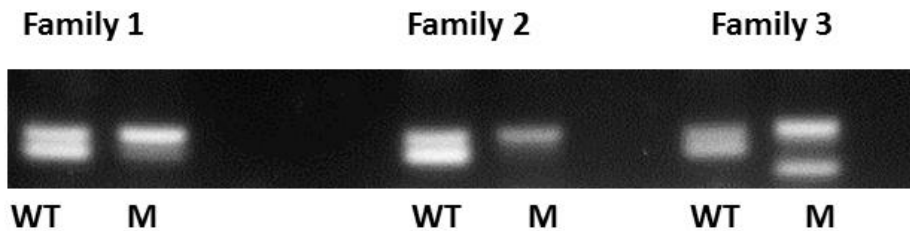
Figure shows PCR products for 48 SSLP markers; each marker was tested on mutant (M) and wild-type (WT) DNA pools (See Appendix table 1). (Hyperladder IV was used on all gels and the LG for each marker is indicated in black above and below the gel).



WT Wild type
M Mutant

Figure 4.8: PCR genotyping with SSLP z1068.

PCR products amplified from WT sibling pools showing three polymorphic alleles (left lane in each pair) and mutant pools (right lane in each pair) which show a high degree of homozygosity for the middle allele. (n=25 WT, 25 Mut, x 5,)



WT Wild type
M Mutant

Figure 4.9: PCR genotyping with SSLP z15031.

PCR products amplified from WT sibling pools showing two polymorphic alleles (left lane in each pair) and mutant pools (right lane in each pair) which show a high degree of homozygosity for the upper allele. (n=25 WT, 25 Mut, x3)

4.2.4 RECOMBINATION FREQUENCY ACROSS LG8

In order to validate the linkage between LG8 and the FB148.5 mutation, individual mutants were tested with a number of LG8 SSLP markers. From this the recombination frequency for each marker was calculated and with 170 mutant embryos, z1068 showed 24.2% recombination frequency whereas z15031 and z7819, which are located at 28.2cM and 30cM on LG8 respectively, showed only a single recombination event (shown in Fig. 4.10, 4.11 and 4.12) when genotyping 45 mutant embryos (Table 4.2). Mutant embryos were analysed by *in situ* hybridization with *olig2* probe to exclude any non-specific abnormal embryos that might interfere with the mapping results. Therefore, a lower number of mutant embryos was genotyped with most of these SSLPs compared with z1068 where embryos were tested without performing *in situ* hybridization first.

The recombination frequency can be used to help determine the relative positions between the linked SSLP markers and the mutation. Other markers in LG 8 were also tested but only 5 more SSLPs were informative, including z34962, z49543 and z24511 which all showed 8.8% recombination frequency (Fig. 4.13, 4.14 and 4.15). Interestingly, these 3 markers were located relatively close together at 30.5, 31.6 and 32 cM respectively. However, SSLP z27391 which is located at 55.1 cM showed 30% (Fig. 4.16) and z21115 at 62 cM showed 44% recombination frequency (data not shown). This suggests that these SSLPs were located further away from the mutation-carrying gene.

	Marker	Position	Recombination %
1	z11922	4.9cM	Uninformative
2	z1637	4.9cM	Uninformative
3	z10731	7.8cM	Uninformative
4	z20180	9cM	Uninformative
5	z1068	13cM	Linkage, 24.2% R
6	Z27279	14.7cM	PCR failed
7	Z6763	14.4cM	Uninformative
8	z9420	19.8cM	Uninformative
9	Z44909	19.8cM	Uninformative
10	z15273	25.7cM	PCR failed
11	z15031	28.2cM	Strong linkage, 2.2% R
12	z7819	30.5cM	Strong linkage, 2.2% R
13	z34962	30.5cM	Linkage, 8.8% R
14	Z49543	31.6cM	Linkage, 8.8% R
15	z24511	32cM	Linkage, 8.8% R
16	z4323	35.2cM	PCR failed
17	z13412	43.3cM	Uninformative
18	z27391	55.1cM	Weak linkage, 30% R
19	Z21115	62cM	Weak linkage, 44% R
20	z7130	65.7cM	PCR failed
21	z14670	70cM	PCR failed
22	z9279	81.5cM	Uninformative
23	z10929	98.4cM	Uninformative

Table 4.1: list of SSLPs analysed from LG 8 with percentage recombination frequency observed.

4.2.5 COMPARISON OF RECOMBINATION EVENTS IN INDIVIDUAL EMBRYOS

Table 4.2 shows the genotyping data for 11 selected individual embryos. Embryo No.1 shows homozygosity at z1068 and recombination at z15031, whereas the other 10 embryos show recombination at z1068 and homozygosity at z15031. Since these recombinant embryos do not share homozygosity between z1068 and z15031, the mutation can be deduced as being between these two markers (Table 4.2) and (Fig.4.10-16). Unfortunately, we were unable to find any informative SSLP markers between z1068 and z15031 to narrow down the candidate region interval, which contains about 50 genes in approximately 4 Mb of genomic DNA (Figure 4.17 and 4.18).

Markers	Z1068/ 13cM	Z15031/ 28.2cM	Z7819/ 30cM	Z34962/ 30cM	Z49543/ 31.6cM	z24511/ 32cM
Mutant embryo No. 1	Homozygous	Recombinant	Recombinant	Recombinant	Recombinant	Recombinant
Mutant embryo No. 2	Recombinant	Homozygous	Homozygous	Homozygous	Homozygous	Homozygous
Mutant embryo No. 3	Recombinant	Homozygous	Homozygous	Homozygous	Homozygous	Homozygous
Mutant embryo No. 4	Recombinant	Homozygous	Homozygous	Homozygous	Homozygous	Homozygous
Mutant embryo No. 5	Recombinant	Homozygous	Homozygous	Homozygous	Homozygous	Homozygous
Mutant embryo No. 6	Recombinant	Homozygous	Homozygous	Homozygous	Homozygous	Homozygous
Mutant embryo No. 7	Recombinant	Homozygous	Homozygous	Homozygous	Homozygous	Homozygous

Mutant embryo No. 8	Recombinant	Homozygous	Homozygous	Homozygous	Homozygous	Homozygous
Mutant embryo No. 9	Recombinant	Homozygous	Homozygous	Homozygous	Homozygous	Homozygous
Mutant embryo No. 10	Recombinant	Homozygous	Homozygous	Homozygous	Homozygous	Homozygous
Mutant embryo No. 11	Recombinant	Homozygous	Homozygous	Homozygous	Homozygous	Homozygous

Table 4.2: Analysis of SSLPs linked with FB148.5 in individual embryos.

Individual mutant embryos were tested to confirm the BSA results. Single mutant embryo No.1 was found to be homozygous with z1068 and recombinant with the rest of the markers. Testing of individual mutant embryos No 2-11 found them to be recombinants with z1068 and homozygous for the other markers. These results determined that the candidate interval lies between z1068 and z15031.

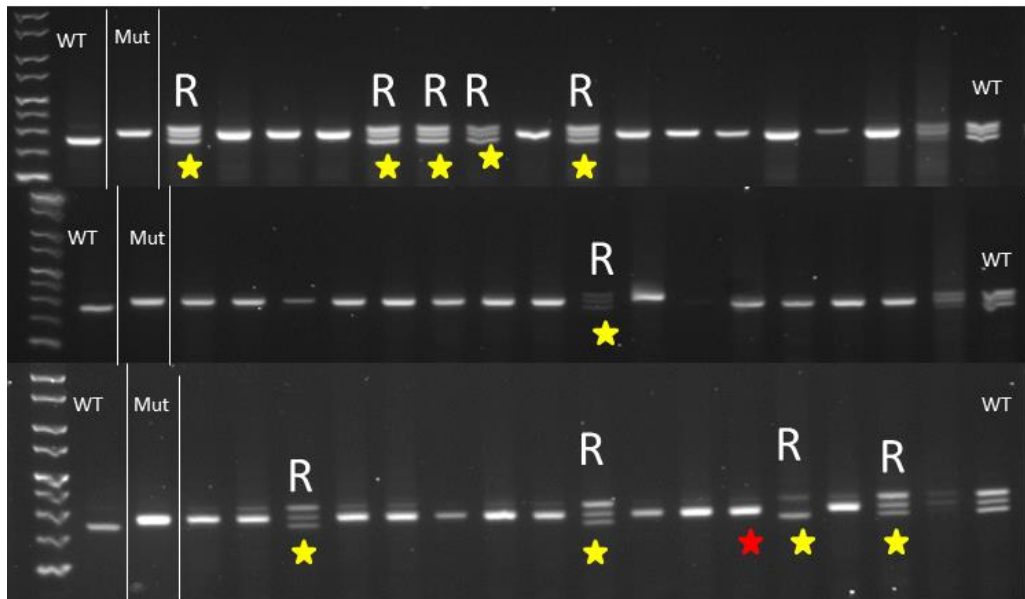


Figure 4.10: Genotyping of mutant embryos with the SSLP marker z1068.

This SSLP is located at 13 cM on LG8. (WT) indicates to the grandparental alleles from the WIK strain, while (Mut) indicates the grandparental allele from FB148.5. 10 of 45 mutant embryos are recombinants showing 3 alleles. Yellow stars indicate the recombinant embryos that are included in Table 4.3. The red star indicates the mutant embryo that didn't showed recombination with this marker but was recombinant with the others (Table 4.3).

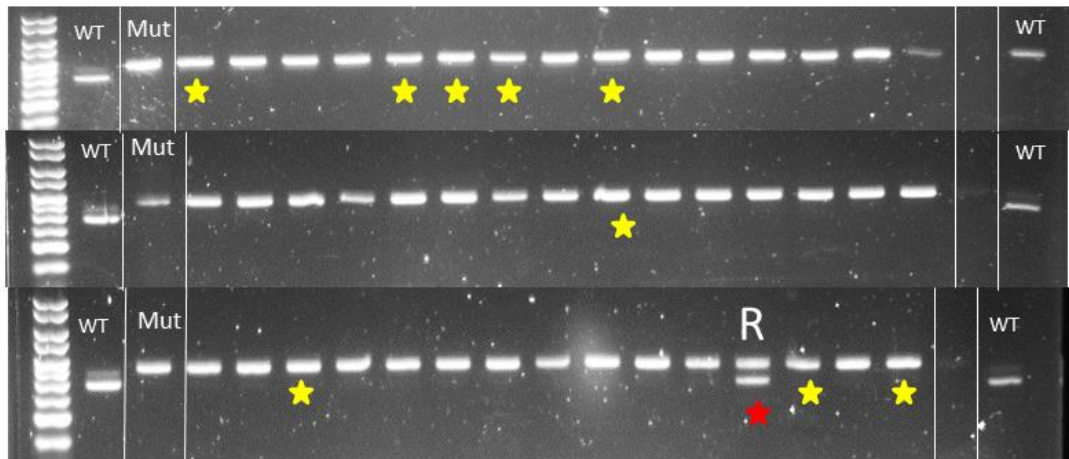


Figure 4.11: Genotyping of mutant embryos with the SSLP marker z7819, which is located at 30 cM.

(WT) indicates the grandparental alleles from the WIK strain, and (Mut) indicates the grandparental allele from FB148.5. One of 45 mutant embryos was a recombinant showing 2 alleles. Yellow stars showed non-recombinant embryos with this marker that is included in Table 4.3. The red star indicates the mutant embryo that showed recombination with this marker as well as with the other markers listed in Table 4.3 except z1068.

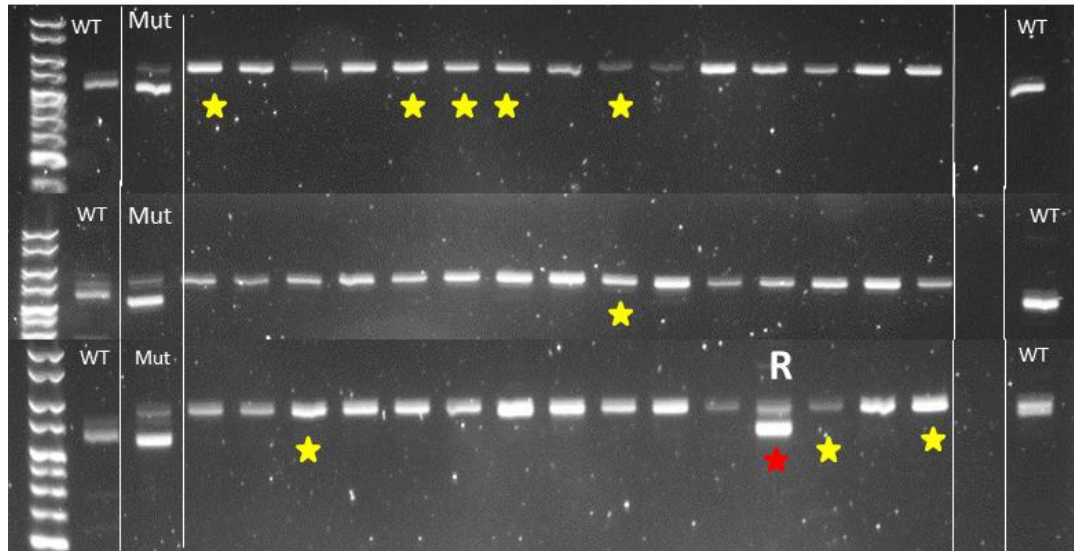


Figure 4.12: Genotyping of mutant embryos with the SSLP marker z15031, which is located at 28.2 cM.

(WT) indicates the grandparental alleles from the WIK strain, while (Mut) indicates the grandparental alleles from FB148.5. One of 45 mutant embryos was a recombinant showing 2 alleles. Yellow stars indicate non-recombinant embryos with these markers that are listed in Table 4.3. The red star indicates the mutant embryo that showed recombination with this marker as well as with the others markers listed in Table 4.3, except z1068.

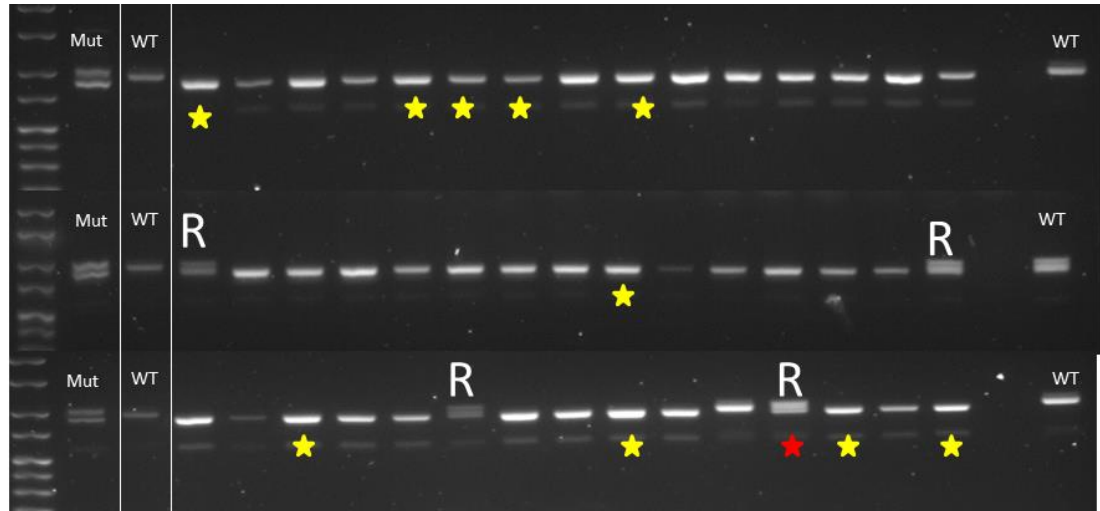


Figure 4.13: Genotyping of mutant embryos with the SSLP marker z34962, which is located at 30 cM.

(WT) indicates the grandparental allele from the WIK strain, while (Mut) indicates the grandparental alleles from FB148.5. Four of 45 mutant embryos were recombinants showing 2 alleles and are labelled with (R). Yellow stars show non-recombinant embryos with these markers that are listed in Table 4.3. The red star indicates the mutant embryo that shows recombination with this marker as well as with the others markers listed in Table 4.3, except z1068.

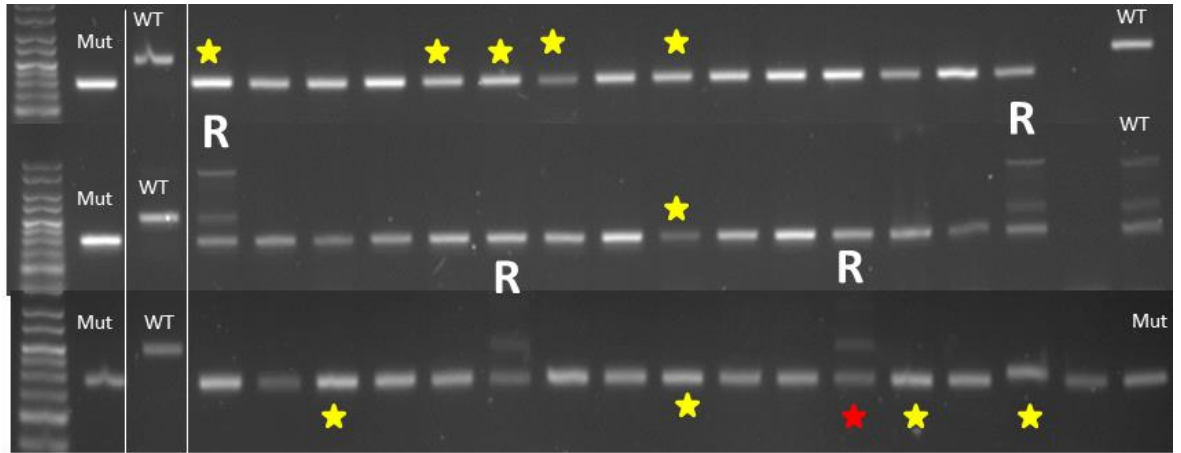


Figure 4.14: Genotyping of single embryos with the SSLP marker z49543, which is located at 31 cM.

(WT) indicates the grandparental allele from the WIK strain, while (Mut) indicates the grandparental allele from FB148.5. Four of 45 mutant embryos were recombinants showing both alleles and are labelled with (R). Yellow stars indicate non-recombinant embryos with these markers that are listed in Table 4.3. The red star indicates the mutant embryo that showed recombination with this marker as well as with the others markers in Table 4.3, except z1068.

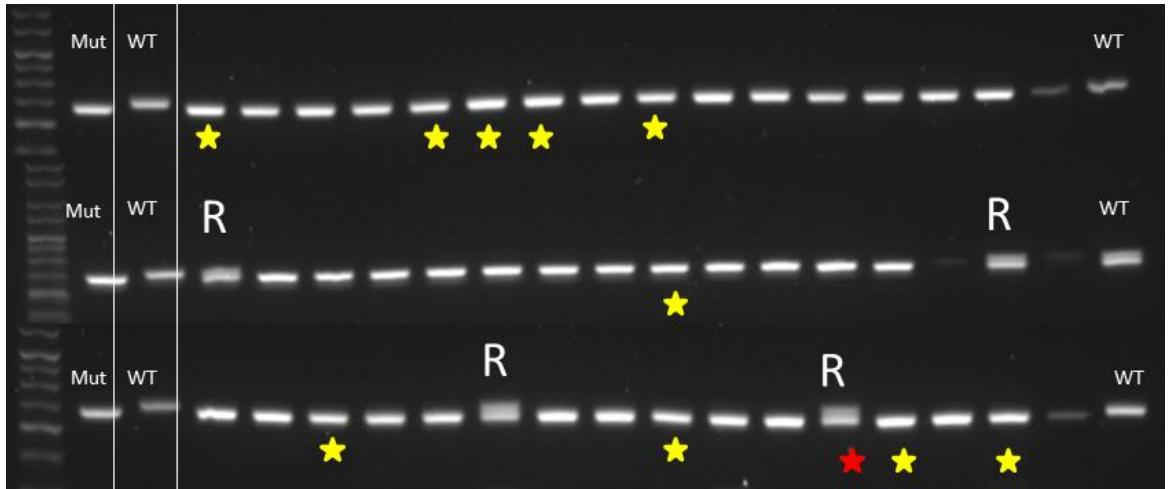


Figure 4.15: Genotyping of single embryos with the SSLP marker z24511, which is located at 32 cM.

(WT) indicates the grandparental allele from the WIK strain, and (Mut) indicates the grandparental allele from FB148.5. Four of 45 mutant embryos were recombinants showing 2 alleles and are labelled with (R). Yellow stars indicate non-recombinant embryos with these markers that are listed in Table 4.3. The red star indicates the mutant embryo that showed recombination with this marker as well as with the others markers in Table 4.3, except z1068.

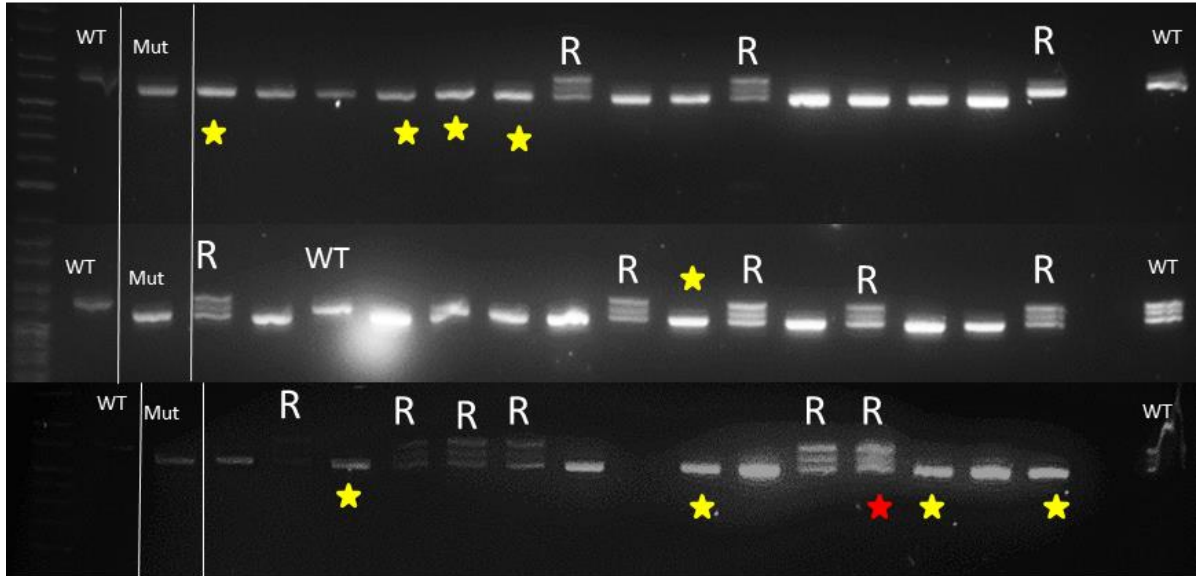


Figure 4.16: Genotyping of single embryos with the SSLP marker z27391, which is located at 55.1 cM.

(WT) indicates the grandparental allele from the WIK strain, while (Mut) indicates the grandparental alleles from FB148.5. Fourteen of 45 mutant embryos were recombinants showing 3 alleles and are labelled with (R). Yellow stars indicate non-recombinant embryos with this marker that is listed in Table 4.3. The red star indicates the mutant embryo that showed recombination with this marker as well as with others markers listed in Table 4.3, except z1068.

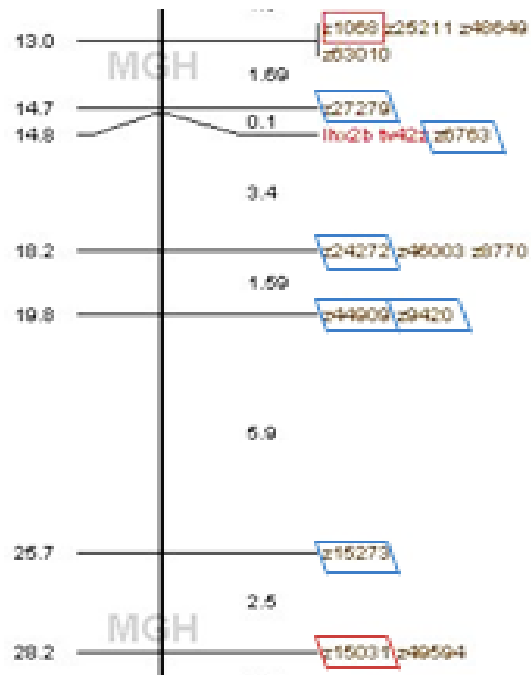


Figure 4.17: Map of SSLP markers between z1068 and z15031 on chromosome 8.
 The region between z1068 and z15031 contained other markers that were tested but either failed or was found to be uninformative.

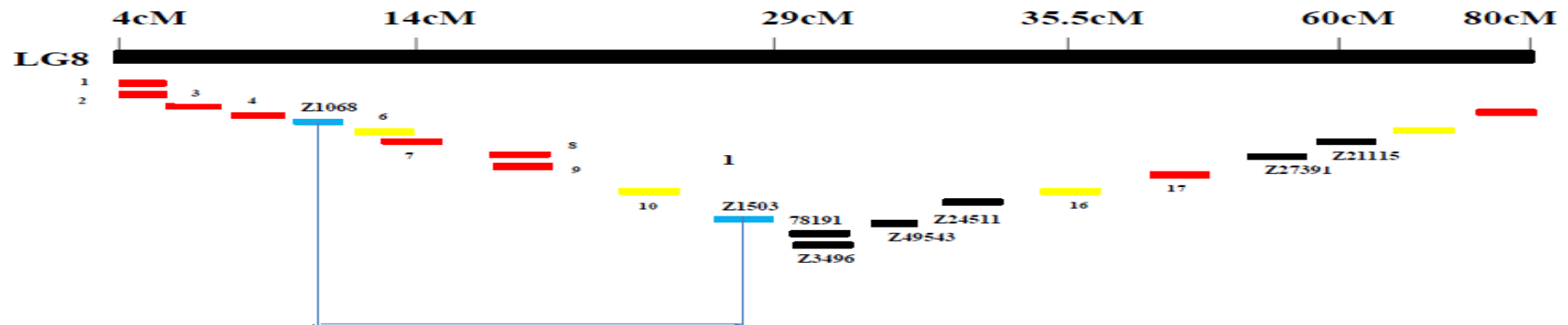
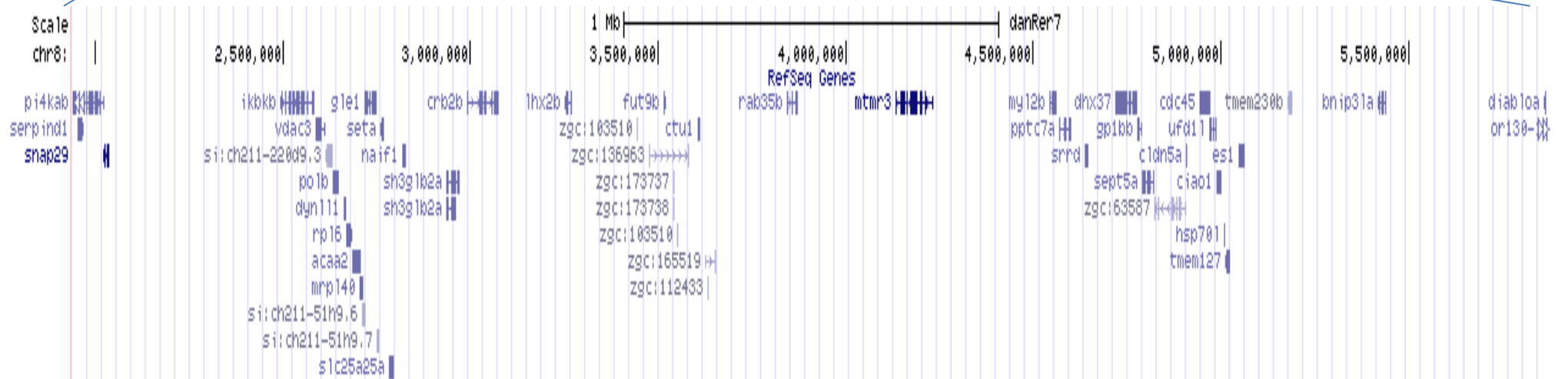
A**B**

Figure 4.18 The genetic map of the candidate region between z1068 and z15031 contains around 50 genes

(A) The genetic map of the candidate interval between z1068 and z15031 showing positions of SSLPs, yellow = PCR failed, Red = uninformative, Black = informative SSLPs and Blue shows SSLPs flanking the candidate region (z1068 and z15031). (B) The physical map of the candidate area showing the genes in this region according to the zebrafish Ref-seq from UCSC track.

4.2.6 SEQUENCING OF INTRONIC REGIONS

As a consequence of the lack of any informative SSLP markers within the candidate region, sequencing of intronic regions to identify informative single nucleotide polymorphisms as novel markers was used. A number of introns from genes spread throughout the candidate region were chosen randomly and were then sequenced. DNA from two pools of WT siblings and homozygous mutant FB148.5 was used and compared to Ensembl reference sequences (Table 4.3). However; no informative SNPs were identified in any of the sequenced introns.

	Gene		Position
1	Enkd1-001 Intron7-8	ENSDART00000141263	8:2,820,746-2,836,633
2	SH2D6-201 Intron 4-5	ENSDART00000124093	8:2,290,123-2,302,348
3	Acaa2-001 Intron 5-6	ENSDART00000056767	8:2,684,693-2,704,946
4	Seta-001 Intron 1, 2, 3 9	ENSDART00000049109	8:2,760,324-2,766,722
5	Ciao1 Intron 1-2	ENSDARG00000059212	8: 4,988,285-4,997,575
6	Plat-001 Intron 19-20	ENSDART00000147275	8: 2,435,980-2,481,545
7	Ccdc64 Intron 1-2	ENSDARG00000074761	8: 3,896,265-3,968,697
8	CIT(1 of2) Intron 37-38	ENSDARG00000088825	8: 4,015,429-4,121,991
9	ihx2b-001	ENSDART00000148020	8: 3,251,922-3,268,194

	Introns 1, 2, 3		
10	CLTCL1 (2 of 2) Introns 1-2	ENSDARG00000091618	8: 2,240,226-2,242,278
11	Gle1 Introns 1-2/12-13	ENSDARG00000043559	8: 2,718,593-2,749,849
13	Ikkkb Introns 6-7/8-9	ENSDART00000140265	8: 2,494,159-2,581,767
14	Pptc7 Introns 1-2/2-3	ENSDART00000015214	8: 4,568,797-4,602,444

Table 4.3: List of genes that had intronic regions sequenced to identify novel SNPs linked with FB148.5.

4.3 CANDIDATE GENES

4.3.1 GENES EXCLUDED BY GENOMIC DNA SEQUENCING

The first gene to be excluded was *dynl1l*, which was considered a good candidate because it encodes dynein, light chain, LC8-type 1, and was originally identified as a light chain of the dynein motor complex which has a role in dynein assembly. It has been found to interact with NDE1, which is a DISC1 interaction partner, and also localises to primary cilia, making it a good candidate to be mutated in FB148.5. However, DNA sequencing for all coding exons of *dynl1l* in genomic DNA showed no mutation in this gene and subsequently it was excluded from the candidate list (Fig. 4.24).

The candidate region contains several genes that when mutated give a phenotype similar to the FB148.5 mutant in some ways (Table 4.4). *Claudin 5a* mutants show interesting phenotypes including abnormal nervous system, small head, and reduction of brain

ventricular volume. *Cldn5a* has also been linked to blood-brain barrier (BBB) development in zebrafish (Xie, Farage et al. 2010) and contains only one exon, making it straightforward to analyse. However, genomic DNA sequencing results for from the mutant pool showed no mutations in this gene, although we found two polymorphisms in *cldn5a*. As shown in (Fig.4.19 A,B), an A>G transition was observed at nucleotide position 458 in WT DNA, causing a codon change of AAA is altered to become AAG yielding same amino acid—lysine in exon 1. The mutant DNA showed AAG, which is the same as the original reference. The other polymorphism is located in the 3'-UTR, and showed a heterozygote at nucleotide position 111 and 112 in both WT and mutant when compared to the reference sequence (Fig. 4.19 C,D). A change like this would suggest that the mutation is not close to *cldn5a* gene.

Genes	
<i>Dynll1</i>	ENSDART00000081325
<i>Gle1</i>	ENSDARG00000043559
<i>Ccdc64</i>	ENSDART00000101125
<i>Rpl6</i>	ENSDART00000115036
<i>Ufd1l</i>	ENSDART00000034968
<i>Ihx2b</i>	ENSDART00000148020
<i>Cldn5a</i>	ENSDART00000064197

Table 4.4: Genes selected on the basis of known phenotypes.

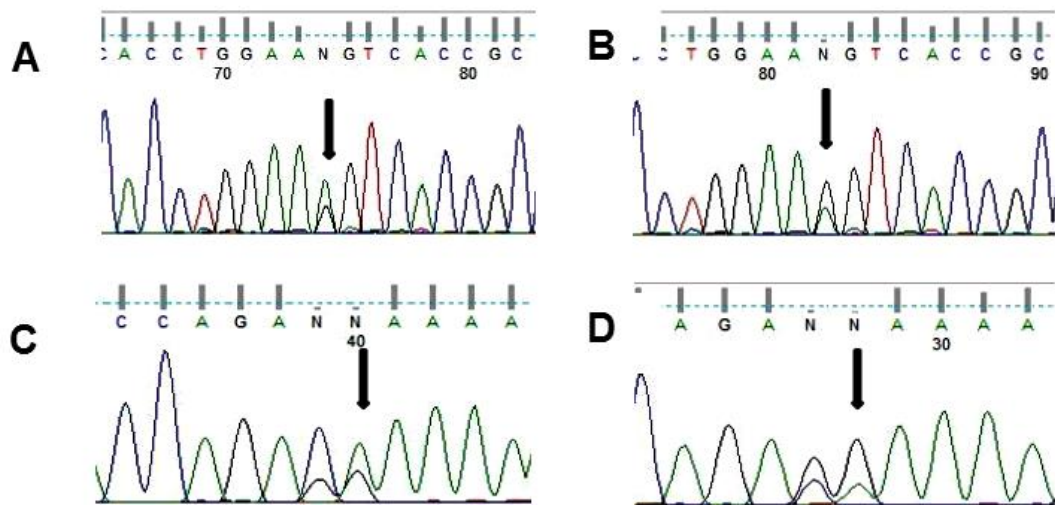


Figure 4.19: Sequence chromatograms for *Cldn5a*.

(A) Sequence chromatogram for *Cldn5a* revealed a SNP with A/G in sibling (WT) DNA. (B) Sequence chromatogram for *Cldn5a* revealed no change in sequence of mutant (M) DNA as the sequence showed A/G too. (C) DNA chromatograms for sequencing at position 111 in WT DNA showed two peaks for C and G and also two peaks for A and G at position 112. (D) Mutant sequencing at position 111 showed same two C and G peaks and at 112 two peaks for A and G were also observed.

4.3.2 GENES EXCLUDED BY CDNA SEQUENCING

Sequencing cDNA is an accurate and fast method to identify point mutations in the coding DNA sequence. Most deleterious mutations are predicted to affect exons or splice sites but since 90% of the zebrafish genome is non-coding, mutations in splice junctions, cis-regulatory elements and promoters will be missed using this method (Henke, Bowen et al. 2013). Several genes in the candidate area have mutants that show similar phenotypes to that seen in FB148.5 mutant fish. Given that these genes have multiple exons, we attempted to sequence the cDNA of these genes from two pools of 20 embryos, one mutant and one WT pool, to identify any nucleotide change, deletion or duplication that could underlie the phenotype. Coiled-coil domain containing 64 (*Ccdc64*) morphants show abnormal brain and eye development and a small head (Schlager, Kapitein et al. 2010). However, we failed to exclude this gene from our list because multiple attempts with different sets of primers failed to amplify the cDNA (Fig. 3 Appendix). Thus, further sequencing analysis is needed in order to exclude *ccdc64*.

The next gene analysed was ribosomal protein L6 (*rpl6*). Mutants for this gene displayed an inflated hindbrain, small eyes and head, and pericardial odema (Uechi, Nakajima et al. 2006). cDNA sequence analysis of the full coding sequence of *rpl6* revealed no mutations so this gene could then most likely be excluded (Fig .4 Appendix).

Ubiquitin fusion degradation 1 like (yeast) (*ufdll*) was also analysed because mutants revealed important phenotypes including a small mis-shapen head, small thick jaw, small eyes and pericardial odema (Amsterdam, Nissen et al. 2004). Sequence analysis identified a single mismatch allele of A to G at position 1870 in WT cDNA. This nucleotide change from GCA to GCG doesn't cause an amino acid change since both

codons encode arginine. The mutant DNA showed heterozygous A/G alleles whereas the reference sequence contains a G (Fig 4.20). Thus, this suggests that this change is a normal polymorphism and also suggested that this gene is found far away from FB148.5 mutation.

Finally, *LIM homeobox 2b (lhx2b)* was also considered as a reasonable candidate gene. In zebrafish, *lhx2b* mutants showed similar phenotypes to FB148.5 such as abnormal brain and eye structures. This gene has been related with eye development, neurogenesis and Wnt signaling (Peukert, Weber et al. 2011). DNA sequence analysis revealed no mutations in *lhx2b* gene that were likely to be the causal mutation in FB148.5. Heterozygous alleles in both WT and mutant DNA were found in the promoter region (Fig.4.21A/B). Two peaks were observed in sequence analysis at position 744; the two nucleotides present were A/G. At position 1472 WT sequencing revealed heterozygous A/T alleles, while the mutant showed only one A allele which is the original nucleotide in the reference sequence. Also, an A/C polymorphism was detected at nucleotide position 1800 in mutant DNA, causing a codon change of CAG to become CCG, changing the amino acid from glutamine to proline (Fig.4.22). The WT DNA showed a CAG codon which is seen in the original nucleotide reference sequence. Other polymorphisms were observed at position 1840, 1870 and 1828; they showed T/C, G/A and G/A respectively (Fig 4.22C/D and 4.23) in 3rd codon positions. All were silent with both alleles encoding Asn, Pro and Ser respectively. As a consequence, this gene has been excluded from the potential genes list. Also, the fact that heterozygous alleles were observed in the mutant DNA samples suggested that this gene is not close to the mutation site.

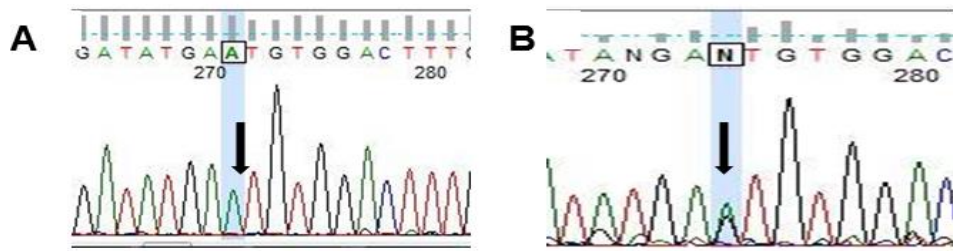


Figure 4.20: Sequence chromatograms for *ufd1l*.

(A) Sequence chromatograms for *ufd1l* revealed a G>A SNP in sibling (WT) DNA. (B) Sequence chromatograms for the mutant (M) DNA also revealed A and G alleles where the reference sequence showed a G.

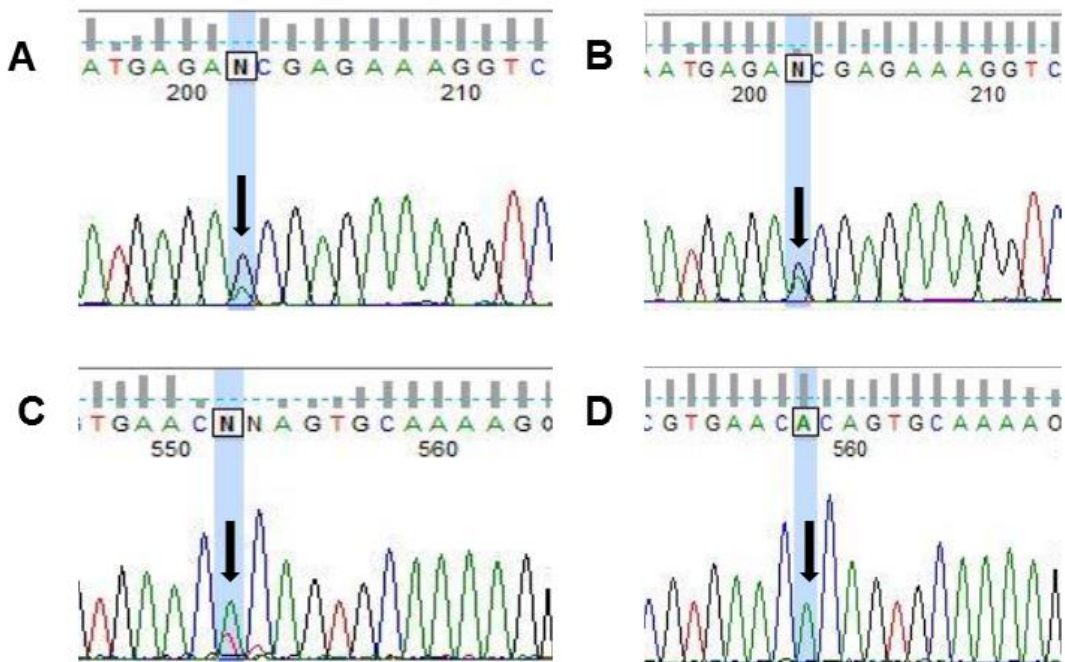


Figure 4.21: Sequence chromatograms for *lhx2b*

(A) Sequence chromatograms for *lhx2b* revealed two peaks for an A/G SNP in sibling (WT) DNA in the promoter region at position 421. (B) Sequence chromatograms for the mutant (M) DNA revealed the same A and G peaks while the reference sequence showed an A. (C) WT sequencing revealed heterozygous T/A alleles at position 1472 encoding Ser/Thr respectively. (D) Mutant sequencing showed homozygosity for the original A nucleotide in the reference sequence which means this variant did not lead to mutation change.

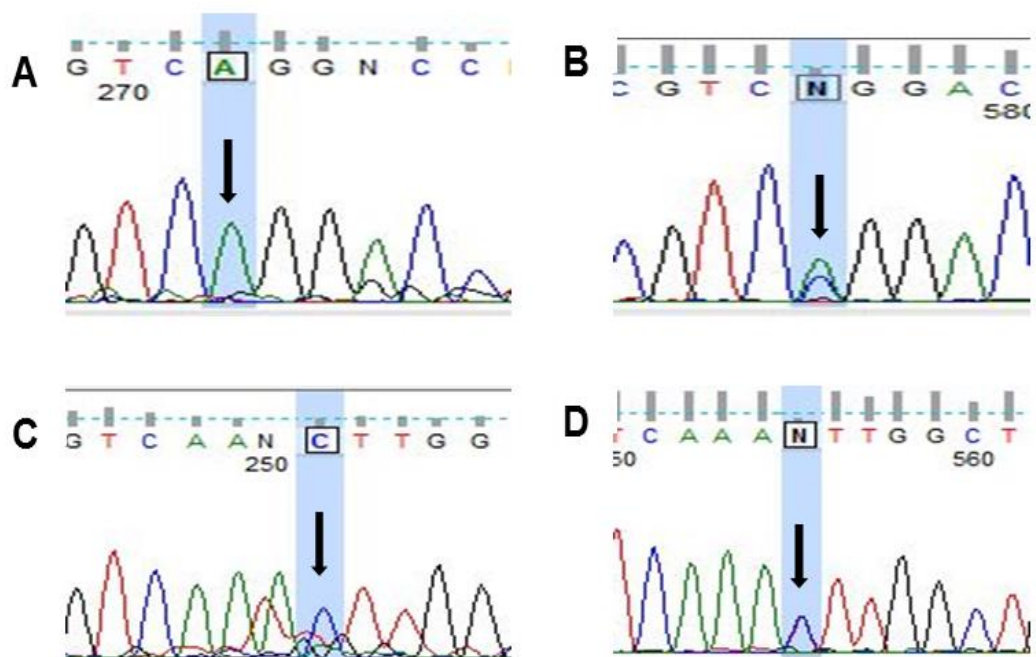


Figure 4.22: Direct sequencing of cDNA encoding *lh2b* gene.

(A) Sequence of WT cDNA showing A allele at position 1800 (B). Sequence of mutant cDNA showing heterozygous A/C alleles encoding Gln/Pro respectively. (C) Sequencing of cDNA of wild-type allele showing C instead of T in the original reference sequence. (D) Sequence of mutant cDNA showing heterozygous T/C alleles at codon 1840 (both encode Asn).

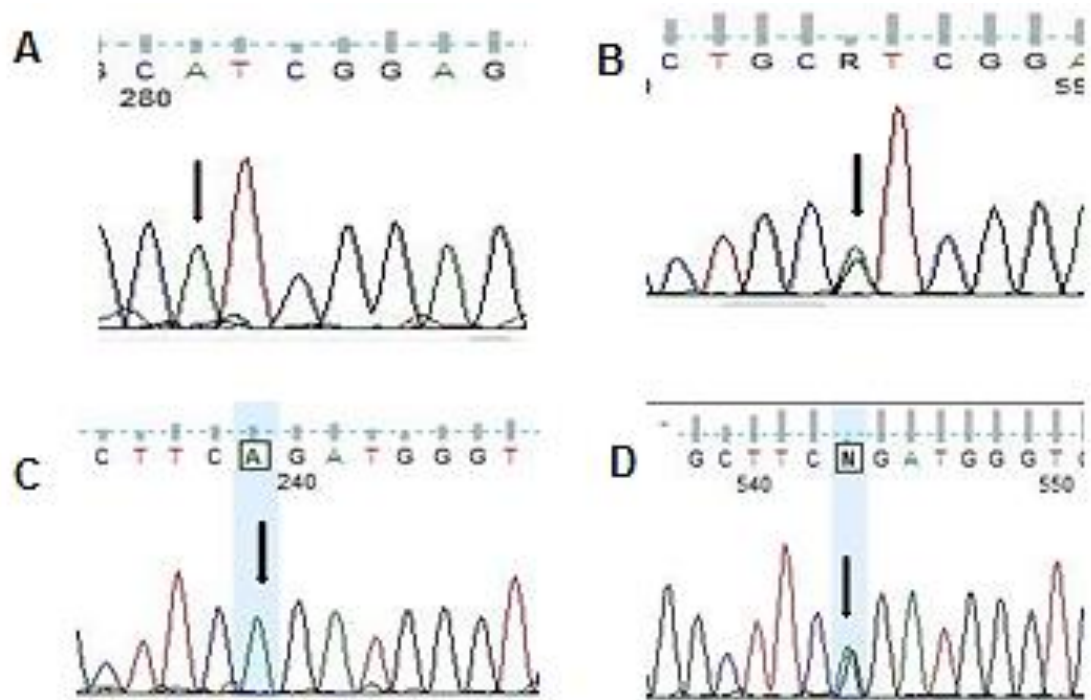


Figure 4.23: Direct sequencing of cDNA encoding *lhx2b* gene.

(A) Sequence of WT cDNA showing A allele. (B) Sequence of mutant cDNA showing heterozygous A/G alleles at position 1870, both encoding Pro. (C) Sequencing of cDNA from wild-type showing C instead of T as in the original reference. (D) Sequence of mutant cDNA showing heterozygous A/C alleles at position 1828, both encoding Ser.

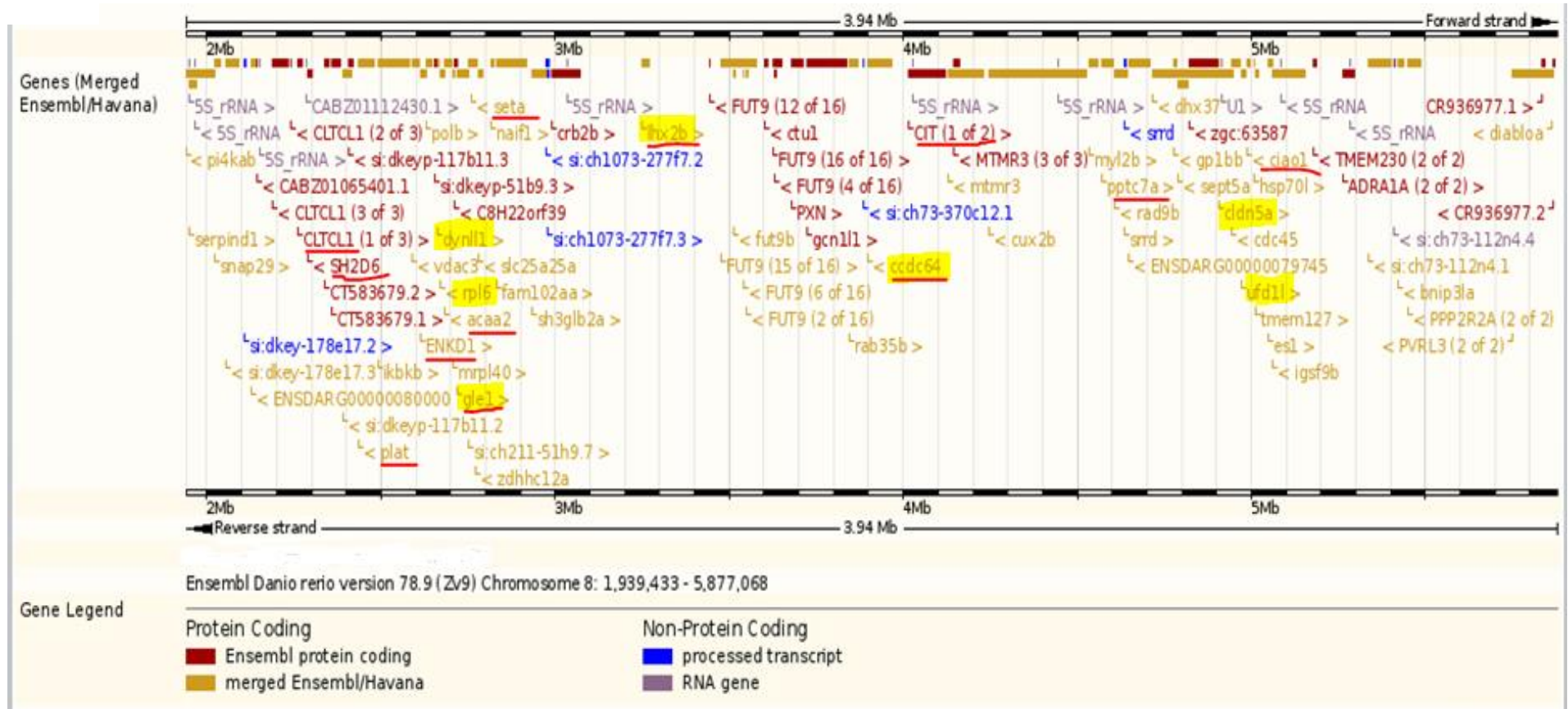


Figure 4.24 Candidate genes from the linkage interval.

Genes that are highlighted with yellow are the phenotypic candidate genes, while genes underlined with red are genes that contained sequenced introns. Image was imported from Ensembl

4.3 DISCUSSION

The aim of positional cloning is to link a mutant phenotype to a specific chromosomal region and involves analysing the segregation of alleles and calculating the frequency of recombination events. This approach has been used in many zebrafish studies to identify the causative gene in mutants obtained through phenotypic screens. In this study, positional cloning has been used to map FB148.5 to linkage group 8 using a panel of 192 SSLP markers originating from the Massachusetts General Hospital (MGH) marker map (Knapik, Goodman et al. 1998). The recombination frequency was determined by testing 45 individual mutant embryos and then the critical interval was defined as 15.2 cM flanked by the markers z1068, which is placed at 13 cM, and z15031 at 28.2 cM. SSLP z1068 showed 24.2% recombination frequency while z15031 showed 2.2%, which suggested that the FB148.5 gene is closer to z15031 than z1068 (Table 4.2). The physical map positions of z1068 and z15031 obtained from the Ensembl genome assembly showed that this 15.2 cM interval corresponded to around 4 Mb and contains around 50 genes (Fig.4 7). Further analyses were performed to test more markers between the two candidate markers to find new closer flanking markers. The physical map in this region showed a small number of additional SSLP markers. These markers were tested and found to be uninformative or the PCRs failed; more specifically, the region from 19.8 cM to 28.2 cM contains only 3 SSLPs, 2 of which were uninformative while the PCR for the other one failed (Fig. 4.17). Therefore, this approach failed to refine the genetic interval to a narrower region because no informative SSLPs were found close to z15031.

As a result of the lack of polymorphic SSLP markers in the region containing the FB148.5 mutation, we attempted to identify intronic SNPs that could be used as markers

for genetic linkage to further refine the FB148.5 locus. It has been reported that the single nucleotide polymorphism (SNP) frequency in non-coding regions is 4.85 SNPs per kb, compared to 1.64 SNPs per kb in coding regions, supporting the use of these SNPs as genetic markers (Zhu, Song et al. 2003). PCR primers (Fig.1 Appendix) were designed to amplify intronic DNA from several genes spanning the defined interval (Fig. 4.18). However, direct sequencing of these regions failed to find any informative SNPs.

As an alternative approach, candidate gene screening was undertaken to try to identify the mutated FB148.5 gene. We selected a number of genes that have mutants with similar phenotypes to FB148.5, an interesting expression pattern or cilia-related function to see if they harboured any potentially deleterious nucleotide change, deletion or duplication. This has been widely used as a successful approach to find mutated genes, but is time and resource costly, and we had insufficient resources to screen all 50 genes in the candidate region in this way. Seven genes were selected as interesting candidate genes in the defined area including; *dyn11l*, *gle1*, *udf1l*, *lhx2b*, *cldn5a*, *rpl6* and *ccdc64*. *Dyn11l* was an interesting candidate gene because it has been reported that DYNLL1 interacts with the DISC1 partner NDEL1. Also, it's a small gene that only contains three exons and therefore was easy to sequence in full. However, it was excluded by DNA sequencing of all coding exons. The *cldn5a* gene was also chosen due to its mutants displaying interesting phenotypes including abnormal nervous system, small head, and reduction of brain ventricular volume (Xie, Farage et al. 2010). DNA sequencing results showed no mutations in this gene, although two polymorphisms were found. Two alleles in both WT and mutant DNA were observed but the change was silent causing codon change of AAA to AAG (both lysine). The other polymorphism was in the 3'-UTR and again showed two alleles at positions 111

and 112 in both WT and mutant DNA (Fig. 4.19). We attempted cDNA sequencing of *ccdc64* but this gene has not been excluded because PCR failed to amplify the cDNA using multiple sets of primer pairs. This gene contains 14 exons and sequencing of all these exons could be undertaken to exclude *ccdc64*. In addition, *rpl6* was selected due to its mutants having phenotypes very similar to FB148.5 such as inflated hindbrain, small eyes and head, and pericardial oedema (Uechi, Nakajima et al. 2006). However, cDNA sequencing analysis revealed no mutations and excluded this gene as a candidate. *Ufd11* was also genotyped owing to mutants having relevant phenotypes that include a small mis-shaped head, small thick jaw, small eyes and pericardial odema (Amsterdam, Nissen et al. 2004). Sequence analysis identified a normal polymorphism mismatch allele of A to G at position 1870 in WT and mutant cDNA (Fig. 4.20). A number of polymorphisms were observed in *Lhx2b*, which we considered another plausible candidate gene for FB148.5, but these were all silent changes (Fig. 4.21.22.23) Finally, *gle1*, which is located at the z1068 end of the candidate region and whose mutants show similar phenotypes to FB148.5, was excluded using a complementation assay. Taken together, none of what we considered the most likely candidate genes were found to harbour a deleterious mutation in FB148.5, although *ccdc64* was not fully analysed. Mutant DNA was found to be heterozygous for SNPs in *cldn5a*, *ihx2b* and *ufd11*. These indicate that mutants have inherited different alleles from each parent. Thus, these genes may be localised far away from the mutation suggesting that the observed linkage to the LG8 locus might be a false positive result (Fig. 4.24). This finding is consistent with WGS results obtained in the following chapter.

Recent advances in DNA sequencing technology means that whole genome sequencing (WGS) now provides a relatively quick and efficient method for genome analysis. Therefore, given the problems that we encountered refining the FB148.5 locus and the

large number of candidate genes in the defined candidate interval, WGS was used for further analysis to try and identify the mutated gene in FB148.5.

CHAPTER V: WHOLE GENOME SEQUENCING

5 INTRODUCTION

5.1 WHOLE GENOME SEQUENCING

Recent advances in whole genome sequencing (WGS) methods provided an alternative method with which to try to identify the FB148.5 mutation. Whole genome sequencing approaches have been applied in many model organisms including *Drosophila*, *Arabidopsis*, *Caenorhabditis elegans* and mice (Blumenstiel, Noll et al. 2009; Cuperus, Montgomery et al. 2010; Doitsidou, Poole et al. 2010; Fairfield, Gilbert et al. 2011). Moreover, WGS has also been successfully utilised in zebrafish to identify phenotype-causing mutations in a number of mutant lines (Gupta, Marlow et al. 2010; Bowen, Henke et al. 2012; Voz, Coppieters et al. 2012).

The Wellcome Trust Sanger Institute in 2001 established the zebrafish genome-sequencing project and used the Tübingen strain as a reference, since this strain was widely used to find mutations causing developmental abnormalities. The newest assembly is Zn9 with a total size of 1.412 Giga bases (Gb) (Howe, Clark et al. 2013). It is known that zebrafish carry a unique genome duplication known as the teleost-specific genome duplication (TSD) (Meyer and Schartl 1999) which complicates accurate annotation of the genome. WGS provides several advantages compared to the SSLP mapping strategy. Firstly, WGS requires a pool of approximately 50 mutants and some WGS strategies do not need WT embryos, which is a much lower number of mutants compared to that typically used in SSLP mapping. The whole library construction, sequencing and analysis takes a few weeks so is less expensive in term of man hours. A

typical WGS run provides 13 Gb of sequence which provides eightfold coverage of the total zebrafish genome and should be sufficient to identify a causative gene mutation (Voz, Coppieters et al. 2012). Genome coverage is described in terms of read depth which is the average number of nucleotide reads to the length of sequence. Thus, 10X coverage means that the genome is sequenced ten times over (Schatz, Delcher et al. 2010).

5.2 MAPPING FB148.5 BY WHOLE-GENOME SEQUENCING

WGS was undertaken because of the lack of informative SSLP markers within the candidate region and because the sequencing of intronic regions also failed to identify informative nucleotide polymorphisms as novel markers. A pool of 50 mutant embryos was sent for library construction and high throughput genomic sequencing at GIGA Genomics in Liege.

The main principle of this technique is to identify the causal mutation region through calculating the level of homozygosity among sequence reads across the genome (Fig.5.1). Recently, the Coppieters group determined the candidate region in the m1045 mutant strain that shows hyperplasia of the exocrine pancreas using an algorithm to calculate the SNP homozygosity score along all the chromosomes so as to map the interval carrying the mutation. They identified an 8 Mb region in chromosome 5 with a homozygosity score close to 1 in m1045 mutants. Sequence analysis of all genes in the candidate region enabled them to determine a nonsense mutation in the *snopc4* gene (Voz, Coppieters et al. 2012).

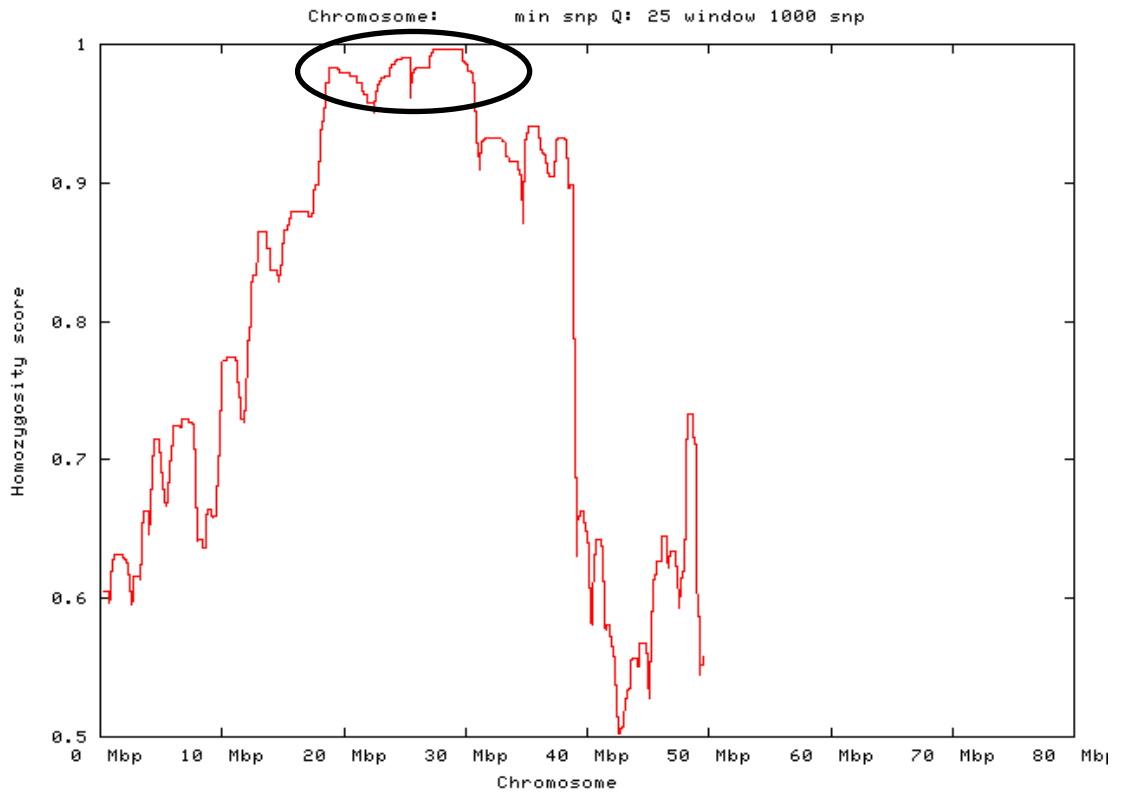


Figure 5.1: An example of high homozygosity score.

Plot showing SNP homozygosity score near to 1 in 18-30 Mbp region of this chromosome as an example; this would be a good candidate region for the mutation.

5.2.1. WHOLE-GENOME SEQUENCING FAILED TO IDENTIFY THE CAUSAL GENE IN FB148.5

The WGS data was generated using an Illumina platform. Paired end sequencing was performed using a library constructed using an Illumina TruSeq kit; the mean insert size was 300bp and mapping was performed using Burrow-Wheeler Aligner (BWA) on danRer7 (Zv9). The homozygosity mapping was done using SAMtools SNP calls while variants were selected by VariantQuerier using the RefGene and Ensembl gene annotations. The percentage of sequencing reads that mapped to Zv9 was approximately 82%.

WGS data revealed that no typical signals corresponding to a homozygous region selected for by a causal mutation were observed in the data set. A correct signal typically has slowly decreasing homozygosity levels on both sides of the homozygous region. Only some relatively small highly homozygous regions were observed (Figure 5.2). These type of signals are typical for homozygous blocks shared by the two crossed strains.

The mutant embryos used in the pools were not all the offspring of a single grandparent carrier, but of multiple grandparent carriers. Depending on the number of generations between these different grandparents to the original mutant, historical recombinations can influence the size of the homozygous region expected in an unpredictable way. The mutation could not be mapped to chromosome 8 as we expected (Figure 5.3), nor did any other chromosome show a typical signal. Since small highly homozygous regions were observed in chromosomes 5, 20 and 23 (Figure 5.2) we retested a number of SSLPs from these regions to ensure that chromosomes 5, 20 and 23 are not

genetically linked with the FB148.5 mutation (Figure 5.4). The results of this analysis demonstrated that none of the SSLPs showed clear genetic linkage with the mutation.

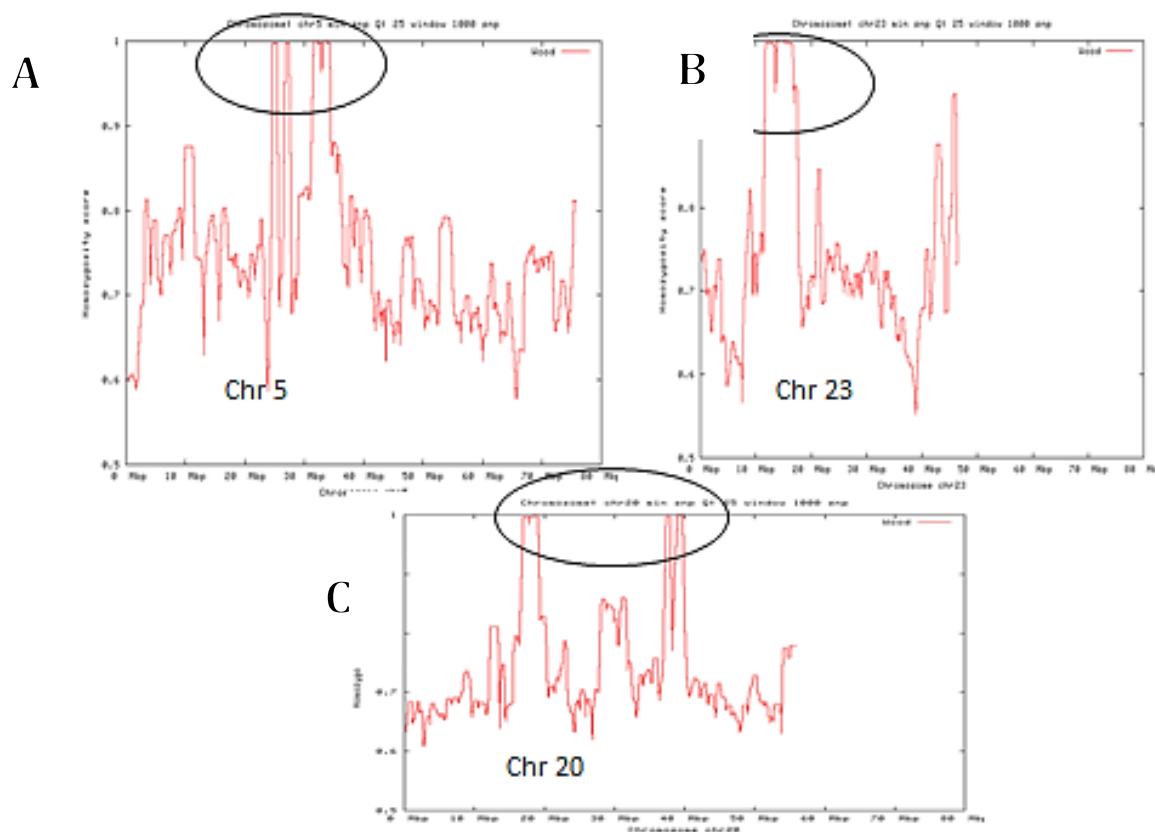


Figure 5.2: Plots showing homozygosity score levels in chr5, chr20 and chr23.

(A) Plot of SNP homozygosity for chromosome 5 showing high score between 24 to 34 Mbp. (B) SNPs show high homozygosity on chromosome 23 between 12 to 18 Mbp. (C) SNPs show homozygosity on chromosome 20 between 15 to 20 Mbp and 37 to 40 Mbp. This suggests possible linkage between these chromosomes and the FB148.5 mutation. These results provided by Dr Wouter Coppieters.

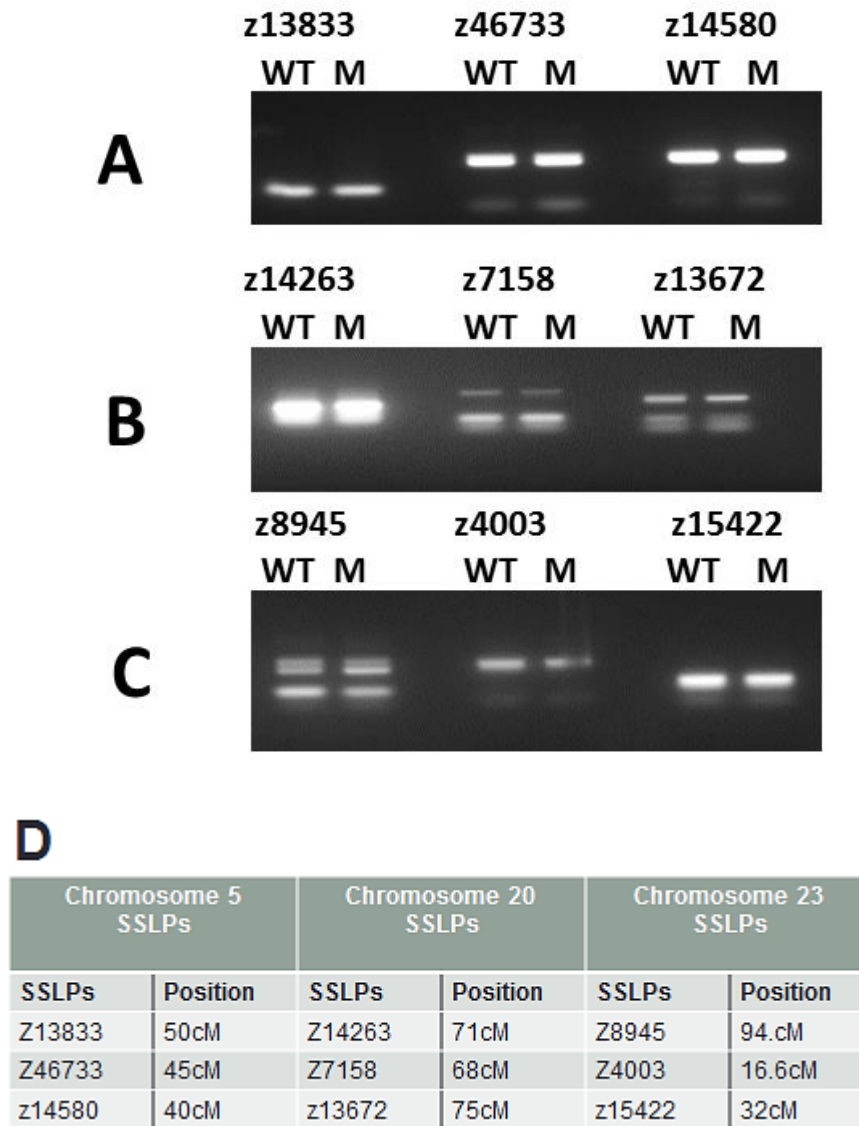


Figure 5.3: Retesting of chromosomes 5, 20 and 23 for homozygosity with SSLP markers.

(A) Genotyping of microsatellites on chromosome 5. (B) PCR products of microsatellites on chromosome 20. (C) PCR products of microsatellites on chromosome 23. The left lane in each case is the PCR product from the wild type (WT) pool and right lane is mutant (M) DNA pool. PCR products for these SSLPs were either uninformative or showed no genetic linkage between these chromosomes and FB148.5 mutation. (D) Table of SSLPs selected for chromosomes 5, 20 and 23.

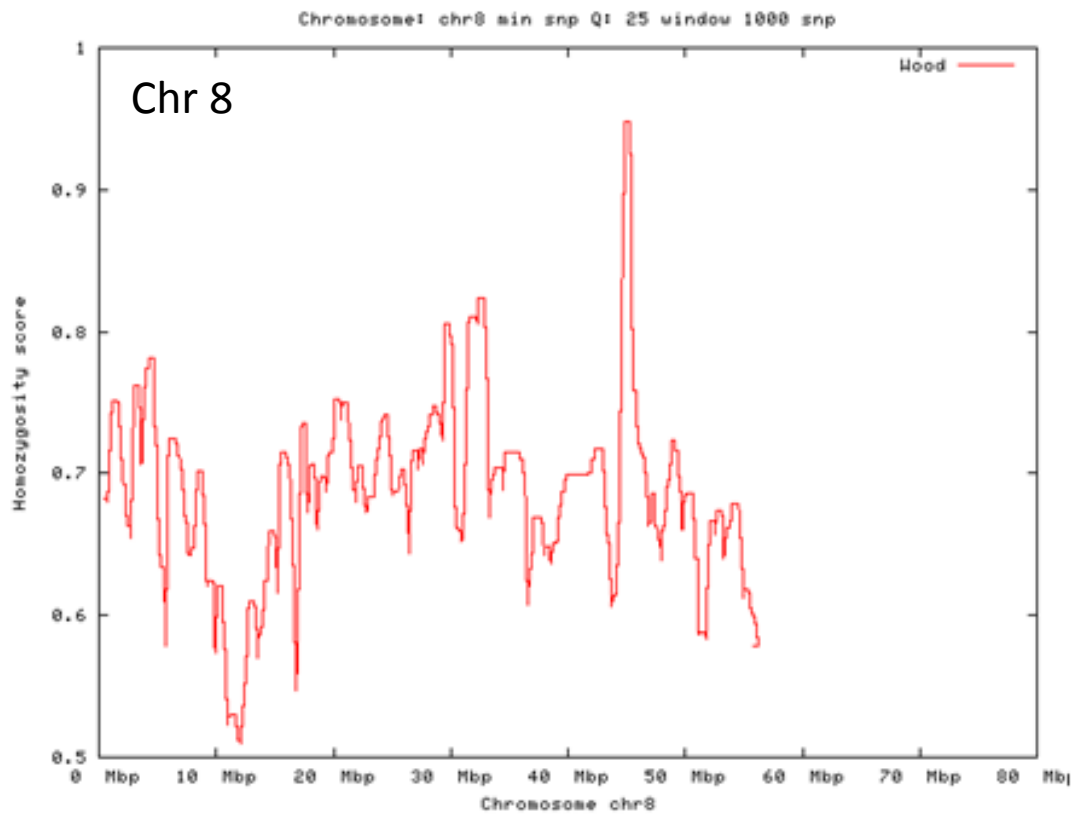


Figure 5.4: Homozygosity score level in chromosome 8.

Analysis of SNP homozygosity for chromosome 8 failed to show typical linkage between this chromosome and the FB148.5 mutation in spite of prior SSLP analysis suggesting that the mutation lies in a candidate interval on this chromosome.

5.2.2 GENES EXCLUDED BY WGS

All regions with a homozygosity score above 0.9 were annotated for candidate causal mutants using a number of toolkits including GATK Unified Genotyper, SAMtools and Variant Querier (Li, Handsaker et al. 2009; McKenna, Hanna et al. 2010) with RefSeq (Zv9) and Ensembl gene annotations by Dr Coppieters. Variants within the critical regions were annotated by their effect on amino acid sequence and splice sites. After that, functional SNPs were filtered using two criteria:

- 1) The SNP has to be private to the mutant line (if the SNP is also observed in another zebrafish line it was excluded as being the causal variant).
- 2) The SNP must be homozygous for the alternative allele.

132 private variants in regions with a homozygosity score above 0.98 were detected, comprising 9 splice site mutations and 7 possible loss of function mutations. These disruptive mutations were checked using the Broad Institute Integrative Genomics Viewer but none were retained as causal. All other mutations identified were missense mutations. Moreover, the variant annotation undertaken by Dr Coppieters provided a list of chromosome 8 genes that revealed interesting functional SNPs that might cause the FB148.5 mutation. Accordingly, PCR primers were designed to amplify around the SNP change for these selected variants and then the DNA was sequenced (Table 5.1). The *dock5* gene was selected since it has a role in cytokinesis, *specc11a* because morphants for this gene show neural crest defects, *fnbp11* because of an interesting expression pattern (CNS, midbrain and neural plate (Thisse and Thisse 2004)) and *iqsec2* since it is related to X-linked mental retardation. However, sequencing revealed that no *dock5* mutation was identified in the FB148.5 mutant DNA pool as illustrated in Fig. 5.5B compared to WT DNA (Fig. 5.5A). In addition, both sibling and mutant pools revealed no SNP change in *fnbp11* gene (Fig. 5.6A and B). A C>G polymorphism was

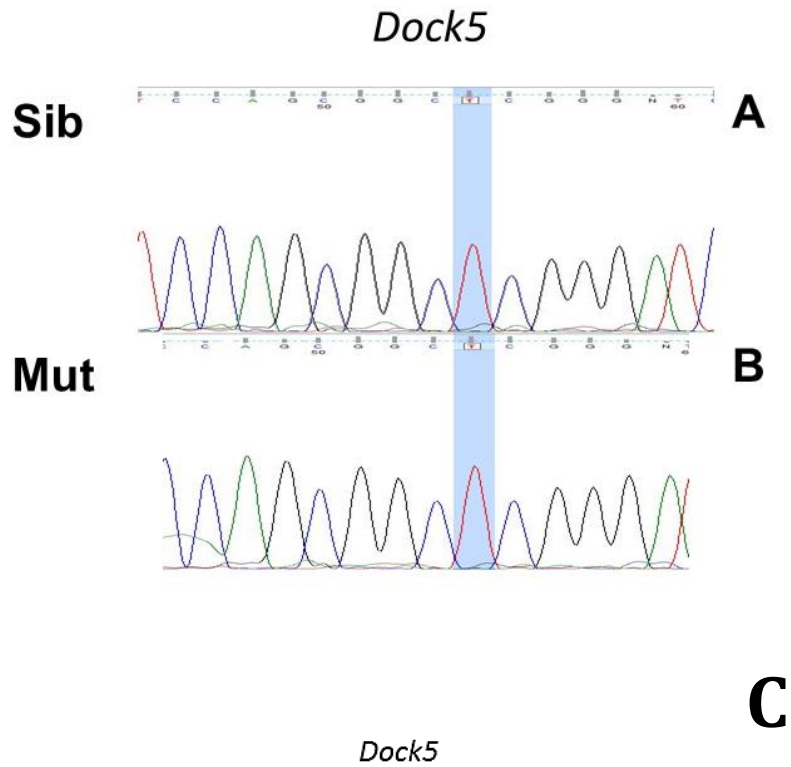
observed in the *specc11a* gene sibling and mutant DNA pools (Fig.5.7A and B) but because the nucleotide change was identified in the WT pool as well as the mutant pool this suggests that this change is not causal in FB148.5. Another SNP that was identified in the *specc11a* gene by WGS was examined and did not reveal a SNP change in the mutant DNA pool (Fig. 5.8). Finally, the *iqsec2* gene showed no SNP change in mutant DNA although the WT showed heterozygous alleles (Fig.5.9A) whereas the mutant sequence showed the original reference nucleotide as illustrated in Fig.5.9B and C. Taken together, DNA sequencing failed to identify any causal mutation among these polymorphisms.

5.2.3 GC CONTENT

It has been reported that GC content may affect genomic sequencing data as these areas cannot be accurately sequenced and give gaps in the high-throughput sequencing dataset (Marx 2013). In addition, the GC content also has been found to affect fragment genome coverage (Benjamini and Speed 2012). Thus, to investigate whether the genes in the candidate interval were previously identified in chromosome 8 are rich in GC content I examined the GC content manually using ABS software (Table 2 Appendix). However, the average GC content in these genes was 45%, suggesting that high GC content is not a likely cause for the failure of WGS to identify the FB148.5 mutation.

No	Genes	Chr	Position	SNP	Ref	Alt	GeneID
1	Docks	Chr8	7239105	SNP	T	G	ENSDART00000135834
2	Fnbp1l	Chr8	15591048	SNP	A	G	ENSDART0000045038
3	Specc1la	Chr8	31471171	SNP	C	G	NM-001039816
4	Specc1la/p	Chr8	31509171	SNP	A	G	NM-001039816
5	Iqsec2	Chr8	38087120	SNP	C	T	ENSDART00000111680

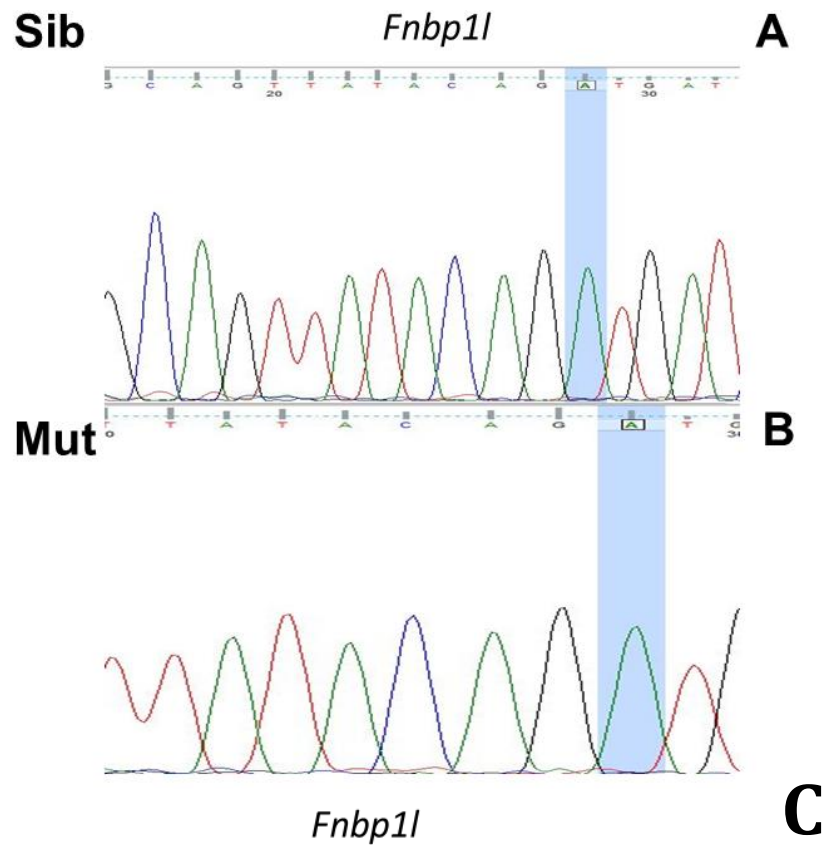
Table 5.1: Candidate LG8 genes identified by WGS and the polymorphism observed.



CCCTGCTCTCTGACAGAGAAGAAAAAGAGTCGTGTTGGTTCAGTGGTGATGCCATATATCATGTCGTCCACAC
 TCAGACGGATGTCCACCATCTCAAATGCCCTCTCCGGTCACTCCAGCGGCTCGGGATCCTCTGACGGGAATC
 CTCCAGACCCGCATCCAGGAgtcagtatccacaaatcaaagctcttattctttatctcctcgctttctgca
 ccacaccgagggctcatttgctgcaggacagaggtttcgggggtcaaggaaaggatgcaatgattcagtttg
 ccgtgtaattacattacttactgctagtggggttgctgctgggttaacaccctttaattggttgttaggtg
 ctggataaat

Figure 5.5: Sequencing of *dock5*.

(A, B) Sequence chromatograms for *dock5* revealed the same SNP in sibling (Sib) DNA and mutant (Mut) DNA. (C) Sequence with highlighted forward primer (yellow), reverse primer (green) and the polymorphism (pink). Sequence was exported from Ensembl genome browser.



```

ttcttctcgttcagTCCTGAAGGCAGTTATACAGATGATCACAGTCAGGAG
CATCGGTCTCCGCCACAGCCGGACCCTCACGAATTTGATGACGAGTTTGAT
GATGACGATCCACTCCCTGCCATCGGCCACTGCAAAGCTCTCTACTCTTTT
GATGgtacaaaacaatgtttactaaattactatacagctcacatgaccga

```

Figure 5.6: Sequencing of *fnbp11* SNP.

(A, B) Sequence chromatograms for *fnbp11* revealed the SNP was present in sibling (Sib) and mutant (Mut) DNA. (C) Sequence with highlighted forward primer (yellow), reverse primer (green) and polymorphism (pink). Sequence was exported from Ensembl genome browser.

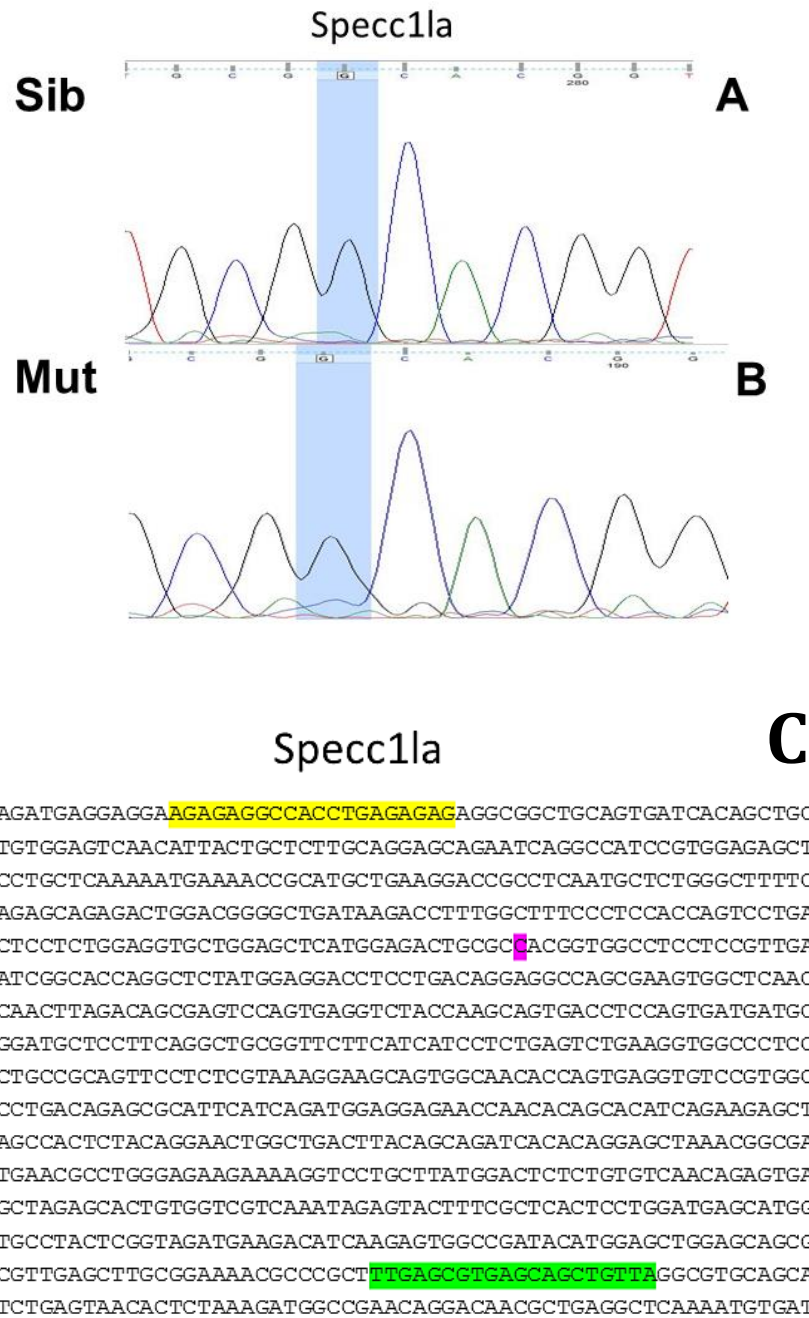
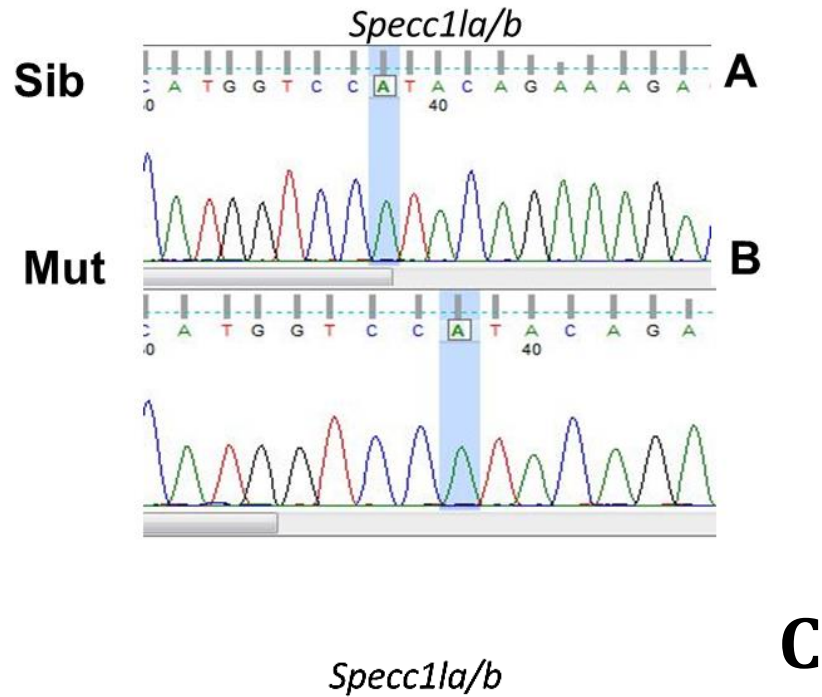


Figure 5.7: Sequencing of *specc1la* SNP.

(A) Sequence chromatograms for *specc1la* shows the SNP change from C to G is present in sequence trace of sibling (Sib) and mutant (Mut) DNA as C to G change (B) suggesting that it is not the causal mutation in FB148.5. (C) Sequence with highlighted forward primer (yellow), reverse primer (green) and polymorphism (pink). Sequence was exported from Ensembl genome browser.



```

ttaagtcataatatatatatatatatatatatatatatatatatatatatatatatatatatatat
atatatatatatatatataataaaccatgaagattcaatgatttcttcttgttcagtt
gagatctgaataagtgacacaattcccctcttccgttcag
GACATCACTGACATGGTCCATACAGAAAGACCGGACTGGCAGAGTGTTATGACTTACGTC
ACCTCCATCTACAAGTATTTTGAGACCTGAGCACATGTCCATTCACAAACTGCCACACCC
AGTGCAACAGATTTCCGCCA ACTAACCAGAGTTCAACTCTCCACCATATCATCCATGCCT
AACCTAGCACAAAGTCACATTACGTTACACCCCCATCACAAGGACAAATTCTGTTAGCG
TATACTGATATGATACTTTGATTTTGGATCTCAGCCGCTAACCCAGAATGAGTTTGCCTT

```

Figure 5.8: Sequencing of second *specc1la/b* SNP.

(A) Sequence chromatograms for *specc1la/b* revealed the SNP was present in sibling (Sib) and (B) mutant (Mut) DNA. (C) Sequence with highlighted forward primer (yellow), reverse primer (green) and polymorphism (pink). Sequence was exported from Ensembl genome browser.

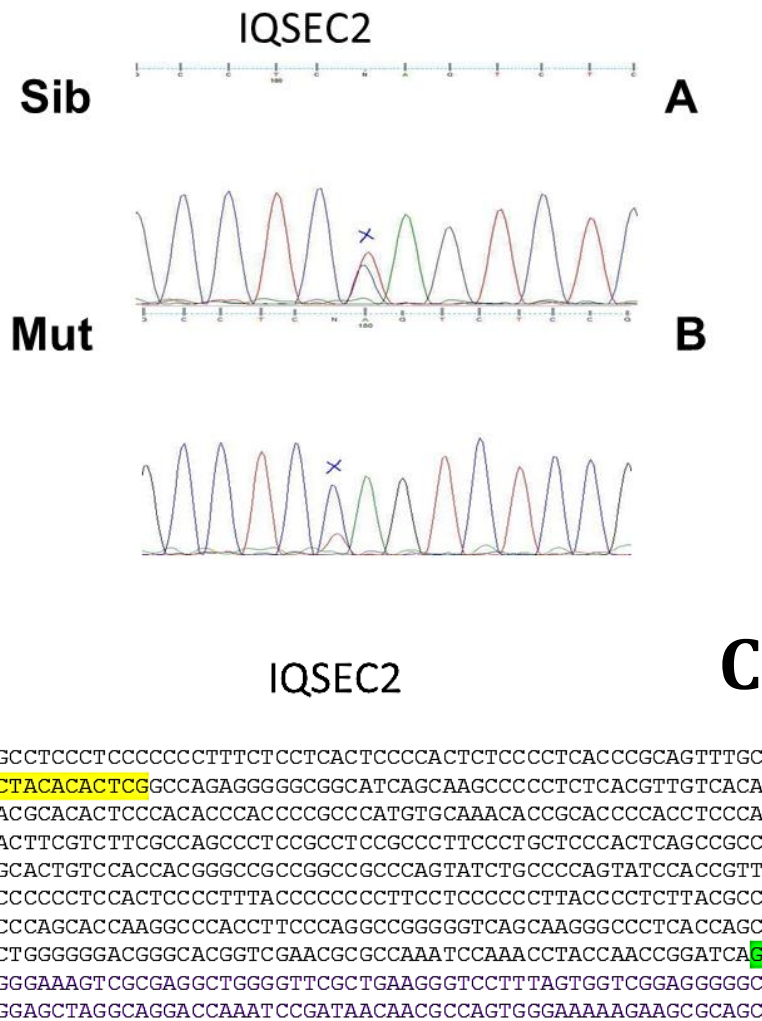


Figure 5.9: Sequencing of *iqsec2* SNP.

(A) Sequence chromatogram for *iqsec2* revealed heterozygous C/T SNP sequence in sibling (Sib) DNA. (B) Sequence chromatogram for *iqsec2* reveals no SNP change compared with reference sequence in mutant (Mut) DNA suggesting that this is not a causal change (C) Sequence with highlighted forward primer (yellow), reverse primer (green) and polymorphism (pink). Sequence was exported from Ensembl genome browser.

5.3 FB148.5 RESCUE BY BAC CLONE INJECTION

Since positional cloning and WGS failed to identify the mutated gene in FB148.5 we tried to rescue FB148.5 mutants using bacterial artificial chromosomes (BACs) encompassing the region of interest on LG8. Microinjection of BAC clones can partially rescue mutant zebrafish phenotypes (Yan, Talbot et al. 1998) but relies on the BAC partitioning to the required cell type. To determine whether appropriate BAC clones can rescue FB148.5 mutants, we found 7 BACs clones (Table, 5.2) in the region of interest by searching through the CHORI-211 BAC library (zfin.org) (Fig. 5.10). These 7 genomic DNA clones were injected in to 1-2 cell embryos and the injected embryos were allowed to develop to 4-5 d.p.f.. To evaluate partial BAC rescue, *in situ* hybridization was performed using the myelination marker myelin basic protein (*mbp*) as a probe so as to identify rescue of oligodendrocyte defects in the hindbrain.

The first BAC clone that was identified in the candidate area was CH211-220D9. This clone contains a number of genes including *ikbkb*, *plat*, *polb*, *si:ch211-220d9.3* and *vdac3*. However, DNA microinjection into mutant FB148.5 embryos did not reveal any increase in oligodendrocyte numbers in the hindbrain (Fig. 5.11C, D). Next, the CH211-51H9 clone was injected into FB148.5 embryos. This clone includes *aca2*, *fam102aa*, *gle1*, *mrpl40*, *naif1*, *seta*, *si:ch211-51h9.6*, *si:ch211-51h9.7*, *slc25a25a* and *zdhhc12a*. Again, the mutant embryos did not show any increased specification of hindbrain oligodendrocytes (Fig. 5.11E, F). Although, CH211-159C13 and CH211-146J7 overlapped and both contain only one gene (*lhx2b*), they were both injected into embryos and tested by *in situ* hybridization for *mbp* as before. Similar to the previous BAC clones they could not rescue FB148.5 defects in the oligodendrocyte lineage (Fig. 5.11G, H and 5.12A, B). CH211-218I18 was also injected into embryos to rescue FB148.5 phenotypes. This clone contains *cux2b* and *mtmr3* genes, but it also failed to

rescue oligodendrocyte defects in mutant embryos (Fig. 5.12C, D). CH211-166A6 was another BAC clone that was identified in the candidate interval and encodes *cux2b*, *myl2b*, *pptc7a*, *rad9b*, *si:ch211-166a6.5* and *srrd*. However, this BAC clone also did not show any rescue for FB148.5 defects in oligodendrocyte specification (Fig. 5.12F, E). Finally, the CH211-2408 clone which contains *diablos* and *or130-1* genes was injected into embryos but it did not demonstrate any rescue of the FB148.5 phenotype (Fig 5.12G, H). It must however be acknowledged that the likelihood of hitting the appropriate neural precursors with the BAC to elicit a partial mosaic rescue is low. In addition, due to time limitations only a small number of mutants were injected with each BAC and embryos that underwent BAC clone DNA microinjection showed lower survival rates than uninjected controls which might be due to the concentration of DNA injected (50 ng/ul) (Table 5.3).

	BAC-name	Genes	Size
1	CH211-220D9	ikbkb, plat, polb, si:ch211-220d9.3, vdac3	201525 bp
2	CH211-51H9	acaa2, fam102aa, gle1, mrpl40, naif1, seta, si:ch211-51h9.6, si:ch211-51h9.7, slc25a25a, zdhhc12a	187161 bp
3	CH211-159C13	lhx2b	137166 bp
4	CH211-146J7	lhx2b	153989 bp
5	CH211-218I18	cux2b, mtmr3	197983 bp
6	CH211-166A6	cux2b, myl2b, pptc7a, rad9b, si:ch211-166a6.5, srrd	151374 bp
7	CH211-2408	Diabloa, or130-1	187860 bp

Table 5.2 List of BAC clones that were identified in the candidate interval with their size and genes encoded listed.

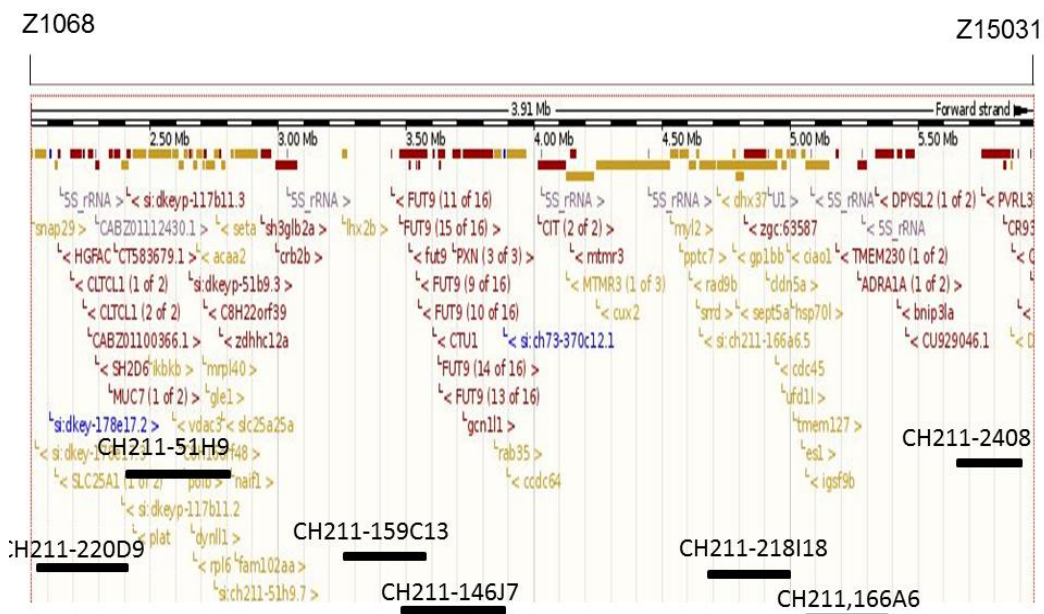


Figure 5.10: BAC clones locations in the linkage interval.

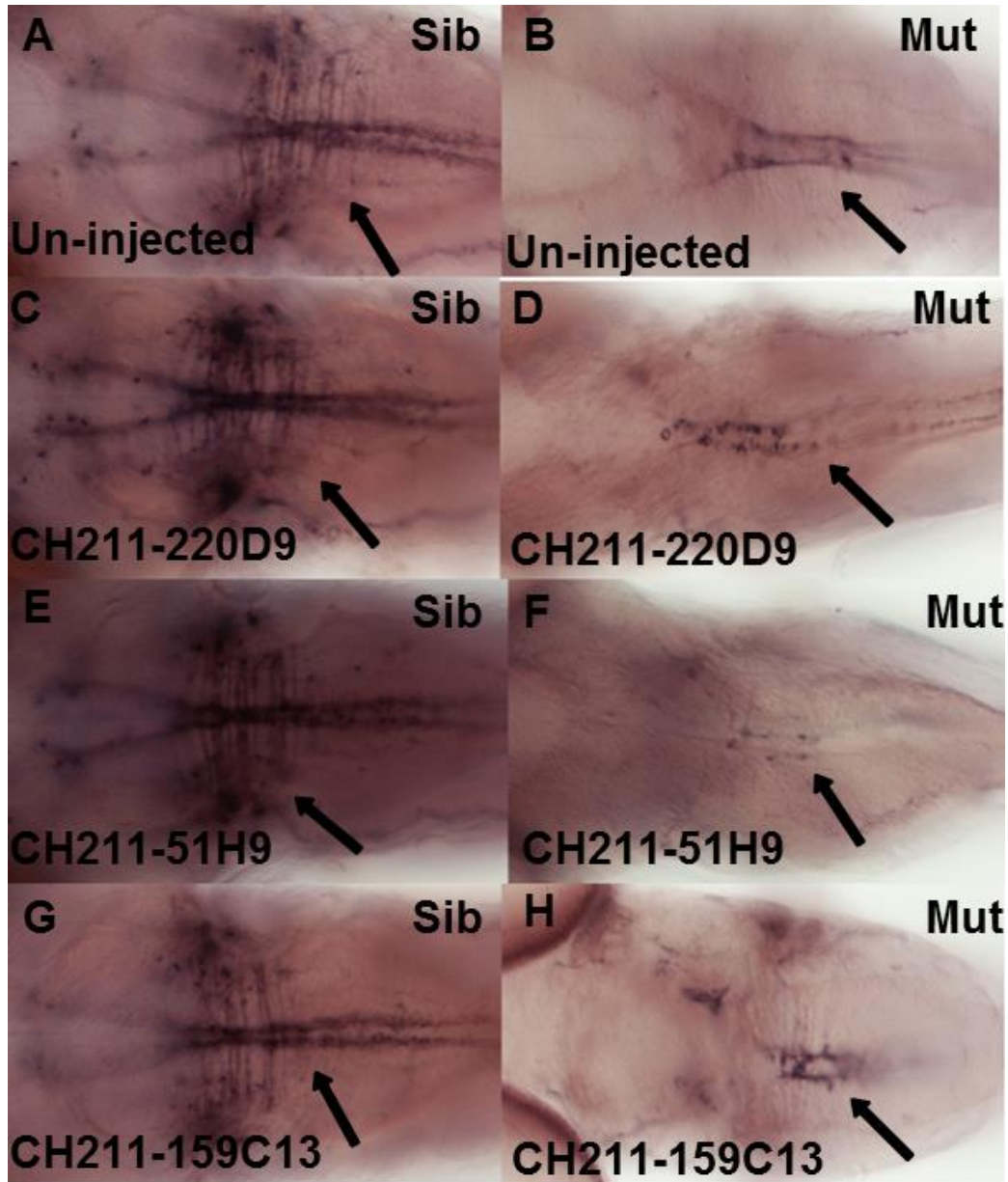


Figure 5.11: BAC clones did not give mosaic rescue of oligodendrocyte defects in 5 d.p.f. FB148.5 larvae.

(A, B) Show *mbp* expression in un-injected WT (A) and mutant (B) embryos. (C to H) BAC clones were injected into 1-2 cell stage embryos then larvae were assayed by *in situ* hybridization with *mbp* probe. (D, F, and H) CH211-220D9, CH211-51H9, and CH211-159C13 clones were injected into mutant FB148.5 embryos and in all cases it was found that the BAC clones could not rescue the oligodendrocyte defects in the hindbrain compared with un-injected mutant FB148.5 embryos. Magnification x20 in all panels. (technical repeat x1).

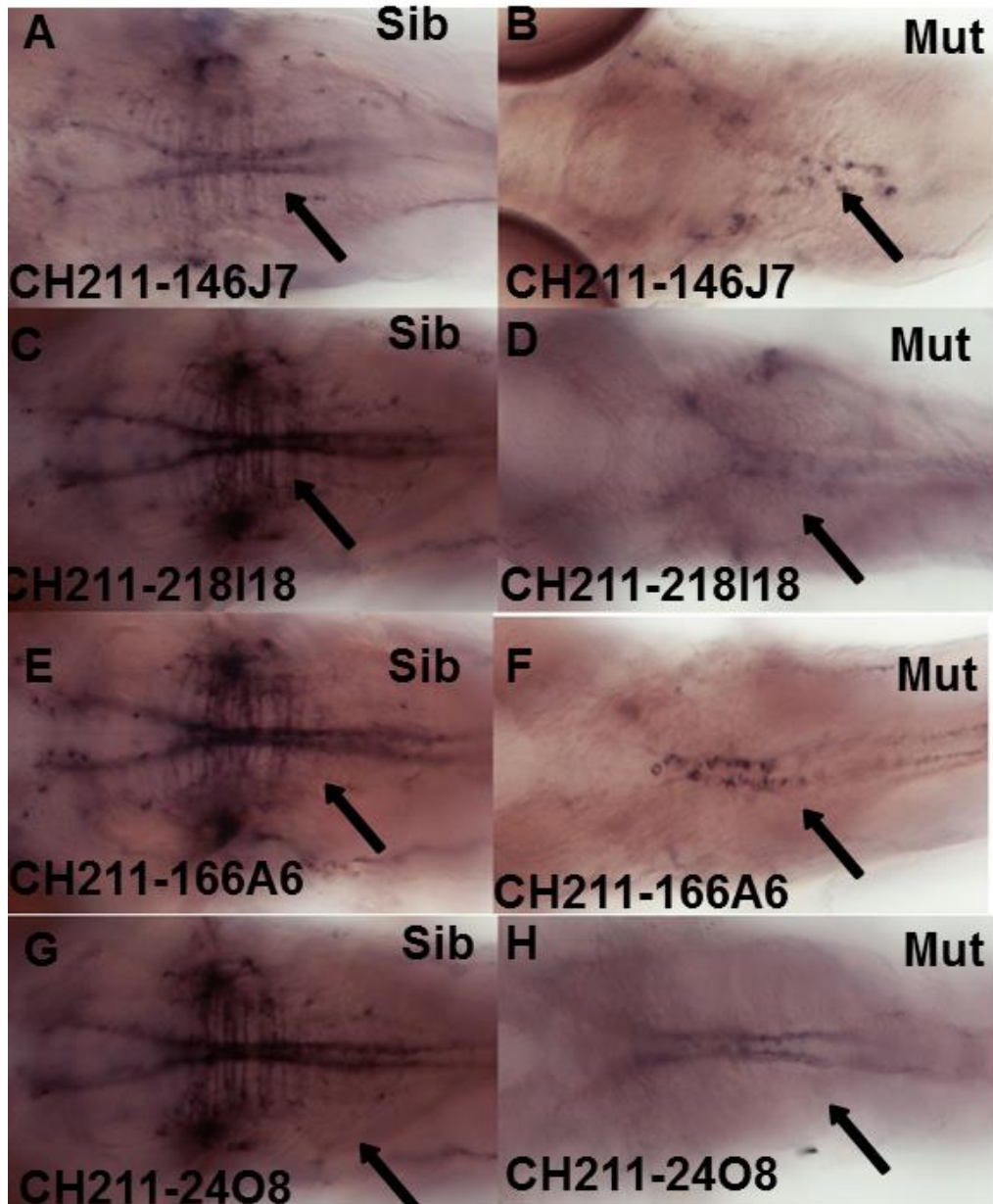


Figure 5.12: BAC clones did not give mosaic rescue of the oligodendrocyte defects in 5 d.p.f. FB148.5 larvae.

(A to H) BAC clones were injected into 1-2 cell stage embryos then larvae were assayed by *in situ* hybridization with *mbp* probe at 5 d.p.f.. (B, D, F, and H) CH211-146J7, CH211-218I18, CH211-166A6 and CH211-24O8 clones were injected in to mutant FB148.5 larvae and all showed that BAC clones did not rescue oligodendrocyte numbers in the hindbrain compared with un-injected mutant FB148.5 embryos. Magnification x20 in all panels. (x1).

BAC Clone	Purified DNA concentration ng/ul	DNA Concentration injected ng/ul	No. Sibling embryos	No. Mutant embryos	Survival Rate %
CH211-220D9	384.8	50	47	9	70%
CH211-51H9	380	50	32	5	32%
CH211-159C13	167	50	50	5	50%
CH211-146J7	93	50	42	7	36%
CH211-218I18	144	50	61	11	44%
CH211-166A6	134	50	58	9	27%
CH211-24O8	125	50	35	4	25%

Table 5.3: Quantification of attempted BAC rescue experiments.

5.3 DISCUSSION

In this chapter WGS was used as an alternative strategy due to the failure of the traditional SSLP mapping approach to refine the locus in the candidate region for FB148.5 on LG8. This approach also has the advantage of taking much less time and we sent a pool of 50 mutant embryos for WGS at GIGA Genomics in Liege. However, WGS failed to determine the FB148.5 mutation in the candidate region. One potential problem was that the mutant embryos that were sent to WGS were collected from more than one grandparental mutant which may have affected the degree of homozygosity around the mutation site. Others labs in the Bateson Centre at the University of Sheffield have had around 50% success rate with other mutants using this approach. It has also been reported that high-throughput sequencing in human samples has been unable to identify causal mutation in number of Mendelian diseases such as medullary cystic kidney disease (Kirby, Gnirke et al. 2013) and a number of possible factors have been suggested for this including the GC richness, presence of repeated bases, missing bases in the initial genome reference sequence and low genome coverage in the candidate region (Marx 2013). Thus, GC content was determined in the defined LG8 region and was found to be of an average level. However, the other factors mentioned above still need to be verified.

We obtained a list of variants within the candidate linkage group which displayed SNP changes in amino acid sequence or at splice sites. We then manually reviewed the list to determine genes with mutants carrying interesting phenotypes or having relevant expression patterns. We were left with a list of 5 candidate genes; *dock5*, *fnbp11*, *specc11a*, *specc11a/b* and *iqsec2*. We however failed to find a causal mutation in any of these genes. Dedicator of cytokinesis 5 (*dock 5*) is a member of the DOCK protein family which regulate cytokinesis. In zebrafish, it has been shown that *dock5* and *dock1*

are required for myoblast fusion (Moore, Parkin et al. 2007). Although the gene function for Formin binding protein 1-like (*fnbp1l*) is not well characterized, it was selected because of its expression pattern. It has been shown to be expressed in the CNS, neural plate and pharyngeal arches, and these regions show abnormal phenotypes in the FB148.5 mutant (zfin.org). Another candidate gene was Sperm antigen with calponin homology and coiled-coil domains 1-like (*specc1l*) since mutation of this gene has been linked with a human developmental disorder and zebrafish lacking *specc1l* function show jaw, facial structure and neural crest defects (Saadi, Alkuraya et al. 2011). Additionally, we selected *iqsec2* since it has been found that mutation of this gene leads to intellectual disability. *Iqsec2* encodes a guanine nucleotide exchange factor for the ADP-ribosylation factor family of small GTPases (Shoubridge, Tarpey et al. 2010). We excluded the identified SNPs in all these genes through PCR and DNA sequencing and thus were unable to identify the FB148.5 mutation through this initial attempt at WGS.

Subsequently, we attempted to rescue FB148.5 mutants using bacterial artificial chromosomes (BACs). We rationalised that microinjection of BAC clones might partially rescue the specification of oligodendrocyte precursor cells in mutant FB148.5 embryos. However, the clones injected did not show rescue of oligodendrocyte numbers in the mutant hindbrain compared with un-injected mutant FB148.5 embryos (Fig. 5.11 and 5.12). The limited number of mutant embryos injected and apparent toxicity of injected BAC DNA were limitations of these experiments which further affected the potential rescue efficiency. In addition, BACs encoding all genes in the candidate region were not available.

If time and resources had allowed, we could have sent a second pool of mutant embryos derived from a single mutant grandparent for further whole genome sequencing to help

find the mutated gene in FB148.5. Sequencing of the whole zebrafish genome in this study was performed with eight-fold genome coverage which is usually sufficient to identify homozygous SNPs, but increased genome coverage (e.g. 30-fold) will increase the chance of SNP discovery, especially in heterozygous positions (Bentley, Balasubramanian et al. 2008). However the best approach to take in future might be to use whole exome sequencing (WES) or RNA-sequencing (RNA-Seq) which can also be used to find causal mutations and give information on gene expression changes and alternative splicing. Other studies have reported that mutations can be found using RNA-Seq which provides a fast and relatively low-cost alternative strategy to determining coding variants (Cirulli, Singh et al. 2010).

6. CHAPTER VI: GENERAL DISCUSSION

The primary aim of this study was to characterise and identify the mutated gene in FB148.5 mutant fish and to define its function and roles during zebrafish development. The FB148.5 mutant was of interest to us since initial characterisation revealed very similar morphological phenotypes to those found in *disc1* morphants (Wood, Bonath et al. 2009). DISC1 has been one of the most intensively studied mental illness susceptibility genes and recent work from our group and others has demonstrated roles for *disc1* in oligodendrocyte development (Wood, Bonath et al. 2009; Katsel, Tan et al. 2011; Hattori, Shimizu et al. 2014). Accordingly, we hypothesized that these two genes may act together in common developmental pathways related to myelination. In order to characterise the FB148.5 mutant phenotype, whole-mount immunostaining and *in situ* hybridization studies were performed with a panel of neurological markers. The previous unpublished studies of the FB148.5 mutant suggested that it may induce a specific myelin phenotype. However, the further characterisation of this mutant described in **chapter 3** indicates that it has important roles in earlier stages of nervous system development. This work was done without performing sense probe controls, although all the probes that were used are well-known and control images are available on ZFIN from multiple publications.

The range of phenotypes described in FB148.5 is not unique to this line. Similar phenotypes have been described in mutants and morphants for other genes such as *pescadillo*, *gle1*, *ccdc64* and *nrg1* (see table 6-1). Mutation of *pescadillo* (*pes*) was mapped to chromosome 5 and causes oligodendrocyte formation defects similar to those in FB148.5 in mutant larvae. Also, these larvae showed similar morphological phenotypes to those found in FB148.5, e.g. defects in the eye, jaw and body length (Simmons and Appel 2012). This gene might be another candidate to investigate that

correlates with FB148.5 function. Notably, *Pescadillo* has important functions in ribosome biogenesis and cell proliferation (Lerch-Gaggl, Haque et al. 2002). *Pes1* mutant mouse embryos die extremely early, at the eight-cell stage (Lerch-Gaggl, Haque et al. 2002). In zebrafish *pes* mutant larvae showed oligodendrocyte defects which resulted from disruption of the cell cycle in neural precursors resulting in a failure to produce oligodendrocyte progenitors (Simmons and Appel 2012).

Neuregulin 1 is another gene that when its function was disrupted using *nrg1* morpholinos showed similar morphological phenotypes to the FB148.5 mutation line: it is also a candidate gene for SZ (Stefansson et al., 2002). It encodes a transmembrane signaling protein that interacts with receptor tyrosine kinases of the ErbB family. It has been reported that *nrg1* morphant zebrafish revealed similar defects in production of *olig2*-positive cells to those that have been demonstrated in *disc1* morphants. This study suggested that *nrg1* and *disc1* perform similar roles in the zebrafish hindbrain during oligodendrocyte precursor specification (Wood et al., 2009). It has been reported that in zebrafish *nrg1* type III is required for Schwann cell proliferation and migration (Perlin, Lush et al. 2011). Additionally, several studies on mouse models found that NRG1 has critical roles in regulating synaptic transmission, axon guidance and neuronal migration (Buonanno et al, 2001; Fischback G.D, 2007; Vartanian et al, 1999). Thus, this gene might be related to FB148.5 function through direct or indirect interactions with *disc1* function.

In addition, *gle1* was considered to be one of the most promising genes in the candidate region of FB148.5 as its mutants show a small head and eyes (Jao, Appel et al. 2012). However, *gle1* mutation was excluded in FB148.5 using a complementation test. Mutation in this gene leads to lethal congenital contracture syndrome type 1 (LCCS1), an autosomal recessive inherited foetal motor neurone disorder (Nousiainen et al.,

2008). Interestingly, further work on *gle1* mutant zebrafish larvae showed severe Schwann cell defects in them (Seytanoglu, Alsomali et al., manuscript in preparation). It is likely that FB148.5 is also involved in Schwann development, possibly playing a similar role to *gle1*.

In addition to the above genes, *ccdc64*, *mybpc1* and *tbx2a* morphants also exhibit similar morphological phenotypes to FB148.5 mutant zebrafish (table 6.1). These genes play different roles in organogenesis and embryo development suggesting that the FB148.5 mutated gene might be correlated with different genes that perform diverse functions during embryogenesis.

	Morphological phenotypes	Function	Chromosomal location	References
1- <i>gle1</i>	<i>gle1</i> ^{-/-} at ~48 hpf showed abnormal phenotypes including small eyes and head, underdeveloped pectoral fins, and cell death in the head and spinal cord. Some embryos also demonstrated upward or downward body axis curvature.	GLE1 mutations lead to LCCS1 fetal motor neuron disease (Nousiainen et al., 2008). Gle1 is an essential mRNA export factor.	Chr: 8	(Nousiainen et al., 2008) (Jao, Appel et al. 2012)
2- <i>nrg1</i>	Morphants showed small head and eyes	Has critical roles in regulating synaptic transmission, axon guidance, and neuronal migration	Chr: 10	(Perlin, Lush et al. 2011), (Wood et al., 2009).
3- <i>pescadillo</i>	Mutant embryos exhibited reduce brain and eye size and a lack of extension of the jaw, probably affected by the lack of cartilage in the branchial arches	Has important functions in ribosome biogenesis and cell proliferation	Chr: 5	(Lerch-Gaggl, Haque et al. 2002)
4- <i>ccdc64</i>	Ccdc64 morphants showed small eyes and head and a curved body axis	Ccdc64 interacts with the microtubule minus-end-directed dynein/dynactin motor complex.	Chr: 8	(Schlager, Kapitein et al. 2010)
5- <i>mybpc1</i>	Morphant embryos displayed pericardial edema and decreased growth of eyes and head. Some <i>mybpc1</i> morphants showed cardiac edema that was correlated with reduced heart	MYBPC1 mutations cause limb contractures characteristic of distal arthrogryposis	Chr: 4	(Ha, Buchan et al. 2013)

	rate			
6- <i>tbx2a</i>	Morphants showed abnormal body curvature, hydrocephalus, heart edema, and reductions in the size of the ears and eyes	Tbx2 is a member of the T-box family of transcription factors essential for embryo development and organogenesis. Tbx2 deficiency affects the development of the pharyngeal arches	Chr: 5	(Thu, Tien et al. 2013)

Table 6.1 List of genes that were found to exhibit similar phenotypes to FB148.5 mutant zebrafish

It has previously been reported that neurogenesis and OPC specification defects may result from neural precursor cell proliferation defects (Garcion and Faissner 2001; Grandel, Kaslin et al. 2006). We found that FB148.5 revealed neurogenesis as well as OPC specification defects, suggesting that FB148.5's effects on OPC specification and neurogenesis may be caused by defects in NPC proliferation. In addition, the jaw cartilage defects (Fig. 3.5) that have been seen in FB148.5 mutant larvae have at least two possible origins: one possibility is that disruption of normal jaw development may directly affect the specification of the relevant precursors. However, it is also possible that the jaw defects might be a secondary effect, since the jaw cartilages are derived from the cranial neural crest (CNC) (Noden 1983) and CNC proliferation and migration could be affected by the profound neural specification defects observed.

Chapter 4 of this study described chromosomal mapping of the FB148.5 mutation to identify the chromosomal location of the mutated gene. This analysis suggested genetic linkage of FB148.5 to LG 8, because several polymorphic SSLPs on this chromosome showed a high degree of apparent homozygosity and this was confirmed in offspring from multiple mapping pairs (table 4.1). Further analysis also suggested that the critical interval was a 15.2 cM interval flanked by the markers z1068 and z15031. This 15.2 cM interval contains around 50 genes (Fig. 4.18) and corresponded to 4 Mb of genomic DNA. However, this approach failed to narrow the candidate region because of an absence of informative SSLPs between the two flanking markers.

A number of limitations were encountered in this study which included the lack of any informative SSLP in the candidate region, the unsuccessful attempts at identifying intronic SNPs as genetic markers and the large number of candidate genes in the defined interval. Together, these factors seriously limited the positional mapping approach. Additionally, while the initial mapping experiments suggested the LG8 locus it should be acknowledged that the genome scan undertaken did not include all genomic regions.

This limitation was the result of a number of un-informative SSLPs and the lack of amplification of PCR products for some markers. It is therefore conceivable that the LG8 locus was a false positive.

Recently, a number of laboratories have developed WGS methods to map zebrafish mutations. These groups used similar strategies involving the sequencing of libraries from pools of 20-50 mutant embryos from a mapping family and then calculating the homozygosity score by analysing SNPs distributed across the whole genome (Gupta, Marlow et al. 2010; Bowen, Henke et al. 2012; Voz, Coppieters et al. 2012). Therefore we sent a pool of 50 mutant embryos for WGS at GIGA Genomics in Liege; however, WGS also failed to determine the FB148.5 mutation in neither the candidate region identified through the SSLP screen nor any other region (Fig. 5.2, 3).

Several limitations might have caused the WGS approach taken to fail such as the mutant embryos that were sent for WGS were derived from more than one grandparental mutant and only around 80% of sequence reads mapped to the reference genome. Other factors such GC content, the presence of repeated bases, missing bases in the initial genome reference sequence and low genome coverage in the candidate region (Marx 2013) could also be factors. Furthermore, a number of heterozygous SNPs were found in genes in the LG8 candidate region. Thus, these SNPs are likely to be distant from the mutation. This suggests that this may not have actually been the true region which was confounded by the mixed grandparental mutant background. Consequently, these findings are consistent with the WGS results.

Future work on FB148.5 mutants should therefore utilise whole exome (WES) or RNA-sequencing (RNA-Seq) as alternative genetic approaches to find the causal mutation (Cirulli, Singh et al. 2010).

6.1 FUTURE WORK

1- In order to determine whether FB148.5 is required for proliferation of neuronal precursor cells, future work would be performed using EdU incorporation as a cell proliferation assay. Crossing FB148.5 with transgenic lines such as *Tg(olig2:EGFP)* would enable proliferation of specific progenitor populations to be measured.

2 - To map the FB148.5 mutation WGS could be repeated using single mutant embryos and compared to single WT embryos rather than using pools of DNA to identify all SNPs that are derived from mutant line. As discussed in chapter 5, whole exome- (WES) or RNA-sequencing (RNA-Seq) could also be utilised as alternative genetic approaches to find the causal mutation (Cirulli, Singh et al. 2010). These have the advantage of utilising lower complexity starting material and less variation would be expected c.f. WGS. The main drawback with these methods is that they only analyse coding regions so certain types of mutation could be missed.

3- It is well known that DISC1 is multi-scaffold protein that interacts with many other proteins, so once the mutant gene has been identified it would be important to determine whether DISC1 interacts with the FB148.5 protein. Yeast two-hybrid and co-immunoprecipitation assays could be done to test this. Additional research will be needed into these genes and their protein products to help our understanding of how they may affect each other or are linked, and which molecular pathways are regulated by them.

To conclude, this study describes FB148.5 mutant zebrafish which show defects in oligodendrocyte precursor specification, neurogenesis, motor axon outgrowth and Schwann cell development. However, mapping this mutant to a known gene using different genetic approaches failed. Therefore, further experiments to identify the gene

mutated in FB148.5 are needed. These studies support the utility of zebrafish as a model system to understand myelination in relation to human disease.

APPENDIX

Table .1: SSLP marker panel for initial mapping (genome scan).

This table shows SSLP locations and their chromosomes.

No.	Marker	Chromosome	Position map cM
1	z1986	1	3.5
2	z728	1	3.5
3	z1525	4	15.6
4	z9920	4	36.7
5	z10785	7	8.9
6	z1206	7	25.1
7	z10789	9	70
8	z49814	9	81.8
9	z4593	1	3.5
10	z3953	1	3.5
11	z21636	4	42.6
12	z11876	4	55.5
13	z4706	7	36.7
14	z3445	7	41.5
15	z4577	9	91.2
16	z6648	10	4.7
17	z22168	1	3.5
18	z10340	1	5.1
19	z984	4	74.8
20	z3275	4	75.8
21	z1182	7	45
22	z1059	7	52.3
23	z15847	10	10.2
24	z26181	10	19.6
25	z3705	1	13.4
26	z5508	1	24.2
27	z15414	5	3.6
28	z11496	5	17.1
29	z8156	7	60.7
30	z1239	7	70.6
31	z13632	10	28.9
32	z9473	10	46.4
33	z1781	1	85.1
34	z7634	2	20.3
35	z26471	5	33.9
36	z13833	5	50.3
37	z13936	7	85.9

38	z1068	8	13
39	z1145	10	44.7
40	z618511	10	36.4
41	z22527	2	46.6
42	z8451	2	47.7
43	z13641	5	57.5
44	z14143	5	77.2
45	z4323	8	35.2
46	z13412	8	43.3
47	z9701	10	77.2
48	z3260	10	92.5
49	z6617	2	62.9
50	z1703	2	82.6
51	z4299	5	83.1
52	z1202	5	103
53	z27391	8	55.1
54	z21115	8	62.3
55	z10919	11	2.8
56	z47548	11	12.2
57	z20550	2	85
58	z872	3	13.1
59	z13275	6	12
60	z6624	6	31.1
61	z7130	8	65.8
62	z14670	8	70.8
63	z8214	11	15.8
64	z13411	11	22.8
65	z8208	3	38.5
66	z15457	3	40.9
67	z17402	6	33.6
68	z51328	6	36.2
69	z9279	8	81.5
70	z10929	8	98.4
71	z22038	11	36.8
72	z1590	11	72.9
73	z9964	3	58.8
74	z10964	3	69.1
75	z22712	6	39.5
76	z5294	17	32.2
77	z1777	9	8.3
78	z6268	9	32.5
79	z1778	12	3.6
80	z3690	12	6.3
81	z20058	3	85.7
82	z9463	3	97.4
83	z13614	6	67.9

84	z4297	6	88.1
85	z54333	9	31.1
86	z4673	9	37
87	z21911	12	21.1
88	z1473	12	30.4
89	z6019	3	107.9
90	z1366	4	10.9
91	z1680	6	89.2
92	z3273	7	1.9
93	z5080	9	48.7
94	z20031	9	64.1
95	z50970	12	40.7
96	z28630	12	41
97	z1400	12	69.1
98	z1358	12	78.7
99	z17410	14	2.3
100	z21155	16	20.7
101	z11380	19	22
102	z4825	19	28.1
103	z10321	22	35.1
104	z21243	22	43.3
105	z1531	13	4.7
106	z6104	13	25.2
107	z6365	16	18.38
108	z23305	16	46.9
109	z7450	19	31.9
110	z3782	19	3.5
111	z9084	22	55.9
112	z8945	23	9.4
113	z5395	13	40
114	z1627	13	40
115	z1215	16	48.9
116	z4670	16	60.1
117	z11403	19	62.5
118	z1803	19	91.6
119	z4003	23	16.6
120	z15422	23	32.2
121	z9868	13	45.3
122	z17223	13	51.5
123	z25049	16	60.2
124	z4268	17	3.8
125	z6804	20	7.9
126	z9334	20	30.6
127	z3157	23	48.6
128	z1773	23	60.2
129	z6657	13	57.3

130	z6007	13	80.7
131	z1490	17	15.1
132	z22083	17	24.6
133	z11841	20	49.8
134	z3964	20	66.2
135	z5075	24	2.5
136	z1233	24	4.8
137	z5436	14	12
138	z5435	14	34.6
139	z22674	17	29.9
140	z9847	17	40.9
141	z21170	20	67.6
142	z4394	20	75.7
143	z1061	24	11.5
144	z1584	24	14.3
145	z11725	14	49.8
146	z22107	14	58.3
147	z1408	14	52.2
148	z4053	17	57.1
149	z13626	20	86.5
150	z24333	20	92.2
151	z5413	24	16.6
152	z23011	24	36
153	z3984	14	84.8
154	z6312	15	9.7
155	z8771	17	69.2
156	z63995	18	1
157	z56034	20	102.4
158	z4329	20	112.3
159	z3399	24	44.1
160	z5657	24	66.3
161	z6712	15	15.4
162	z21982	15	34.1
163	z1136	18	4.3
164	z1144	18	7
165	z3476	21	2.3
166	z1274	21	2.3
167	z3901	24	72.2
168	z1243	24	76.9
169	z11320	15	54.1
170	z13822	15	73.3
171	z8488	18	32.5
172	z10008	18	44.2
173	z4492	21	20.5
174	z10960	21	38.4
175	GOF15	25	1.1

176	z8238	25	32.2
177	z7381	15	79.6
178	z732	15	87.5
179	z3558	18	55.4
180	z5321	18	70
181	z4425	23	34
182	z42626	21	71.5
183	z3490	25	36.4
184	z22028	25	50.5
185	z41067	15	92.2
186	z5223	15	98.2
187	z4009	19	12.7
188	z7964	19	18.5
189	z1497	21	119
190	z10673	22	12.6
191	z5669	25	52
192	z1462	25	64.2

Table 2 %G~C content in the genes in the LG8 candidate region

No.	Gene	GC%	No.	Gene	GC%
1	CTU1	47%	29	<u>dock5</u>	46%
2	Seta	42%	30	<u>neflb</u>	47%
3	Cux2	42%	31	<u>lhfl4b</u>	38%
4	ADRA1A	51%	32	<u>specc11a</u>	37%
5	ccdc64	51%	33	<u>IQSEC2</u>	38%
6	dynll2	42%	34	UFD1I	48%
7	PVRL3	36%	35	Cdc45	47%
8	snap29	34%	36	Cldn5a	62%
9	PPP2R2A (2 of 2)	51.69%	37	dhx37	50%
10	bnip3la	55.60%	38	sept5a	47%
11	si:ch73-112n4.4-001	34.10%	39	gp1bb	59%
12	si:ch73-112n4.1-201	55.70%	40	cux2b	57%
13	ADRA1A (2 of 2)-	52.70%	41	srrd	47%
14	TMEM230	48.60%	42	rad9b	48%
15	igsf9b	46.30%	43	pptc7a	52%
16	es1	52%	44	myl2b	51%
17	Ciao1	52.20%	45	mtmr3	54%
18	naif1	59.8	46	CIT	54.70%
19	seta	46.4	47	rab35b	46.5%
20	rpl6	54.1	48	gcn11l	55.6%
21	gle1	53.6	49	pxn	52.6%
22	mrp140	49.3	50	ctu1	54.2%
23	acc2	53.8	51	fut9	42.3%
24	vdac3	52.5	52	ihx2b	54.8%
25	polb	46.4	53	crb2b	53.1%
26	enk01	56.1	54	fam102aa	54.3%
27	ikbkb	52.7	55	naif1	59.8%
28	plat	52.6	56	seta	46.4%

Figure 1: Intronic PCR primers used

Enkd1-001

Intron 7-8

```
atctttgatgacatccataactaagtaaggaataggttgaaaagagcaagagaggcag
aaaaggcaggcagctgtgtcattatagcaaaaatttgaacatatgttcaaaaagactgcc
aacagggttaaggctaaagttaacttactccctcacagatgaaaaactgtccctatctgtg
aggttctaggctaaactggccgattagctgggaagtcctgtttatttattgactgtcca
gtacatgacctccctttgcttattttttcaataactgtcctacgaaggctttaaagc
cagcggagtcctcagctgtcagatgtcacttcacagcaaaaggcgtaatcccatcacgt
ctgtgtttttgaggctgtttggtcacttcattcgttttattctgatcggatataaaatccg
atcgctcaaaccacttcagaagggtgactgggatgcatccagatgaaatggacaggtt
tttagacaaaattaataaaataaaactaattatgacctggagataatctgacctgccc
tgaacacactgtgggtgcttttacagccaaaattctatataaatatgtttacgtaag
cattaaacgtgttctaaatttcaggcctgtagccaggggggggttcggaagaccacc
ccacactgacaaagggtccagaatttgtcccatatatgagctcatttgcctattctgact
```

Figure 1A: Primers used for *enkd1* intron 7-8. The forward primer is highlighted in yellow and the reverse primer in green.

SH2D6-201

Intron 4-5

```
gtttgtgtgcgtttatgtgtgaattgtttttttttttgtattgtcatgcttatccctat
ttggaagtgttttagtcgaggtatacttttcagaattaaatgtgtatataacatttgggt
gacacgggtggctcagtggttagcactgtggcctcacagcaagaaggctcactggttcgagt
cctggctgggtcgcttggcatatctgtttggagtttgcagttctccccgtgttggcgtg
ggtttccctccgggtgctttggttttcccacagtgcaaagacatgtgtaaatgggtgtag
gagtcacatctattagctcaatgacgaaactaacagcatggtcgaagggtttaaagcatgta
agccttttctagtgttctgaaaagaattttattttatttagaattttatattatattag
tttttagctccgaattcaatctgactccaatttcaatgatcctaaaatgtaaattatatt
tctaattgtaagaacggatcacattcatcatttatgatattaatttagagttctgatattt
tctgaggtccgatattataagttgtacgttcattagggacctacgtcgctcagagttcca
cgccccgggtttgcatttcttctcaggacaatatgtctgcactctgaaaatagtcagag
```

Figure 1B: Primers used for *sh2d6* intron 4-5. The forward primer is highlighted in yellow and the reverse primer in green.

Acaa2-001

Intron 5-6

gtcagcgcaagatatacaccaca^{gtcagcgcaagatatacaccaca}tatcctggataaattctgcattaatataactagcactt
ccgtttaggtcataactcatgctattaactacctgcccaatgttaaagtcacagtgaaat
tacaataaagtttttagatgtagtttcagtcgttaaggatatctataatctagtggtg
atccaaaatagtgacaatttacattaagtaaataaaaactgataaaaaatccaagcct
gtcacttcgcctatatgcatcattgtttttgttttttttacatcacctcatgctatagt
ttctcatccaattttctgaccaatcaaatgctctcttttgtctgacatgccccgccctt
tttcatttgcttttcatttaattcgcttgagcttaaccactctcactggcagagctgtga
gaaaaccaaagctattggctgtttatataaaaagggaggagctactcagtcgcaccctc
tctcatggttcagtttagattacgtcagacataaaacaaaagtcacatttcaaagcac
ttcgtggaacctttaaataaattaaaagtgtgaaaaagtaaatggagaactctttgtggg
gagagaaaatgtttgtggatgttatctgttcacatacactcatactc^{acactctctctct}
^{ctgctgcag}

Figure 1C: Primers used for *acaa2* intron 5-6. The forward primer is highlighted in yellow and the reverse primer in green.

Seta-001

Intron 1-2

ctattattgtagttgattcgctttgtgtggttagact^{gaggtagctctgctggatggcgg}
cggcggcagcagtagtaaccggcggcggaggccatgtttgatttctagccgaactataag
cgcgccacaaagccccattaggacatgaagaaactgctgtatttattgctaatcaaactg
caaggggtttgtttatgaatcacacaggttattttattagaaaagcagctgcattttaa
acgcatgaaacatgcggaacggaagcgtccgcgcgccgctttatgttgtgtgttttag
cttttagcttagcagaagcgcgtctccgccatgatgcagcacgatctaattggaggtttacg
gactttaaataggcgaataatggtggaattaaatgctggagtggtttttgtgtgtattttc
ggctcatgtgggatgtgttctcgggtggcggcgggaagcaggtgcagcgcgagcggggaag
cgcacatttaaaccacgcgcatctgcgcggctccgttcagttccaatgatacactgcact
cgcacaaatacacgcttttctcaagatgtaatgcacggagtttatttacaataaccca
tttaatgctactgcacgtgtagagcaacgcttgattagaaataaaa^{gctgtttcgatcg}
^{ttttgcg}catttatttgattttattttaaacagaatatcatgcaattgtacaaatatac
atcaacaaaatatttagttattcatalccgcgtaaaaataacactgcattctatgaagca

Figure 1D: Primers used for *seta* intron 1-2. The forward primer is highlighted in yellow and the reverse primer in green.

Seta-001
Intron 3-4

gtgagtttaacttccttgaatgcttttacagaattttgatgccagaatggttttgctggg
ggtttcagtgatatttagagtcctccatcctaagatttaaagcatatatggttatTTTTTgt
gtagatcca taagttatagtagatataaatgaacctaaatattgTTTTTaaacattta
gcttctattaatctctcttttatatttagtttacttttaatggttcatttaagatggtta
aaaaattgTTTaaacttttataaaaacatctatagtttatTTTacttatttcaccaacagt
aatttaattataaaaataaaaagctataaataaacctaaactattgTTTTTaaatattta
aaagttaaaataatgTTTTctcagggttctgcagggctcttatatactttatcttaatg
tcttcaatctcaaaa tccaaatTTTtaggtcttaaaaaggctcttaaatttatggaaatatt
gtgTTgTcggtcttaaatTTTaaaagggtcttcatttcccttTgTTtatgtattgctg
cttaatctagccaaaaccatatacaatcatcaacaatctatctaaaaactTTTaaactTTT
atTTTaaaatgcaatTTTaaacctatTTTatcaaatggtttatTTTccctTgcaataaca
ttgTTTTaaatgTtctccatgattTtactgctgga gacaccgacctgcacggattgtgc

Figure 1E: Primers used for *seta* intron 3-4. The forward primer is highlighted in yellow and the reverse primer in green.

Seta-001
Intron 9-10

gtgagacttggggttgagttatgtggcaaaaatataataatcacacaatTTTcattTTTg
gtgaactaactcttcttaataatttaagggttagttcaccacaatgtcaagtgtgt
catttactcagccttgactagttgcaacttgTTTaaTTTtgagttggctgttgaaaagc
ataaagatgctgtgaaatagttggaaccggttaaccattgatTTTccctcatattgtTT
TTcctacaatggaagttaatcgTTacaagTTTTtgataTTTcttaaaatgatcattTTTg
ctcaacagaacccaaaaaattTTTaaaacggTTTggacaagTccaaatgggagtaaTga
ctTTTaaTTTttgagtgaaaaatccctTTaatgctgccagctTTgaaaaagTaaaTTTta
atTaaaggaaaaaataataatgacgggtcatttaattattTaaagccacctgatgtgctt
agcacagtggtgttacacctgtgtgcattataataattcagTggcttatcaattgttc
cataTtgagccaaaactTTTcttgaactctTTTtagtctgtggttatctgaataaat
gccacagctTTgaaacagaggtgcccAAactcagTcctggatggccggTTTcctgcataTT
TtagTtccaaatctgaattaaatgcattTgaactaataaagctctTctgggtacactaga
aactTccaggtaggtTgtTgaagaaagTtgaggctaaaaatTcaggacaccggccctc
caggaccaagTTTgggcaccCCAatcttagaatgtTcaatagccaatcaataTcaagca
ccaacagctctgtagtgaattaagTtacaatgatagattaacacgaacaaatTcacat

Figure 1F: Primers used for *seta* intron 9-10. The forward primer is highlighted in yellow and the reverse primer in green.

Ciao1
Intron 1-2

tcagctttgaatttgatgcgagcagcaactggcagccagtgcaaacggatgagtagcggag
gtgacgtgttctttcaggttcattaaagaccactcgtgctgctgctgttctgaagcagctg
aagaggtttgatagagttagctggaagccatatataaaatataataaaacaatttttt
aaatacttttattgtttcagaaaaatgtgatacataatgtattagtaaccaaataccaat
caaagaacacccaaccccatcccgcagagacataatataatataatataatataatata
tataatataatataatataatataatgtttacacatacagtacatgcaaaaaatattaat
taataaatgaataaaagtaaaaactaaaataagataaaaataataataaaaaaggg
caattttgaaaaaaaaagacattaaagacaatgacagttcaacacacatacattccaatga
aagtgaaaaagatattaagttagtcataacaaacacagtgacattaacacagtcacat
tgtttgtgattactaaacgttcaggccattcttacttaaaaaataaagaaagaagtccca
aatcttgtaaaatagtgcattttttgtttgactgagtaagtcagtccttgcatgctat
acaagaagacatttcctcaatccagagtgacaaagatggaccatgaatacttctccagtg
aatggcagtcaggcatttcgtatgcaatagacacagattttaaaacttctgttcatatga
cttcagcagataaggcaggtgggaaaagaccaagaacacagatttagggcaaacagggatt

Figure 1G: Primers used for *ciao1* intron 1-2. The forward primer is highlighted in yellow and the reverse primer in green.

Plat-001
Intron 19-20

gtaagagaaggtgaaaaagaagtaaaatagtggttttttactcatgtaaaagtgctctgtga
tgtaacgtgtgctgtatgcatataaacacaagagtttaagatggtatcttccactttc
caaaaattaaacaaaaataagcattgaaacgtgcatgtgtgacctcaaaattctaatta
tgaggggaaaaatgctactccgggtatatacaggaatcagagagtgaaattcaatacttt
ataacacctatataaagacattttaactggtaacactggcgacatttgaacgtacttata
ttgactaaatactgattgtaagaaagtgtgaagagttatgcaaaaactcttattcagtcaca
atthaattcagaatggtggtaacgaagaatagtaagtgaaagaatcgtgcctgatgtgaa
ggtttgaaagtgtttgtactgtatttaatgtcagcttgaacgttgaataaacagcaattt
ggatattgctgccacctgctgctggatttgggtgtgttttttttatccatgactgaact
gaaccaaagtaccaactgtacaacaatgagcaaaaatattgtttaattatcttataatata
gcttatacattatattttatatacacatttttctgacttcaactgtataaatatata
taatgtatatgtctgtaaaaaactaaaaactctatttttgtcttcaatacagcacaagt
gtgagtttttcccctcatcttttctccgtgtgtgtctgtcag

Figure 1H: Primers used for *plat* intron 19-20. The forward primer is highlighted in yellow and the reverse primer in green.

ccdc64
Intron 1-2

ccatcttaca~~aa~~atagttataagctattcacacaataaaaaaagaactg~~cg~~gga~~cg~~ctcg
tgtataaaccagacttaagaacttgggtggttttgccttaataattggttgcctagaagagtgt
tgagaatgcaattcctggttcaagaaatgagc~~ca~~actaatgatgaaaaactgaaatata
aacataataataat~~ac~~attaagaagtgtcctgctctggagagacaggtgacagctagataa
tagagtagaacagcttcacgagcaggtaaagcctagtaaagacagacagcataaatgttt
agctaattgagttgaacatatgtgctgtgttggacagatgctttctgttgccg~~cg~~cgca
cagggggt
tgtcaaaaagcttga~~cccc~~agcagctaatctgatcagagagacgcattg~~c~~actaatta
cattacaaagggttagagggggtggg~~cg~~gtgggggagacacacaaaaacagac~~ct~~acat
ttcattacggagatgagctgattttgac~~ct~~ttttataatagatgatctcattgactttat
gttcaactggtagactggagggtt~~g~~aggaaatgaaatcaca~~aa~~gcaaaatcagt~~aat~~g~~cc~~ag
~~at~~cacactgca~~ca~~at~~ttt~~tagccctgatttcttgcctcggtcgctagatttctatccaaaa

Figure 1I: Primers used for *ccdc64* intron 1-2. The forward primer is highlighted in yellow and the reverse primer in green.

CIT(1 of2)
Intron37-38

gtcagagtcactctgtaaattcacttcactaactaatctga~~ct~~aactg~~ct~~t~~g~~ctgagctgc
gcattagctgtccctccagttacata~~tg~~caaaataaccaataactaactgctcaaccaat
cagccccaccaatctgaatgcttactgataccgtttaaccttcagccaatcaaaaa
tcttttatctgtccagcagttcagctaat~~ta~~aaaccactgatatctttccagttttcag
cfaatcagaacactttcatcggtccagccgttcaaccaatcagagttcttgaatctatcc
agccctaccaatcagaatgcttactgtctccattaaccttttagccaatcagaact
ctttcatttgcagcagttcagctaat~~ta~~aaaacattgacatctttccagtccttcggc
aaattagaacaccttcactggtccagccactcaaccaatcagaattcttctatctatcca
gccatacgaatcagaatgcttactgtattcctctagcctttcagccaatcagaatc
ttccatctgtccagcccttagccaatcagaacgctcggttctat~~tt~~tagettcaaccaat
ccgaatactgtattgtattcgtctaatcttttagccaatcagaactggttcactgtcc
aggccttaaccaatcagaacgctctatctatccagacttaaccaatcagatcactgt
attgtattcgtctaatctt~~tc~~agccaactgtccagc~~ct~~ttcaaccaatcagtagg

Figure 1J: Primers used for *cit* intron 37-88. The forward primer is highlighted in yellow and the reverse primer in green.

lkbkb-001
Intron6-7

tagtttacattactttggtagcttaaagcgatgaaacaccatttaactagtga~~cg~~gc
tgcattc~~g~~aaacactg~~ct~~tcac~~gg~~agcttcaaaaacttgacaaatctcctggtttgaaatc
agtggtttgagcagctatttaaaaaaagtgttaaggtcacatgattttagtaaacgag
gatttgttatggtataactttcgaacggttaaaaaaatcaatgattctctactgacgg
gtgatctgtgtaacaccataaaatccacataaatcatgtaggtgactcagatcgcccc
taatggctaatcactaaacaggttttatagttttacctgatcagtttgcgatggtttt
tccaaatgtaactgtctg~~cg~~gactgcaatagagggcgtaacatgaaaggagcgtgactt
gtagttatcaagatccaattgaacctg~~cg~~aggtgtcaaatgtttcatgattcaacatg
at~~tt~~gata~~tatt~~atcattcattca~~tt~~aaggaactctactcgtgacttctcatctgt
ttttttcatgacagtttagcctactcgcctgccccctggttgcaattaacagtaca
atggcagtcaaatatgaaagcctccataactcgcggtgaatgttaataactgtgattg
ttaggttagatttgggaaagggtgaaaccttaataacctgtgatgattgggttagggtt
gggggtagacattagtaactgtgttagttaagtttaggttgggaaaggcctcaggacatt
aataactat~~gat~~gg~~tt~~ggggaagg~~tt~~ggacattaataactgtgatggtgggttaggt

Figure 1K: Primers used for *ikbkb* intron 6-7. The forward primer is highlighted in yellow and the reverse primer in green.

Ikbkb-001
Intron8-9

```
caataagcatttgatatagaatcctcatgtcttttataaaaaacaat tcatttccatgg
tttccatgtctaaaattcatagagacttttataatcaccttattctttgctgacgagc
gggcgcagccatttcagtctttttggctcaagtcttccggtctcatacacttccattcat
ttttagacattaaaaactgctcgtttcgtgtttgatgttgcaactgatattttcttat
tatattatctacttagtctgtatagtcatgcaaacatttgttgtagagcaagtagttt
gactgtttctgccgtttattattcctagtcattttctcataggcgactgaatcggaag
ttctaaaaaatcgcaaaaacaggcgacttccacattttagaataaggtcaataccttg
gattttcaagactgtgggaatcttagtttcagctgttttggatgttaagctgaatacat
ttttggcctcaaatcctgctccaaaacatgtctttgattatgacgtgtaaagtgaggaa
attacagcattttctaaaataattaataaaaaacaacttctttttcttatacgtcgaaa
tagtgccagtataaattcagaataacaggttacctgttgaattcatcagaaaaaaagc
aaaaataaccacaatcacacaatttaagccatgacctgtcagtgtaggtacagatcct
gttccccatgcagaaaaaccttgataactcatgataaagcactattgttgtaacttctt
atgcttgcgtaagataataatccccctcacagcagtggttattgcagagagatctctgt
actgtgatggcgttctccagtattgtcaacacacaaaactgttttataaataatctc
tgagaatgaaagaa aaatcaagactgacgcggggctcaagggtgtgtgtaaaacaacc
```

Figure 1L: Primers used for *ikbkb* intron 8-9. The forward primer is highlighted in yellow and the reverse primer in green.

gle1
Intron2-3

```
ttacgcacaacgctgtgttagctacaaaaaaaaacaacaaatcaaatgcttgtggtaatc
ataaccataagatgcgatttgatcacttaagatgtg cgcacaggcttcacttctagtgc
agctcacgtgtgatctcccgctccgcaaatacatcattacatgaagacagaaatgacattt
ctgggtgaattgtaccttataaaatcacagatgtgacacttttaacaccatttgaagggtg
caatgttgtgaatgactgtacgactcctgcaaccactttaagcttctcttctgaccttg
aaaataataattggctgaatcatagaaaagctgaattaagatcgtgtgtagggctgaaatcg
agattgtgatctttttcgattaatcgtacagctcactgtatgggtaaaaaatattgac
attgtaactaggttaatttcgatttttaataatttaaaatttaagaaaatattaattgaa
tattttggcctttgttctttgtgttttggctggttttgaacagtttttgggctgaaaa
aagtcaactatactgggaacagagctctgaaaactgacctttcaggctttgatcctaatt
gtgacatcttgggtgactgtcgttttaaatctaatgagattgtgctcttttcaaaagagg
gtggagctagaaaggcctgcgtgtcagcatagtggcaga ccacagatggctactaatccg
```

Figure 1M: Primers used for *gle1* intron 2-3. The forward primer is highlighted in yellow and the reverse primer in green.

gle1
Intron12-13

gtggtggtggtgcttctgtccat taata tcacaataatcaatatatcgattgatcatgcaat
actcagagatgacctcaaatcatgtttgcatgcaatatagatttacaattcacaat
aacattaaagccattttacagtgcaccagtgaggtagtcataacttcaataacggggtc
ctggaggccgggtgctctgcatactttagtttcaaccacaattaacacacctgaaccag
ttaatcaagctctttctaggataactaaaacttccaggcagggtttggtgaaggaaagtgg
agctaaactatgtaggagaccggccctcaaggaccaagttggaaccccttctttataa
tcatgacaatgcgaatgagttttatacatgcttttgacacttaataacagttgtcgtaa
gcatgaataaggtctcattcacattcacgatgtgtttcatgaatcatgatcataaaggtt
taatgtcagacccttcaagtagtgacccaaaattagtagcaccacaattaatatgttgg
gggaaaatattaaa taagat tttaacgaaacagggaaaatcactagaaaataaaaatatt
caaatataggtgat tttttttgtttgtttgtttgcaataactgaatttaaatgtgttat
at tttctataccaaaataaaaaataaaaataaaaactcatttcaaacgcacaaaata
tgttacctatattcattgagaaatggaacaaacgggctactcattatgctgagcact
gtatgttatttaactgagat tttttatgactctgtttatataatgtgaata **tgtagcaatt**
ctggctgcatcag

Figure 1N: Primers used for *gle1* intron 12-13. The forward primer is highlighted in yellow and the reverse primer in green.

pptc7-001
Intron 1-2

gtatgtaat **tgctacaacgattaaggcgca**tttg tttttacacgcgaagatcatttgcta
gggagaactggttagtcaggatgttcgtggttgactcgcttctgacgtcacgactgtc
gcacatcagtgccgcgacaaaagcctttacaacctctatataacgttacacgatgaag
at tttatgaggatacataactttccaattacttttaaaaaatttcacctagtggttaagg
ctattccagctggttaaatacaactaattaataatcacctttatgatgagtgcaaaaa
gataggctactcccagaattaaaaatgacgggtgtgaaatactttctctatcataaat
aataaaaaattagacaactgtttcaatctaaacataaaaatatcccctagtagagggaaat
at tattggaatgaaaaaaaatattaatattataaatggaaagctacctggtcaatgcc
tttaaatttttaatttaagaagtgcactttaaaatacttcacaaaatgtatccttgcaa
gcaactttatctaaatcatgaatattgataatacttgacattttgtaatacacaagag
gaagacttatctttctataactgatgtatctcttaaat ttcggaatgatgtt **agtgga**
tgttat tttgggcaaagaaatgttaataacaggctctctttaaagatgtcatttgcaatt

Figure 1O: Primers used for *pptc7* intron 1-2. The forward primer is highlighted in yellow and the reverse primer in green.

pptc7-001

Intron 2-3

gtaagtacgttcacttttaatgaactgaattcagtggaatcttacttcaaagagag
ttgcatggaaatcatttattttccgtcttacttttttacgcgcaaacagtggaatgctgt
tttttagaggctgttgggtctattacagcattatgctctggcttcaattaaggtgcggtg
tgcaattttgtgttctgttcacttccattcatgcgcttacgtaaacagaggagcatgcgt
catalcttctgctacacactgaagttcacttcaacttgtgcatcaaataatcacagtt
tgacatctatcttaaatctaggtcaactatccatacagtgatggttaagcagagtaaccac
acaaacatagtcttattttacttagcgtgcactgacatgagagacacgtggttacacat
aaaactccggaatggatggtttagttctgggacgggtacaagtgaatgttttattttcctg
acttgggagggacaagggtttttgggaacggcttggctcatgtttctcaggatgagatca
aagccgtaactaaaatataatagactgaaatgagtcattgtagagtgcgtttttcctcaa
aaacacgctgtgggctggatgagtcacgaacagagtgtactgggtcacaagattggattt
tggtattaatctgcacagattcaaatcaattacaggtttttgtgagggtttggccttt

Figure 1P: Primers used for *pptc7* intron 2-3. The forward primer is highlighted in yellow and the reverse primer in green.

lhx2b-001

Intron 1-2

taacaacaaaacaaga caatggcaagcttcacggttaattcctttggcatgacagattt
ttagcattttctctaatagcagtgcaacttaaaatataatgtggcaattcaaattctaagt
tatatacaaaaatgtaaatccataactacacaaagaaattataaaggatttaattttacg
acttaaatgtgaatataggattttcagattgtttgctgtcgtctatataaagccacaaaa
cacgatcaaacacaataaaaacacacctctgattaatttacttaaaaatgcattggattt
tacgaaattcttatgttaaaagtgaaaaaacacgcaaatggatgcatgcacaatataata
cattctatctgttgatcctctttatgcatgatcctccgttgacagggaaatgtaa
aaaaaattaaagtagcctatataatcggtcttattcactctaaactgtgtatttatctt
ctgaatttgttctcagccccctccattctatacacaagtgagcactattttactcttag
catgtttttttatacccagcaaatgcgtaaaaatagtggtttacactcatccctaaagccat
taccattataatttacaatctgccttttaatatcattgctgcaacataagagagaatgg
tgagaaaaaaaatctgtgtttgtgtaagaattgggatttgagttcgtgcaatttaatgagt

Figure 1Q: Primers used for *lhx2b* intron 1-2. The forward primer is highlighted in yellow and the reverse primer in green.

lhx2b-001

Intron 2-3

aagtaaaaaacgatgcaacatgcattaatctcgtcgggaatatatcatgcagaactgattt
ttaacgccatttaaatatttacataactaaaagttacttatctaactcgttacctaaagt
aaatgatgctctttgtttgggaaaaaacagcaacaacctgtaaaaattgtccaaaaata
aattattatgtgatgttgcacttagctgactgtgcaattgattgtgtatgtcattgcac
aattgaataatcaagagggagggcgagaggcctattaagataatcatatggcgttacc
tcgccatgctcagtcfaatctccattgtaagcaatttaagtaattattggagacgtgatt
attgagactggattccactgcgagactcactacatttgcctgctgcatctgtttaa
tgcgttgttttactttagcagtgccaaggataacatccaatatttaaaatacaaatc
aatctcgaattctaaatgatgattgatccaaaggtatggtgggaagcagcttattta
gtcaggctcgtgagtggggggccaccttctgcttgaagagtgctgaaagtcacagctg
ctctattctccgcag

Figure 1R: Primers used for *lhx2b* intron 2-3. The forward primer is highlighted in yellow and the reverse primer in green.

lhx2b-001

Intron 3-4

attgttaattgaagtggcaaatttatcagaccggcgggtctcgtttgctgaactaagcag
cttctgaagcactgttaaatttacatggacgtaaaatggaggagaaaaaagagagaaat
caaatgaaacgttttgaatcagatcaacgggttcgacaaaaacagagttactagtgagt
gaactttgtgtgtgtgtgtgtgctctcttgagtgtgagactcagatcattgctgcccc
atcagctcacactttaacaacagcagcaagaatcaaacctgaaaaataagaacaataa
gacatcttctttttgtttatgcatcattgcaatactacagtcaacaaaataaactcc
gcgttcagataactattcctggcagcgcgtcgtgtagtaaggtaacagatatttctcaat
gaccatatttatatgagcaggaaacatttgttcgccatgtgcagcgttgtaaagcattca
aggtaattatccgaagtgttgatcagaccatttttcaatgactaatattttagtgtgc
agagaaaacataattctgaaactgtcatgctctagcaacacataaacttctgccaaagaat
ttggaactggcgcaaacacatttctgacacattcagacaggcctatctcctaacaacttg

Figure 1S: Primers used for *lhx2b* intron 3-4. The forward primer is highlighted in yellow and the reverse primer in green.

CLTCL1 (2 of 2)-201

Intron1-2

ctgaatttggtaaactacctggtggtgcaaatattggtgacttgaaaagcgagacaaag
gtggcggagtcgagagcccctcgtcggccttcccatctttacaccacctgctccgacgg
atcaggcagtatacgcagcaaaaccaattcttcataaagcacatcttataattctaatt
tgaaagcttatttcaccgcaatTTTaaagaattctgtcatcttaataagtcacettac
agcagcga tcgaactgtcctggtgacaggtccgaggagataaaa aggttggggaccactg
acatagcgtataatggtgta tgagta tgataggtgttctcactgatgggttcagcta
gaagggcatccgctgtgtaaaacata tgctggataagt tgggtggttcattccactgttgc
gaccccagattaataaaaggactaagctgaaaagaaa tgaatgaaggaaactatgccatt
aaatgagtttatatTTTgagactatTTTaaaatttgagcacattcttcagtgacttatt
ttctagttccagttagtttaatTTTTTactcattgtgaattttgtgTTTTatttcagc
taacagaaatgTTTTTgaccgatagTTTTtagttggtttggttgagtttcaagggtggtt
ttgtggtcattctcgtctctctctctctctcag

Figure 1T: Primers used for *cltcl1* intron 1-2. The forward primer is highlighted in yellow and the reverse primer in green.

Ccdc64

cDNA

```
ATGTCGGCTGCTGCTGGATCTGATTTTCAAGCCACCCAGCCGGACAGCGACCCGCTC  
GACCGAGCCCTAATCCCGGGGGCCAGACTCGCCAGACACCCGGGGGCACTCACGCTG  
CTACACACCGGGGGGGGGGGCTCGGCATGGCTCTGAGCAGGAGGTTGGCCATGCTGACC  
GGGACCCAGGCGCCAGCTCCAGCCATCCCGGGGGAGCACCCCTGTGAGCCGGCCAGGAC  
TCTGACCTACTGTGCTCTCTTCCGGCCAGAAAGAGAGGACTTGGTGTCTGGCTGCTAAACTG  
GGCAAGCTCTACTTGAAGAAGAACCCAGACCTCACTAAGCATTATGACAAAATGACCTAG  
GATTTAAACGACAGACTGGAGCTGCTGGAGCAGGAGAGACAGAGCTGGCGGGGGGCTGTG  
GAGAGCCGTGAGGGCCAGTGGGAGGGGGGGCTGCTGACTGGAGCCGGATCTGCAGCAC  
CTGCAGGGGAGCTGGAGAGACATCAGCTCCAGTGGGGAGCCGACCCGAAAGAGCC  
CGAGCCATCAGTCAACTTTTCAAGACAGACCCACCCGCTGCTGGAGCAGCTCAGCAGGGCC  
GGGAGCTGGAGAACAGCTGTCAACTCAGGTTCTATTCTATTACGGGAGCATTCAAGAG  
AAAGCATCTCCAGCACCCAGCAGATGACGGGGCTGGAGACGCTGCAGCTGAGATCCGG  
ATGCTGTGGAGCCGAGCAGGATCTGGAGGGAGGGTCTGTGCTGTTCTGGAGGAAGAC  
CAGCAGCTGCAGAACCCGCTGGAGGAGCTGAGAGAGAGCCGCTGGAGCTGGAGAACAC  
TGGCACCATAAGACTGCCAGAAATTTTACCTGAGACCTGTTAACAATTATTAACTT  
AAAACAACTATTTCACAAAAAAGAAAAAAGACAGACCCATCCATCCATCTTTATACACAGA  
CGTGCACATCTCACTTGTGTAGAGCCGCTCAGAACTCCAAAGTTCCATCCGGAAGCTTA  
TCAGCTGTCTGCTCCATACAGACCCAAAGATTGTGATTTGTTTCTCTCTAGCTCCCT  
CTGCACTTCTGGGAGCCCTACTGTCAGCTGGCTCCATCTGCTCTCAGCTCAGAGGAAAT  
GACATCACAGACTCCGCTTATCCACCGACTCGTCCATGGATGAGTCTTCAGAGACACTC  
TGGCTAAGGAGCTCCGGAGGGGGCAGTTTGCACCTTAGTCTTCTGGAGCTGGGAGACTT  
ACACAAAACCTGCTGGAGGGCCATGANTCAACGGTGGGGCTGCTCTCAGTGGAGGTTTCT  
TCTTCAAGAGAGACAGACCCAGCCGCTTGGAGCCGATGACAGAGTACCCAGACCCAAAGAA  
CAGTTCCAGAGCCCTATACAGACAGAGATGAGCCATGCCAAGAGAAAGCCGCTGGAG  
ATGGAGCTGGCCAAAGTAAAGATCGACATCATGTCITTCAGCAGTCAAGCTGCTGGACGCA  
ATACAGCAGAACTCAACCTGTCTCAGAGTTAGAGCCCTGGCAGGATGACATGCCACAGA  
GTAATCGATCAGCAGCTGATCCGCAAAACCCAGGAGGATCCCTCCCTTCTCC  
TTCCAGGAGGAGGAGGGGGCTGCTTCCAGACCAACACAGGGGGCTGGCAGCAACAGCAG  
CCACTCTTTCATTTCTCAAGAGAACTGA
```

Figure 3: Primers used for sequencing of *ccdc64*.

Highlighted are forward primer (yellow) and reverse primer (green) sequences. The sequence was exported from Ensembl genome browser.

Rpl6 cDNA

```
TCGGTCTTTTTTCTAGTTGAAGGTAAATGTGGCTTCCATGTCTGTTTTTCTCCACACACA  
ATCTGCAATTAATCT CAGTCAATCAATGGGCTTATGCGTCAGCCCGCATACAGAGAGAGCTTGGC  
CGTAAGCATGGCAGCCGTAACCCCTGAGCTGGTTCAGCCCGCATGGCCCGCTATTCCCGCTCC  
GCCATGTTTGGCTGGCCGGCCATGTACRAGAGGAGACTTAAGCTCCAGTGCAGGAGGTG  
GAAAAGAAATCAAGCAGAAAGAGCTCAGCCAGACTCAAGCAATCCACCCCGCCCATC  
AAGACTGTCCGGGAGACAAAAATGGAGGCCACTCGTGTGTCTCARRC TGGCGGAAATCCG  
CGTTATT ATCCACAGAGAGATGTCGGCTCTAAGCTGGCGACTCATGCTATCAGCCCTTC  
ACTCAGCAAGCCAGGAAACTGGCCAAAACCATCAACCCCTGGAACTGTGCTCATCATGCTG  
ACCGGACGGCAACCGTGGAAAAGCCGGTGGTTTTTCTCAGCCAGCTAGACAGCCGGCCCTCTC  
CTCGTCAACCGTCCCTTGGCCATCAACCCCGTCCCTCTGGCTAGAGCTCAGCCAGAACTTC  
TGCATGGCCACAAACACCAAACTGGACATCTCTGGCCATCAGATGCCACAGAACTCAGC  
GACTCTTACTTCAGCAGAGAGAGCTCAGGAAACCCAGCCACCCAGGAGGGAGAG CAATCTTC  
GACACCGAGAGGAGCACTACCGTTTGCAGGAGCAGCCAGGGCAGACCAGAGAGCCGTG  
CAGTCTCAGCTGCTCTCTCTATCAAGAGCTTCTCTCAGCTCAGCCGT TACCTGGCCCTCC  
ATGTTCTCCCTGTCTAATCG ACTCTACCCACACAACTGGTTTTCTAAAATGCTAATAAA  
ACGTCAACCCAGA
```

Figure 4: Primers used for sequencing *rpl6*.

Highlighted are the forward primer (red) and reverse primer (green) sequences. Sequence was exported from Ensembl.

lhx2b cDNA

```
TGTAGAGGGGCTTCAGTAGCTGGTATGTCCCTCAAAGCTCCGGAAATGCTCTCATAGGCTAA  
ACCAATCTGGGCTGCATGCTTTGGGATCTCTGATATACTCTGATGCATTTCAAAGANTCC  
GTCAGAATACAGAGCTGACAGTTCTGATAAACCAGTGGCCGTTTCAGACCCGATCAGACACTG  
CTAACGGGAATTATTTAATGAGGAGGAGAAAGGTCATATGAACTGCCACAGGCTTAGAAGT  
GGCTCTCACGGAAATCTTGGGTTGCAGATCTCCGCGCAACAGCTCTATTGGGTCTCATC  
TGCGGCAACGATGCTTTTCCACGGTCTGGCTGGAGGGCGAGATGCATGGTGTATGGGAAG  
AATGGAGCCGAGAGGAAAGAGCCGATTCGGCGACTATCAGCTCGGGCCATAGATATGGGGCA  
AACACACACCAACCTTCCTTCATCAGCGGGGENTGGGTTGGCTCTGTGCGGGGGCTGGGG  
AGGCAAGATTTGGGATCGCTACTACCTGCTGGCGTGGACAAGCAATGGCACATGGCGTG  
TCTGAAGTCTGCGAGTGTAAACTGAACTGGAGTCTGAGCTCAGCTGCTTCAGCARAGA  
CGGAAGCATCTACTGCAAGAAGACTATTACAGAGGTTTTTGGGTGCAGAGATGTGCCCCG  
GTGCCACCTCGGGATCTCGGGCTCGGAAATGGTCAATGAGGGCCAGGGATTTGGTGTACCA  
CTTGAACTGTTTCACTGCAAGACTTGGAAACAAATGCTGAGGACTGGGGGACCACTTCGG  
CATGAAAGACAGTCTGGTGTACTGCAGGCTACACTTTGAAACGCTCATCCAGGGAGACTT  
CCCCAGGCATTTCAATCACACGGATGTAGGGCTAATAAAGGACTGAGCAGCAGGGGGCC  
TCTAGGACTGTCTTATTATAACGGCGTGAACAGCTGCAAAAGGGCCCGGGCCCGAAGAG  
GAAGAGCCCTGGGGCCGGAGCGGACTTGGGGGGGTATATGTCAGCAATTGAGCTGCANTGA  
TATGAGAACTCATTTAAACACCATCAGCTGAGGACCATGAACTGGTATTTGGCCATCAA  
CCCAATCCTGACGCAAGGATCTGAACAGCTGGGCCGAAAAACAGGACTCCCAAGGGG  
GGTGGTACAGCTGTGTGTTTCAGAACGCTCGAGCGAAGTTTCAGACCAATCTTCTGGGTCA  
GGAGAACACCGGTGTGGACAGGCTTGGGATGGGTCAAAATTTGGCTGGAGGAACGGCGT  
GGGACTGGTTCGGAGATATCAAACGGCTCCATGAGCCCTTCCAGCAGCCCGACCACTCT  
CACAGACCTGACCAACCCCAATGCCCACCGTCACTCCGTACTGACCTCTGTCCCGGG  
CAGCTGGAGGTTCAAGGATGGCGGATCCATGGCAAAGCACTTAACCAGGCTCTTCTG  
ATGCACAGACTAACAAAGTCACTTTATCTGCTCCCTAAGAAGACCGGATCATGGATGCA  
TCCATCATTTTACCCCACTGCAAAAACAAAAGAGTTCTTGCTTAGTGTTCCTGTCTCAT
```

Figure 6: Primers used for sequencing of *lhx2b*.

Forward primers (grey), reverse primers (green) and polymorphisms (pink) are highlighted. Sequence was exported from Ensembl genome browser.

REFERENCES

- Aboitiz, F. and J. Montiel (2007). "Co-option of signaling mechanisms from neural induction to telencephalic patterning." Reviews in the Neurosciences **18**(3-4): 311-342.
- Akbarian, S., W. E. Bunney, et al. (1993). "Altered distribution of nicotinamide-adenine dinucleotide phosphate—diaphorase cells in frontal lobe of schizophrenics implies disturbances of cortical development." Archives of general psychiatry **50**(3): 169-177.
- Aleman, A., R. S. Kahn, et al. (2003). "Sex differences in the risk of schizophrenia: evidence from meta-analysis." Archives of general psychiatry **60**(6): 565.
- Allende, M. L. and E. S. Weinberg (1994). "The Expression Pattern of Two Zebrafish achaete-scute Homolog (ash) Genes Is Altered in the Embryonic Brain of the cyclops Mutant." Developmental biology **166**(2): 509-530.
- Amsterdam, A., R. M. Nissen, et al. (2004). "Identification of 315 genes essential for early zebrafish development." Proceedings of the National Academy of Sciences of the United States of America **101**(35): 12792-12797.
- Aston, C., L. Jiang, et al. (2004). "Microarray analysis of postmortem temporal cortex from patients with schizophrenia." Journal of neuroscience research **77**(6): 858-866.
- Atanasoski, S., L. Notterpek, et al. (2004). "The Protooncogene Ski Controls Schwann Cell Proliferation and Myelination." Neuron **43**(4): 499-511.
- Austin, C., B. Ky, et al. (2004). "Expression of Disrupted-In-Schizophrenia-1, a schizophrenia-associated gene, is prominent in the mouse hippocampus throughout brain development." Neuroscience **124**(1): 3-10.
- Avila, R. L., B. R. Tevlin, et al. (2007). "Myelin structure and composition in zebrafish." Neurochemical research **32**(2): 197-209.
- Back, S. A., N. L. Luo, et al. (2001). "Late oligodendrocyte progenitors coincide with the developmental window of vulnerability for human perinatal white matter injury." The Journal of neuroscience **21**(4): 1302-1312.
- Banisadr, G., T. J. Frederick, et al. (2011). "The role of CXCR4 signaling in the migration of transplanted oligodendrocyte progenitors into the cerebral white matter." Neurobiology of disease **44**(1): 19-27.
- Bansal, R., K. Stefansson, et al. (1992). "Proligodendroblast Antigen (POA), a Developmental Antigen Expressed by A007/O4-Positive Oligodendrocyte Progenitors Prior to the Appearance of Sulfatide and Galactocerebroside." Journal of neurochemistry **58**(6): 2221-2229.

- Baraban, Y. W. S. C. (2007). "Granule cell dispersion and aberrant neurogenesis in the adult hippocampus of an LIS1 mutant mouse." Dev Neurosci **29**: 91-98.
- Baranzini, S. E. (2011). "Revealing the genetic basis of multiple sclerosis: are we there yet?" Current opinion in genetics & development **21**(3): 317-324.
- Barateiro, A. and A. Fernandes (2014). "Temporal oligodendrocyte lineage progression: In vitro models of proliferation, differentiation and myelination." Biochimica et Biophysica Acta (BBA)-Molecular Cell Research.
- Barbin, G., M. Aigrot, et al. (2004). "Axonal cell-adhesion molecule L1 in CNS myelination." Neuron glia biology **1**(01): 65-72.
- Barres, B. A. and M. C. Raff (1999). "Axonal control of oligodendrocyte development." The Journal of Cell Biology **147**(6): 1123-1128.
- Barros, C. S., T. Nguyen, et al. (2009). " β 1 integrins are required for normal CNS myelination and promote AKT-dependent myelin outgrowth." Development **136**(16): 2717-2724.
- Baumann, N. and D. Pham-Dinh (2001). "Biology of oligodendrocyte and myelin in the mammalian central nervous system." Physiological reviews **81**(2): 871-927.
- Benjamini, Y. and T. P. Speed (2012). "Summarizing and correcting the GC content bias in high-throughput sequencing." Nucleic acids research: gks001.
- Benninger, Y., T. Thurnherr, et al. (2007). "Essential and distinct roles for cdc42 and rac1 in the regulation of Schwann cell biology during peripheral nervous system development." The Journal of Cell Biology **177**(6): 1051-1061.
- Bentley, D. R., S. Balasubramanian, et al. (2008). "Accurate whole human genome sequencing using reversible terminator chemistry." Nature **456**(7218): 53-59.
- Bjelke, B. and A. Seiger (1989). "Morphological distribution of MBP-like immunoreactivity in the brain during development." International Journal of Developmental Neuroscience **7**(2): 145-164.
- Blackwood, D., A. Fordyce, et al. (2001). "Schizophrenia and affective disorders— cosegregation with a translocation at chromosome 1q42 that directly disrupts brain-expressed genes: clinical and P300 findings in a family." The American Journal of Human Genetics **69**(2): 428-433.
- Blader, P., N. Fischer, et al. (1997). "The activity of neurogenin1 is controlled by local cues in the zebrafish embryo." Development **124**(22): 4557-4569.

- Blumenstiel, J. P., A. C. Noll, et al. (2009). "Identification of EMS-Induced Mutations in *Drosophila melanogaster* by Whole-Genome Sequencing." Genetics **182**(1): 25-32.
- Bowen, M. E., K. Henke, et al. (2012). "Efficient mapping and cloning of mutations in zebrafish by low-coverage whole-genome sequencing." Genetics **190**(3): 1017-1024.
- Bradley, K. M., J. B. Elmore, et al. (2007). "A major zebrafish polymorphism resource for genetic mapping." Genome biology **8**(4): R55.
- Bradshaw, N. J. and D. J. Porteous (2011). "DISC1-binding proteins in neural development, signalling and schizophrenia." Neuropharmacology.
- Bramon, E., E. Dempster, et al. (2006). "Is there an association between the COMT gene and P300 endophenotypes?" European psychiatry **21**(1): 70-73.
- Brandon, N., E. Handford, et al. (2004). "Disrupted in Schizophrenia 1 and Nudel form a neurodevelopmentally regulated protein complex: implications for schizophrenia and other major neurological disorders." Molecular and Cellular Neuroscience **25**(1): 42-55.
- Brennan, A., C. Dean, et al. (2000). "Endothelins Control the Timing of Schwann Cell Generation *in Vitro* and *in Vivo*." Developmental biology **227**(2): 545-557.
- Brinkmann, B. G., A. Agarwal, et al. (2008). "Neuregulin-1/ErbB signaling serves distinct functions in myelination of the peripheral and central nervous system." Neuron **59**(4): 581-595.
- Britsch, S., D. E. Goerich, et al. (2001). "The transcription factor Sox10 is a key regulator of peripheral glial development." Genes & development **15**(1): 66-78.
- Brösamle, C. and M. E. Halpern (2002). "Characterization of myelination in the developing zebrafish." Glia **39**(1): 47-57.
- Buckley, C. E., P. Goldsmith, et al. (2008). "Zebrafish myelination: a transparent model for remyelination?" Disease models & mechanisms **1**(4-5): 221-228.
- Buckley, C. E., A. Marguerie, et al. (2010). "Temporal dynamics of myelination in the zebrafish spinal cord." Glia **58**(7): 802-812.
- Bunge, R. P. (1968). "Glial cells and the central myelin sheath." Physiol. Rev **48**(1): 197-251.

- Camargo, L., V. Collura, et al. (2006). "Disrupted in Schizophrenia 1 Interactome: evidence for the close connectivity of risk genes and a potential synaptic basis for schizophrenia." Molecular Psychiatry **12**(1): 74-86.
- Cannon, T. D., W. Hennah, et al. (2005). "Association of DISC1/TRAX Haplotypes With Schizophrenia, Reduced Prefrontal Gray Matter, and Impaired Short- and Long-term Memory." Arch Gen Psychiatry **62**(11): 1205-1213.
- Carson, J. H., K. Worboys, et al. (1997). "Translocation of myelin basic protein mRNA in oligodendrocytes requires microtubules and kinesin." Cell Motil Cytoskeleton **38**(4): 318-328.
- Charles, P., M. Hernandez, et al. (2000). "Negative regulation of central nervous system myelination by polysialylated-neural cell adhesion molecule." Proceedings of the National Academy of Sciences **97**(13): 7585-7590.
- Chen, Y., H. Wu, et al. (2009). "The oligodendrocyte-specific G protein-coupled receptor GPR17 is a cell-intrinsic timer of myelination." Nature neuroscience **12**(11): 1398-1406.
- Chenn, A. and C. A. Walsh (2002). "Regulation of cerebral cortical size by control of cell cycle exit in neural precursors." SCIENCE **297**(5580): 365.
- Cheung, M. and J. Briscoe (2003). "Neural crest development is regulated by the transcription factor Sox9." Development **130**(23): 5681-5693.
- Chubb, J., N. Bradshaw, et al. (2007). "The DISC locus in psychiatric illness." Molecular Psychiatry **13**(1): 36-64.
- Cirulli, E. T., A. Singh, et al. (2010). "Research Screening the human exome: a comparison of whole genome and whole transcriptome sequencing." Genome biology **11**: R57.
- Clapcote, S. J., T. V. Lipina, et al. (2007). "Behavioral phenotypes of Disc1 missense mutations in mice." Neuron **54**(3): 387-402.
- Clapcote, S. J. and J. C. Roder (2006). "Deletion polymorphism of Disc1 is common to all 129 mouse substrains: implications for gene-targeting studies of brain function." Genetics **173**(4): 2407-2410.
- Coe, T., P. Hamilton, et al. (2009). "Genetic variation in strains of zebrafish (*Danio rerio*) and the implications for ecotoxicology studies." Ecotoxicology **18**(1): 144-150.
- Colognato, H., C. ffrench-Constant, et al. (2005). "Human diseases reveal novel roles for neural laminins." Trends in neurosciences **28**(9): 480-486.

- Concha, M. L., C. Russell, et al. (2003). "Local tissue interactions across the dorsal midline of the forebrain establish CNS laterality." Neuron **39**(3): 423-438.
- Consortium, S. W. G. o. t. P. G. (2014). "Biological insights from 108 schizophrenia-associated genetic loci." Nature **511**(7510): 421-427.
- Corfas, G., M. O. Velardez, et al. (2004). "Mechanisms and roles of axon-Schwann cell interactions." Journal of Neuroscience **24**(42): 9250.
- Craig, A., N. Ling Luo, et al. (2003). "Quantitative analysis of perinatal rodent oligodendrocyte lineage progression and its correlation with human." Experimental neurology **181**(2): 231-240.
- Crowley, J. J., C. E. Hilliard, et al. (2013). "Deep resequencing and association analysis of schizophrenia candidate genes." Molecular psychiatry **18**(2): 138.
- Cuperus, J. T., T. A. Montgomery, et al. (2010). "Identification of MIR390a precursor processing-defective mutants in Arabidopsis by direct genome sequencing." Proceedings of the National Academy of Sciences **107**(1): 466-471.
- Czopka, T., C. French-Constant, et al. (2013). "Individual Oligodendrocytes Have Only a Few Hours in which to Generate New Myelin Sheaths In Vivo." Developmental Cell **25**(6): 599-609.
- Czopka, T. and D. A. Lyons (2011). "Dissecting mechanisms of myelinated axon formation using zebrafish." Methods Cell Biol **105**: 25-62.
- D'Antonio, M., A. Droggiti, et al. (2006). "TGF β type II receptor signaling controls Schwann cell death and proliferation in developing nerves." The Journal of neuroscience **26**(33): 8417-8427.
- de Castro, F., A. Bribián, et al. (2013). "Regulation of oligodendrocyte precursor migration during development, in adulthood and in pathology." Cellular and Molecular Life Sciences **70**(22): 4355-4368.
- Dean, J. M., M. D. Moravec, et al. (2011). "Strain-specific differences in perinatal rodent oligodendrocyte lineage progression and its correlation with human." Developmental neuroscience **33**(3-4): 251-260.
- Devon, R. S., S. Anderson, et al. (2001). "Identification of polymorphisms within Disrupted in Schizophrenia 1 and Disrupted in Schizophrenia 2, and an investigation of their association with schizophrenia and bipolar affective disorder." Psychiatric genetics **11**(2): 71.

- Doitsidou, M., R. J. Poole, et al. (2010). "C. elegans mutant identification with a one-step whole-genome-sequencing and SNP mapping strategy." PLoS One **5**(11): e15435.
- Drerup, C. M., H. M. Wiora, et al. (2009). "Disc1 regulates foxd3 and sox10 expression, affecting neural crest migration and differentiation." Development **136**(15): 2623.
- Drerup, C. M., H. M. Wiora, et al. (2009). "Disc1 regulates foxd3 and sox10 expression, affecting neural crest migration and differentiation." Development **136**(15): 2623-2632.
- Dubois-Dalcq, M., T. Behar, et al. (1986). "Emergence of three myelin proteins in oligodendrocytes cultured without neurons." The Journal of Cell Biology **102**(2): 384-392.
- Duff, B. J., K. A. N. Macritchie, et al. (2013). "Human brain imaging studies of DISC1 in schizophrenia, bipolar disorder and depression: A systematic review." Schizophrenia research **147**(1): 1-13.
- Dugas, J. C., T. L. Cuellar, et al. (2010). "Dicer1 and miR-219 Are required for normal oligodendrocyte differentiation and myelination." Neuron **65**(5): 597-611.
- Eastwood, S. L., M. Walker, et al. (2010). "The DISC1 Ser704Cys substitution affects centrosomal localization of its binding partner PCM1 in glia in human brain." Human Molecular Genetics **19**(12): 2487.
- Edenfeld, G., G. Volohonsky, et al. (2006). "The Splicing Factor Crooked Neck Associates with the RNA-Binding Protein HOW to Control Glial Cell Maturation in Drosophila." Neuron **52**(6): 969-980.
- Edgar, N. and E. Sibille (2012). "A putative functional role for oligodendrocytes in mood regulation." Translational psychiatry **2**(5): e109.
- Eisen, J. S. and J. C. Smith (2008). "Controlling morpholino experiments: don't stop making antisense." Development **135**(10): 1735-1743.
- El Waly, B., M. Macchi, et al. (2014). "Oligodendrogenesis in the normal and pathological central nervous system." Neurogenesis **8**: 145.
- Emery, B. (2010). "Regulation of oligodendrocyte differentiation and myelination." Science **330**(6005): 779-782.
- Enomoto, A., N. Asai, et al. (2009). "Roles of disrupted-in-schizophrenia 1-interacting protein girdin in postnatal development of the dentate gyrus." Neuron **63**(6): 774-787.
- Esain, V., J. H. Postlethwait, et al. (2010). "FGF-receptor signalling controls neural cell diversity in the zebrafish hindbrain by regulating olig2 and sox9." Development **137**(1): 33-42.

- Ettinger, U., M. Picchioni, et al. (2006). "Antisaccade performance in monozygotic twins discordant for schizophrenia: the Maudsley twin study." American Journal of Psychiatry **163**(3): 543.
- Fairfield, H., G. J. Gilbert, et al. (2011). "Mutation discovery in mice by whole exome sequencing." Genome biology **12**(9): R86.
- Fancy, S. P., S. E. Baranzini, et al. (2009). "Dysregulation of the Wnt pathway inhibits timely myelination and remyelination in the mammalian CNS." Genes & development **23**(13): 1571-1585.
- Fields, R. D. (2008). "White matter in learning, cognition and psychiatric disorders." Trends in neurosciences **31**(7): 361-370.
- Fingerprinting, G. (2007). "Risk alleles for multiple sclerosis identified by a genomewide study." N engl J med **357**: 851-862.
- Finzsch, M., C. C. Stolt, et al. (2008). "Sox9 and Sox10 influence survival and migration of oligodendrocyte precursors in the spinal cord by regulating PDGF receptor α expression." Development **135**(4): 637-646.
- Fleming, J. (2013). "Helminth therapy and multiple sclerosis." International journal for parasitology **43**(3): 259-274.
- Ford-Perriss, M., H. Abud, et al. (2001). "Fibroblast growth factors in the developing central nervous system." Clinical and Experimental Pharmacology and Physiology **28**(7): 493-503.
- Fruttiger, M., L. Karlsson, et al. (1999). "Defective oligodendrocyte development and severe hypomyelination in PDGF-A knockout mice." Development **126**(3): 457-467.
- Fuccillo, M., M. Rallu, et al. (2004). "Temporal requirement for hedgehog signaling in ventral telencephalic patterning." Development **131**(20): 5031-5040.
- Furusho, M., J. L. Dupree, et al. (2012). "Fibroblast growth factor receptor signaling in oligodendrocytes regulates myelin sheath thickness." The Journal of neuroscience **32**(19): 6631-6641.
- Gaj, T., C. A. Gersbach, et al. (2013). "ZFN, TALEN, and CRISPR/Cas-based methods for genome engineering." Trends in biotechnology **31**(7): 397-405.
- Gandhi, R., A. Laroni, et al. (2010). "Role of the innate immune system in the pathogenesis of multiple sclerosis." Journal of neuroimmunology **221**(1): 7-14.

- Garcia-Lopez, R. and S. Martinez (2010). "Oligodendrocyte precursors originate in the parabasal band of the basal plate in prosomere 1 and migrate into the alar prosencephalon during chick development." Glia **58**(12): 1437-1450.
- Garcion, E. and A. Faissner (2001). "Knockout mice reveal a contribution of the extracellular matrix molecule tenascin-C to neural precursor proliferation and migration." Development **128**(13): 2485-2496.
- Ge, X., C. L. Frank, et al. (2010). "Hook3 interacts with PCM1 to regulate pericentriolar material assembly and the timing of neurogenesis." Neuron **65**(2): 191-203.
- Geisler, R., G.-J. Rauch, et al. (2007). "Large-scale mapping of mutations affecting zebrafish development." BMC genomics **8**(1): 11.
- Gelfman, S., D. Burstein, et al. (2012). "Changes in exon-intron structure during vertebrate evolution affect the splicing pattern of exons." Genome research **22**(1): 35-50.
- Georgieva, L., V. Moskvina, et al. (2006). "Convergent evidence that oligodendrocyte lineage transcription factor 2 (OLIG2) and interacting genes influence susceptibility to schizophrenia." Proceedings of the National Academy of Sciences **103**(33): 12469.
- Geren, B. B. and F. O. Schmitt (1954). "The structure of the Schwann cell and its relation to the axon in certain invertebrate nerve fibers." Proceedings of the National Academy of Sciences of the United States of America **40**(9): 863.
- Ghislain, J. and P. Charnay (2006). "Control of myelination in Schwann cells: a Krox20 cis-regulatory element integrates Oct6, Brn2 and Sox10 activities." EMBO reports **7**(1): 52-58.
- Gilmour, D. T., H.-M. Maischein, et al. (2002). "Migration and function of a glial subtype in the vertebrate peripheral nervous system." Neuron **34**(4): 577-588.
- Gottesman, I. I. and T. D. Gould (2003). "The endophenotype concept in psychiatry: etymology and strategic intentions." American Journal of Psychiatry **160**(4): 636-645.
- Grandel, H., J. Kaslin, et al. (2006). "Neural stem cells and neurogenesis in the adult zebrafish brain: origin, proliferation dynamics, migration and cell fate." Developmental biology **295**(1): 263-277.
- Gritli-Linde, A., P. Lewis, et al. (2001). "The whereabouts of a morphogen: direct evidence for short-and graded long-range activity of hedgehog signaling peptides." Developmental biology **236**(2): 364-386.
- Grunwald, D. J. and G. Streisinger (1992). "Induction of recessive lethal and specific locus mutations in the zebrafish with ethyl nitrosourea." Genetical research **59**(02): 103-116.

- Gupta, T., F. L. Marlow, et al. (2010). "Microtubule actin crosslinking factor 1 regulates the Balbiani body and animal-vegetal polarity of the zebrafish oocyte." PLoS genetics **6**(8): e1001073.
- Guryev, V., M. J. Koudijs, et al. (2006). "Genetic variation in the zebrafish." Genome research **16**(4): 491-497.
- Ha, K., J. G. Buchan, et al. (2013). "MYBPC1 mutations impair skeletal muscle function in zebrafish models of arthrogryposis." Human molecular genetics: ddt344.
- Hakak, Y., J. R. Walker, et al. (2001). "Genome-wide expression analysis reveals dysregulation of myelination-related genes in chronic schizophrenia." Proceedings of the National Academy of Sciences **98**(8): 4746-4751.
- Hamshere, M. L., P. Bennett, et al. (2005). "Genomewide Linkage Scan in Schizoaffective Disorder: Significant Evidence for Linkage at 1q42 Close to DISC1, and Suggestive Evidence at 22q11 and 19p13." Arch Gen Psychiatry **62**(10): 1081-1088.
- Hanafy, K. A. and J. A. Sloane (2011). "Regulation of remyelination in multiple sclerosis." FEBS letters **585**(23): 3821-3828.
- Hartman, B. K., H. C. Agrawal, et al. (1979). "A comparative study of the immunohistochemical localization of basic protein to myelin and oligodendrocytes in rat and chicken brain." Journal of Comparative Neurology **188**(2): 273-290.
- Hattori, T., S. Shimizu, et al. (2014). "DISC1 (Disrupted-in-Schizophrenia-1) Regulates Differentiation of Oligodendrocytes." PLoS One **9**(2): e88506.
- Hayashi, M. A. F., J. R. Guerreiro, et al. (2010). "Assessing the role of endooligopeptidase activity of Ndel1 (nuclear-distribution gene E homolog like-1) in neurite outgrowth." Molecular and Cellular Neuroscience **44**(4): 353-361.
- Heasman, J. (2002). "Morpholino oligos: making sense of antisense?" Developmental biology **243**(2): 209-214.
- Hébert, J. M. (2005). "Unraveling the molecular pathways that regulate early telencephalon development." Current topics in developmental biology **69**: 17-37.
- Henke, K., M. E. Bowen, et al. (2013). "Perspectives for identification of mutations in the zebrafish: making use of next-generation sequencing technologies for forward genetic approaches." Methods **62**(3): 185-196.
- Hennah, W., A. Tuulio-Henriksson, et al. (2005). "A haplotype within the DISC1 gene is associated with visual memory functions in families with a high density of schizophrenia." Mol Psychiatry **10**(12): 1097-1103.

- Hennah, W., T. Varilo, et al. (2003). "Haplotype transmission analysis provides evidence of association for DISC1 to schizophrenia and suggests sex-dependent effects." Human Molecular Genetics **12**(23): 3151.
- Hernández, F., E. Gómez de Barreda, et al. (2010). "GSK3: a possible link between beta amyloid peptide and tau protein." Experimental neurology **223**(2): 322-325.
- Hodgkinson, C. A., Q. Yuan, et al. (2008). "Addictions biology: haplotype-based analysis for 130 candidate genes on a single array." Alcohol and alcoholism **43**(5): 505.
- Howe, K., M. D. Clark, et al. (2013). "The zebrafish reference genome sequence and its relationship to the human genome." Nature.
- Howng, S. Y. B., R. L. Avila, et al. (2010). "ZFP191 is required by oligodendrocytes for CNS myelination." Genes & development **24**(3): 301-311.
- Huangfu, D., A. Liu, et al. (2003). "Hedgehog signalling in the mouse requires intraflagellar transport proteins." Nature **426**(6962): 83-87.
- Hwang, W. Y., Y. Fu, et al. (2013). "Efficient genome editing in zebrafish using a CRISPR-Cas system." Nat Biotech **31**(3): 227-229.
- Innocenti, G., F. Ansermet, et al. (2003). "Schizophrenia, neurodevelopment and corpus callosum." Molecular psychiatry **8**(3): 261-274.
- Iorio, M. V., M. Ferracin, et al. (2005). "MicroRNA gene expression deregulation in human breast cancer." Cancer Research **65**(16): 7065-7070.
- Jaaro-Peled, H., A. Hayashi-Takagi, et al. (2009). "Neurodevelopmental mechanisms of schizophrenia: understanding disturbed postnatal brain maturation through neuregulin-1-ErbB4 and DISC1." Trends in neurosciences **32**(9): 485-495.
- Jakovcevski, I., R. Filipovic, et al. (2009). "Oligodendrocyte development and the onset of myelination in the human fetal brain." Frontiers in neuroanatomy **3**.
- Jakovcevski, I., Z. Mo, et al. (2007). "Down-regulation of the axonal polysialic acid-neural cell adhesion molecule expression coincides with the onset of myelination in the human fetal forebrain." Neuroscience **149**(2): 328-337.
- Jao, L.-E., B. Appel, et al. (2012). "A zebrafish model of lethal congenital contracture syndrome 1 reveals Gle1 function in spinal neural precursor survival and motor axon arborization." Development **139**(7): 1316-1326.

- Jeserich, G., K. Klempahn, et al. (2008). "Features and functions of oligodendrocytes and myelin proteins of lower vertebrate species." Journal of Molecular Neuroscience **35**(1): 117-126.
- Jeserich, G. and A. Stratmann (1992). "In vitro differentiation of trout oligodendrocytes: evidence for an A2B5-positive origin." Developmental brain research **67**(1): 27-35.
- Jeserich, G. and T. Waehneltd (1986). "Characterization of antibodies against major fish CNS myelin protein: Immunoblot analysis and immunohistochemical localization of 36K and IP2 proteins in trout nerve tissue." Journal of neuroscience research **15**(2): 147-158.
- Jessen, K., A. Brennan, et al. (1994). "The Schwann cell precursor and its fate: a study of cell death and differentiation during gliogenesis in rat embryonic nerves." Neuron **12**(3): 509-527.
- Jessen, K. R. and R. Mirsky (2005). "The origin and development of glial cells in peripheral nerves." Nature Reviews Neuroscience **6**(9): 671-682.
- Jones, S. A., D. M. Jolson, et al. (2003). "Triiodothyronine is a survival factor for developing oligodendrocytes." Molecular and cellular endocrinology **199**(1): 49-60.
- Kakalacheva, K. and J. D. Lünemann (2011). "Environmental triggers of multiple sclerosis." FEBS letters **585**(23): 3724-3729.
- Kamiya, A., K. Kubo, et al. (2005). "A schizophrenia-associated mutation of DISC1 perturbs cerebral cortex development." Nature cell biology **7**(12): 1067-1078.
- Katsel, P., K. L. Davis, et al. (2005). "Variations in myelin and oligodendrocyte-related gene expression across multiple brain regions in schizophrenia: a gene ontology study." Schizophr Res **79**(2-3): 157-173.
- Katsel, P., W. Tan, et al. (2011). "Expression of mutant human DISC1 in mice supports abnormalities in differentiation of oligodendrocytes." Schizophrenia research **130**(1): 238-249.
- Kazakova, N., H. Li, et al. (2006). "A screen for mutations in zebrafish that affect myelin gene expression in Schwann cells and oligodendrocytes." Developmental biology **297**(1): 1-13.
- Kelly, P. D., F. Chu, et al. (2000). "Genetic linkage mapping of zebrafish genes and ESTs." Genome research **10**(4): 558-567.
- Kerns, D., G. S. Vong, et al. (2010). "Gene expression abnormalities and oligodendrocyte deficits in the internal capsule in schizophrenia." Schizophr Res **120**(1-3): 150-158.

- Kessaris, N., M. Fogarty, et al. (2005). "Competing waves of oligodendrocytes in the forebrain and postnatal elimination of an embryonic lineage." Nature neuroscience **9**(2): 173-179.
- Kessaris, N., N. Pringle, et al. (2008). "Specification of CNS glia from neural stem cells in the embryonic neuroepithelium." Philosophical Transactions of the Royal Society B: Biological Sciences **363**(1489): 71-85.
- Kim, H. J., H. J. Park, et al. (2008). "Association study of polymorphisms between DISC1 and schizophrenia in a Korean population." Neuroscience Letters **430**(1): 60-63.
- Kim, J. Y., Q. Sun, et al. (2003). "The role of ErbB2 signaling in the onset of terminal differentiation of oligodendrocytes in vivo." The Journal of neuroscience **23**(13): 5561-5571.
- Kimmel, C. B., W. W. Ballard, et al. (1995). "Stages of embryonic development of the zebrafish." American Journal of Anatomy **203**(3): 253-310.
- Kirby, A., A. Gnirke, et al. (2013). "Mutations causing medullary cystic kidney disease type 1 lie in a large VNTR in MUC1 missed by massively parallel sequencing." Nature genetics **45**(3): 299-303.
- Knapik, E. W., A. Goodman, et al. (1998). "A microsatellite genetic linkage map for zebrafish (*Danio rerio*)." Nature genetics **18**(4): 338-343.
- Kondo, T. and M. Raff (2000). "Oligodendrocyte precursor cells reprogrammed to become multipotential CNS stem cells." Science **289**(5485): 1754-1757.
- Koudijs, M. J., M. J. den Broeder, et al. (2008). "Genetic analysis of the two zebrafish patched homologues identifies novel roles for the hedgehog signaling pathway." BMC developmental biology **8**(1): 15.
- Law, A. J., C. Shannon Weickert, et al. (2004). "Neuregulin-1 (NRG-1) mRNA and protein in the adult human brain." Neuroscience **127**(1): 125-136.
- Lawson, N. D. and S. A. Wolfe (2011). "Forward and reverse genetic approaches for the analysis of vertebrate development in the zebrafish." Developmental Cell **21**(1): 48-64.
- Lee, F. H. F., M. P. Fadel, et al. (2011). "Disc1 Point Mutations in Mice Affect Development of the Cerebral Cortex." Journal of Neuroscience **31**(9): 3197-3206.
- Lee, X., Z. Shao, et al. (2014). "LINGO-1 regulates oligodendrocyte differentiation by inhibiting ErbB2 translocation and activation in lipid rafts." Molecular and Cellular Neuroscience **60**(0): 36-42.

- Lerch-Gaggl, A., J. Haque, et al. (2002). "Pescadillo is essential for nucleolar assembly, ribosome biogenesis, and mammalian cell proliferation." Journal of Biological Chemistry **277**(47): 45347-45355.
- Li, D., D. A. Collier, et al. (2006). "Meta-analysis shows strong positive association of the neuregulin 1 (NRG1) gene with schizophrenia." Human Molecular Genetics **15**(12): 1995.
- Li, H., B. Handsaker, et al. (2009). "The sequence alignment/map format and SAMtools." Bioinformatics **25**(16): 2078-2079.
- Li, H., Y. Lu, et al. (2007). "Olig1 and Sox10 interact synergistically to drive myelin basic protein transcription in oligodendrocytes." The Journal of neuroscience **27**(52): 14375-14382.
- Liu, A., J. Li, et al. (2006). "A molecular insight of Hes5-dependent inhibition of myelin gene expression: old partners and new players." The EMBO journal **25**(20): 4833-4842.
- Lo Nigro, C., S. S. Chong, et al. (1997). "Point mutations and an intragenic deletion in LIS1, the lissencephaly causative gene in isolated lissencephaly sequence and Miller-Dieker syndrome." Human Molecular Genetics **6**(2): 157.
- Long, M. and M. Deutsch (1999). "Association of intron phases with conservation at splice site sequences and evolution of spliceosomal introns." Molecular biology and evolution **16**(11): 1528-1534.
- López-Bendito, G., A. Cautinat, et al. (2006). "Tangential neuronal migration controls axon guidance: a role for neuregulin-1 in thalamocortical axon navigation." Cell **125**(1): 127-142.
- Lu, Q. R., T. Sun, et al. (2002). "Common Developmental Requirement for *Olig* Function Indicates a Motor Neuron/Oligodendrocyte Connection." Cell **109**(1): 75-86.
- Lynch, M. and J. S. Conery (2003). "The origins of genome complexity." Science **302**(5649): 1401-1404.
- Lyons, D. A., H.-M. Pogoda, et al. (2005). "*erb3* and *erb2* Are Essential for Schwann Cell Migration and Myelination in Zebrafish." Current Biology **15**(6): 513-524.
- Lyons, David A. and William S. Talbot (2012). "Targeting Mechanisms in Myelinated Axons: Not All Nodes Are Created Equal." Developmental Cell **22**(1): 7-9.
- Majewski, J. and J. Ott (2002). "Distribution and characterization of regulatory elements in the human genome." Genome research **12**(12): 1827-1836.

- Mao, Y., X. Ge, et al. (2009). "Disrupted in Schizophrenia 1 Regulates Neuronal Progenitor Proliferation via Modulation of GSK3 [beta]/[beta]-Catenin Signaling." Cell **136**(6): 1017-1031.
- Marx, V. (2013). "Next-generation sequencing: The genome jigsaw." Nature **501**(7466): 263-268.
- Maycox, P., F. Kelly, et al. (2009). "Analysis of gene expression in two large schizophrenia cohorts identifies multiple changes associated with nerve terminal function." Molecular psychiatry **14**(12): 1083-1094.
- McKenna, A., M. Hanna, et al. (2010). "The Genome Analysis Toolkit: a MapReduce framework for analyzing next-generation DNA sequencing data." Genome research **20**(9): 1297-1303.
- Mecklenburg, N., R. Garcia-López, et al. (2011). "Cerebellar oligodendroglial cells have a mesencephalic origin." Glia **59**(12): 1946-1957.
- Mela, A. and J. E. Goldman (2013). "CD82 blocks cMet activation and overcomes hepatocyte growth factor effects on oligodendrocyte precursor differentiation." The Journal of neuroscience **33**(18): 7952-7960.
- Merchán, P., A. Bribián, et al. (2007). "Sonic hedgehog promotes the migration and proliferation of optic nerve oligodendrocyte precursors." Molecular and Cellular Neuroscience **36**(3): 355-368.
- Meyer, A. and M. Schartl (1999). "Gene and genome duplications in vertebrates: the one-to-four (-to-eight in fish) rule and the evolution of novel gene functions." Current opinion in cell biology **11**(6): 699-704.
- Mi, S., R. H. Miller, et al. (2005). "LINGO-1 negatively regulates myelination by oligodendrocytes." Nature neuroscience **8**(6): 745-751.
- Millar, J. K., J. C. Wilson-Annan, et al. (2000). "Disruption of two novel genes by a translocation co-segregating with schizophrenia." Human Molecular Genetics **9**(9): 1415.
- Milo, R. and E. Kahana (2010). "Multiple sclerosis: geoepidemiology, genetics and the environment." Autoimmunity reviews **9**(5): A387-A394.
- Ming, G.-l. and H. Song (2009). "DISC1 Partners with GSK3² in Neurogenesis." Cell **136**(6): 990-992.
- Miron, V. E., T. Kuhlmann, et al. (2011). "Cells of the oligodendroglial lineage, myelination, and remyelination." Biochimica et Biophysica Acta (BBA)-Molecular Basis of Disease **1812**(2): 184-193.

- Mironov, A. A., J. W. Fickett, et al. (1999). "Frequent alternative splicing of human genes." Genome research **9**(12): 1288-1293.
- Mirsky, R., K. R. Jessen, et al. (2002). "Schwann cells as regulators of nerve development." Journal of Physiology-Paris **96**(1): 17-24.
- Mitkus, S. N., T. M. Hyde, et al. (2008). "Expression of oligodendrocyte-associated genes in dorsolateral prefrontal cortex of patients with schizophrenia." Schizophrenia research **98**(1): 129-138.
- Miyamoto, Y., N. Yamamori, et al. (2014). "Rab35, acting through ACAP2 switching off Arf6, negatively regulates oligodendrocyte differentiation and myelination." Molecular biology of the cell **25**(9): 1532-1542.
- Miyoshi, K., A. Honda, et al. (2003). "Disrupted-In-Schizophrenia 1, a candidate gene for schizophrenia, participates in neurite outgrowth." Molecular Psychiatry **8**(7): 685-694.
- Moens, C. B., T. M. Donn, et al. (2008). "Reverse genetics in zebrafish by TILLING." Briefings in functional genomics & proteomics **7**(6): 454-459.
- Monk, K. R., S. G. Naylor, et al. (2009). "AG protein-coupled receptor is essential for Schwann cells to initiate myelination." Science **325**(5946): 1402-1405.
- Monuki, E. S., G. Weinmaster, et al. (1989). "SCIP: a glial POU domain gene regulated by cyclic AMP." Neuron **3**(6): 783-793.
- Moore, C. A., C. A. Parkin, et al. (2007). "A role for the Myoblast city homologues Dock1 and Dock5 and the adaptor proteins Crk and Crk-like in zebrafish myoblast fusion." Development **134**(17): 3145-3153.
- Morris, J. A., G. Kandpal, et al. (2003). "DISC1 (Disrupted-In-Schizophrenia 1) is a centrosome-associated protein that interacts with MAP1A, MIPT3, ATF4/5 and NUDEL: regulation and loss of interaction with mutation." Human Molecular Genetics **12**(13): 1591.
- Nasevicius, A. and S. C. Ekker (2000). "Effective targeted gene 'knockdown' in zebrafish." Nature genetics **26**(2): 216-220.
- Nery, S., H. Wichterle, et al. (2001). "Sonic hedgehog contributes to oligodendrocyte specification in the mammalian forebrain." Development **128**(4): 527-540.
- Nickols, J. C., W. Valentine, et al. (2003). "Activation of the transcription factor NF- κ B in Schwann cells is required for peripheral myelin formation." Nature neuroscience **6**(2): 161-167.

- Nodari, A., D. Zambroni, et al. (2007). " β 1 integrin activates Rac1 in Schwann cells to generate radial lamellae during axonal sorting and myelination." The Journal of Cell Biology **177**(6): 1063-1075.
- Noden, D. M. (1983). "The role of the neural crest in patterning of avian cranial skeletal, connective, and muscle tissues." Developmental biology **96**(1): 144-165.
- Norton, W. H., M. Mangoli, et al. (2005). "Monorail/Foxa2 regulates floorplate differentiation and specification of oligodendrocytes, serotonergic raphe neurones and cranial motoneurones." Development **132**(4): 645-658.
- O'Donovan, M. C., N. J. Craddock, et al. (2009). "Genetics of psychosis; insights from views across the genome." Human genetics **126**(1): 3-12.
- Ogata, T., S.-i. Yamamoto, et al. (2006). "Signaling axis in schwann cell proliferation and differentiation." Molecular Neurobiology **33**(1): 51-61.
- Ohya, W., H. Funakoshi, et al. (2007). "Hepatocyte growth factor (HGF) promotes oligodendrocyte progenitor cell proliferation and inhibits its differentiation during postnatal development in the rat." Brain research **1147**: 51-65.
- Olivier, C., I. Cobos, et al. (2001). "Monofocal origin of telencephalic oligodendrocytes in the anterior entopeduncular area of the chick embryo." Development **128**(10): 1757-1769.
- Ono, K., R. Bansal, et al. (1995). "Early development and dispersal of oligodendrocyte precursors in the embryonic chick spinal cord." Development **121**(6): 1743-1754.
- Ono, K., Y. Yasui, et al. (1997). "Focal ventricular origin and migration of oligodendrocyte precursors into the chick optic nerve." Neuron **19**(2): 283-292.
- Orentas, D. M., J. E. Hayes, et al. (1999). "Sonic hedgehog signaling is required during the appearance of spinal cord oligodendrocyte precursors." Development **126**(11): 2419-2429.
- Osburn, N., J. Li, et al. (2011). "Genetic and functional analyses identify DISC1 as a novel callosal agenesis candidate gene." American Journal of Medical Genetics Part A **155**(8): 1865-1876.
- Ozeki, Y., T. Tomoda, et al. (2003). "Disrupted-in-Schizophrenia-1 (DISC-1): mutant truncation prevents binding to NudE-like (NUDEL) and inhibits neurite outgrowth." Proceedings of the National Academy of Sciences of the United States of America **100**(1): 289.

- Pan, Y., C. B. Bai, et al. (2006). "Sonic hedgehog signaling regulates Gli2 transcriptional activity by suppressing its processing and degradation." Molecular and cellular biology **26**(9): 3365-3377.
- Park, H.-C., A. Mehta, et al. (2002). "< i> olig2</i> Is Required for Zebrafish Primary Motor Neuron and Oligodendrocyte Development." Developmental biology **248**(2): 356-368.
- Park, H. C., A. Mehta, et al. (2002). "olig2 is required for zebrafish primary motor neuron and oligodendrocyte development." Developmental biology **248**(2): 356-368.
- Park, T. J., S. L. Haigo, et al. (2006). "Ciliogenesis defects in embryos lacking inturnd or fuzzy function are associated with failure of planar cell polarity and Hedgehog signaling." Nature genetics **38**(3): 303-311.
- Parkinson, D. B., A. Bhaskaran, et al. (2004). "Krox-20 inhibits Jun-NH2-terminal kinase/c-Jun to control Schwann cell proliferation and death." The Journal of Cell Biology **164**(3): 385-394.
- Pastink, A., C. Vreeken, et al. (1989). "Sequence analysis of N-ethyl-N-nitrosourea-induced vermilion mutations in *Drosophila melanogaster*." Genetics **123**(1): 123-129.
- Paus, T. (2010). "Growth of white matter in the adolescent brain: myelin or axon?" Brain and cognition **72**(1): 26-35.
- Perlin, J. R., M. E. Lush, et al. (2011). "Neuronal Neuregulin 1 type III directs Schwann cell migration." Development **138**(21): 4639-4648.
- Peters, A., S. L. Palay, et al. (1991). The fine structure of the nervous system: neurons and their supporting cells, Oxford University Press New York.
- Peukert, D., S. Weber, et al. (2011). "Lhx2 and Lhx9 determine neuronal differentiation and compartment in the caudal forebrain by regulating Wnt signaling." PLoS biology **9**(12): e1001218.
- Philips, T., A. Bento-Abreu, et al. (2013). "Oligodendrocyte dysfunction in the pathogenesis of amyotrophic lateral sclerosis." Brain **136**(2): 471-482.
- Placzek, M. (1995). "The role of the notochord and floor plate in inductive interactions." Current opinion in genetics & development **5**(4): 499-506.
- Pogoda, H.-M., N. Sternheim, et al. (2006). "A genetic screen identifies genes essential for development of myelinated axons in zebrafish." Developmental biology **298**(1): 118-131.
- Poliak, S. and E. Peles (2003). "The local differentiation of myelinated axons at nodes of Ranvier." Nature Reviews Neuroscience **4**(12): 968-980.

- Poncet, C., C. Soula, et al. (1996). "Induction of oligodendrocyte progenitors in the trunk neural tube by ventralizing signals: effects of notochord and floor plate grafts, and of sonic hedgehog." Mechanisms of development **60**(1): 13-32.
- Prabakaran, S., J. Swatton, et al. (2004). "Mitochondrial dysfunction in schizophrenia: evidence for compromised brain metabolism and oxidative stress." Molecular psychiatry **9**(7): 684-697.
- Qian, X., A. A. Davis, et al. (1997). "FGF2 concentration regulates the generation of neurons and glia from multipotent cortical stem cells." Neuron **18**(1): 81-93.
- Qu, M., F. Tang, et al. (2007). "Positive association of the Disrupted-in-Schizophrenia-1 gene (DISC1) with schizophrenia in the Chinese han population." American Journal of Medical Genetics Part B: Neuropsychiatric Genetics **144B**(3): 266-270.
- Raphael, A. R., D. A. Lyons, et al. (2011). "ErbB signaling has a role in radial sorting independent of Schwann cell number." Glia **59**(7): 1047-1055.
- Rauch, G.-J., M. Granato, et al. (1997). "A polymorphic zebrafish line for genetic mapping using SSLPs on high-percentage agarose gels." Technical Tips Online **2**(1): 148-150.
- Remahl, S. and C. Hildebrand (1990). "Relation between axons and oligodendroglial cells during initial myelination I. The glial unit." Journal of neurocytology **19**(3): 313-328.
- Richardson, W. D., N. Kessar, et al. (2006). "Oligodendrocyte wars." Nature Reviews Neuroscience **7**(1): 11-18.
- Richardson, W. D., H. K. Smith, et al. (2000). "Oligodendrocyte lineage and the motor neuron connection." Glia **29**(2): 136-142.
- Riethmacher, D., E. Sonnenberg-Riethmacher, et al. (1997). "Severe neuropathies in mice with targeted mutations in the ErbB3 receptor." Nature **389**(6652): 725-730.
- Rio, C., H. I. Rieff, et al. (1997). "Neuregulin and erbB Receptors Play a Critical Role in Neuronal Migration." Neuron **19**(1): 39-50.
- Robu, M. E., J. D. Larson, et al. (2007). "p53 activation by knockdown technologies." PLoS genetics **3**(5): e78.
- Ross, C. A., R. L. Margolis, et al. (2006). "Neurobiology of schizophrenia." Neuron **52**(1): 139-153.
- Rowitch, D. H. (2004). "Glial specification in the vertebrate neural tube." Nature Reviews Neuroscience **5**(5): 409-419.

- Saadi, I., F. S. Alkuraya, et al. (2011). "Deficiency of the cytoskeletal protein SPECC1L leads to oblique facial clefting." The American Journal of Human Genetics **89**(1): 44-55.
- Sadovnick, A., H. Armstrong, et al. (1993). "A population-based study of multiple sclerosis in twins: Update." Annals of neurology **33**(3): 281-285.
- Salzer, J. L. (2003). "Polarized Domains of Myelinated Axons." Neuron **40**(2): 297-318.
- Sander, J. D., L. Cade, et al. (2011). "Targeted gene disruption in somatic zebrafish cells using engineered TALENs." Nature biotechnology **29**(8): 697.
- Schatz, M. C., A. L. Delcher, et al. (2010). "Assembly of large genomes using second-generation sequencing." Genome research **20**(9): 1165-1173.
- Schlager, M. A., L. C. Kapitein, et al. (2010). "Pericentrosomal targeting of Rab6 secretory vesicles by Bicaudal-D-related protein 1 (BICDR-1) regulates neuritogenesis." The EMBO journal **29**(10): 1637-1651.
- Schlager, M. A., L. C. Kapitein, et al. (2010). "Pericentrosomal targeting of Rab6 secretory vesicles by Bicaudal-D-related protein 1 (BICDR-1) regulates neuritogenesis." The EMBO journal **29**(10): 1637-1651.
- Schmidt, R., U. Strähle, et al. (2013). "Neurogenesis in zebrafish-from embryo to adult." Neural Dev **8**(3).
- Schumacher, J., G. Laje, et al. (2009). "The DISC locus and schizophrenia: evidence from an association study in a central European sample and from a meta-analysis across different European populations." Human Molecular Genetics **18**(14): 2719.
- Schurov, I. L., E. J. Handford, et al. (2004). "Expression of disrupted in schizophrenia 1 (DISC1) protein in the adult and developing mouse brain indicates its role in neurodevelopment." Molecular Psychiatry **9**(12): 1100-1110.
- Schweitzer, J., T. Becker, et al. (2006). "Evolution of myelin proteolipid proteins: gene duplication in teleosts and expression pattern divergence." Molecular and Cellular Neuroscience **31**(1): 161-177.
- Selemon, L. D. and P. S. Goldman-Rakic (2001). "The reduced neuropil hypothesis: a circuit based model of schizophrenia." The Science of Mental Health: Schizophrenia: 259.
- Seshadri, S., A. Kamiya, et al. (2010). "Disrupted-in-Schizophrenia-1 expression is regulated by β -site amyloid precursor protein cleaving enzyme-1-neuregulin cascade." Proceedings of the National Academy of Sciences **107**(12): 5622-5627.

- Sherman, D. L. and P. J. Brophy (2005). "Mechanisms of axon ensheathment and myelin growth." Nature Reviews Neuroscience **6**(9): 683-690.
- Shiomi, K., H. Uchida, et al. (2003). "Ccd1, a Novel Protein with a DIX Domain, Is a Positive Regulator in the Wnt Signaling during Zebrafish Neural Patterning." Current biology : CB **13**(1): 73-77.
- Shoubridge, C., P. S. Tarpey, et al. (2010). "Mutations in the guanine nucleotide exchange factor gene IQSEC2 cause nonsyndromic intellectual disability." Nat Genet **42**(6): 486-488.
- Siegel, G. J., B. W. Agranoff, et al. (1999). "Myelin Formation, Structure and Biochemistry."
- Simmons, T. and B. Appel (2012). "Mutation of pescadillo disrupts oligodendrocyte formation in zebrafish." PLoS One **7**(2): e32317.
- Singh, K. K., X. Ge, et al. (2010). "Dixdc1 Is a Critical Regulator of DISC1 and Embryonic Cortical Development." Neuron **67**(1): 33-48.
- Sivkov, S. T. and V. H. Akabaliev (2003). "Minor physical anomalies in schizophrenic patients and normal controls." Psychiatry: Interpersonal and Biological Processes **66**(3): 222-233.
- Sivron, T., A. Cohen, et al. (1990). "Glial response to axonal injury: in vitro manifestation and implication for regeneration." Glia **3**(4): 267-276.
- Skromne, I. and V. E. Prince (2008). "Current perspectives in zebrafish reverse genetics: moving forward." Developmental Dynamics **237**(4): 861-882.
- Solnica-Krezel, L., A. F. Schier, et al. (1994). "Efficient recovery of ENU-induced mutations from the zebrafish germline." Genetics **136**(4): 1401-1420.
- Stefansson, H., H. Petursson, et al. (2002). "Neuregulin 1 and susceptibility to schizophrenia." The American Journal of Human Genetics **71**(4): 877-892.
- Stewart, H. J., A. Brennan, et al. (2001). "Developmental regulation and overexpression of the transcription factor AP-2, a potential regulator of the timing of Schwann cell generation." European Journal of Neuroscience **14**(2): 363-372.
- Stolt, C. C., S. Rehberg, et al. (2002). "Terminal differentiation of myelin-forming oligodendrocytes depends on the transcription factor Sox10." Genes & development **16**(2): 165-170.
- Streisinger, G., C. Walker, et al. (1981). "Production of clones of homozygous diploid zebra fish (*Brachydanio rerio*)." Nature **291**(5813): 293.

- Sullivan, P. F., D. Lin, et al. (2008). "Genomewide association for schizophrenia in the CATIE study: results of stage 1." Molecular psychiatry **13**(6): 570-584.
- Sun, N. and H. Zhao (2013). "Transcription activator-like effector nucleases (TALENs): A highly efficient and versatile tool for genome editing." Biotechnology and bioengineering **110**(7): 1811-1821.
- Syroid, D. E., P. J. Maycox, et al. (2000). "Induction of postnatal Schwann cell death by the low-affinity neurotrophin receptor in vitro and after axotomy." The Journal of neuroscience **20**(15): 5741-5747.
- Talbot, W. S. and A. F. Schier (1998). "Positional cloning of mutated zebrafish genes." Methods in cell biology **60**: 259-286.
- Taveggia, C., M. L. Feltri, et al. (2010). "Signals to promote myelin formation and repair." Nature Reviews Neurology **6**(5): 276-287.
- Taveggia, C., G. Zanazzi, et al. (2005). "Neuregulin-1 Type III Determines the Ensheathment Fate of Axons." Neuron **47**(5): 681-694.
- Taya, S., T. Shinoda, et al. (2007). "DISC1 Regulates the Transport of the NUDEL/LIS1/14-3-3 Complex through Kinesin-1." The Journal of Neuroscience **27**(1): 15.
- Taylor, M. S., R. S. Devon, et al. (2003). "Evolutionary constraints on the Disrupted in Schizophrenia locus." Genomics **81**(1): 67-77.
- Tekki-Kessarlis, N., R. Woodruff, et al. (2001). "Hedgehog-dependent oligodendrocyte lineage specification in the telencephalon." Development **128**(13): 2545-2554.
- Thisse, B. and C. Thisse (2004). "Fast release clones: a high throughput expression analysis." ZFIN direct data submission **2**.
- Thomson, P. A., S. E. Harris, et al. (2005). "Association between genotype at an exonic SNP in DISC1 and normal cognitive aging." Neuroscience Letters **389**(1): 41-45.
- Thu, H. N. T., S. F. H. Tien, et al. (2013). "tbx2a Is required for specification of endodermal pouches during development of the pharyngeal arches." PLoS One **8**(10): e77171.
- Timsit, S., S. Martinez, et al. (1995). "Oligodendrocytes originate in a restricted zone of the embryonic ventral neural tube defined by DM-20 mRNA expression." The Journal of neuroscience **15**(2): 1012-1024.
- Topilko, P., S. Schneider-Maunoury, et al. (1994). "Krox-20 controls myelination in the peripheral nervous system."

- Tran, P. B. and R. J. Miller (2003). "Chemokine receptors: signposts to brain development and disease." Nature Reviews Neuroscience **4**(6): 444-455.
- Tripathi, R. B., L. E. Clarke, et al. (2011). "Dorsally and ventrally derived oligodendrocytes have similar electrical properties but myelinate preferred tracts." The Journal of neuroscience **31**(18): 6809-6819.
- Tsai, H.-H., E. Frost, et al. (2002). "The chemokine receptor CXCR2 controls positioning of oligodendrocyte precursors in developing spinal cord by arresting their migration." Cell **110**(3): 373-383.
- Uechi, T., Y. Nakajima, et al. (2006). "Ribosomal protein gene knockdown causes developmental defects in zebrafish." PLoS One **1**(1): e37.
- Uranova, N., D. Orlovskaya, et al. (2001). "Electron microscopy of oligodendroglia in severe mental illness." Brain Res Bull **55**(5): 597-610.
- Vallstedt, A., J. M. Klos, et al. (2005). "Multiple dorsoventral origins of oligodendrocyte generation in the spinal cord and hindbrain." Neuron **45**(1): 55-67.
- Vartanian, T., G. Fischbach, et al. (1999). "Failure of spinal cord oligodendrocyte development in mice lacking neuregulin." Proceedings of the National Academy of Sciences **96**(2): 731-735.
- Verity, A. and A. Campagnoni (1988). "Regional expression of myelin protein genes in the developing mouse brain: in situ hybridization studies." Journal of neuroscience research **21**(2-4): 238-248.
- Vierkotten, J., R. Dildrop, et al. (2007). "Ftm is a novel basal body protein of cilia involved in Shh signalling." Development **134**(14): 2569-2577.
- Vlkolinský, R., N. Cairns, et al. (2001). "Decreased brain levels of 2', 3'-cyclic nucleotide-3'-phosphodiesterase in Down syndrome and Alzheimer's disease." Neurobiology of aging **22**(4): 547-553.
- Voyvodic, J. T. (1989). "Target size regulates calibre and myelination of sympathetic axons."
- Voz, M. L., W. Coppieters, et al. (2012). "Fast homozygosity mapping and identification of a zebrafish ENU-induced mutation by whole-genome sequencing." PLoS One **7**(4): e34671.
- Waehneltd, T., J.-M. Matthieu, et al. (1986). "Appearance of myelin proteins during vertebrate evolution." Neurochemistry international **9**(4): 463-474.

- Waggener, C. T., J. L. Dupree, et al. (2013). "CaMKII β Regulates Oligodendrocyte Maturation and CNS Myelination." The Journal of neuroscience **33**(25): 10453-10458.
- Wang, Q., E. Charych, et al. (2010). "The psychiatric disease risk factors DISC1 and TNIK interact to regulate synapse composition and function." Molecular Psychiatry.
- Wang, S., A. Sdrulla, et al. (2001). "A role for the helix-loop-helix protein Id2 in the control of oligodendrocyte development." Neuron **29**(3): 603-614.
- Waxman, S. and M. Bennett (1972). "Relative conduction velocities of small myelinated and non-myelinated fibres in the central nervous system." Nature **238**(85): 217-219.
- Webster, H. d., J. R. Martin, et al. (1973). "The relationships between interphase Schwann cells and axons before myelination: a quantitative electron microscopic study." Developmental biology **32**(2): 401-416.
- Wegner, M. (2008). "A Matter of Identity: Transcriptional Control in Oligodendrocytes." Journal of Molecular Neuroscience **35**(1): 3-12.
- Wienholds, E., S. Schulte-Merker, et al. (2002). "Target-selected inactivation of the zebrafish rag1 gene." SCIENCE **297**(5578): 99.
- Wienholds, E., F. van Eeden, et al. (2003). "Efficient target-selected mutagenesis in zebrafish." Genome research **13**(12): 2700-2707.
- Wolff, C., S. Roy, et al. (2004). "iguana encodes a novel zinc-finger protein with coiled-coil domains essential for Hedgehog signal transduction in the zebrafish embryo." Genes & development **18**(13): 1565.
- Wolff, C., S. Roy, et al. (2004). "iguana encodes a novel zinc-finger protein with coiled-coil domains essential for Hedgehog signal transduction in the zebrafish embryo." Genes & development **18**(13): 1565-1576.
- Wood, J. D., F. Bonath, et al. (2009). "Disrupted-in-schizophrenia 1 and neuregulin 1 are required for the specification of oligodendrocytes and neurones in the zebrafish brain." Human molecular genetics **18**(3): 391-404.
- Wood, J. D., F. Bonath, et al. (2009). "Disrupted-in-schizophrenia 1 and neuregulin 1 are required for the specification of oligodendrocytes and neurones in the zebrafish brain." Human Molecular Genetics **18**(3): 391.
- Woodhoo, A., M. B. D. Alonso, et al. (2009). "Notch controls embryonic Schwann cell differentiation, postnatal myelination and adult plasticity." Nature neuroscience **12**(7): 839-847.

- Woodhoo, A. and L. Sommer (2008). "Development of the Schwann cell lineage: from the neural crest to the myelinated nerve." Glia **56**(14): 1481-1490.
- Xie, J., E. Farage, et al. (2010). "A novel transgenic zebrafish model for blood-brain and blood-retinal barrier development." BMC developmental biology **10**(1): 76.
- Yan, Y.-L., W. S. Talbot, et al. (1998). "Mutant rescue by BAC clone injection in zebrafish." Genomics **50**(2): 287-289.
- Ye, F., Y. Chen, et al. (2009). "HDAC1 and HDAC2 regulate oligodendrocyte differentiation by disrupting the β -catenin–TCF interaction." Nature neuroscience **12**(7): 829-838.
- Yoshida, M. and W. B. Macklin (2005). "Oligodendrocyte development and myelination in GFP-transgenic zebrafish." Journal of neuroscience research **81**(1): 1-8.
- Young-Pearse, T. L., S. Suth, et al. (2010). "Biochemical and functional interaction of DISC1 and APP regulates neuronal migration during mammalian cortical development." The Journal of neuroscience: the official journal of the Society for Neuroscience **30**(31): 10431.
- Yu, W.-M., M. L. Feltri, et al. (2005). "Schwann cell-specific ablation of laminin γ 1 causes apoptosis and prevents proliferation." The Journal of neuroscience **25**(18): 4463-4472.
- Zhang, H., L. Vutskits, et al. (2004). "A role for the polysialic acid–neural cell adhesion molecule in PDGF-induced chemotaxis of oligodendrocyte precursor cells." Journal of cell science **117**(1): 93-103.
- Zhang, H., L. Vutskits, et al. (2003). "VEGF is a chemoattractant for FGF-2–stimulated neural progenitors." The Journal of Cell Biology **163**(6): 1375-1384.
- Zhao, X., X. He, et al. (2010). "MicroRNA-Mediated Control of Oligodendrocyte Differentiation." Neuron **65**(5): 612-626.
- Zheng, W., H. Wang, et al. (2012). "The possible role of the Akt signaling pathway in schizophrenia." Brain research **1470**: 145-158.
- Zhou, Q. and D. J. Anderson (2002). "The bHLH transcription factors OLIG2 and OLIG1 couple neuronal and glial subtype specification." Cell **109**(1): 61-73.
- Zhu, Y., Q. Song, et al. (2003). "Single-nucleotide polymorphisms in soybean." Genetics **163**(3): 1123-1134.

